Università degli Studi della Tuscia di Viterbo

Dipartimento di SCIENZE ECOLOGICHE E BIOLOGICHE (DEB)

Corso di Dottorato di Ricerca in

ECOLOGIA E GESTIONE SOSTENIBILE DELLE RISORSE AMBIENTALI - **XXXIV ciclo**

TITOLO TESI DI DOTTORATO DI RICERCA

The resistance of Antarctic black fungus and stability of fungal biomolecules: a support for habitability and biosignature detection beyond Earth

Settore scientifico-disciplinare
(per es. **s.s.d. BIO/03**)

Tesi di dottorato di:
Dott. Alessia Cassaro

Tutore
Prof. Silvano Onofri

Coordinatore del corso
Prof. Claudio Carere

Co-tutore
Dott. Claudia Pacelli

A.A. 2020/21

Abstract

The search for life outside Earth mainly depends on the concept of habitability of a planetary body and on the definition of signs of extant or extinct life (biomarkers). Since space exploration missions are expensive and require long-term organization, the preliminary study of terrestrial environments and their inhabiting microorganisms, is an essential step to support extraterrestrial *in situ* operations. Terrestrial extreme environments are considered as analogues of extraterrestrial planetary surfaces and could be helpful in understanding the limits of life, habitability and the adaptation mechanisms of life in hostile environments. One of the best terrestrial analogues is the Antarctic continent, described as the most inhospitable and isolated continent on Earth, whose conditions lie on the edge of habitability. In particular, the McMurdo Dry Valleys are one of the larger ice-free areas of the continent, characterized by a cold and dry climate (Onofri et al., 2007; Øvstedal and Lewis Smith, 2001), low water availability, minimum annual precipitations, strong katabatic winds, salt concentration, desiccation, and high incident solar and ultraviolet (UV) radiation. Here, the cryptoendolitic black fungus *Cryomyces antarcticus* CCFEE 515 has been isolated and for its astonishing ability to survive in extreme conditions is considered one of the relevant test organisms used in astrobiology studies.

In this context, the primary goal of this thesis was to investigate the responses of the *C. antarcticus* colonies desiccated or in metabolically active conditions, after the exposure to increasing doses of i) heavy ions and ii) γ-rays, being part of the cosmic radiation environment. In addition, in the frame of Life in space ASI project, the survivability after the growth in different Martian relevant perchlorates was determined through culture-dependent and microscopic approaches.

The second purpose of the thesis concerned the fungal biomarkers detection after i) the exposure of *C. antarcticus* colonies, grown on two Martian regolith analogues, to ground-based tests (EVT and SVT treatments) and to real space exposure in Low Earth Orbit (LEO) and ii) the exposure of colonized Antarctica sandstone fragments in LEO, in the frame of BIOMEX and LIFE projects. The stability or degradation of different classes of biomolecules (mainly focused on pigments and nucleic acids) were investigated through spectroscopic and molecular techniques.

The obtained results have deep implications to support the ongoing and near future life-detection missions beyond Earth. The results from the study of *C. antarcticus* contributed to expands our knowledge about the limits of life, confirming the amazing adaptive abilities of *C. antarcticus*, with strong implication on the Martian habitability. The second results about biomarkers detection will be helpful to prepare exploration missions and to support extraterrestrial *in situ* operations (e.g. during Rosanlind Franklin and Perseverance rovers' operations).

Contents

1. Introduction *7*

1.1 Astrobiology and the search for life beyond Earth **7**

1.2 What is life? **8**

1.2.1 Life as we know it 9

1.3 Habitability **9**

1.3.1 Instantaneous habitability 11

1.3.2 Continuous habitability 14

1.4 Mars **16**

1.4.1 Habitability on the Martian surface: past and present scenario 16

1.4.2 Ice and water 17

1.4.3 Organic compounds 19

1.4.4 Salts 20

1.4.5 Radiation 21

1.4.6 Martian atmosphere 24

1.5 Martian subsurface **24**

1.5.1 Biosignatures 25

1.5.2 Biomarkers: a way to delineate a biological origin 26

1.5.3 Biomarkers detection through Rosalind Franklin rover 28

1.6 Not only Mars **30**

1.7 Research on Earth **31**

1.7.1 Planetary Field analogues (PFAs) 32

1.7.2 Mars analogue sites on Earth: the Antarctica continent 33

1.7.3 Antarctic McMurdo Dry Valleys (MDVs) as Martian surface analogue 36

1.7.4 The cryptoendolithic communities 37

1.7.5 Meristematic rock-inhabiting black fungi 42

1.7.5.1 The black yeast-like fungus Cryomyces antarcticus: an example of extreme eukaryotic life 44

1.8 Astrobiology projects **46**

1.8.1 The Italian National Project of Astrobiology—Life in Space—Origin, Presence, Persistence of Life in Space, from Molecules to Extremophiles 47

1.8.2 The BIOlogy and Mars Experiment (BIOMEX) project 49

1.8.3 The Lichens and Fungi Experiment: LIFE 51

1.8.4 STARLIFE project 52

1.9 Aims of the thesis and chapter description **53**

2. Insights into the habitability *56*

2.1 Insights into the survival capabilities of *Cryomyces antarcticus* hydrated colonies after exposure to Fe particle radiation **56**

2.1.1 Introduction 57

2.1.2 Materials and Methods 60

2.1.2.1 Test organism 60

2.1.2.2 Samples preparation and performed analyses 60

2.1.3 Results 62

2.1.3.1 Cultivation test 62

2.1.3.2 Metabolic activity assessment 63

2.1.3.3 Cell membranes integrity 64

2.1.3.4 DNA integrity 65

2.1.4 Discussion 66

2.2 Could radiation affect fungal cells survivability in an aqueous environment? **70**

2.2.1 Introduction 71

2.2.2 Material and Methods 73

2.2.2.1 Fungal cultures preparation 73

2.2.2.2 Irradiation parameters 74

2.2.2.3 Survival analysis 75
2.2.2.3.1 Cultivation test 75
2.2.2.4 Metabolic activity estimation by MTT (3-(4,5-dimethylthiazol-2-yl)-2,5-diphenyltetrazolium 75
2.2.2.5 Membranes damage assessment 75
2.2.2.5.1 Propidium MonoAzide (PMA) assay 75
2.2.2.6 Nucleic acids integrity assessment 76
2.2.2.7 Nucleic acids amplification and estimation of DNA lesions 76
2.2.3 Results 77
2.2.3.1 Cultivation test 77
2.2.3.2 Metabolic activity measurements 77
2.2.3.3 Membranes damage assessment 78
2.2.3.3.1 Propidium MonoAzide (PMA) assay 78
2.2.3.4 Nucleic acids amplification and estimation of DNA lesions 79
2.2.3.5 Nucleic acid integrity assessment 81
2.2.4 Discussion 82

2.3 Fungal growth tolerance, metabolic activity recovery and ultrastructural damages in hypersaline substrata 87
2.3.1 Introduction 88
2.3.2 Materials and methods 90
2.3.2.1 Test-organism, perchlorates medium preparation and activity water measurement 90
2.3.2.2 Metabolic activity estimation by MTT (3-(4,5-dimethylthiazol-2-yl)-2,5-diphenyltetrazolium) assay 92
2.3.2.3 Ultrastructural investigation 93
2.3.3 Results 93
2.3.3.1 Growth tolerance to perchlorate salts 93
2.3.3.2 Growth tolerance to Mars-relevant perchlorate salts 94
2.3.3.3 Water activity measurements 95
2.3.3.4 MTT assay 95
2.3.3.5 Ultrastructural investigation: TEM observations 97
2.3.4 Discussions 100
2.3.5 Conclusions 103

3. Insights into the biosignatures detection 105

3.1 The ground-based BIOMEX Experiment Verification Tests for life detection on Mars 105
3.1.1 Introduction 106
3.1.2 Materials and Methods 108
3.1.2.1 Sample preparation and cultivation conditions 108
3.1.2.2 Test facilities and exposure conditions 109
3.1.2.3 DNA integrity assay 111
3.1.2.3.1 DNA extraction and quantification 111
3.1.2.3.2 DNA amplification 111
3.1.2.3.3 Statistical analysis 112
3.1.2.4 Fungal melanin assay 112
3.1.2.4.1 Pigment extraction and quantification 112
3.1.2.4.2 Pigment detection 112
3.1.2.5 Fungal organic compound detection 113
3.1.3 Results 113
3.1.3.1 DNA damage assessment 113
3.1.3.2 Pigment characterization by UV-Vis spectrophotometry 114
3.1.3.3 Pigment characterization by Raman spectroscopy 117
3.1.3.4 Organic compounds characterization by FT-IR spectroscopy 119
3.1.4 Discussion 122
3.1.5 Conclusions 127

3.2 Fungal biomarkers stability in Mars regolith analogues after simulated space and Mars-like conditions 128
3.2.1 Introduction 129
3.2.2 Materials and Methods 132
3.2.2.1 Science Verification Tests (SVTs) 132
3.2.2.2 Fungal melanin extraction 133
3.2.2.3 Spectrophotometric analysis 134

3.2.2.4 Confocal Raman spectroscopy analyses 134
3.2.2.5 Nucleic acid analysis 135
3.2.2.5.1 Nucleic acid Extractions from synthetic Mars and terrestrial soils 135
3.2.2.5.2 Acid nucleic detection through quantitative real-time PCR (qPCR) 135
3.2.2.6 Statistical analyses 136
3.2.2.7 Organic compounds detection by Gas Chromatography-Mass Spectrometry 136
3.2.3 Results 137
3.2.3.1 Detection of pigments by spectrophotometric analyses 137
3.2.3.2 Detection of pigments by Confocal Raman spectroscopy 138
3.2.3.3 Detection of nucleic acids through amplification method 139
3.2.3.3.1 Organic compounds detection by Gas Chromatography associated to Mass Spectrometry 141
3.2.4 Discussion 143
3.2.5 Conclusions 147

3.3 Fungal biomarkers are detectable in Martian rock-analogues after space exposure: implications for the search of life on Mars 149
3.3.1 Introduction 150
3.3.2 Materials and Methods 152
3.3.2.1 Test organism 152
3.3.2.2 Mars analogues composition and preparation 152
3.3.2.3 Exposure conditions aboard the ISS 153
3.3.2.4 Timing and conditions of space exposure 155
3.3.2.5 Pressure 155
3.3.2.6 Solar irradiation 155
3.3.2.7 Temperature 156
3.3.2.8 Cosmic radiation 156
3.3.2.9 Mission timeline 156
3.3.2.10 Raman spectroscopy analyses 157
3.3.2.11 Fourier-transform infrared spectroscopy 159
3.3.2.12 Lipid extraction and fractionation and gas chromatography-mass spectrometry analysis 159
3.3.2.13 Nucleic acids extraction and quantitative PCR 160
3.3.3 Results 161
3.3.3.1 Raman spectroscopy analyses 161
3.3.3.2 Pigments detection by Raman spectroscopy 161
3.3.3.3 Melanin pigments vs amorphous carbon detection 162
3.3.3.4 Raman analyses interpretation 162
3.3.3.5 Organic compounds detection by Fourier Transform Infrared Resonance (FTIR) spectroscopy 165
3.3.3.6 Organic compounds detection by gas chromatography associated to mass spectrometry 168
3.3.3.7 Nucleic acids detection by quantitative Polymerase Chain Reaction (qPCR) 170
3.3.4 Discussion 171
3.3.5 Implications for the search of Earth-like life on Mars 176

3.4 Spectroscopic investigations of fungal biomarkers after exposure to heavy ion irradiation 179
3.4.1 Introduction 180
3.4.2 Materials and Methods 183
3.4.2.1 Fungal colonies and mineral mixtures preparation 183
3.4.2.2 Radiation exposure 184
3.4.2.3 Fourier transformed infrared resonance (FT-IR) spectroscopy analysis 184
3.4.2.4 Data analysis 185
3.4.2.5 Confocal Raman spectroscopy analysis 185
3.4.3 Results 186
3.4.3.1 Fourier Transform Infrared Resonance Spectroscopy (FT-IR) detection 186
3.4.3.2 Mineralogy 188
3.4.3.2 Organics 188
3.4.3.3 MIR spectra of samples exposed to Ar ions 191
3.4.3.4 MIR spectra of samples exposed to He ions 192
3.4.3.5 Heatmap (HM) analysis on the FT-IR spectra 193
3.4.3.6 Pigment detection by confocal Raman spectroscopy 194
3.4.4 Discussion 196

3.5 The protective role of Antarctica sandstone: new results from Lichens and Fungi EXperiment 201

3.5.1 Introduction 202
3.5.2 Materials and Methods 204
3.5.2.1 Colonized Sandstone 204
3.5.2.2 Hardware and exposure conditions 205
3.5.2.3 Confocal Raman spectroscopy analysis 208
3.5.2.4 Fourier transformed infrared resonance (FT-IR) spectroscopy analysis 208
3.5.3 Results 209
3.5.3.1 Detection of pigments by Confocal Raman spectroscopy 209
3.5.3.2 Infrared spectroscopy analysis: organic and inorganic detection 211
3.5.4 Discussions 214
3.5.4.1 The preservation of molecular biomarkers in quartz minerals 214
4. General discussion 221
5. Conclusion 230
References 233

1. Introduction

1.1 Astrobiology and the search for life beyond Earth

The term astrobiology, previously named exobiology, includes the study of the origin of life on Earth and the search for life on other planetary bodies (Dick and Strick, 2005; Dick, 2007). The exobiology coincided with the era of space missions, such as Viking missions (started in 1976), aiming to search for microbial life on Mars (DiGregorio, 1997; Jones, 2004).

The astrobiology term was introduced for the first time in 1941 by A.L. La Fleur, but only in 1995, astrobiology acquired its definitive name given by Wes Huntress from NASA (Catling, 2013), replacing the term exobiology, coined by Lederberg in 1960. Although this field may be considered as a "modern" discipline if compared to other sciences, its origins can be correlated to ancient Greece. Different Greek philosophers such as Thales of Miletus (624–546), Epicurus (341–270), and Metrodorus of Lampsacus (331–278), assumed the existence of other inhabited worlds beyond Earth. Some centuries later, Thomas Digges and Giordano Bruno completely changed the "geocentric idea" of the Earth, supporting the Copernican theory and believing in the "plurality of worlds", which sustains that in an infinite Universe there are an infinite number of inhabited worlds. 400 years later, the first exoplanet was discovered. These theories were also confirmed by the so-called "age of space investigation", were some of the most popular astronomers (Galileo Galilei (1564–1642), Johannes Kepler (1571–1630) and Giovanni Cassini (1625–1712)), discovered other planets and Moon, confirming that Earth was not at the center of the Universe and different potentially inhabited worlds existed. Nowadays, astrobiology is a rapidly expanding field and the space explorations include the whole Universe: from neighbor planets or icy moons to faraway exoplanets. The specific goals of this scientific field include understanding the emergence of life on Earth, determining how the early terrestrial life interact and evolved with its changing environment, understanding the evolutionary mechanisms and environmental limits of life, exploring the habitable environment in the Solar System

and searching for life or its sign on Earth and on other worlds (Kolb, 2018). To achieve these goals, astrobiology requires bringing together many disciplines, such as biology, chemistry, physics, geology, planetary science and astronomy. For this reason, it is considered as a multidisciplinary scientific field. Many years after the emergence of astrobiology as a scientific field, scientists have made several progresses in understanding the origin and the limits of life, the planetary habitability potential and the way for life-detection, enough to make the possibility of life elsewhere almost certain. In the next decades, one of the most important challenges of astrobiology will be to find it. In this moment, the search for life outside our planet is based on the habitability potential and on the biosignatures detection methods. The next paragraphs will discuss these two topics.

1.2 What is life?

Since one of the main focuses of astrobiology is to search for life or it remains on other planets (*see the paragraph above*), it is important to define what life is. "*What is life?*" Erwin Schrodinger (1945) famously asked, returning to a question that was asked in the past by Aristotle. The answer of this question requires many considerations, including the point of view from which we would like to define (Chyba and Hand, 2005). Most of the proposed definitions face problems in the form of robust counter-examples. For example, if we define life from a metabolic point of view, it is difficult to exclude fire, since it is able to grow and reproduce through chemical reactions, similarly to what happens in organisms. A thermodynamic definition should include minerals, since they can grow, reach an equilibrium and even move in response to stimuli (Chyba and Hand, 2005). For these reasons, it is important to define life through an appropriate scientific theory, based on the nature of living systems and to the features that we currently associate with life (Chyba and Hand, 2005). Nowadays, the most general definition of life, adopted by the NASA exobiology program in 1992 is: "*Life is a self-sustained chemical system capable of undergoing Darwinian evolution*". This definition of life implies the system uses matter and energy provided by the environment and primitive life could be defined as an open chemical system capable of self-reproduction. Thus,

primitive life may evolve as a chemical system, and thanks to the random errors during the transfer of chemical information, the complexity and the efficiency of the systems was enhanced. In this way, life was adapted to change within the constraints of the environment. From an astrobiology point of view, life is defined from all the characteristics possessed by terrestrial life. The possibility that extraterrestrial life, if it exists, could be different, should be considered. For this reason, in the astrobiological research we referred to "*life as we know it*".

1.2.1 Life as we know it

As explained above, the search for life in the Universe is referred to "life as we know it". This assumption has three fundamental requirements: a complement of basic chemical elements, an available source of metabolic energy and the presence of liquid water (McCollom, 2006) (for further details see the paragraph below). Terrestrial biomass is mainly composed of organic molecules, formed by C, H, O, N, P and S backbone, with the addition of K-, Ca- and Mg-salts and a few traces of metal (Fe and Co), which acts as co-factors for enzymes. While the discovery of carbon-based molecules and energy sources was reported throughout the Solar System, the presence of liquid water is limited on thin transient films or trapped in ice. In our Solar System, Europa and Mars showed the possibility to host or hosted liquid water in the past (Kargel, 2004; Chyba and Phillips, 2005): the search for life is mainly focused on these extraterrestrial planetary bodies.

1.3 Habitability

The definition of life is strictly correlated to habitability: life cannot originate without habitability.
To proceed through the definition of habitability, we have to consider that terrestrial life is the only example we have and the assessment of habitability is confined by the terrestrial biological knowledge (Cockell et al., 2019).

To define habitability, astrobiologists focused on the basic requirements for life to be metabolically active or to reproduce in planetary environments. The word habitability comes from the verb "*habitare*", which means "*to live or dwell*". Actually, the most common definition of habitability is based on the term "*habitat*", which means "*it lives/dwells*". As reported in Cockell et al. (2016), a habitat is ''an environment capable of supporting the activity of at least one known organism,'' where ''activity'' (and thus ''living'') is metabolic activity allowing for survival, maintenance, growth, and reproduction.

One of the main debate points about habitability concerns the question if an environment may be considered habitable across a continuum or is a binary (yes or no) decision (Cockell et al., 2019).

The US National Academies of Sciences, Engineering and Medicine proposed habitability as not a binary property, but a continuum degree of habitability, due to the complexity of interactions among physical, chemical, and biological parameters and processes. In conclusion, they define habitability as: "an environment's ability, or inability, to support life, which can be misinterpreted as a simple yes/no proposition". Cockell et al. (2019), changed this point of view by proposing habitability as a continuous sequence of binary answers to the question if the studied environment or a planet can sustain life. According to this definition, habitability is binary at a fundamental level and, once an environment has been established as habitable, a series of non-binary questions may be asked about life. Apparently, the habitability may be defined as a binary property, but time and species richness should be considered. Indeed, we should consider an environment as an ecosystem, where the habitability of a given organism is dependent on the other organisms present. If we ask all the organisms in an ecosystem if the environment is habitable, we should integrate all these answers, producing a continuum. Thus, we can start to define habitability as a continuum derived from a binary state (yes or not for each organism). In the same way, we consider time in the habitability answers. An environment may change over time, becoming inhabitable for some organisms. Also in this case, a series of binary answers may be integrated in a continuum.

The term habitability could be divided into two categories: instantaneous and continuous habitability. Instantaneous habitability refers to a range of conditions in a given place in an instant in time that will support habitability. On the contrary, continuous habitability is defined as a set of parameters on (or in) a planetary body, which support habitable conditions, at least in a part of the planet, over geological time scale (Cockell et al., 2016). The difference between the terms is correlated to the scale of applicability: the instantaneous once could be applied to localized scale, in which conditions may support the activity of organisms; in contrast, continuous habitability may be referred to the ability of a planetary bodies to support habitable conditions in all the surface or in its interior, over geological time scales.

1.3.1 Instantaneous habitability

To allow the instantaneous habitability, a range of parameters for all known organisms to be active, may be identified:

- A solvent,
- physico-chemical conditions,
- available energy,
- major elements required by all known life (CHNOPS),
- other elements required by a specific organism (Fig. 1).

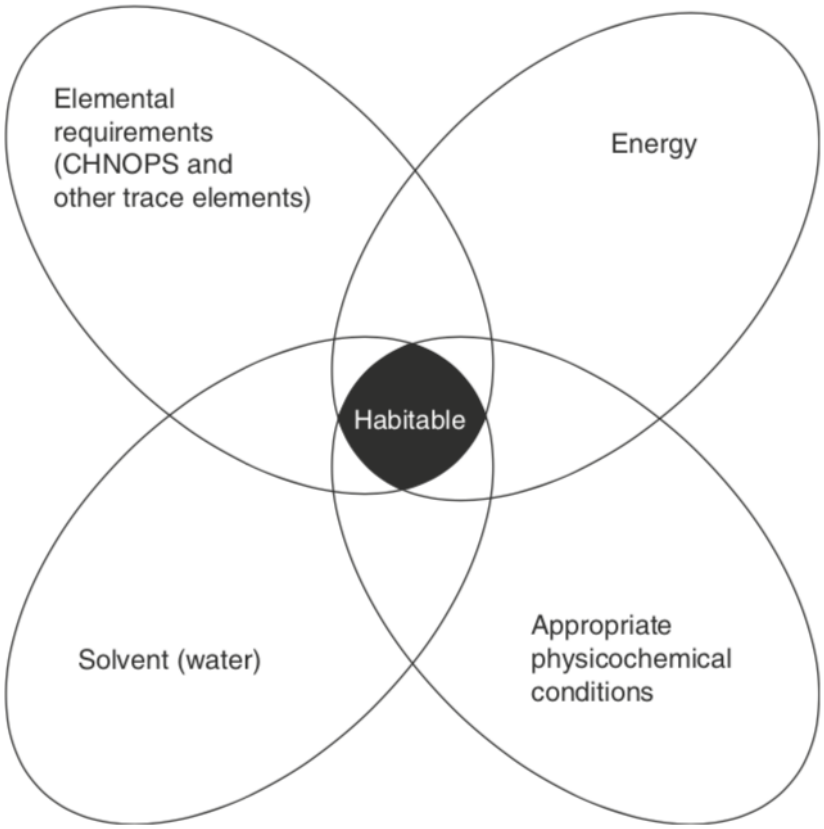

Figure 1. Instantaneous habitability. A diagram illustration of the physico-chemical requirements that allow organisms to be active in a given environment (from Cockell et al., 2016).

Liquid water is the solvent essential for biochemical reactions within terrestrial organisms. Actually, water is the only compound known to be used by life, even if other solvents have been proposed: liquid ammonia, organic solvents (such as methane and ethane), formamide, and even sulfuric acid (Benner et al., 2004; Schulze-Makuch and Irwin, 2006). However, no evidence of organisms using alternative solvents have been reported. The presence of liquid water in a planetary body's surface is determined by environmental conditions of temperature, pressure, and chemical impurities, which allow water to descend into the defined liquid phase space of the equation of state. Despite the importance of water for life as we know it, its presence may not define an environment as suitable for life.

In addition, to maintain liquid water, the correct physicochemical conditions are required. Liquid water can exist at below -15 °C and above the current upper limit for microbial growth: 122 °C (Kashefi and Lovley, 2003; Takai et al., 2008). The processes of growth, reproduction and maintenance require energy. Energy may be derived from inorganic electron donors (chemolithotrophy) or through organic compounds as the electron donor (chemoheterotrophy). On the contrary, if the organisms use sunlight as an energy source, it is designated phototrophy. Of all the elements in the Periodic Table six are required for life: C, H, N, O, P and S (Cockell et al., 2012). Carbon is the major constituent of the macromolecules backbone and hydrogen is covalently linked to carbon and other atoms in macromolecules. Similarly, nitrogen is found in long-chained molecules, such as proteins and base pairs of DNA, together with phosphorus. The latter element may be also used in energy-molecules (ATP). Oxygen is used in alcohols, sugars, and a variety of molecules and sulfur in protein bridges or in iron-sulfur clusters in molecules involved in energy acquisition. Additionally, other elements (e.g. magnesium and tungsten), are used in different organisms to exploit different functions. Wackett et al. (2004), explains in a simplistic way as the evolution selected six elements to build the chassis of life and then, the other elements have been associated thanks to their chemical properties of use in particular biochemical functions or environments. The availability of these elements on the planetary body surfaces is determined by the environmental conditions, for example in an oxidative environment, sulfate and ferric iron are predominant.

Even if a planetary body surface hosts all the requirements for life, life does not necessarily have to live there. Indeed, an important question to ask is “Could life have originated and evolved there?”. Currently, Earth is the only example of habitable planet and for this, it is considered as unique if compared to other planets of our Solar System. Indeed, our planet hosts liquid water, an atmosphere with a greenhouse effect, which allows it to maintain its surface above freezing and the right mass to maintain tectonics (Kasting et al., 1993). Earth orbits around the Sun, in a so-called “Habitable Zone (HZ)” region, a zone where planets can maintain liquid water on the surface. The term is an old

concept proposed by Huang (1960), which defined the HZ as a spherical shell around a star where a planet with an atmosphere may support liquid water at a given time. The distance and the width of the shell depends on the star luminosity that modifies during the star's lifetime (Hart, 1979). The inner part of the HZ is defined as the distance where the greenhouse effect vaporizes the water reservoirs, which induce the photodissociation of water vapor and the loss of hydrogen to space (Kulikov et al., 2007; Tian et al., 2009). On the contrary, the outer edge is the distance from the star where the greenhouse effect does not allow keeping the planet surface above the freezing point or the distance from the star where CO_2 starts condensing (Kasting et al., 1993). The HZ may influence the continuous habitability.

1.3.2 Continuous habitability

The presence of liquid water allows distinguishing two types of planetary bodies. In planets with liquid water on the surface and in the interior, the maintenance of water in liquid state is due to the combination of internal heating and stellar energy (Cockell et al., 2016). Earth is an example of a "surface liquid water worlds". In the second type, the stellar energy flux is not sufficient to allow the presence of liquid water on the surface, but it may exist on the interior. These planetary bodies are defined as "interior liquid water worlds" (McMahon et al., 2013). To maintain surface liquid water, essential for sustaining an energy source for an organism's activity, the appropriate temperature conditions are necessary. It depends on the greenhouse force. If the stellar energy and the greenhouse gases in the atmosphere are excessive, the temperature values will be high and the water will evaporate, generating a moist greenhouse effect (Kasting, 1988). The moist greenhouse may result in a runaway greenhouse effect (Nakajima et al., 1992); and as observed on Venus, this effect will cause the complete loss of water from the planet, making it uninhabitable. On the contrary, planets located far from a star, experience the effects of the carbon dioxide: this greenhouse gas may condense onto the surface, contributing to low temperatures and in a frozen surface (Noack et al., 2014). In regards to the main elements for life, there are different sources of CHNOPS available to life over geological

time scale, on or within a planetary body. Some events, such as geological turnover (plate tectonics) or atmospheric chemistry, may increase the abundance of compounds that contain these atoms, enhancing also the instantaneous habitability. The availability of the main elements is listed below:

- Carbon is always available as CO_2 in the atmosphere during all the lifetime of a planet. It is present on Venus (96.5%), Earth (*400 ppmv) and Mars (96%), demonstrating the availability of the most types of terrestrial-type rocky planets.
- Hydrogen depends on its source. The serpentinization reaction cannot sustain this element over geological times, unless the geological activity sustains liquid water through the crust (Okland et al., 2012). On the contrary, it may be obtained from molecules endogenously produced by Urey-Miller-type reactions (Bada, 2013); or from carbon compounds within meteoritic material (Sephton, 2002).
- Nitrogen is present in the atmospheres of Venus (3.5%), Earth (78.1%), and Mars (1.9%). An environment may be considered habitable if it contains N_2 at a partial pressure suitable for biological nitrogen fixation (Mancinelli and Banin, 2003). If the biological source of nitrogen is absent, nitrogen compounds (e.g. ammonia, nitrite, nitrate), should be available. Some abiotic processes, such as impact events, hydrothermal activity and lightning discharge may favor the production (Brandes et al., 1998; Segura and Navarro-Gonzalez, 2005; Summers and Khare, 2007).
- Oxygen is not always accessible to life (e.g. atoms bound to silicon in silicates). Available sources of oxygen may be found in compounds as sulfates and iron oxides, largely found on Earth and Mars (Bibring et al., 2007). In addition, oxygen atoms may exist in organic molecules, such as alcohols and carboxylic acid groups.
- Phosphate is accessible from igneous (e.g. apatite and merrillite) and other rocks, as a direct consequence of the rock cycle (Usui et al., 2008). Furthermore, these atoms may be delivered on the planetary body surfaces through meteoritic material (Pasek et al., 2007).

- Sulfur may be available in the form of sulfides, sulfates, and compounds of intermediate oxidation state such as thiosulfate (Morris et al., 2006).

1.4 Mars

The Universe encloses an unlimited number of planetary systems and stars: many planets are comparable to Earth-size and are located in the HZ around their star (see the paragraph #1.3.1, "*Instantaneous habitability*"). Our Solar System hosts evidence of habitable environments (Borucki et al., 2013), such as the Mars' planet; it constitutes the main planetary target of astrobiological research. The current conditions on Mars suggest similarities to early Earth conditions, since it hosts carbon, potential energy sources for life and water in different forms (Malin and Edgett, 2000, 2003; Rasmussen et al., 2009).

1.4.1 Habitability on the Martian surface: past and present scenario

The habitability of Mars has been investigated for a long time. Starting from the definition of habitability (see the paragraph #1.3 "*Habitability*"), the Martian surface could be considered as not habitable. Indeed, for example, the massive volcanisms and the plate tectonics once active on the planet are now almost geologically stopped (Acuna et al., 1999). As a consequence, the end of plate tectonics could shut down the negative climate feedback of the CO_2 cycle (Kasting and Catling, 2003) and probably greatly reduce the surface availability of biologically useful sources (Weiss et al., 2000). Some of the geological young features detected on the Mars' surface, may be associated with changes in solar insolation over time. Despite that, the discovery of sulfate (jarosite) and perchlorate deposits (at the Opportunity rover and Phoenix lander landing sites), may have led the scientists to assert the presence of liquid water on the Martian surface during the past (Squyres et al., 2004). In addition, the Spirit rover has been found sulfur-rich compounds and layered deposits, also indicative of liquid water (Squyres et al., 2004). Ground-based spectroscopy investigation revealed the presence of methane in Martian atmosphere via its 3.3 μm band (Mumma et al., 2003) at a 10 ± 3 ppb mixing

ratio (Krasnopolsky et al., 2004). A 10 ± 5 ppb mixing ratio was also detected through the Mars Express spacecraft (Formisano et al., 2004).

Considering these discoveries, Mars could be considered partially habitable. The conditions that may make Mars habitable or limit the origin of life, are listed in the following subparagraphs.

1.4.2 Ice and water

Since liquid water is a critical aspect for activity of life, the search for habitability on Mars is closely correlated to the search of water, so much so that NASA has adopted "Follow the Water" as the main aim of the exploration of the planet.

Although liquid water is unstable at the surface of Mars, due to the extremely cold conditions and low atmospheric pressure, evidence for water and ice date from many years ago. In the seventeenth century, bright polar caps were discovered, even if the exact composition (H_2O or CO_2 ice) have been fully understood in the twenty-first century (Kieffer et al., 1976; Plaut et al., 2007). The spacecraft Mariner 9, detected dendritic valley networks, braided channels attributed to fluvial processes (McCauley et al., 1972). Data obtained from Curiosity rover, suggested the presence of an aged freshwater lake in Gale Crater (Grotzinger et al., 2015). Hydrothermal environments on Mars, associated with craters from impact and volcanism, may provide a source of water (Westall et al., 2013). Studies and observational data have shown sedimentary processes on Mars, which are most likely the product of earlier aqueous flows (Malin and Edgett, 2003; Ehlmann and Buz, 2015). In addition, images taken by the Mars Global Surveyor (MGS) Mars Orbiter Camera (MOC) and Mars Odyssey Thermal Emission Imaging System (THEMIS), revealed structures similar to large drainage basins. The Observatoire pour la Minéralogie, l'Eau, les Glaces et l'Activité (OMEGA) on Mars Express, identified elevated concentrations of layered hydrated sulfates but also phyllosilicates (Poulet et al., 2005). On Earth, phyllosilicates form in weathering and sedimentary environments over timescales, suggesting persistent aqueous fluids on early Mars (Price et al., 2005). Radioisotope

measurements by Curiosity rover suggest sulfate formation from subsurface fluids some ~2-3 Gyr ago (Martin et al., 2017). Smaller-scale valleys and fluvio-lacustrine deposits dated to the Amazonian Period (past ~3 Gyr) have been identified in several regions of Mars (Fassett et al., 2010; Grant and Wilson 2011, 2019).

Furthermore, the study of the ALH 84001 Martian meteorite revealed the presence of Mg-Fe-Ca carbonates along fractures; these minerals are the results of precipitation from aqueous fluids and may represent the sites of paleolakes on Mars, supporting the idea of a warmer and wetter environment in the past (Ehlmann et al., 2008). Despite the multiple discoveries that can demonstrate the past presence of water, the presence of water on Mars was debated. Recent discoveries demonstrated that water may persist on Mars only in certain circumstances and for a short period of time, because of the conditions of the surface (e.g. low temperature and atmospheric pressure) (Orosei et al., 2020). Precisely, water on Mars exists as polar ice caps, subsurface ice deposits, frosts, water vapor, hydrated salts, groundwater (Michalski et al., 2013) and a recently discovered subglacial lake (Orosei et al., 2018).

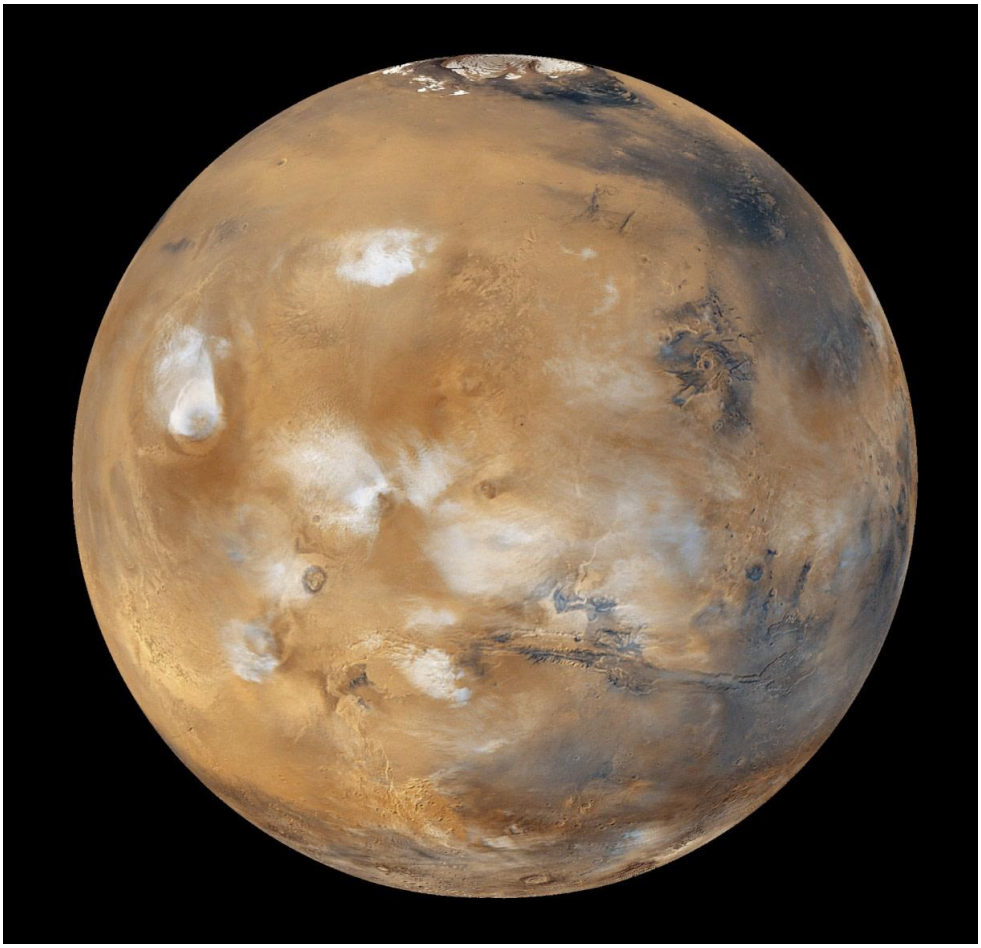

Figure 2. Martian northern ice cap. (photo credit: NASA/JPL)

Water in ice form is mainly present at the polar regions (Fig. 2). Furthermore, in 2016, NASA identified a large amount of underground water on Mars, but the first identification of a subglacial stable water body, located 1.5 km beneath the South polar ice cap reaching 20-km across, was obtained in 2018 by the orbital radar sounding (Orosei et al., 2018). It is currently known that, on Martian surface, water can be only found below the cryosphere, suggesting that in early Mars water flow percolates in the ground, creating an aquifer similarly to Earth (Orosei et al., 2020).

1.4.3 Organic compounds

Atoms contain in organic molecules are one on the prerequisite for life as we know it (see the paragraph #1.3.1, "*Instantaneous habitability*"). Although the first Viking mission in 1976 did not find any organic compounds, if life existed or existed on Mars, organics would be present (Yoshimura, 2019). The main problem during the Viking mission might have been the presence of

perchlorates in Martian soil (for further information about perchlorates, see the subparagraph below). Indeed, the only found chlorinate compounds by Viking mission, could be the reaction product of indigenous organic compounds and perchlorates during pyrolysis of the soil samples at 500 °C (Steininger et al., 2012; Lasne et al., 2016). The first discovery of organic molecules occurred through the Sample Analysis at Mars (SAM) instrument onboard the Curiosity rover, which found chlorobenzene (150–300 ppb) and C_2 to C_4 dichloroalkanes (up to 70 ppb) (Freissinet et al., 2015). Organic sulfur compounds, such as thiophene, methylthiopenes, methanethiol, dimethylsulfide, benzothiopene, carbonyl sulfide, CS_2, H_2S, and SO_2, in addition to O_2, CO, and CO_2, have been detected in lacustrine mudstones of the 3.5-billion-year-old Murray formation located at Pahrump Hills, at the Gale Crater (Eigenbrode et al., 2018). The Gas Evolved Analysis (EGA) onboard the Curiosity rover, detected aliphatic and aromatic compounds such as benzene, toluene, alkylbenzenes, and the possible presence of chlorobenzene and naphthalene. The studies of a similar lacustrine environment on Earth showed that the detection of sulfides on Mars could indicate microbial activity (McMahon et al., 2020). Currently, even if certain organic compounds have been detected on Martian surface, the degradation by ionizing and ultraviolet radiation, and the highly oxidizing conditions, are still under debate. In addition, it is still unknown if the detection of molecules may be attributed to biotic or abiotic factors and if they may have functions in terms of habitability. For these reasons, preliminary tests about the stability of biomolecules are of utmost importance (see paragraph *#1.5.1 Biosignatures*).

1.4.4 Salts

During the NASA Viking lander mission (1970s), the scarcity of organics detected, was attributed to the presence of oxidizers on Mars surface (Klein, 1978). Among oxidizers, the distribution of chlorine was confirmed by several missions (e.g. Mars Pathfinder, Gellert et al., 2004; Spirit and Opportunity, Rieder et al., 2004 and Odyssey orbiter, Keller et al., 2006). Through the launch of NASA Phoenix Mars and Mars Science Laboratory (MSL) landers, the chemical nature of these oxidizer compounds

was attributed to perchlorate salts (Li et al., 2015), mainly present in regolith as mixture of $Ca(ClO_4)_2$ and $Mg(ClO_4)_2$ with a concentration of 0.4-0.6 wt%; and a small amount of Na^+ and K^+ (Hecht et al., 2009). Theoretical studies on perchlorate conditions found at the Phoenix landing site, demonstrated that these salts maintain a liquid state during the summer (Chevrier et al., 2009). Although the presence of perchlorates could represent a challenge task in Martian habitability, their characteristic to lower the freezing temperature of water (Möhlmann and Thomsen, 2011) and to form stable hydrated compounds and liquid solutions by absorbing atmospheric water vapor through deliquescence (Zorzano et al., 2009; Nuding et al., 2014), may exploit by hypothetical life-forms on Mars. Perchlorate compounds are highly oxidizing species, soluble in water and toxic to humans even at low concentrations. However, a large number of microorganisms are able to survive in presence of perchlorates or to utilize these species as electron acceptors (Coates and Achenbach, 2004). For these reasons, the widespread detection of perchlorates in Martian soil does not seem to create a barrier for surface habitability. However, the combination with other factors (e.g. radiation, Martian soil compounds) should be considered.

1.4.5 Radiation

The habitability of Mars's surface depends on the protection from radiation (Dartnell, 2011; Rummel et al., 2014). The lack of a global dipole magnetic field and a sufficient atmosphere (<1%) did not allow the deflection of energetically charged particles. Indeed, the Martian surface is reached by different energetic particles, among which Galactic Cosmic Rays (GCRs) and Solar Energetic Particles (SEP).

The first one derived from cosmic events (e.g. supernova explosion; Chancellor et al., 2018) and are mainly composed of energetic particles, that may be distinguished in light particles (85% of hydrogen-ions and 14% of helium ions) and in High charged Z and Energy particles (HZE). The HZE particles constitute only the 1% of GCRs, but are able to deeply penetrate the organic matter, causing the ionization of atoms inside molecules (Ferrari and Szuszkiewicz, 2009; Horneck et al., 2010,

2016). The interaction of radiation and organic matter occurs through an ionization process that may induce direct effects on molecules by the absorption of energy or indirect effects through the radical formation (Moeller et al., 2010). The ionization in a medium is strictly correlate to the Linear Energy Transfer (LET), the average energy transferred by a single particle and deposited per unit length (expressed in keV/μm, which is referred to a particle's charge and velocity—energy per nucleon—and the elemental composition of the traversing medium) (Hamada et al., 2010). On the contrary, SEP are composed of non-ionizing UV radiation, X-rays and solar flares (Sliney, 2007). These particles penetrate the thin Martian atmosphere and react with regolith: as result, additional particles are created, resulting in an oxidizing environment on the planet surface.

The HZE particles have high LET values (> 10 keV μm^{-1}) and are considered the main component of radiation-induced cellular damages and health risks for the astronauts (Cucinotta et al., 2001; Nikjoo et al., 2001; Cucinotta and Durante, 2006; Friedland et al., 2011; Arena et al., 2014). The LET values of electromagnetic ionizing radiations (X-rays and γ-rays) are relatively lower than high LET radiation (α-particles, neutrons, protons and heavy ions) but have a high penetration power into matter (Reisz et al., 2014). While low-LET radiation can produce only sparse ionization (which results in lesions that are distant from each other) (Hagiwara et al., 2019), the high-LET radiation causes dense ionization. Their energy along their tracks may cause a mix of dense ionization and secondary ionizations (γ-rays) of varied energies that spread in various directions and distances from the particle trajectory (Cucinotta et al., 2000; Sridharan et al., 2015). Indeed, the consequences of particles with a large atomic number are dependent not only on the LET value, but also on the spatial distribution of ionizing energy along the particle's trajectory. The energy depositing released by high LET radiation can be subdivided into a densely ionizing core and a penumbra where energy transfer takes place by far reaching secondary electrons (Baltschukat et al., 1986), excluding only localized effects. The effects of space radiation are mainly DNA damages (single- or double-strand breaks), which activates cellular responses leading to cell cycle arrest and appropriate DNA repair mechanisms

(base-excision repair, homologous recombination or non-homologous end-joining repair) depending on the damages (Zhou and Elledge, 2000).

The biological effects of low-LET are lower than those induced by the same dose of high-LET radiation. The significant cellular effects produced by X- and γ-rays is due to the generation of reactive oxygen species (ROS) (H_2O_2, $O_2•^-$, and •OH) and other reductants (H• and e_{aq}-) (Reisz et al., 2014; Desiderio et al., 2019). These highly reactive agents cause DNA breaks (single strand breaks, SSBs), protein fragmentation, protein structure deterioration and cell membrane function and permeability changes, while dense radiation (high-LET) may induce clustered DNA damages, such as double strand breaks (DSBs). The lipid layer within cell membranes is another biomolecule targeted by radiation-generated ROS. Radiation causes lipid peroxidation, particularly of polyunsaturated fatty acids (PUFAs), which increases membrane permeability, disrupts ion gradients and other transmembrane processes, and changes membrane-associated protein activity.

On Mars, the calculated radiation dose reaching the Martian surface by the Radiation Assessment Detector (RAD) carried by the MSL rover, was estimated to be around to be 0.210 ± 0.040 mGy/day (average total dose), while the SEP dose was 50 μGy (Hassler et al., 2014). The UV radiation at < 200 nm may be attenuated by the high concentration of CO_2 in the atmosphere, but UV wavelengths > 200 nm still reach the surface (Horneck, 2008). However, the dust storms and the first few centimeters of the Martian surface may provide an effective screen (Rontò et al., 2003). On the contrary, it has been demonstrated that GCRs decrease 3 meters beneath the surface. These data were used to determine the potential for microbial survival and to assess how the radiation may influence the preservation of organic matter (Checinska Sielaff and Smith, 2019).

Based on this result, the ongoing robotic ExoMars mission will drill the surface to investigate the subsurface up to 2 meters (Vago et al., 2017).

1.4.6 Martian atmosphere

The Martian atmosphere is completely different from Earth's atmosphere: it is almost anoxic. Firstly, the atmospheric measurements on Mars revealed a composition of 95.3% CO_2, 2.7% N_2, 1.6% Ar, and 0.1% O_2 (Owen et al., 1977). The most recent investigation of the SAM onboards the Curiosity rover, shows an atmosphere composed of 96% CO_2, 1.93% Ar, 1.89% N_2, 0.145% O_2, and <0.1% CO (Mahaffy et al., 2013). In addition, the Martian atmosphere hosts a small amount of water vapor at a pressure of 10^{-3} mbar, depending on the seasonal removal of water from ice caps at polar regions (Jakosky and Phillips, 2001). Another characteristic that distinguishes it from the terrestrial atmosphere is the low pressure, estimated to be around ~6 mbar (Jones et al., 2011).

1.5 Martian subsurface

It is reasonable to think that long time ago, hospitable conditions for life existed on the Martian surface. Many studies reported the possibility that life emerged on Mars (McKay et al., 1992; Dartnell, 2007) and disappeared during the deterioration of climatic conditions, in the Late Noachian/Early Hesperian period (Friedmann and Koriem, 1989). The current dry surface conditions (see paragraph *#1.4.1 Habitability on the Martian surface: past and present scenario)*, instead, appear inhospitable for any hypothetical life form. However, scientists agree to consider the subsurface of Mars the most probable place where life may continue its existence, a place to survive and thrive (Michalski et al, 2013; Cockell, 2014). Actually, it is estimated that life may exist at depths up to 8 km in the subsurface (Michalski et al, 2018). The shallow surface offers protection against radiation and the atmospheric pressure, which is considered as a limiting factor when at low values, is expected to be higher (Pavlov et al., 2010). Fisk and Giovanonni (1999), reported that some subsurface conditions could sustain life, such as water, temperature between 0 to 120 °C, major elements and energy sources. In addition, as reported above (see paragraph *#1.4.2 Ice and water*), there is evidence of subsurface water and subglacial lakes (Orosei et al., 2018). The subsurface is not only considered as a harbor of extant life, but also for extinct life. Indeed, signatures of past life, related to the

morphological, organic and metabolic characteristic of an organism, may be preserved and detected beneath the surface (Westall et al., 2000; Cady et al., 2003; Summons et al., 2011; Westall and Cavalazzi, 2011). For these reasons, the future ESA-Roscosmos ExoMars mission, equipped with a drill to collect material, will search for signatures of extant or extinct life, up to 2 m-depth in the subsurface (Vago et al., 2017).

1.5.1 Biosignatures

The search for signs of extant or extinct life is one of the main scientific drivers of the exploration of Mars. The signs of life are commonly named "biosignatures", defined as "any object, substance, and/or pattern whose origin specifically requires a biological agent" (Des Marais et al., 2008). The usefulness of a biosignature is determined not only by the probability that life produced it, but also by the improbability that nonbiological processes produced it. Biosignatures may include isotopic patterns (Bernard and Papineau, 2014), molecular biomarkers or their remains (Summon et al., 2008), fossil-like structures (Schopf and Kudryavtsev, 2012) or microbial influenced structures (e.g. stromatolites, Grotzinger and Knoll, 1999; Berelson et al., 2011; Pepe-Ranney et al., 2012). The term biosignature may have a multiple shape. An "abiosignature" is a substance, object, or pattern from nonbiological origin, which is produced with probability from an abiotic source and with improbability from biological processes. The importance of abiosignatures lies in the capacity to correctly detect and delineate biosignatures. "Ambiguous biosignatures" is a term indicating a substance of uncertain origin that needs more data to be classified in one of the above-mentioned categories. Lastly, "agnostic biosignatures", are substances of biological origin, but may include also features that might not have originated on Earth (Johnson et al., 2018). The search for life beyond Earth is based on the idea that a biosignature will be identifiable within the context of an extraterrestrial environment. While, the astrobiological investigation needs to consider how

biosignatures might have originated, preserved and detected in that context (Des Marais and Jahnke, 2019).

1.5.2 Biomarkers: a way to delineate a biological origin

One of the most debated points in the search for biosignatures is the biological or non-biological origin. In this context, we can introduce the term "biomarker", referring to structures or stereochemical variations of organic compounds useful in tracing biological sources (Peters et al., 2004; Summons, 1993), including biomolecules, fossil derivatives, and complex chemicals characteristic of biotic processes (National Research Council, 2007). Biomolecules include a range of chemical components such as nucleic acids, proteins, carbohydrates, and intermediary metabolites, as essential parts of carbon-based life and potential molecular biosignatures. On Earth, these compounds are liable to degradation over geological timescale (National Research Council, 2007). On other hands, if exposed to the cold and dry Martian climate conditions, they might be better preserved, and used as a biosignature of life (Sephton, 2010). Lipids, as membrane lipids, are extremely valuable molecules for identifying living biota or its fossilized remains and considered as a universal biomarker of life (Georgiou and Deamer, 2014). Isoprenoids, which have no known abiotic source, derive from unique structural building blocks (e.g., isoprene units) specific to life (Summons et al., 2008).

The three domains of life use lipid compounds for maintaining the membrane integrity and regulating its fluidity in response to physio-chemical conditions like temperature or pH (Aerts et al., 2014).

Biological lipids and their derivatives may survive for billions of years in the geological record, such as in the 2.7 billion-year-old shales from the Pilbara Craton, Australia (Brocks et al., 1999).

It is expected that lipids are able to be preserved up to 3-4 × 10^9 years (Engel and Macko, 1993; Simoneit et al., 1998); hydrocarbons, for examples, are known to be stable on Earth over billion-year timescales: their chemical structures could be as diagnostic for biogenicity as those of amino acids or other biomolecules (Brocks and Summons, 2003; Peters et al., 2004). Another peculiarity of lipids is

their higher resistance to enzymatic degradation than proteins or nucleic acids, which is of relevant interest since these molecules are the main component of cellular membranes (Sephton, 2010).

Other biomolecules considered as good biomarkers of life, due to their potentially long geological preservation, are pigments and their derivatives (*e.g.* phytane and pristine, porphyrins, carotenoids, melanins, scytonemin) (Schwieterman et al., 2015; Suo et al., 2007; Varnali et al., 2009; Vítek et al., 2009). For example, melanin pigments are produced by many organisms of all the kingdoms of life. Their utilization of melanin as biomarkers has been largely reported (Pacelli et al., 2020, 2021b, c; Cassaro et al., 2021). The analyses of pigmented microorganisms after the exposure to simulated Martian or real space conditions, revealed a higher resistance of these species than the non-melanized counterpart (Pacelli et al., 2017, 2021c). Moreover, spectroscopic analyses on the extracted melanin pigments after the treatments, showed no structural changes in the acquired spectra.

Peptides are considered as another important class of biomarkers, present in all extant life on Earth. They are the main constituent of the 20 amino acids. These compounds are relatively easy to abiotically form (Sephton, 2002; Martins et al., 2007), questioning their use to search for life. However, most amino acids appear as levorotatory (L-) and dextrorotatory (D-) enantiomers. Under natural processes amino acids could become racemic (an equal amount of L- and D-configuration); deviations from racemic mixture hints at a biological origin, providing support in the use of these compounds as indicators for life (Meierhenrich, 2008). However, they are rapidly degraded when exposed to ionizing radiation (Dartnell, 2011; Pavlov et al., 2012), but may survive at 2 meters depth and without enzymatic degradation may persist up to 3.5 billion years (Aubrey et al., 2006; Kminek and Bada, 2006).

The most debated biomarkers of life are nucleic acids. They may be considered as clear evidence of life, since all known terrestrial life is used as genetic material. The finding of a nucleic acid trace could indicate unambiguously the presence of life and/or an organism with common ancestries to those on Earth (Mojarro et al., 2017; Pontefract et al., 2018). On Earth, DNA has an estimated half-life at -25 °C in the order of 10^7 years (Millar and Lambert, 2013). Studies have extracted ancient

DNA and living organisms (with intact DNA) from samples dated millions of years old (Vreeland et al., 2000; Panieri et al., 2010). The conditions persisting during the Amazonian period on Mars, theoretically, could have permitted the preservation of DNA beyond 10 million years. Despite that, nucleic acids show a higher instability in comparison to lipids and amino acids. Nucleic acids may be rapidly destroyed by the UV and ionizing radiation of Martian surface (Martins, 2011), but in the subsurface they might be protected from the harsh environment. On Mars, DNA could be binding to clay minerals, which may have a protective function against the enzymatic digestion (Scappini et al., 2004) and radiation (Ciaravella et al., 2004). On the contrary, the presence of minerals may represent a challenge in extraction and detection of nucleic acids.

1.5.3 Biomarkers detection through Rosalind Franklin rover

The upcoming missions on Mars are focused on the search for past and putative present life (e.g., Mars 2020 and the ESA-Roscosmos ExoMars), and the primary aim is the direct detection of biomarkers (Grotzinger, 2014; Domagal-Goldman and Wright, 2016; Rull et al., 2017). The rovers will have onboard a suite of miniaturized instruments dedicated to the detection of organic molecules. The ESA-Roscosmos ExoMars mission's rover, Rosalind Franklin, will have a lifetime of 218 sols (*7 Earth months), during which it will move in various areas relying on solar array electrical power. The rover will host a payload with all the scientific instruments, the Pasteur payload, capable of providing evidence for, or against, the existence of a range of biosignatures at each searched location (Vago et al., 2017). The Pasteur payload contains (Fig. 3):

(a) Panoramic instruments: cameras, an infrared (IR) spectrometer, a ground-penetrating radar, and a neutron detector,

(b) contact instruments: a close-up imager and an IR spectrometer in the drill head,

(c) a subsurface drill capable to acquire (3-cm-long by 1-cm-diameter) samples (solid, fragments, or powder) at depths ranging between 0 and 2 m,

(d) a sample preparation and distribution system (SPDS),

(e) an analytical laboratory.

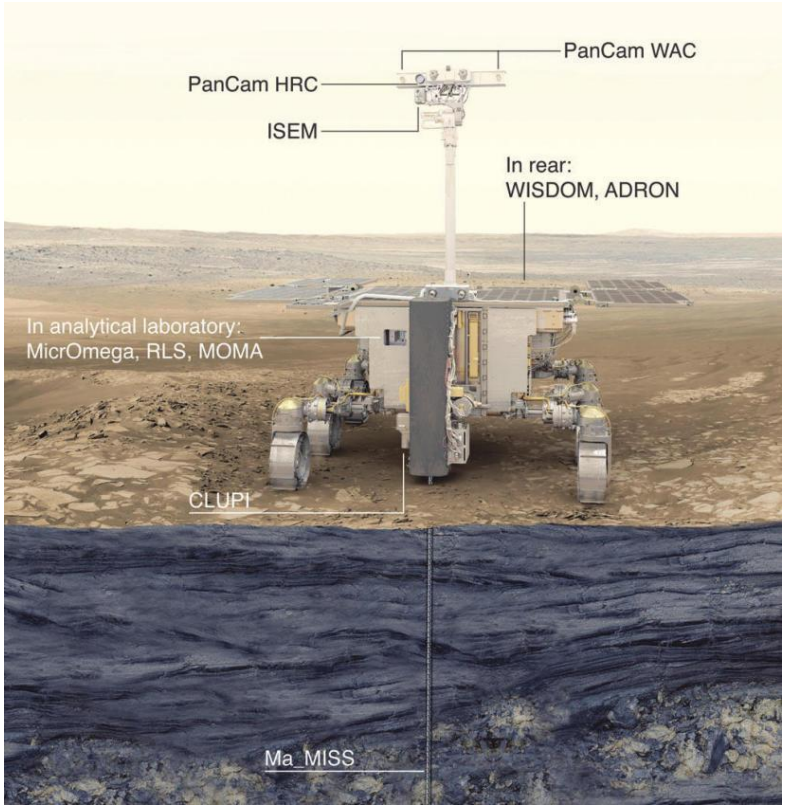

Figure 3. ExoMars Rosalind Franlink rover representation with the nine Pasteur payload instruments (from Vago et al., 2017)

The Panoramic Camera system (PamCam) is designed to perform digital terrain mapping for the ExoMars rover mission. PanCam, will enable the science team to characterize the geological environment at the sites the rover will visit—from panoramic (tens of meters) to millimeter scale. It will be used to examine outcrops, rocks, and soils in detail, and to image samples collected by the drill before they are delivered to the analytical laboratory for analysis. The pencil-beam IR spectrometer (ISEM) is coaligned with the PamCam is (Korablev et al., 2015, 2017). ISEM will record IR spectra of solar light reflected off surface targets, such as rocks and soils, to determine their bulk mineralogical composition. Due to its sensitivity, it is able to discriminate among various classes of minerals. A ground-penetrating radar (WISDOM), will allow to generate two- and three-dimensional subsurface maps to improve our understanding of the depositional environment. Among

contact instruments, the close-up imager (CLUPI) will be used to obtain high-resolution color images to study the depositional environment (Josset et al., 2017). In addition, it will recognize potential morphological biosignatures, such as biolamination, preserved on surface rocks, if present. A miniaturized IR spectrometer, Ma_MISS (Mars multispectral imager for subsurface studies), will be integrated in the drill tool to elaborate images of the borehole wall as the drill is operated (De Angelis et al., 2013; De Sanctis et al., 2017). To study the mineral grain and unravel their geological origin, structure, and composition, the Micro observatoire pour la mineralogie, l'eau, les glaces et l'activite´ (MicrOmega) (Pilorget and Bibring, 2013; Bibring et al., 2017) will image the crushed sample material. A Raman laser spectrometer (RLS) (Edwards et al., 2013; Foucher et al., 2013; Lopez-Reyes, 2015; Rull et al., 2017), will provide geological and mineralogical information on igneous, metamorphic, and sedimentary processes. In addition, it also permits the detection of a wide variety of organic functional groups. Lastly, MOMA is the largest instrument within the rover, which targets chemical biosignatures. This instrument may identify a wide range of organic molecules, even if present at low concentrations (Arevalo et al., 2015; Goetz et al., 2016; Goesmann et al., 2017). It has two operational modes: the LDMS, to study large macromolecules and inorganic minerals (Busch, 1995; Bounichou, 2010), and the GCMS, for the analysis of volatile organic molecules.

All the above-explained instruments will cooperate trying to identify biomarkers on the Martian subsurface. Since the detection could be affected by the environmental conditions of Mars or by the mineral matrix during the sample's extraction, preliminary ground-based tests using those instruments may provide support for the upcoming life-detection missions on Mars.

1.6 Not only Mars

Mars is not the only planetary body in the spotlight of the space agencies. The Moon represents a great interest, even if it was demonstrated to never have supported any form of life on its own. Many missions passed on its surface, from the Soviet Union Luna program to Apollo missions, followed by

Hiten and SELENE spacecraft to Chang'e and SMART-1. The lunar surface conditions are characterized by temperature fluctuation between -171 and 140 °C (Langseth et al., 1972), pressure values that may reach 10^{-10} Pa (Schuerger, 2004), high doses of ultraviolet (UV) irradiation (26.8 Wm^{-2} UVC/UVB) and high levels of ionizing radiation (Schuerger et al., 2019). Despite these conditions, the Moon may be considered a celestial body where to develop the ability to go further in space exploration. Indeed, the return on the Moon has a dual aspect: i) it will offer an ideal platform for studies relative to the origin, evolution and distribution of life in an environment different from Earth and Low Earth Orbit, and ii) it will serve as a training ground for testing instrumentation for future missions to Mars and other destinations. The lack of geological activity and active erosional processes, could have maintained the surface with the same characteristics of 3 and 4.5 billion years ago in some areas (Jaumann et al., 2012), allowing the preservation of records of the early geological evolution of the Earth (Crawford et al., 2010). Another important point for the investigation of life is due to the highly radiative environment, which allows us to test the effects of ionizing and cosmic radiation, solar energetic particles on biomolecules. The lunar environment may be used as a test-bed for the development of bioregenerative life support systems and for long-term deep space exploration missions (Gronstal et al., 2007; Crawford, 2010).

1.7 Research on Earth

Since the research on extraterrestrial celestial bodies is limited, expensive and requires long-term organization, the preliminary study of terrestrial environments is an essential step to prepare and support exploration missions. The Earth hosts a multitude of extreme environments whose characteristics resemble celestial bodies in our Solar System. In these environments, the physico-chemical properties partly match extraterrestrial environments, and could clarify limits and adaptation mechanisms of life, the mineralogical or geochemical context, and support and interpret data sent back from the planetary space missions.

1.7.1 Planetary Field analogues (PFAs)

To achieve the above-mentioned astrobiology goals (see the paragraph #1.1, "*Astrobiology and the search for life beyond Earth*"), and to support research on other planets, we necessarily start from the only inhabited place we know, the Earth. On Earth there are a multitude of places, that for some past or present geological, environmental, or biological conditions are analogues to some extraterrestrial environments; they are known as "Planetary Field Analogues (PFAs)". Researches on these areas support planetary missions and are essential in the robotic and human exploration of our Solar System and in assessing the habitability of other worlds. Such analogue sites offer critical test-bed for astrobiological studies in characterizing the physical and chemical boundaries within which life may exist on Earth and in assessing the habitability of other planets, understanding the biological mechanisms for survival in extreme environments and investigating the potential preservation and detectability of biosignatures. Analogues are generally considered an efficient tool to plan and guide the future human exploration of the Solar System: they can be used for *in situ* testing of technologies and methodologies (e.g., rovers and their payloads), for verifying laboratory methods and protocols for life-detection, for training astronauts, and for improving data interpretation. The perfect analogue that exactly matches all the characteristics of an extraterrestrial place or samples does not exist (Preston and Dartnell, 2014). Therefore, every terrestrial analogue has to be chosen depending on its characteristic and relevance, its scientific use, availability and limitations (Foucher et al., 2021). Generally, these environments are known as "extreme". Indeed, the discovery of places on Earth that were once thought to be hostile for supporting life from an anthropocentric point of view has boosted the search for life beyond Earth. The study of terrestrial extreme environments and the comprehension of the biology of the inhabiting organisms (extremophiles) along with their niches of habitability and adaptation, would aid hypotheses regarding the search for life beyond Earth, as also the origin and evolution of terrestrial life. The discoveries of extremophiles have expanded the boundaries of life on Earth, and our concept of habitability. We broaden our knowledge of what might be considered a habitable environment on other worlds by reference to extreme terrestrial environments and survival

strategies employed by the microbial life referred to as extremophiles. Several organisms able to tolerate extreme conditions have been discovered on Earth, expanding the limits within which life is possible on Earth, and redefining the habitability of a target celestial body. These analogues also inform researchers on the potential for the long-term preservation of signs of past life, and thus guide the selection of which potential biosignatures to target and the most appropriate analytical methods for space detection missions.

1.7.2 Mars analogue sites on Earth: the Antarctica continent

Six of the eight planets are permanently cold. Mars is very cold when compared to our planet; thus, the coldest habitat on Earth serves as a natural laboratory to expand knowledge about habitability and the limits of life and support life-detection missions. Furthermore, Earth's biodiversity is the only lesson of life, and extreme terrestrial environments are useful to understand the environmental limits for life and evolved strategies to cope with it (see the paragraph #1.6.1, "*Planetary Filed Analogues (PFA)*").

In this context, the Antarctic continent represents one of the best analogue sites on Earth for the above-mentioned celestial body. The physico-chemical conditions and geomorphic features make the entire continent a good terrestrial PFA, where the habitability limits encountered can be assessed in situ (Heldmann et al., 2013). In addition, Antarctica could provide an important analogue and test-bed to validate robotic space mission technology and instruments (Léveillé, 2009). The extension of the entire continent allows the identification of various extraterrestrial environments and different analogue categories (Preston and Dartnell, 2014). The majority of Antarctic analogue sites are devoted to Mars. Antarctica, due to its cold and dry conditions, is one of the most remote and inhospitable places on Earth. The large surface of Antarctica (about 13.6-14 million km^2), may be divided into two major geographical units: West and East Antarctica, which are separated from each other by one of the longest (about 3500 km) mountain ranges on the Planet, the Transantarctic Mountains (Fig. 4). West Antarctica, including the Antarctic Peninsula, is the "lower" part of the

continent (on average 850 m high) and lies between 150° E and 60° W. East Antarctica, on the other hand, comprises about two-thirds of the total area of the continent (with an average altitude of 2300 m) and lies between 30° W and 150° E (Bargagli, 2005; Turner et al., 2009).

The continent is characterized by extreme conditions, such as low temperatures, fluctuating ultraviolet (UV) radiation, strong desiccating winds, frequent freeze-thaw and wet-dry cycles, low humidity, and nutrient paucity (Bargagli, 2005; Wynn-Williams, 1990; Robinson et al., 2003). Low temperatures are predominantly caused by the permanent ice cover creating an albedo effect (*i.e.* reflecting solar radiation), the average altitude of over 2 km, and long periods of (nearly) complete darkness (*i.e.* the austral winter) combined with the aphelion position (Bargagli, 2005).

The entire continent is characterized by different climate regions: i) the sub-Antarctic region is characterized by an oceanic climate with a mean annual temperature above 0 °C and precipitation over 1000 mm; ii) the maritime region is predominantly cold, with mean temperatures above 0 °C in the warmer period, but rarely below -15 °C in winter, precipitation could range from 250 to over 1000 mm; and iii) the coastal climate, with a cold climate characterized by temperature below 0 °C during the summer and ranging from -15° to -25°C during the winter; iv) the ice plateau is dominated by mean temperatures near -15 °C and up to -50 °C during the winter (Øvstedal and Lewis-Smith, 2001). As a consequence of these low temperatures combined with low humidity and strong winds (with a maximum speed of about 320 km/h (Onofri et al., 2007)), most snowfall sublimates before reaching the surface (Campbell et al., 2009; Nylen et al., 2004). The remaining precipitation, mainly as snowfall, reached an average of 171 mm water equivalent (WE) per year (Bockheim, 2015; Palerme et al., 2014; Turner et al., 2009), making Antarctica the coldest desert on Earth.

98% of the continent is covered by the Antarctic Ice Sheet, a large single piece of ice having an average elevation of about 2.5 km, reaching 4 km above sea level near the center of the continent. Nevertheless, there are several ice-free areas, referred to as “Dry Valleys”.

Figure 4. Map of Antarctica. It shows the topography (as blue lines), ice-free rock areas (in brown), and ice shelves (in grey). (photo credit: Landsat Image Mosaic of Antarctica (LIMA) Project.)

1.7.3 Antarctic McMurdo Dry Valleys (MDVs) as Martian surface analogue

The MDVs (Fig. 5) are a series of glacially carved valleys located along the coastal edge of East Antarctica (76° to 78°S, 160° to 164°E) in Southern Victoria Land. Mainly due to the damming effects of the Transantarctic Mountains, which block the ice sheet flow from the Polar Plateau, the MDVs are the largest (4500 km^2) relatively ice-free region of the continent (Levy, 2013).

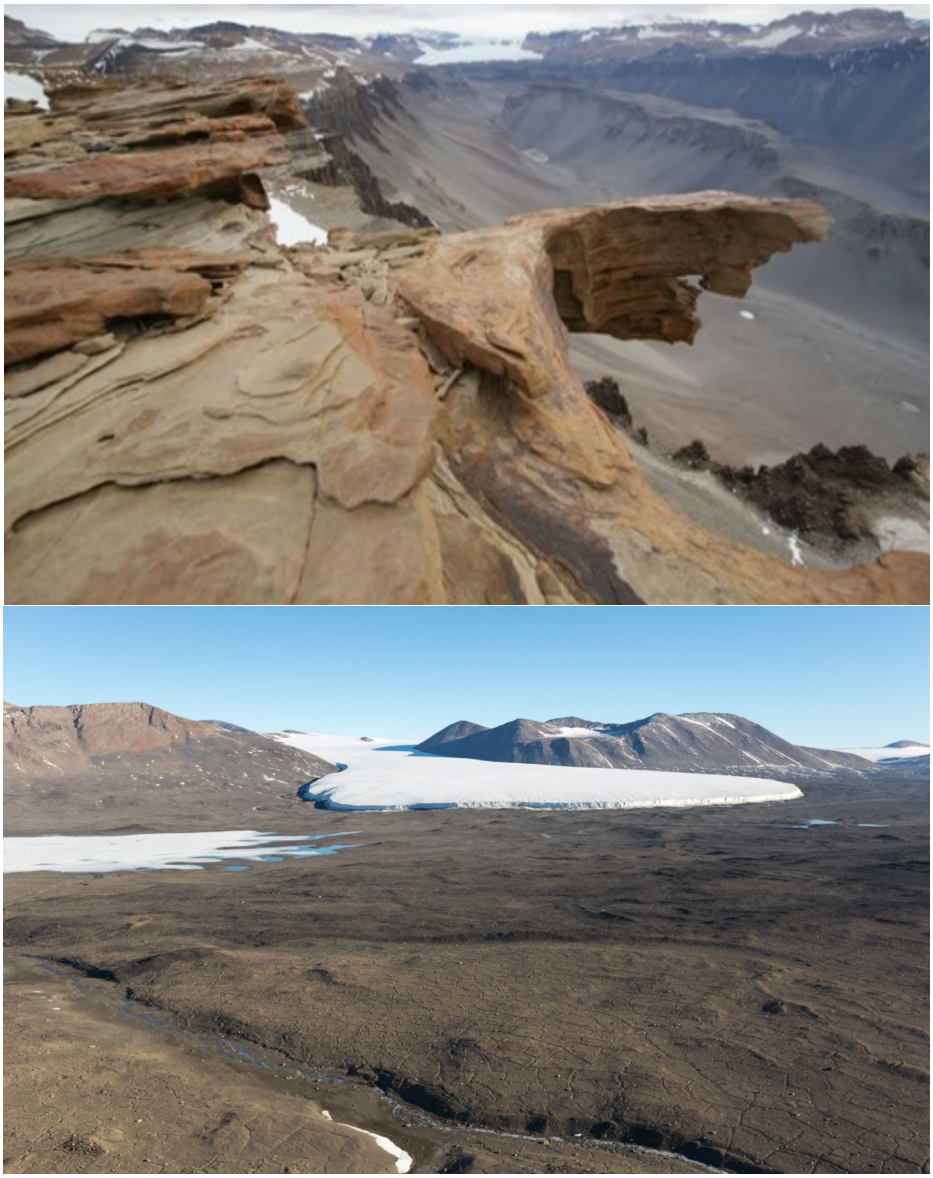

Figure 5. McMurdo Dry Valleys. (photo credit: Mike White)

The region is widely acknowledged to host the coldest hyperarid desert on Earth (Cowan and Tow, 2004), presenting low mean annual air temperature, (around -20°C, with winter minimum down to -60 °C and summer maximum up to +10°C; Doran et al., 2002), precipitation only limited to snow,

elevated levels of ultraviolet B (UV-B) solar radiation caused by stratospheric ozone depletion (Smith et al., 1992), moisture deficit (<10 cm y^{-1} water equivalent precipitation), oligotrophic conditions, and physico-chemical disturbances (e.g., high salt content, katabatic winds, steep geochemical gradients) (Wynn-Williams, 1990). In these regions, liquid water is scarce and the hydrologic cycle is dominated by ice and vapor phase processes such as sublimation (Wentworth et al., 2005). Despite the scarcity of precipitation, rocks maintain water internally for several days, thanks to the snowmelt, favoring a rapid oscillation in temperature and wetting-drying cycles. Considering these harsh surface conditions, the Dry Valleys are considered one of the best analogues of the conditions existing on the Mars' surface (Friedmann, 1982; Gibson et al., 1983) (Fig. 6).

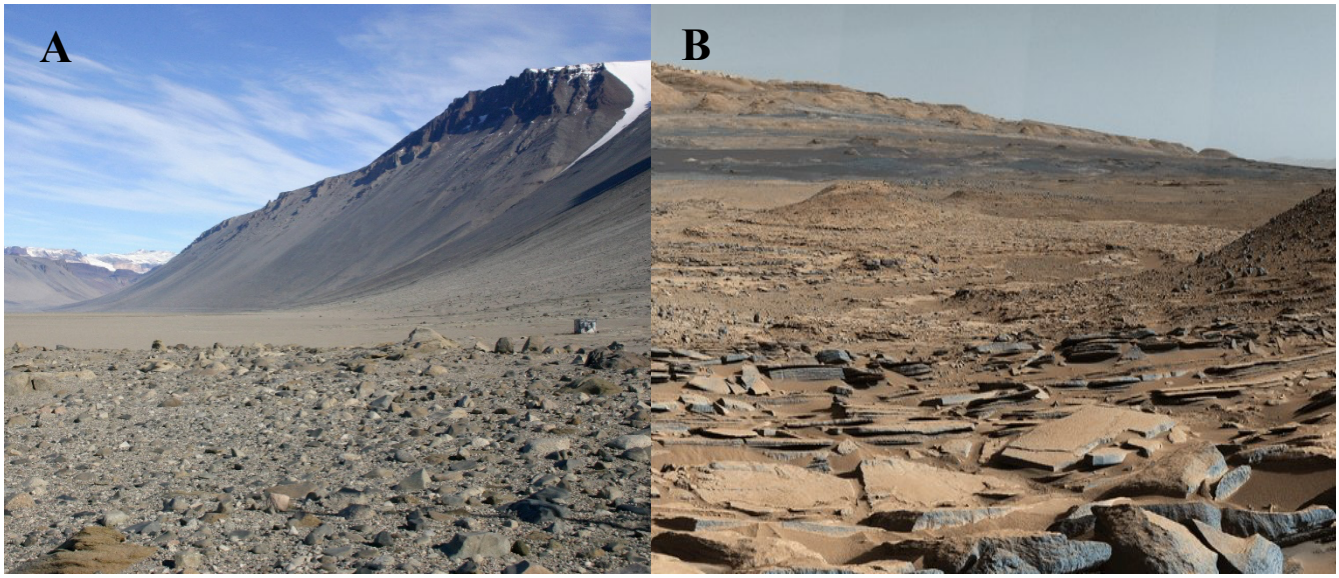

Figure 6. Comparison between landscapes: (A) the Wright Valley, one of the McMurdo Dry Valleys (photo credit: David Saul); (B) Mount Sharp on Mars (photo credit: NASA/Caltech/JPL/MSSS).

1.7.4 The cryptoendolithic communities

Under the extreme conditions of the MDVs, such as dramatic temperature fluctuations (Nienow et al., 1988; Nienow and Friedmann, 1993), low water availability and high solar radiation fluxes, the lithobiontic ecological niches are considered as environmental refuge for life (Friedmann, 1982; Pointing and Belnap, 2012). Indeed, a small group of microbes, the so-called "extremophiles" are

adapted to living in communities in specific niches of these areas, that provide protection against the most destructive effects of the environment, as a stress avoidance strategy (Walker and Pace, 2007; Pointing and Belnap, 2012).

The lithic environments represent the main substrata for microbial communities. These lithic habitats may be classified into different categories, depending on where the microorganisms are found on/or within the substrate (Golubic et al., 1981; Wierzchos et al., 2012):

i. in the *epilithic* habitat, microorganisms colonized the exposed rock surface that is directly exposed to the sun;
ii. in the *hypolithic* habitat, microorganisms are found beneath the rock in contact with the soil;
iii. in the *endolithic* habitat, microorganisms colonized the interior of the rock, generally within a few millimeters beneath the rock surface. The endolithic habitat can be further divided into three subcategories: (i) the *chasmoendolithic* habitat, that consists fissures directly connected to the rock surface; (ii) the c*ryptoendolithic* habitat, corresponding to pore spaces within the mineral matrix; and (iii) the *hypoendolithic* habitat, in which microorganisms are found within the bottom of the rock.

The microorganisms that inhabiting these habitats are known as endolithic microorganisms and from a functional perspective, they may be divided into: euendoliths, which are able to actively carve rocks from the surface to the interior, thus promoting biogenic weathering of rocks, and (ii) autoendoliths, whose metabolism induces mineral precipitation, thus leading to rock formation (Marlow et al., 2016) (Fig. 7).

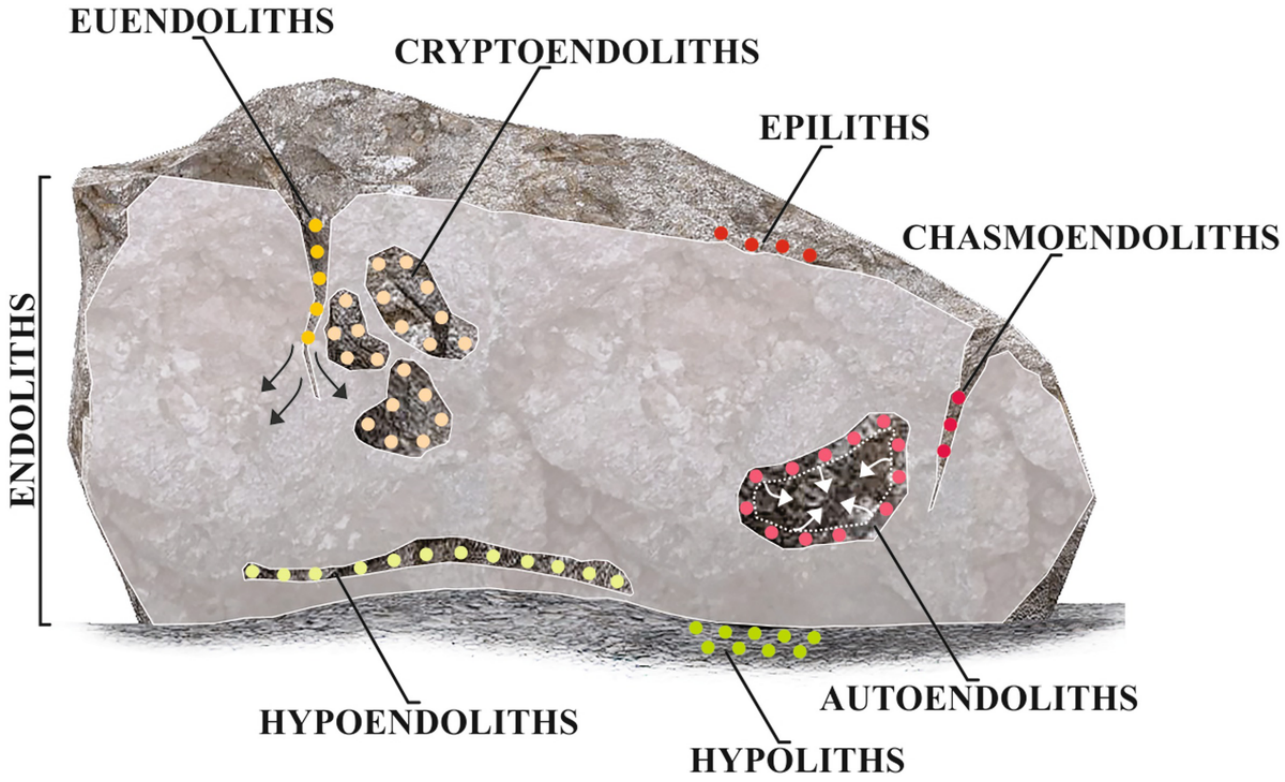

Figure 7. Schematic representation of endolithic habitats. Epilithic habitat (red dots) is located on the upper surface of the rock, while hypolithic habitat (green dots) is found beneath the rock. The rock interiors may be divided into: cryptoendolithic habitats (orange) are those within the pore space, chasmoendolithic habitats (fucsia) are found between cracks or fissures, and hypoendolithic habitats (light green) found within spaces on the underside of the rock that are not in contact with the soil. Autoendolithic habitats (pink) are those created by the microorganism's metabolism, which induce the mineral precipitation, whereas euendolithic habitats (yellow) are those created by microorganisms who actively carve rocks. (from Amarelle et al., 2019).

The type of colonization is correlated to the conditions of a particular Antarctic area: in the coastal areas, characterized to permissive climatic conditions, the epilithic habitat are the most favored while, at the higher latitudes of Antarctic inland, the endolithic habitats are predominant, with a decrease in biodiversity as the stresses environmental conditions increase (Broady, 1996; Smith, 1992, 1996; Wynn-Williams, 1996).

The prevalence of endolithic habitats is due to the fact that mean winter temperatures at rock surfaces generally lie 2 °C below the outside air temperature (Friedmann et al., 1987). In summer, rock surface temperatures may reach 20 °C above that of outside air (Nienow and Friedmann, 1993). Wide thermal fluctuations at exposed sites contribute to the practically sterile conditions at the outside, while within

the rock the nanoclimate supplies milder and more stable conditions for life (Nienow and Friedmann, 1993).

Two classes of endolithic communities have been described, based on the primary producers: lichen- and cyanobacteria-dominated communities (Nienow and Friedmann, 1993).

The most common and extensively studied is the "cryptoendolithic lichen-dominated community", discovered for the first time in the McMurdo Dry Valleys (Friedmann, 1982). These communities colonize an optimal location beneath the surface of translucent sandstone (quartz, limestone, gypsum, carbonate), that is called the colonization zone, and it is located 10 mm deep under the rock crust (Friedmann, 1982; Wierzchos et al., 2012). The first layers of the mineral matrix provide protection from UV radiation and excessive photosynthetically active radiation (PAR), thermal buffering, protection from freeze-thaw events, physical stability, and enhanced water availability (Walker and Pace, 2007). On the contrary, the possibility of a rocks to be colonized depends on its physical and chemical properties (Walker and Pace, 2007), while the intrinsic properties of the microbial community to survive the extreme xeric stress, include the production of the extracellular polymeric substances (EPS) with hygroscopic characteristics, the alternation of grow in short periods which correspond with the availability of the water, and the capability to delay metabolic activity during dehydration (Harel et al., 2004).

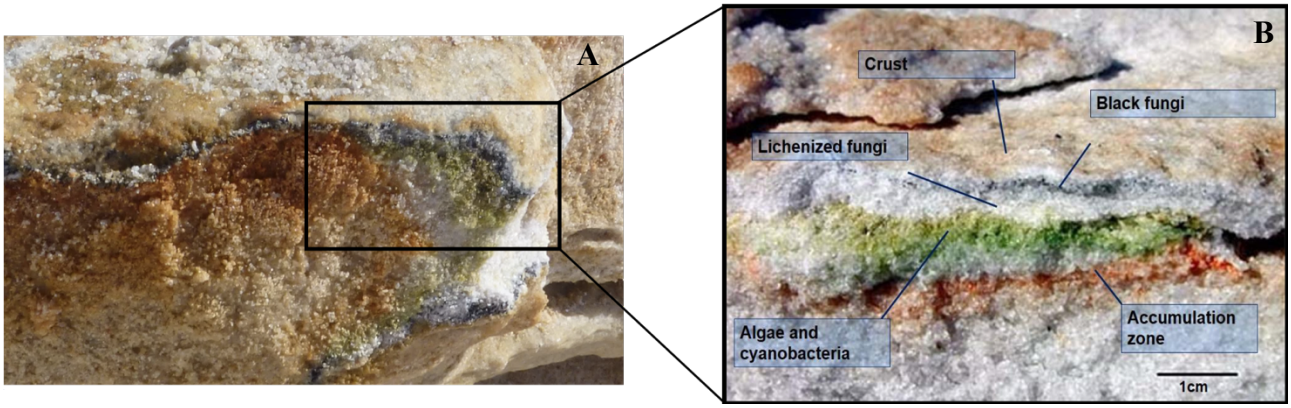

Figure 8. (A) Overview of a sandstone fragment, colonized by a stratified cryptoendolithic lichen-dominated community. (B) Zoom and description of the colonization layers: silicified, reddish brown crust; black zone colonised by lichenised and non-lichenised fungi; white zone colonised by lichenised fungi and lichenised algae; green zone colonised by non-lichenised algae and cyanobacteria.

Within the sandstone, the microbial growth leads to a characteristic stratification with various colored and biologically distinct bands (Fig. 8A). The stratification is the result of the different physiological requirements (e.g. exposure to solar radiation) and/or abilities (e.g. production of antibiotic substances) by each associated microbial type (Ocampo-Friedmann and Friedmann, 1993).

The upper zone, under the silicified, reddish brown rock crust, is formed by a cryptoendolithic lichens zone. This zone may be divided into an upper black zone and a lower white zone. The black zone may be formed by two structures: (i) lichen soredia with pigmented phycobiont filaments and (ii) non-lichen-forming dark pigmented fungi. These microorganisms, known as "black fungi", often showing meristematic growth *in vitro*, have been isolated as regular members of the lichen-dominated community (Ruisi et al., 2007), e.g. *Friedmanniomyces endolithicus* (Onofri et al., 1999) and *Cryomyces antarcticus* (Selbmann et al., 2005). Otherwise, the white zone appears to be formed by lichens and/or hyaline soredia (Friedmann et al., 1988). The lower zone of the lichen-dominated community, defined as "green zone", is characterized by the presence of non-lichenised algae, among which the endemic chlorophycean alga *Hemichloris antarctica* is predominant, and several of the most extremophilic prokaryotes known to date, e.g. the cyanobacteria *Chroococcidiopsis* sp. and *Gloeocapsa* sp. (Friedmann et al., 1988) (Fig. 8B).

The microorganisms that inhabiting the microbial communities represent the one of the focus of many astrobiological researches, since they evolved and adapted in the conditions that best mimic the ones on Mars and, if a hypothetical life-form has ever existed on the planet could have evolved the same strategy (Friedmann and Ocampo-Friedmann, 1976; Nienow and Friedmann, 1993). Besides, cryptoendolithic life has been suggested as a suitable diagnostic indicator for putative extinct microbial life preserved in Martian rocks (Walker et al., 2005).

For this reason, cryptoendolithic microorganisms might be suitable analogues for detecting forms of life on Mars (Wynn-Williams and Edwards, 2000).

1.7.5 Meristematic rock-inhabiting black fungi

For long time, exobiology and astrobiology focused their attention mainly on the prokaryotes rock-inhabiting microorganisms, to study the habitability and the limits of life in other planets, thanks to their scarce complex organization, the earlier emergence and putative higher resistance to stresses compare to eukaryotes. In recent years, eukaryotes microorganisms also demonstrated their ability to survive and thrive in different extreme environments (Amaral Zettler et al., 2002). For this reason, they attracted interest for astrobiological studies, becoming a good test organism for these studies.

Among eukaryotes, black fungi are one of the most stress-tolerant microorganisms known (Gorbushina, 2003), occurring in diverse environments and under oligotrophic conditions (Sterflinger et al., 1999). The term "black fungi" is referred to a particular group of fungi, characterized by a thick-walled, melanised cells (Harutyunyan et al., 2008). They are also known as "dematiaceous fungi", "meristematic fungi", "microcolonial fungi" (MCF), or "rock-inhabiting fungi" (RIF), with respect to their prominent morphological or ecological characteristics (Sterflinger, 2006; Sterflinger et al., 1999). These fungi are widespread in hot and cold deserts (Nienow and Friedmann, 1993; Selbmann et al., 2005), in temperate regions (Gorbushina et al., 2005; Ruibal et al., 2005; Sert et al., 2007), in acidic and contaminated sites (Hölker et al., 2004; Isola et al., 2013), including contamination by radionuclides (Zhdanova et al., 2004). Black fungi usually shown a meristematic growth, which term, introduced by de Hoog and Hermanides-Nijhof (1977), indicate a slow expanding, cauliflower-like aggregates and reproduce by isodiametric enlargement with subdividing cells. Their growth can shift among yeast-like, filamentous, and meristematic growth (Gostinčar et al., 2012). The latter is less frequent and is particularly typical of fungi under stressing conditions (Wollenzien et al., 1995), as provides the fungus an optimal surface/volume ratio for enhanced stress tolerance (Sterflinger and Krumbein, 1995). Under the stressful conditions of MDV (see the paragraph #1.6.2, "*Antarctic MDV as Martian surface analogue*"), the meristematic growth represent a stable character (Selbmann et al., 2015), allowing to grown on elevated temperatures, low water availability, UV radiation (Wollenzien et al., 1995), high salt concentration (Zalar et al., 1999).

Although the meristematic growth represents a good adaptation against harsh conditions, the strong melanization of the thick cell walls has an important role in protection against excessive temperatures, pH extremes, dryness, hyperosmolarity, and UV radiations (Bell and Wheeler, 1986; Butler and Day, 1998; Dadachova and Casadevall, 2008; Gostinčar et al., 2012). The cell wall melanin consists of negatively charged hydrophobic molecules often aggregated to proteins and carbohydrates, formed by phenols and indolic compounds polymerization (Butler and Day, 1998). Melanins may be synthetized by DOPA-melanin (3,4-dihydroxyphenylalanine) or DHN-melanin (1,8-dihydroxynaphtalene) pathways (Butler and Day, 1998), in the interior of the cell wall or as extracellular polymers (Kogej et al., 2006).

Furthermore, the production of protective compounds provides support against an oligotrophic and stress-tolerant lifestyle (Gostinčar et al., 2012): carotenoids, are antioxidant able to stabilize membranes and filter UV-light (Gorbushina et al., 2008), intracellular mycosporines act as UV-filters, antioxidants, and extracellular polymeric substances (EPS) containing lipids, polysaccharides, and proteins act as an additional irradiation filter (Gorbushina et al., 2008). In addition, the accumulation of trehalose (Nakamura et al., 2009) and polyols (Blomberg and Adler, 1992) stabilizes enzymes, membranes and the osmotic potential of the cells (Sterflinger et al., 2012). Black fungi usually lack of sexual reproduction that implies energetic costs that cannot be maintained when energy must be employed for survival and stress resistance (Ruibal et al., 2008; Selbmann et al., 2015). An asexual reproduction by clonal reproduction is favored. Due to their extraordinary adaptations to extreme conditions, both alone or complex with the entire community, black fungi have been selected for astrobiological studies, to give new insights about the habitability and the search for life on Mars.

1.7.5.1 The black yeast-like fungus Cryomyces antarcticus: an example of extreme eukaryotic life

Among the isolated Antarctic black fungi, *Cryomyces antarcticus* was described in 2005, based on a strain (CCFEE 534) isolated by R. Ocampo-Friedmann from weathered sandstone samples collected at Linnaeus Terrace (Dry Valleys) by E.I. Friedmann during the Antarctic expedition 1981-1982. Generally, this fungus has slow-growing cerebriform colonies, black and thick-walled torulose hyphae, and dark and very thick-walled conidia (Fig. 9).

Figure 9. SEM micrograph showing the micro-colonial black fungi with yeast-like organization *C. antarcticus* CCFEE 515 (from Onofri et al., 2015).

It's growth optimum spanning from 0 to 20 °C, tolerates strong thermal fluctuations and produces extracellular polysaccharides in response to extreme conditions, protecting against cycles of desiccation, and freeze/thawing. Despite that, it may survive up to 90 °C for 1 hour in laboratory conditions and to 50 cycles of heating (+20 °C) and cooling (-20 °C) within 2 weeks (Onofri et al., 2008). Low temperatures are correlated to a number of additional stress such as dehydration and osmotic stress. Since most of the Antarctic water is trapped as ice, causing depletion of liquid water available for active life, black fungi evolved desiccation-tolerant strategies, in order to overcome long periods of deep dehydration (Onofri et al., 2007; Selbmann et al., 2015). In dehydrated conditions,

C. antarcticus is able to survive to different simulated and real exposure tests, such as radiation: (i) up to 56 kGy of gamma rays (^{60}Co, Pacelli et al., 2017a), (ii) up to 1000 Gy of helium ions (Pacelli et al., 2017b), (iii) up to 0.3 Gy of X-ray (Pacelli et al., 2018), (iv) to space and simulated Martian conditions experienced in LEO for 16 months (Onofri et al., 2012, 2015, 2019) and (v) accelerated iron and helium ions up to 1000 Gy in the presence of Martian regolith analogues (Aureli et al., 2020; Pacelli et al., 2020a). In addition to the ability of recovering after exposure to the above-mentioned parameters in de-hydrated conditions, the fungus showed a good survivability also in hydrated conditions (up to 2000 Gy of accelerated iron ions; Pacelli et al., 2021a). *C. antarcticus* has been also shown to retaining colony-forming ability after UV-B exposure at lethal doses for *Saccharomyces pastorianus*, and with no evident effects on DNA integrity (Onofri et al., 2007; Selbmann et al., 2011). Recently, it has been discovered that *C. antarcticus* possesses the ability to produce both 1,8-dihydroxynaphthalene (DHN) and L 3-4 dihydroxyphenylalanine (L-DOPA) melanins (Pacelli et al., 2020b), suggesting a possible involvement in protection against different kinds of radiation. In addition, in cold desert desiccation may be favored by the evaporation, allowing the accumulation of high salt concentrations on rocks surface (Selbmann et al., 2015). Although this fungus is not classified as a halophile species, its high stress tolerance acts as an adaptation to osmotic stress, allowing it to tolerate high salt concentrations (Selbmann et al., 2015). *C. antarcticus* showed active colonies after the exposure to NaCl concentrations of 24% (w/v) (Onofri et al., 2007). Recent study reported a good survivability of fungal colonies after growth on Martian relevant perchlorates [$Mg(ClO_4)_2$+ $Ca(ClO_4)_2$]; 145 mM of $Mg(ClO_4)_2$, 80 mM of $KClO_4$, 200 mM of $Ca(ClO_4)_2$, 220 mM of $NaClO_4$] (Cassaro et al. unpublished). Basing on all these results about the stress tolerance, *C. antarcticus* is considered as one the most extremotolerant eukaryotic organisms known to date (Selbmann et al., 2015), and for this reason, it is selected as a good test organism for astrobiological studies (Onofri et al., 2012, 2015, 2019; Selbmann et al., 2017; Pacelli et al., 2017a, 2019, 2020a, 2021a, b, c; Cassaro et al., 2021).

1.8 Astrobiology projects

To establish the habitability potential of planetary bodies and to investigate the detection of hypothetical traces of extant or extinct forms of life, experimental procedures and tools for life-detection need to be settled. A significant amount of preparation and investigation is required to prevent and eliminate bias, during the effective investigation on a planetary body surface. For this reason, the space agencies fund different astrobiology projects, with the aim to conduct a series of experimental procedures to i) test and chose the appropriate instruments for life-detection onboard space exploration rovers, ii) define the correct protocol to use, iii) understand the limits of habitability and the adaptive strategies of life forms, iv) to define detectable biomolecules (could be used as biosignatures) from extant or recently extinct life and their preservation over the time, v) to select the best landing sites for the rovers.

Usually, astrobiology projects are organized into a multi-step approach combining field, laboratory, and space research is necessary (Fig. 10) (de Vera et al., 2019, 2020) to perform and support life-detection missions beyond Earth. The use of terrestrial environments to study the ability of life to persist in hostile extraterrestrial environments and how to detect it, is important since Earth is the only planet supporting life so far. Since no actual terrestrial places closely exhibit the complete environmental parameter range described on the other planetary bodies, the use of planetary simulation facilities is a required step of these investigations. In addition, for a complete study, the exposure to the harsh conditions of real space is needed, considering that no laboratory is equipped with facilities that can simultaneously test all the conditions that samples could undergo in real space.

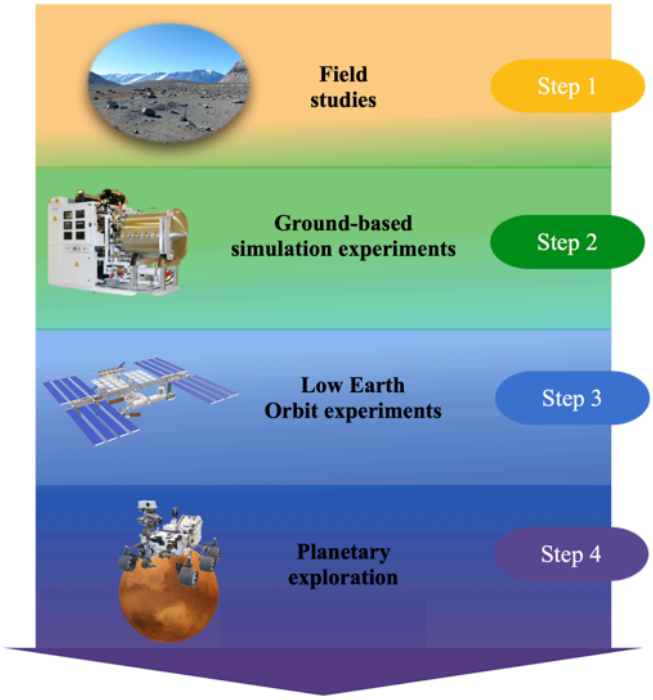

Figure 10. Schematic representation of a multi-step approach for astrobiological investigations.

Among astrobiology projects who follow this or part of the above-mentioned procedure, we may mention: Life in space, BIOMEX, LIFE and STARLIFE projects.

1.8.1 The Italian National Project of Astrobiology—Life in Space—Origin, Presence, Persistence of Life in Space, from Molecules to Extremophiles

The Italian Space Agency (ASI)-funded "Life in Space" project was funded in the wake of the proposal for the development of a network of institutions and laboratories conceived to implement Italian participation in space astrobiology experiments. One of the main aims of the project is the study of the origin and evolution of life in the Universe, spanning from prebiotic chemistry to astrobiology and astrophysics (Onofri et al., 2020).

The project embraces the four most important topics in astrobiological research:

- Origins and evolution of organic compounds of biological significance in space (comets, asteroids, rocky planets, and moons);
- Prebiotic syntheses, origin of life, and early life;

- The limits of life and biological habitability: origin, evolution and adaptation of life in extreme environments on Earth and in space;
- Biomarkers for life detection in the Solar System and on exoplanets.

The first topic includes the study of prebiotic organic compounds formation on ice and gas for conditions expected on different ice-covered planetary bodies, such as Pluto, Icy Moons, and comets, and explores the possible synthesis of prebiotic compounds in non-aqueous solvents such as liquid methane/ethane that is abundant, for example, on Titan. The “Prebiotic syntheses, Origins, and Early Life” topic develops on the idea of formamide as a precursor to complex organic matter and will follow molecular evolution from simple chemical precursors to the basic intermediates of cellular processes, including the detection of organic life markers in planetary and space conditions. The third topic, “Limits of Life", will investigate different aspects in the life-detection question. For example, the biology and limits of adaptation of extremophilic Archaea and microbiomes from extreme solfataric environments, will be investigated. Microorganisms (mainly fungi) and radioprotective pigments (melanin) will be evaluated under space-relevant radiation or other extreme conditions (perchlorates, analogue regolith mixtures), to study the protective effects on biological systems and materials. In addition, astrobiological models such as cyanobacteria and microfungi will be investigated by the modern -omics technologies under simulated Mars and icy moon conditions and M-star simulated irradiation with the intent to highlights the limits of life and adaptability under non-Earth conditions, as well as the permanence of biomarkers. Cyanobacteria will also be evaluated, with biochemical and -omics methods, to determine the limits and mechanisms of adaptability of oxygenic photosynthetic microorganisms to simulated M-type light sources at ground conditions and increasing CO_2 concentrations (in N_2) up to 100% Mars-like concentrations. Microfungi will be investigated through a transcriptomic and metabolomic approach to elucidate the adaptation mechanisms at the basis of their high resistance. A data set of atmospheric biosignatures generated under a variety of tested conditions will be produced as part of the “Biomarkers for Life Detection”

topic. This topic will also include laboratory irradiation studies of biomolecule interactions with mineral surfaces, identification of atmospheric and reflectance spectroscopic biomarkers of gases and pigments, respectively, from oxygenic photosynthetic extremophiles. Exoplanets that could accommodate a biosphere will also be selected for remote biosignature study.

This project provides only planetary field and ground-based experiments. One of the objectives of the third topic, is mainly performed on the Antarctic black fungus *C. antarcticus* (see paragraph #1.6.5.1 *The black yeast-like fungus* Cryomyces antarcticus*: an example of extreme eukaryotic life*). In this context, the fungus is exposed to different simulated Martian and space conditions (ionizing and non-ionizing radiation, perchlorates, desiccation, vacuum, etc), and then, analyzed through vitality and molecular tests. Radiation exposure were performed at the Calliope facility of the National Agency for New Technologies, Energy and Sustainable Development (ENEA-Casaccia; Rome, Italy), a pool-type irradiation facility equipped with a ^{60}Co γ-source (Baccaro et al., 2019). The results of these experiments were analyzed in this thesis (Chapter 2 "Insights into the habitability").

1.8.2 The BIOlogy and Mars Experiment (BIOMEX) project

The ESA-supported (Italian Team funded also by ASI) BIOMEX was an interdisciplinary experiment which aimed to investigate i) the habitability of Mars by survivability tests, ii) the potential preservation of biomolecules, and iii) the limits of life under real space and simulated Mars-like conditions. In addition, samples have been also tested for their resistance to space environment, as support to the Lithopanspermia theory (de Vera et al., 2012, 2019). Thus, the aim of BIOMEX project was dual: the investigation of the limits of life and the consequent evaluation of the habitability of Mars surface, and the detection of the biosignatures stability, developing a biosignature database that might be helpful for the upcoming space exploration missions.

For the BIOMEX project, a variety of extremophile organisms, representing the three domains of the tree of life (algae, archaea, lichens, bacteria, fungi and bryophytes), has been selected. This selection is determined by several factors, such as the extraordinary ability of some of these organisms to resist a wide range of stressors and because they are considered among the oldest organisms on Earth (Campbell et al., 2003; Yuan et al., 2005). Organisms never tested before allowed to investigate new resistance capability of different life-forms (de Vera et al., 2019).

Mainly, these organisms were exposed to different treatments after grown on two different Martian regolith analogues, terrestrial sandstone and lunar regolith analogue, with the aim to determine if the presence of a mineral matrix could interfere or cause toxic effects on microorganisms. For the second purpose of this project, a series of biomolecules, such as pigments, secondary metabolites, and cell surfaces in contact with a terrestrial and Mars analogue mineral environment, have been selected and exposed to simulated- and real space environment, in order to evaluate their stability or degradation over time (de Vera et al., 2012, 2019). This project provides the multi-step investigation of the astrobiological studies (see paragraph #1.7 "*Astrobiological projects*"). Indeed, after the selection of the best extremophilic organisms sampled in planetary field analogues on Earth, the exposure into planetary simulation facility and to LEO, was performed.

In particular, two series of ground-based simulation tests, including EVTs and Science Verification Tests (SVTs, Rabbow et al., 2017) were carried out for BIOMEX before the space exposure. They were performed at the PSI of the DLR. EVTs simulated individual space conditions, while SVTs experiments were performed inside the same exposure platform used aboard the ISS (EXPOSE-R2), and simultaneously simulated all the environmental stresses expected in the LEO exposure. The real space mission was launched to the ISS on July 24th, 2014 on board the space cargo Progress 56P, and on August 18th, the EXPOSE-R2 facility (where samples were accommodating), was installed outside the ISS on the Russian Svezda module for 16 months.

During this period, samples were not only exposed to space conditions, but also to a simulated Mars-like environment (CO_2 atmosphere and UV > 200 nm). Samples returned on Earth in June 2016 (de

Vera et al., 2019). Among the microorganisms, BIOMEX included the Antarctic cryptoendolithic black fungus *C. antarcticus*, as a eukaryotic test organism for investigating astrobiological topics. Colonies of the fungus were grown on different Martian regolith analogues or sandstone, where it naturally occurs. The results on EVTs, SVT and SPACE exposure tests were analyzed in this thesis (Chapter 3 "Insights into the biosignatures detection").

1.8.3 The Lichens and Fungi Experiment: LIFE

Funded by ESA, LIFE project provided the exposure of fragments of Antarctic sandstone colonized by cryptoendolithic communities and microcolonial cryptoendolithic black fungi to simulated space and Mars conditions on Earth and to long-term exposure outside the ISS onboard the EXPOSE-E facility for 1.5 years. The aims of LIFE were to i) investigate the limits of life in different conditions to those experienced on Earth, ii) expose microbial communities in their natural substrate (Antarctica rocks) to evaluate the role of substratum in protecting microorganisms, and iii) provide evidence in support to the Lithopanspermia theory (Onofri et al., 2012, 2015; Horneck et al., 2010).

This project involved ground-based experiments such as the EVTs to test the survivability of samples before the real exposure in LEO. The tests have been carried out at the DLR where individual and combined simulated space and Martian conditions were tested. For the real space exposure, samples were loaded in a small chamber (1.4 cm in diameter) on the EXPOSE-E facility, a part of the European Technology Exposure Facility (EuTEF) developed to expose different type of samples under space environment and launched onboard the Space Shuttle STS-122. On 15 February 2008, the facility was installed outside the Columbus module by an extravehicular activity. The infrastructure EXPOSE-E was brought back to Earth on 12 September 2009 with STS-128. Once back on Earth, samples were subjected to molecular (e.g., qPCR, PCR, MTT, PMA assays) and cultivation analyses to estimate survival and viability of microbial communities and black fungi (Onofri et al., 2012, 2015; Scalzi et al., 2012). In this work, spectroscopic analyses were performed

in order to detect any possible biomolecule after space exposure and to investigate the protective role of mineral rocks towards organic compounds. The results of this work are reported in this thesis (Chapter 3 “Insights into the biosignature detection”).

1.8.4 STARLIFE project

Similarly to the Life in space project (see paragraph #1.7.1 “*The Italian National Project of Astrobiology—Life in Space—Origin, Presence, Persistence of Life in Space, from Molecules to Extremophiles”*), STARLIFE project, did not foresee the exposure of samples in LEO, but only ground-based simulations. The entire project was focused on the exposure of different selected extremophilic organisms to different kind of ionizing radiation (x-rays, gamma-rays, heavy ions), representingpart of the galactic cosmic radiation spectrum. Low and high-energy charged particles radiation experiments have been performed at the HIMAC facility (Heavy Ion Medical Accelerator) at the National Institute of Radiological Sciences (NIRS) in Chiba, Japan. X- or γ-rays were used as reference radiation at DLR (German Aerospace Center, Cologne, Germany) (Moeller et al., 2017). After the exposure, samples were analyzed through biochemical and molecular biological methods, in order to understand the effect of radiation on extremophiles and to extend the limits of life. In this context, colonies of the fungus *C. antarcticus*, were exposed to high doses of heavy ions (Fe, Ar, He), in order to evaluate i) the survivability of hydrated colonies after the exposure to Fe ions, and the ii) biosignature detection after the exposure to Fe, Ar and He ions, when mixed to Martian regolith analogues. The results are reported in this thesis (Chapters 2 and 3, “Insights into the habitability” and “Insights into the biosignature detection”; respectively).

1.9 Aims of the thesis and chapter description

The present thesis work aimed to illustrate the dual approach to search for hypothetical life forms or their signs beyond Earth by investigating the habitability limits on Earth and by studying the biosignatures detection. In this context, the thesis work investigated **i**) the resistance of the black fungus *Cryomyces antarcticus* MNA-CCFEE after the exposure to simulated extraterrestrial conditions, in order to understand the limits of life as we know it and to define the limit of terrestrial habitability; **ii**) the stability or degradation of fungal biomolecules after the exposure to simulated Martian and space conditions and to real space exposure outside the ISS in dedicated exposure platforms, in order to understand which fungal molecules may be considered as a good biosignature of life and to provide support for the ongoing space exploration missions.

The introduction chapter is a presentation of the astrobiology field, focusing on the main approaches used to search for life beyond Earth: the habitability potential and the biosignatures detection. To support the astrobiological researches, the study of the terrestrial extreme environments and the inhabited microorganisms is of utmost importance, since terrestrial life is the only example we have so far. The McMurdo Dry Valleys in Antarctica represent one of the most studied extreme environments, thanks to their similar conditions with Martian surface, which is one of the main targets of space agencies for searching for life beyond Earth. The introduction continues with the description of the cryptoendolithic communities, which live inside the rocks as a survival strategy against the harsh environmental conditions on the surface, and of *C. antarcticus*, one of the most resistant eukaryotes known to date. This fungus is used as a perfect astrobiology test organism due to the high survival reported in previous projects. The end of the introduction describes different astrobiological projects, in which the fungus was selected to study the survivability or biosignatures detection.

The following chapters describe the results obtained, in the frame of Life in space and Starlife projects, about the survival of the fungus *C. antarcticus* after the exposure to simulated extraterrestrial conditions (mainly perchlorates and irradiation). In addition, in the context of BIOMEX and BioSigN

projects, the study of the behavior of the fungal molecules after the exposure to ground-based experiments and real space exposure was investigated.

In particular, chapter 2 describes the results obtained by growing the fungus *C. antarcticus* in different perchlorate concentrations, similar to those found on Mars, were described. The survivability was investigated as the percentage of colony forming units (CFUs), while an estimation of metabolic activity recovery of exposed samples in comparison to controls, was obtained through the MTT assay. To investigate the effects of oxidant species on cellular membranes integrity, a PMA assay coupled with a quantitative PCR (qPCR), was performed. This chapter focuses also on the investigation of ultrastructural damages through transmission electron microscope (TEM) analysis. Samples grown on perchlorate culture media, were exposed to increase doses of gamma rays (^{60}Co) at the ENEA Center (Rome), in presence/absence of Martian regolith analogues, in order to investigate the survivability (CFUs), metabolic activity (MTT), cellular membranes integrity (PMA) and nucleic acid damages (qPCR). Since the presence of perchlorates in hyper arid environments could provide the presence of a transient liquid water film, the radiation effects on the metabolically active state fungal colonies were also investigated. Fungal colonies were irradiated with increased doses of gamma rays (^{60}Co) at the ENEA Center (Rome) and then investigated with the same techniques reported above.

Chapter 3 deals with the results of the study of fungal biomolecules after the exposure to ground-based test and to real space exposure onboard the ISS. First, in the frame of BIOMEX project, fungal colonies were grown on i) two Martian regolith analogues and ii) a lunar regolith analogue and exposed to simulated Martian and space conditions through the Experiment Verification Tests (EVTs) and Scientific Verification Tests (SVTs). After the exposure, the detection of fungal biomolecules was investigated through Raman and Infrared spectroscopies, similar to those installed in Mars 2020 and ExoMars 2022 mission's rovers. Additionally, qPCR assay and Gas Chromatography-Mass Spectrometry techniques were used to detect nucleic acids and low molecular weight compounds,

respectively. Similarly, samples exposed to real space conditions were analyzed. Again, fungal biomolecules were investigated after the exposure to different radiation types (heavy ions, gamma rays) as a part of Starlife irradiation campaign. In the frame of LIFE project, Antarctica sandstone fragments colonized by cryptoendolithic microbial communities, were analyzed after the exposure to real space and Martian-like conditions outside the ISS for 1.5 years. This study provided evidence for the protective role of minerals against biological molecules. The results were obtained via a combination of two techniques including Raman and Infrared spectroscopies. General discussion and conclusions are presented in chapters 4 and 5.

2. Insights into the habitability

2.1 Insights into the survival capabilities of *Cryomyces antarcticus* hydrated colonies after exposure to Fe particle radiation

Abstract

The modern concept of the evolution of Mars assumes that life could potentially have originated on the planet, possibly during the end of the late heavy bombardment, and could then be transferred to other planets. Since then, physical and chemical conditions on Mars changed, and now strongly limit the presence of terrestrial-like life forms. These adverse conditions include scarcity of liquid water (although brine solutions may exist), low temperature and atmospheric pressure, and cosmic radiation. Ionizing radiation is very important among these life-constraining factors because it damages DNA and other cellular components, particularly in liquid conditions where radiation-induced reactive oxidants diffuse freely. Here, we investigated the impact of high doses (up to 2 kGy) of densely-ionizing (197.6 keV/µm) space-relevant iron ions (corresponding on the irradiation that reach the uppermost layer of the Mars subsurface), on the survival of an extremophilic terrestrial organism – *Cryomyces antarcticus* – in liquid medium and under atmospheric conditions, through different techniques. Results showed that it survived in metabolically active state to high doses of Fe ions, being able to repair eventual DNA damages. It implies that some terrestrial life forms can withstand prolonged exposure to space-relevant ions radiation.

Keywords: radiation, melanin, DNA, radioresistance, metabolically active cells

Pacelli, C., Cassaro, A., Siong, L. M., Aureli, L., Ralf, M., Fujimori, A., Shuryak, I. & Onofri, S. (2021a). Insights into the Survival Capabilities of *Cryomyces antarcticus* Hydrated Colonies after Exposure to Fe Particle Radiation. Journal of Fungi, 7(7), 495.

2.1.1 Introduction

Outer space and the surface of most celestial bodies are subjected to high fluxes of ionizing radiation, which constitute the major damaging factor in space. The radiation environment consists of high energy photons (such as gamma rays and X-rays) and particles. Galactic Cosmic Rays (GCRs) are high-energy charged particles that originate beyond the Solar System. They consist of 98% nuclei and 2% electrons that markedly differ in their relative abundance; 85% of the nuclei component is represented by protons, 12% by alpha particles and 1.5% by heavier nuclei (Ferrari and Szuszkiewicz, 2009). Although they represent only about 18 x 10^{-3}% of the GCRs spectrum (Mewaldt, 1994), Fe ions are the most significant components of GCRs when the particle flux is weighted according to the energy deposition (Edwards, 2001; Durante and Cucinotta, 2011). They are harmful for any form of terrestrial life since they can interact either directly or indirectly with all relevant biomolecules, causing dense ionization along the trajectory of the particles, and secondary ionizations of various energies that can diffuse in multiple directions and to varying distances from the particle trajectory. Shielding from this kind of radiation is challenging and poses one of the principal difficulties in understanding its effects on any (terrestrial) biological organisms.

Indeed, habitability in space and on the Martian surface is highly dependent on the protection from UV and ionizing radiation, such as heavy ions (Dartnell, 2011; Rummel et al., 2014). Differently to Earth, Mars does not have a magnetic field to deflect energetically charged particles, including GCRs and Solar Energetic Particles (SEP). These particles penetrate the thin Martian atmosphere and react with the regolith, dust deposit covering solid rocks, creating an oxidizing environment on the Martian surface.

The highly radiative environment on Mars has implications for life-detection missions, since hypothetical life-forms or their remains may be damaged by ionizing radiation field (Dartnell et al., 2007); this could be one of the possible explanations of the for the failure of the curiosity rover to detect any trace of life.

Indeed, the radiation dose received by Mars is quantified by theoretical calculation and determined by the data from the Curiosity rover, which is about 0.05-0.06 or 0.076 Gy/year, respectively (Dartnell et al., 2007; Pavlov et al., 2012; Hassler et al., 2014).

While the UV photons are limited in the upper layer of Martian sub-surface, as they are absorbed by rocks (Pavlov et al., 2012; Hassler et al., 2014), GCRs have the capability to penetrate to 1-2 meter in the sub-surface in spite of chemical and physics features of rocks, or ice content (Pavlov et al., 2012). Besides, UV flux depends in function of latitude and some molecular targets (e.g. amino acids) could be easily destroyed when embedded in highly UV-penetrated materials (Laurent et al., 2019).

In addition, it was demonstrated that 1-2 mm of Mars simulant regolith layer is able to shield biological samples against UV flux (Marschall et al., 2012).

On the contrary, damages provoked by ionizing irradiation are considered as one of the most dangerous. As reported in (Pacelli et al., 2017) an increase reduction of amplicons in a 2000 bp amplification occurs in fungal samples exposed to different doses of ionizing radiation.

At a depth of more than 2 meters it is more plausible that a hypothetical life form has been able to adapt, since the environment is partially shielded from ionizing radiation. Potentially microbial life on Mars could have persisted in protected niches in the Martian sub-surface in dried or in freezing conditions. The estimated survival duration for cryoconserved microorganisms could be about 3.3 million years at 2 meters depth (Dartnell, 2011).

However, the presence of hygroscopic salts on Mars surface create a transient liquid film that could be important for a putative life-form on Mars, since water is essential for life as we know it (McKay, 2004). In fact, perchlorates are helpful for the presence of liquid water, but the biochemical adaptation of life in brine should be taken into account (Gault and Cockell, 2021). A plausible hypothesis could be represented by the idea that deliquescence provoked by salts concentration could sustain hypothetical active microbial life under extremely radiative and dry conditions, as occur in hyper-arid Atacama Desert (Davila et al., 2010). It has been demonstrated that deliquescence in specific

Martian regions, could be pro-vided to i) the low thermal inertia and temperature, which allow the increment of humidity level, or by ii) movements on the Martian surface (Pal et al., 2019).

In the presence of transient liquid water, what effects does radiation have on microorganisms?

In this context, the study of the microbial survivability against radiation effects, is of importance to deepen the biological mechanisms that hypothetical life forms could assume in an extraterrestrial habitat (Domagal-Goldman et al., 2016). Previous studies demonstrated the survivability of cyanobacteria, bacteria, lichens and microfungi after exposure to simulated space and Martian conditions (de Vera et al., 2010; Onofri et al., 2012, 2015, 2019; Musilova et al., 2015).

Despite this recognizable role of radiation in life endurance, effects of space relevant radiation metabolically active terrestrial organisms are still not well characterized, due to the difficulties to fully reproduce the space radiation environment. The capability of the Antarctic cryptoendolithic black fungus *C. antarcticus* in resisting the space-relevant radiation has already been demonstrated. Indeed, in desiccated conditions, the fungus was able to survive the radiation environment experimented in Low Earth Orbit (LEO), outside the International Space Station (ISS) (Onofri et al., 2012, 2015, 2019; Scalzi et al., 2012), and high doses of ionizing radiation exposure (gamma rays up to 55 kGy, Pacelli et al., 2017). Here, for the first time, we investigated the survival capability of the fungus under increasing doses of accelerated outer space-relevant Fe ions radiation, in hydrated (metabolically active) conditions. Indeed, in the frame of STARLIFE irradiation campaign (Moeller et al., 2017) fungal colonies were irradiated, in liquid medium, with accelerated Fe ions doses (up to 2 kGy), at the HIMAC (Heavy Ion Medical Accelerator in Chiba) facility at the National Institute of Radiological Science (NIRS) in Chiba, Japan. Survival, metabolic activity recovery and DNA damages were investigated.

2.1.2 Materials and Methods

2.1.2.1 Test organism

The test organism is the black fungus *C. antarcticus* MNA-CCFEE 515, isolated by R. Ocampo-Friedmann from sandstone collected at Linnaeus Terrace in McMurdo Dry Valleys (Southern Victoria Land, Antarctica) by H. Vishniac, during the Antarctic expedition of 1980-1981 (Selbmann et al., 2005). This fungus was isolated through culture-dependent approach on Malt Extract Agar (MEA) Petri dishes. This microcolonial fungus, is widely used in astrobiological-related studies, due its tolerance to various stressors. It is a cryophilic organism, with a growth optimum below 15 °C, which lives dwelling inside the porous of sandstone, as refuge against the harsh Antarctica environment. A detailed description of *C. antarcticus* morphology and adaptation is reported in (Onofri et al., 2020).

2.1.2.2 Samples preparation and performed analyses

The fungal samples were grown at 15 °C for 3 months and then transferred into 200 µl of Malt Extract (ME) liquid medium for the irradiation (fungal concentration 1000 CFU/ml). The irradiation was performed using accelerated Fe ions (Fe^{26+}, Energy: 418.3 MeV/n, LET in water: 197.6 keV/µm; range in water: 74.4 mm) doses (up to 2 kGy), as reported in Table 1. The survival of *C. antarticus* was quantified by the CFU number on cultivation test with 5 technical replicates. The integrity of cell membranes was investigated by Propidium MonoAzide (PMA) assay and followed by quantitative PCR (qPCR) according to the protocol reported in (Pacelli et al., 2017). The metabolic activity was evaluated using MTT (3-(4,5-dimethylthiazol-2-yl)-2,5-diphenyltetrazolium bromide), through a spectrophotometric assay. Detailed procedures are reported in Supplementary Materials. Lastly, the intactness of DNA regions (ITS-LSU) was examined using single gene amplifications, RAPD fingerprinting, and quantitative PCR. Conditions for DNA amplifications are reported in Supplementary Materials.

Table 1. Accelerated Fe ions radiation doses applied for each sample.

Samples[a]	**Applied/ Received dose (Gy)**
Control	0
Irradiated colonies	100
Irradiated colonies	250
Irradiated colonies	500
Irradiated colonies	1000
Irradiated colonies	2000
Positive control[b]	0

[a] metabolically active fungal cells irradiated in liquid media

[b] metabolically active fungal cells maintained in optimal growth conditions

Based on surviving colony counts, mathematical modelling of cell survival dose response was performed. To quantitatively model the radiation dose response for colony survival, we used the standard linear quadratic (LQ) model of radiation-induced cell death. This formalism is commonly used in radiation biology and oncology, and here we used a variant that takes into account the inducibility of DNA repair (Jones, 2001; Sach et al., 1997).

The selected formalism describes the natural logarithm of the number of surviving clonogens or colony forming units (lnS) after an exposure to an acute radiation dose d by the following equation, where lnB is the number of colonies expected without radiation, α is the linear dose response component and β is the quadratic component that quantifies the dose response "curvature":

$$lnS=lnB-\alpha\times d-\beta\times d^2 \quad (1)$$

Importantly, DNA repair, which affects cell survival, potentially exhibits dose-dependent inducibility. This phenomenon was not taken into consideration by the classic LQ model, but was investigated in models such as the one from (Marples et al., 1993). Here, we used a simple variant of

an "inducible repair" model, described by the following equation, where the term q×dr with adjustable parameters q and r represents repair induction:

$$\ln S = \ln B - \alpha/(1+q\times d^{r})\times d - \beta/(1+q\times d^{r})\times d^{2} \quad (2)$$

At low doses, this model (Eq. 2) exhibits behaviours similar to the classic LQ model (Eq. 1). At high doses, however, the dose response slope (the derivative dlnS/dd) is reduced and can approach zero if parameter r approaches 2. We fitted the model (Eq. 2) to the data (ln-transformed colony counts per plate) using robust nonlinear least squares method-ology implemented by the nlrob function in R 3.6.2 software. To minimize the chances of finding the global optimum best-fit solution rather than a local optimum, we performed the fitting 1000 times with random initial conditions (drawn from log-normal distributions) for the adjustable parameters (lnB, α, β, q, r), and retained the best fit. All parameters (except lnB) were restricted to non-negative values, and parameter r was restricted to $0 \le r \le 2$ to maintain biological plausibility. The quality of the best fit was assessed by coefficient of determination (R2), root mean squared error (RMSE), and examination of residuals for consistency with the normal distribution (by Shapiro-Wilk test and Q-Q-plot).

2.1.3 Results

2.1.3.1 Cultivation test

As showed in Fig. 1A, *C. antarcticus* retained the colony-forming ability after radiation treatments. A gradual increase of mortality was recorded with increasing radiation doses, but a considerable percentage of survivors were observed even after 1000 Gy and 2000 Gy irradiation (13% and 9%, respectively, Fig. 1A). Survival counts were fitted by a dose response curve using robust regression as shown in Fig. 1B. Visual inspection suggests decent fit quality for the dose response model of radiation-induced cell death (described in Supplementary materials), and this is supported by the high R2 (0.92) and relatively low RMSE (0.29 on ln scale) values. The best-fit value of the linear dose response component (parameter α) was not significantly different from zero. The other parameters

had the following best-fit values and standard errors (SE): ln-transformed background colony count (lnB) = 7.69, SE = 0.12; quadratic dose response component (β) = 6.42, SE = 3.23 kGy-2; repair induction parameter (q) = 2.19, SE = 1.66 kGy-2; repair induction dose dependence power (r) = 2.0, SE = 0.38. The minimum robustness weight in the regression was 0.60, and model residuals were consistent with the Normal distribution (Shapiro-Wilk p-value = 0.65).

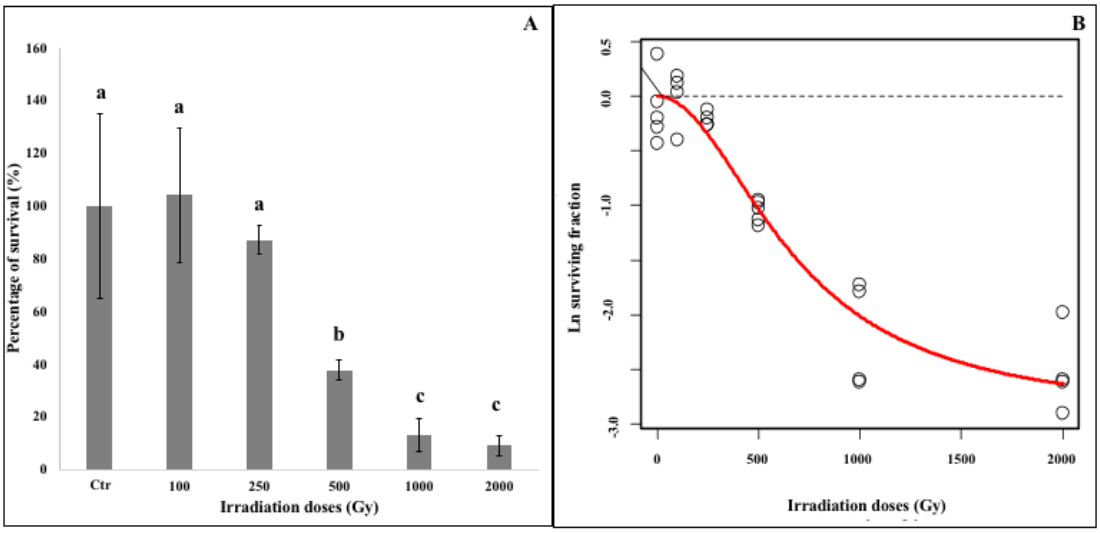

Figure 1. A) Survival of fungal colonies in liquid media exposed to accelerated Fe ions. B) Mathematical model of cell survival dose response. The same letters above bars indicate that the values are not statistically significant according to the t test ($p \leq 0.05$).

2.1.3.2 Metabolic activity assessment

No difference in the overall metabolic activity after 48 and 72 hours-rehydratation was recorded in irradiated fungal colonies, compared with related controls (Fig. 2). The fluorescent signal exhibited higher values with increasing irradiation doses. However, there was an unexpected decrease of Optical Density (O.D.) value in the samples that were treated with 500 Gy irradiation. Positive control samples that were kept on agar plates with sufficient required nutrient and under optimal growth conditions have shown to have higher metabolic activity than the control (Ctr, in dried conditions) sample. On the other side, samples that received irradiation doses treatments displayed high O.D. value compared to positive control samples. This phenomenon may indicate that the metabolic activity is higher in irradiated cell due to the damage repair mechanism activated upon irradiation.

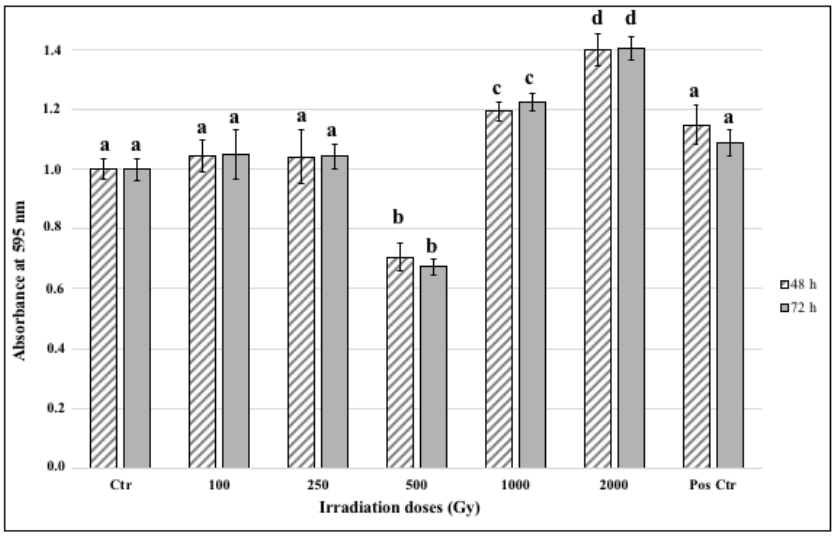

Figure 2. Metabolic activity of fungal cells after 48h and 72 h re-hydratation. Striped bars indicate 48 h re-hydratation; grey bars indicate 72 h re-hydratation. Pos Ctr= DNA of *C. antarcticus* colony growth in physiological conditions. Statistical analysis as in Figure 1.

2.1.3.3 Cell membranes integrity

The integrity of cell-membrane in irradiated cells was assessed by using qPCR combined with the pre-treatment of cells with the dye PMA. This molecule penetrates cells with compromised cell-membranes and inhibits DNA amplification. Accordingly, this analysis revealed a progressive damage with the increasing of treatments; an average of 39% damaged cells were recorded at the dosed of 100, 250, 500 and 1000 Gy (Fig. 3). No cells with intact cell membranes was reported at the dose of 2000 Gy, according to the survival test.

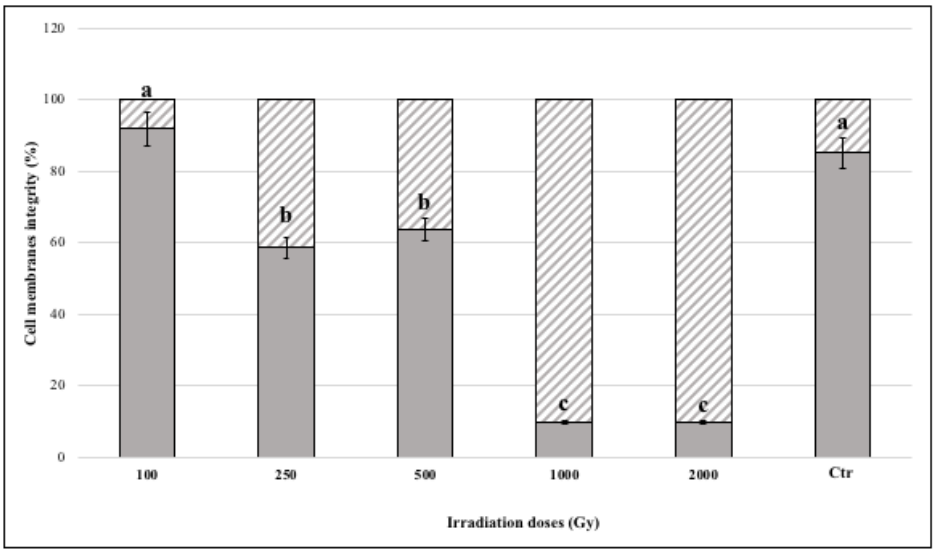

Figure 3. Percentage of intact and damaged cell-membranes measured with PMA assay coupled with qPCR of *C. antarcticus* exposed to accelerated Fe ions. Pos Ctr= DNA of *C. antarcticus* colony growth in physiological conditions. Statistical analysis as in Figure 1.

2.1.3.4 DNA integrity

Amplicons were obtained both for ITS and LSU regions (fragments length of 700 bp, 1600 bp and 2000 bp) of *C. antarcticus* genome after irradiation treatments. DNA amplification revealed a good DNA integrity without any differences despite gene length and treatments (Fig. 1SA, B and C). The overall RAPD profiles were showed to be preserved (Fig. 2S). The quantification of LSU gene fragment amplification in Figure 4 shows that an average of 15000 DNA copies were obtained from the sample treated with doses up to 1000 Gy and approximately 1500 DNA copies from the sample treated with 2000 Gy dose. The tests highlighted a common trend for all the samples. Surprisingly, a high number of DNA copies were reported for 2000 Gy sample, although low survival rate was observed.

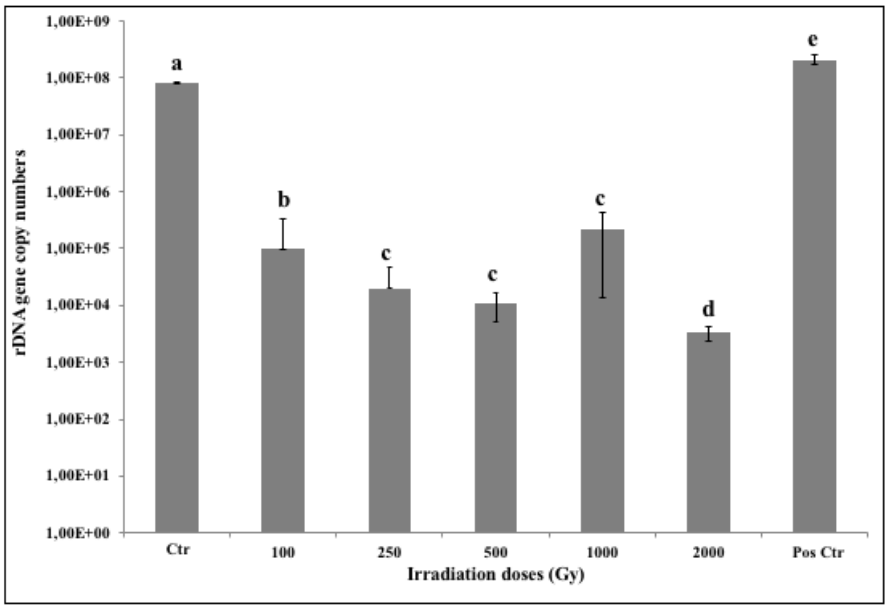

Figure 4. Quantitative PCR of a 939 bp (base pair) target gene (LSU) of *C. antarcticus* DNA, after exposure to Fe ions irradiation. Pos Ctr= DNA of *C. antarcticus* colony growth in physiological conditions. Statistical analysis as in Figure 1.

2.1.4 Discussion

In space, microorganisms have to cope with an interplay of various adverse environ-mental factors (Horneck, 1981). Besides high vacuum and extreme temperatures, they are exposed to a complex radiation environment. Assuming no shielding, the flux of cosmic ray iron (Z= 26) with energies between 100 and 1000 MeV/nucleon is approximately 4 nuclei/cm^2 day. The ultimate limit for survival of spores in space (not on Martian surface, where the limits of life are established through a multitude of factors) may be set by the heavy ions from cosmic radiation. An approximate estimation for survival could be given on the basis of known data on the radio-resistance of terrestrial organisms. However, it must be considered that physical conditions can significantly change the amount of radiation damage in cells at the same dose. It is known, that in aqueous environments most of radiation damages are caused by indirect effects as the formation of highly reactive oxygen species like free radicals OH, O2H, etc. (Baumstark-Khan and Facius, 2002; Ghosal et al., 2005). In the present

experiment, fungal cells were exposed to accelerated Fe ions within liquid medium. However, given the Linear Energy Transfer (LET) and range values of incident ions, no significant shielding was made against radiation, independently of the position of the fungal cells during exposure.

In the optic of the search for life on Mars, such conditions allowed to assess the effects of part of the radiation environment occurring on the surface and in the uppermost layer of Martian subsurface, where microorganisms would be directly exposed to incident CRs.

The radiolysis of water molecules in the solution by high LET Fe ions may have led to an increase of free radicals and molecular products in the environment surrounding the cells (Pimblott, 1994). A correlation between the LET and the radical and molecular yields in water exists. In this respect, it was shown, that desiccated microbial cells survive higher irradiation doses than cells in suspensions (Verseux et al., 2017). Dormant cells can accumulate damage at high levels; whereas metabolically active cells could be able to mitigate some damage (Brandt et al., 2017). However, even if cells in a desiccated state show a greater resistance to radiation exposure and could protect against any residual radiation-induced formation of Reactive Oxygen Species (ROS) (Messen et al., 2013), the additional damaging consequences of dehydration (Sibirny, 2017) should be taken into account. On the other hand, previous work demonstrated that radiation and desiccation resistance is due to the ability to regenerate intact chromosomes from scattered fragments (Soppa, 2013; Stan-Lotter and Fendrihan, 2015).

Here, in the framework of STARLIFE project, hydrated fungal samples were irradiated with iron ions, which energy (~ 500 MeV) represent the flux of GCRs near the Martian surface (Turner et al., 2008); thus, could be considered as representative not only of Fe particles, but also of most of cosmic rays making up the space and Martian radiation environments.

For the first time, our experiment evaluated the effects of high LET particles exposure on *C. antarcticus* cells in metabolically active conditions. Our results are consistent with the previously observed high resistance of the fungus to different kind of ionizing radiation (Selbmann et al., 2018; Pacelli et al., 2017, 2018), and to other factors encountered in space aboard the ISS (Onofri et al.,

2019). Even if the number of alive cells decreased with the increase of radiation doses, robust fungal survival was reported, still at the higher doses (1000 and 2000 Gy, Fig. 1A). A similar decrease of survival was observed for *Halobacterium salinarum* NRC-1 when irradiated with Fe ions up to 2 kGy (Leuko and Rettberg, 2017). The mathematical model (Fig. 1B) used to describe the dose-response behavior of fungal cells, is characterized by an initially shallow inactivation response (shoulder) at low doses, where the majority of cells survive, followed by a "tail" at higher doses. The "tail", where most of the cells are dead but a few survive even at high doses, can indicate a distinct subpopulation within the fungal population that is able to survive, maybe due to the activation of DNA damage repair mechanisms. Future researches focusing on re-irradiation of this resistant subpopulation should be performed for clarifying if fungal cells can evolve a mechanism of radio resistance. The activation of some resistance mechanisms is confirmed by the results of metabolic activity assay. Figure 2 shows an increased metabolic activity at the highest doses, probably due to the activation of an intense cell repair mechanism. Accordingly, to the survival and metabolic activity results, the analysis on cell membranes integrity showed a reduction in the number of cells with intact membranes (and therefore presumably alive) at the dose of 500 Gy (around 60%, Fig. 3); no relevant differences have been detected in control samples. Moreover, the fact that around 10% and 6% of cells have intact cell membranes at the dose of 1000 and 2000 Gy (Fig. 3) confirmed the survival reported from the cultivation tests and the hypothesis of the presence of radioresistant cell subpopulations. In addition, DNA damages has been tested through PCR and qPCR gene amplification. In general, PCR single gene amplifications (Fig. 1S) were successful even at highest dose and longest gene sequences tested; in the same way RAPD amplification results show a good preservation of the fingerprinting profiles (Fig. 2S). Basing on the principle that certain DNA lesion terminate the correct course of any polymerase on the template, and any nucleic acids damage may be measured as a decrease in amplification of the fragment of interest, qPCR analyses were performed. Our results showed that DNA amplification was not impaired by extreme radiation, even at the dose of 2000 Gy (Fig. 4), that reported more than 3000 copies of amplified DNA. A good amplification was detected for control

samples (Fig. 4). As previously reported in (Leuko and Rettberg, 2017), the exposure of different bacteria strains to heavy ions reported only few lesions in DNA, if referring to iron ions up to 1 kGy, compared with the irradiation with Ar ions. This could be explained that DNA damage induced by ionizing radiation is localized (Terato and Ide, 2004). To conclude, the obtained results revealed that *C. antarcticus* could be considered as a suitable candidate to search on planet beyond Earth, especially on Mars that is characterized by the presence of transient liquid water on the surface and a highly radiation environment, also in a metabolic active state. However, the mechanisms involved in the fungal radiation resistance in presence of thin water layer should be further investigate through -omics approaches. In addition, a further investigation about the stability of fungal biomolecules (biomarkers) after irradiation exposure, could be required. The ongoing and future in situ life-detection missions on planetary bodies of our Solar System (e.g. Mars), will drill the surface (Vago et al., 2017; Kereszturi et al., 2016) in order to detect sign of past or present life. Assessing the biomarkers preservation under a highly radiative environment is of outmost importance to support these missions and to estimate the stability/degradation rates of biological molecules (Da Pieve et al., 2021). Besides, the investigation of the techniques could be used to evaluate the hypothetical biomolecules damages, is a test bed for the future Mars Samples Return (MSR) on Earth (Muirhead et al., 2020).

Acknowledgments: We acknowledge the HIMAC team at the NIRS in Chiba, Japan for the irradiation. We thank the PNRA (Italian National Program for Antarctic Research) for supporting sample collection in Antarctica, and the Italian National Antarctic Museum “Felice Ippolito”, for funding CCFEE (Culture Collection of Fungi from Extreme Environments).

2.2 Could radiation affect fungal cells survivability in an aqueous environment?

Abstract

Liquid water is one of the required conditions for life as we know it. Nowadays, its presence is widely reported outside the Earth. There are ample geological and mineralogical evidences that water once flowed on Mars; and the recent discovery of present ice-water on the planet surface is one of the driving factors for life-detection missions. Nevertheless, the highly radiative environment of the Martian surface in combination with aqueous thin layers could be considered prohibitive for hypothetical forms of life on the planet. Here, in the context of the Italian "Life in space" project, we analyzed the survivability and the DNA damages of hydrated colonies of the Antarctic black fungus *Cryomyces antarcticus* after exposure to increased doses of γ-rays.

Keywords: water on Mars, hydrated cells, gamma rays, fungal survivability

Cassaro A., Pacelli C., Leo P., Catanzaro I., Onofri S. Could radiation affect fungal cells survivability in an aqueous environment? Prepared for the submission on "Life" (special issue: "Advances in space biology").

2.2.1 Introduction

The search for life on other celestial bodies is based on "life as we know it", meaning life based on liquid water, a biogenic element (carbon atoms) and an available source of energy (Chyba and Hand, 2005; Wright et al., 2016). Water is one of the required elements, which until recently was thought to be quite rare outside the Earth, but indispensable for chemical and metabolic reactions, enough to be identified as an "universal solvent" because of its i) ability to create hydrogen bonds with polar solutes, ii) high heat capacity, and iii) large range of temperatures for liquid stability (Nazari-Sharabian et al., 2020). Terrestrial life is strictly dependent on liquid water as an internal medium in which molecules dissolving and reactions take place. Over the time, water substitute solvents have been hypotheses, such as liquid ammonia. However, ammonia and other solvents at atmospheric pressure maintain their liquid state at colder temperatures than water (Barrow and Tipler, 1986). Since liquid water is an indispensable element for life as we known it, the life-detection missions within our Solar System will be focus on those planetary bodies known to currently host liquid water or have hosted it in the past, such as Mars (Kargel, 2004), Icy Moons that host subsurface oceans (Chyba and Phillips, 2005), and large asteroids with liquid deep interiors (Merk and Prialnik, 2006). Hospitable conditions such as wet surfaces existed during Mars' history. 3.8 billion years ago climate conditions on Mars have been more favorable (higher surface temperatures as well as a denser atmosphere), suggesting large amounts of surface water in form of vast ocean, possibly covering one-third of the planet (Pollack, 1979; Fairén, 2010; Dohm et al., 2009). Large outflow channels, networks of river valleys, lakebeds and hydrated-minerals provide geological evidence of liquid water on the planet. These evidences have been indagated for decades: in the seventeenth century, bright polar caps were discovered (Kieffer et al., 1976; Plaut et al., 2007), while data obtained from Curiosity rover suggest the presence of an aged freshwater lake in Gale Crater, which could be an ideal habitat for hypothetical life-forms (Grotzinger et al., 2015). In addition, the study of the ALH 84001 Martian meteorite revealed the presence of Mg-Fe-Ca carbonates along fractures; these minerals are the results of precipitation from aqueous fluids and may represent the sites of paleolakes on Mars,

supporting the idea of a warmer and wetter environment in the past (Bandfield et al., 2003; Ehlmann et al., 2008).

Nowadays, it is demonstrated that water may persist on Mars only in certain circumstances and for a short period of time because of the surface conditions (*e.g.,* low temperature and atmospheric pressure) (Orosei et al., 2020). Most water reservoirs on Martian surface are in the form of ice, vapor in the atmosphere, transient liquid brines in shallow soil areas or locked into water-rich materials (Nazari-Sharabian et al., 2020; Orosei et al., 2020). In 2016, NASA identified a large amount of underground water on Mars, but the first identification of a subglacial stable water body, located 1.5 km beneath the South polar ice cap reaching 20-km across, was obtained only in 2018 by orbital radar sounding (Orosei et al., 2018). It is currently known that on Martian surface water can be only found below the cryosphere, suggesting that in early Mars water flow percolated in the ground, creating an aquifer similar to Earth (Orosei et al., 2020). Although there is evidence of water on present Mars, its surface still remains inhospitable for terrestrial life forms because of cosmic and solar radiation reaching it. Based on the idea that Martian life could be related to life on Earth, radiation and an aqueous environment may be considered as limiting factors for microorganisms' survivability. Exposure of living systems to ionizing radiation could cause a direct ionization of DNA (direct effect), the ionization of the first hydration shell able to transfer damage to DNA (quasi direct effect) and ionization of water (indirect effect), causing OH•, H• and aqueous electron (e^-_{aq}) formation (Becker and Sevilla, 1993; von Sonntag, 2006), which could be added to the C=C bonds of the DNA bases. These highly reactive oxygen species cause most of radiation damages on biological macromolecules such as DNA, enzymes, and lipid membranes (Adam et al., 2003; Krieger, 2004) in aqueous environments (Halliwell and Gutteridge, 2015; Baumstark-Khan and Facius, 2002; Ghosal et al., 2005). Considering these conditions, could putative Earth-like life survive on Mars? Are the fungal cells irreversibly affected by radiation in the presence of liquid medium or could they repair the damages and survive?

Many extremophilic terrestrial microorganisms are known to survive exposure to different ionizing radiation when in dehydrated conditions (Baqué et al., 2013; Selbmann et al., 2018, Pacelli et al., 2017, 2018, 2020; Onofri et al., 2019; Verseux et al., 2017, Billi et al., 2019). However, only a few studies of γ-rays exposure on hydrated state microorganisms (Brandt et al., 2017; Verseux et al., 2017) have been performed so far, and never before on fungal species. Different archaea species (*Halobacterium salinarum NRC-1, Halococcus hamelinensis, and H. morrhuae*) have been exposed to γ-rays (^{60}Co), showing a survivability rate up to 6 kGy only in *Halococcus* spp. (Leuko and Rettberg, 2017). Moreover, nucleic acids alterations in *Chroococcidiopsis* spp. have been detected after 48 and 113.25 kGy of γ-rays irradiation (Verseux et al., 2017).

To answer our questions and in the frame of the Italian project of astrobiology "Life in space" (Onofri et al., 2020), hydrated colonies of the polyextremotolerant black fungus *Cryomyces antarcticus* were exposed to different doses of (up to 117 kGy) at the Gamma irradiation Calliope facility at ENEA-Casaccia research center (Rome, Italy). We aim at understanding if metabolically active fungal cells can withstand γ-rays exposure by studying fungal survivability, metabolic activity changes and nucleic acid damages.

2.2.2 Material and Methods

2.2.2.1 Fungal cultures preparation

The Antarctic cryptoendolithic black fungus *C. antarcticus* MNA-CFEE 515, isolated from sandstones at Linnaeus Terrace (McMurdo Dry Valleys, Southern Victoria Land, Antarctica) by H. Vishniac during the Antarctic expedition of 1980-1981, was used as the test organism in this study.

The fungus was spread and grown on MEA (Malt Extract Agar: malt extract, powdered 30 g/L; peptone 5 g/L; agar 15 g/L; AppliChem GmbH, Darmstadt-Germany); then incubated in laboratory for 3 months at 15 °C. Before irradiation, samples were dehydrated in a sterile laminar flow hood for

24 hours. Once dried, micro-colonies were removed from the Petri dishes culture medium and transferred into 400 µL of Malt Extract (ME) liquid medium.

2.2.2.2 Irradiation parameters

The irradiation of fungal colonies was carried out at the Calliope facility of the National Agency for New Technologies, Energy and Sustainable Development (ENEA-Casaccia; Rome, Italy).

The Calliope facility is a pool-type irradiation facility equipped with a ^{60}Co γ-source in a high volume (7×6×3.9 m^3) shielded cell (Baccaro et al., 2019). Irradiation tests were performed through the use of a dedicated software of the Calliope plant, which allows to update daily the value of dose intensity, to determine the duration of the irradiation, and to calculate the absorbed dose value. Samples were exposed to increasing doses of γ-rays. All tested doses are reported in Table 1. Each sample was irradiated in triplicate. During the experiment, the following environmental conditions were maintained constant: air temperature (25 °C), atmospheric pressure (1 atm). After treatment, samples were stored at 4 °C for the following analysis.

Table 1. List of the samples and irradiation parameters experienced during the experiment

Samples	**Average of dose intensity [Gy/h] $_{air}$**	**Time of irradiation (hh:mm:ss)**	**Absorbed dose [kGy$_{air}$]**
Pos Ctr		Not-irradiated	
hydrated colonies	1814.33	14:55:12	27.06
hydrated colonies	1811.05	30:56:48	56.04
hydrated colonies	1814.96	64:29:32	117.04

2.2.2.3 Survival analysis

2.2.2.3.1 Cultivation test

The survivability of *C. antarticus* irradiated colonies were quantified by measuring colony forming ability as percentages of CFUs (Colony Forming Units). Micro-colonies were counted through a Bürker chamber under a light microscope and diluted to obtain a final concentration of 2000 CFUs per 0.1 mL. 100 µL of each diluted sample were spread on MEA Petri dishes and incubated for 3 months at 15 °C. Non-irradiated samples (Pos Ctr), used as the "positive control", were analyzed using the same procedure. All the experiments were performed in quintuplicate.

2.2.2.4 Metabolic activity estimation by MTT (3-(4,5-dimethylthiazol-2-yl)-2,5-diphenyltetrazolium

For the investigation of metabolic activity, a suspension containing 100 µL of fungal micro-colonies (3.5×10^5 cells/mL) and a solution of 0.5 mg/mL of MTT in Phosphate-Buffered Saline (PBS) was placed into 96-well microplates. After incubation at room temperature for 48 and 72 hours, the MTT solution was removed with a multi-channel pipette, and 100 µL of DMSO (DiMethyl SulfOxide) was then added. The absorbance of each treated well was read at 595 nm subtracting the absorbance relative to those containing only MTT. Absorption results were normalized by the number of cells per well, while these values were normalized by dividing by the non-irradiated samples (Pos Ctr).

2.2.2.5 Membranes damage assessment

2.2.2.5.1 Propidium MonoAzide (PMA) assay

Quantitative PCR (qPCr) with PMA was performed to assess membrane integrity after irradiation exposure. A solution of 5 µL of PMA (Biotium, Hayward, CA, United States) was added to treated micro-colonies and kept in the dark in a constant-shaking incubator for 1 h. PMA solution penetrates only damaged membrane cells and crosslinks the DNA preventing PCR after being exposed to light. DNA extraction, purification, normalization at the same concentration of 0.1 ng/mL was performed

using the Qubit dsDNA HS Assay Kit (Thermo Fisher Scientific, Massachusetts, USA). qPCR assay was performed to quantify the number of fungal Internal Transcribed Spacer (ITS) ribosomal DNA fragments (281 bp) present in treated and non-treated samples. A detailed protocol is provided by Onofri et al. (2012). All tests were performed in triplicate.

2.2.2.6 Nucleic acids integrity assessment

Fungal DNA was extracted from colonies using the Nucleospin Plant kit (Macherey-Nagel, Düren, Germany) as reported in Selbmann et al. (2014). Before molecular analyses, DNA was quantified and normalized at the same concentration (0.1 ng/µL) using Qubit dsDNA HS Assay Kit (Thermo Fisher Scientific, Massachusetts, USA). Internal Transcribed Spacer (ITS) and Large SubUnit region (LSU) were amplified using BioMix (BioLine GmbH, Luckenwalde, Germany). To amplify the selected fungal rDNA regions, ITS4 (TCCTCCGCTTATTGATATGC) (White et al., 1990), ITS5 (GGAAGTAAAAGTCGTAACAAGG) (White et al., 1990), LR5 (TCCTGAGGGAAACTTCG) (Vilgalys and Hester, 1990), and LR7 (TACTACCACCAAGATCT) (Vilgalys and Hester, 1990) primers were used. Amplification conditions were as reported in Selbmann et al. (2011). Moreover, to verify the integrity of the whole genome, a fingerprinting analysis (Random Amplified Polymorphic DNA, RAPD) was performed using GGA_7 (GGAGGAGGAGGAGGAGGAGGA) primer (Kong et al., 2000), according to Selbmann et al. (2011).

2.2.2.7 Nucleic acids amplification and estimation of DNA lesions

Real-time PCR was used to quantify the total LSU fragments number. For the amplification of the target region, LR0R (ACCCGCTGAACTTAAGC) (Cubeta et al., 1991) and LR5 (TCCTGAGGGAAACTTCG) primers were used. Amplifications were carried out in triplicate. Final reaction mixture consists of 7.5 of µL of qPCR cocktail (iQ SYBR Green Supermix, Bio-Rad, MI, Italy) mixed with 1 µL of DNA template (0.1 ng/µL) and 1 µL of each primer for a final volume of 5

pmol/μL. Biorad CFX96 real-time PCR detection system (BioRad, Hercules, CA) was programmed to operate at 94 °C for 5 min followed by other 45 sec at 94 °C, annealing at 52 °C for 30 min, and elongation at 72 °C for 2 min. Fluorescence measurements were recorded at the end of each annealing step. After 35 cycles, a melt curve analysis was performed by recording changes in fluorescence as a function of raising the temperature from 60 °C to 95 °C in 0.5 °C per 5 s increments. All data were carried out performing $n \geq 3$ qPCR protocols, each one including n= 3 replicates. The relative amount of DNA lesion in a 0.9 kb amplification product was calculated in samples exposed to different doses of γ-rays (Cassaro et al., in press). Poisson distribution was calculated as reported in Hunter et al. (2010): lesions/amplicon = $-\ln(A_t/A_o)$, where A_t represents the amplification of treated samples and A_o is the amplification of untreated controls.

2.2.3 Results

2.2.3.1 Cultivation test

The survivability of the hydrated colonies of the fungus *C. antarcticus* after irradiation with γ-rays was determined by counting the numbers of colonies formed on MEA plates, compared to the controls. Surprisingly, only control samples (Pos Ctr), showed a good survivability. A complete loss of vitality was detected for exposed samples (data not shown).

2.2.3.2 Metabolic activity measurements

Through the reduction of MTT in formazan by mitochondrial succinate dehydrogenase, an MTT assay is able to detect the percentage of metabolically active cells after radiation exposure. The absorbance of the final solution was estimated after 48 and 72 hours of incubation and measured at the wavelength of 595 nm by a spectrophotometer. Figure 2 shows values obtained from spectrophotometric measurements at the wavelength of 595 nm of the solution with cells and MTT. All samples show a detectable metabolic activity, even at the dose of 117 kGy. Samples show a

common trend with an increase in formazan absorbance, and therefore in metabolic activity, as the radiation dose increases (Fig. 2).

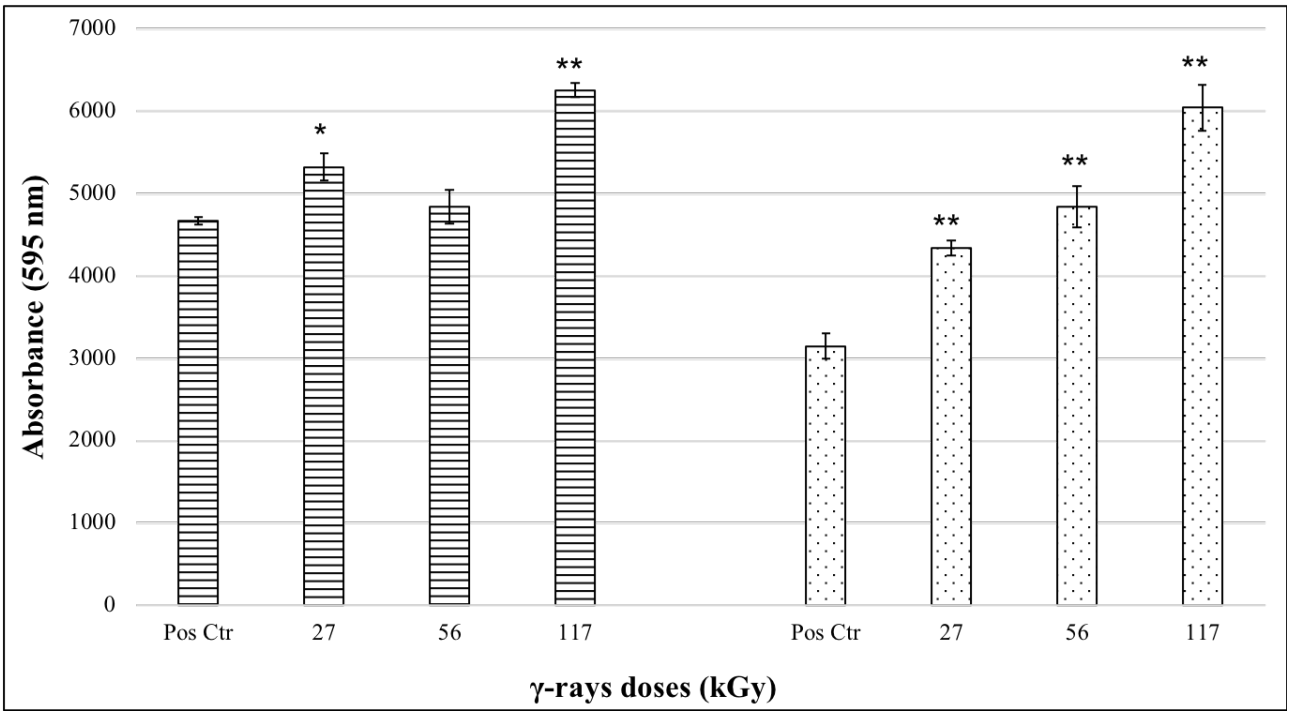

Figure 2. Metabolic activity of hydrated fungal cells exposed to increasing doses of γ-rays after 48 (striped bars) and 72 (pointed bars) h of incubation. Pos Ctr= DNA from *C. antarcticus* colonies grown under physiological conditions. Significant differences were calculated by *t test* with * = $p < 0.05$ and ** = $p < 0.001$.

2.2.3.3 Membranes damage assessment

2.2.3.3.1 Propidium MonoAzide (PMA) assay

PMA assay was performed on hydrated *C. antarcticus* colonies after the exposure to increased doses of γ-rays. The results of PMA assay shows a decrease of the percentage of cells with undamaged cellular membrane as the irradiation dose increases (Fig. 3). Although a high increment of damaged cellular membranes is reported for samples exposed to 117 kGy, 2% of undamaged cellular membranes is still detected (Fig. 3).

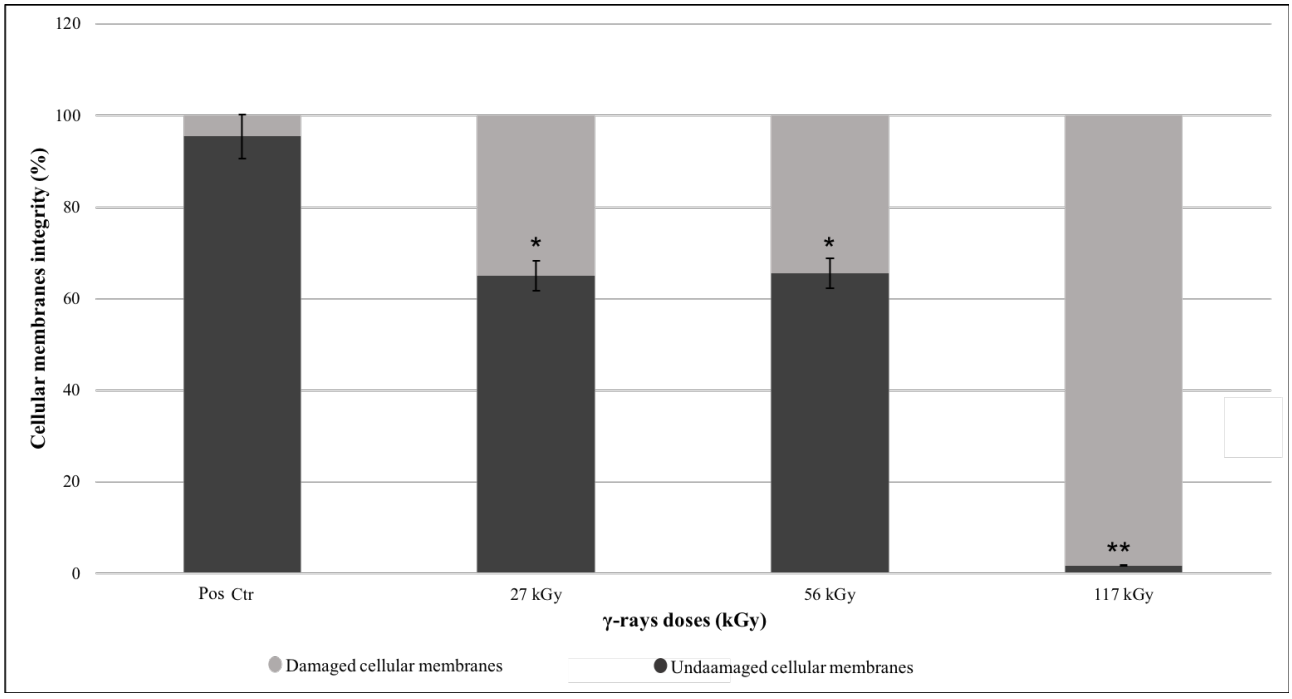

Figure 3. Percentage of undamaged and damaged cellular membranes measured with PMA assay coupled with qPCR of hydrated *C. antarcticus* colonies exposed to increased doses of γ-rays. Pos Ctr= DNA from *C. antarcticus* colonies grown under physiological conditions. Significant differences were calculated by *t test* with * = $p < 0.05$ and ** = $p < 0.001$.

2.2.3.4 Nucleic acids amplification and estimation of DNA lesions

Amplification of DNA extracted from hydrated colonies of *C. antarcticus* after irradiation treatment was performed on a 939 bp length gene. Figure 4 reports the quantity of amplicons detected on fungal DNA after exposure to increased doses of γ-rays. Overall, amplification was obtained for all extracted DNA, with a drastic decrease even at the low irradiation dose. The amplified copy numbers decrease as the radiation dose increases (Fig. 4), while an average of ~4300 DNA copy numbers were detected. Amplification values were used to estimate nucleic acid lesions after irradiation in comparison with Pos Ctr not exposed to any treatments. The relative amount of amplified DNA (Table S2, column 4) decreased with the increasing of irradiation doses. Consequently, a similar trend was obtained for the amount of DNA lesions calculated by Poisson distribution on a ~0.9 kb fragment: extended nucleic acid lesions as radiation doses increased (Table S1, column 6). The estimation of DNA damages for 0.9 kb gene are reported in Fig. S2.

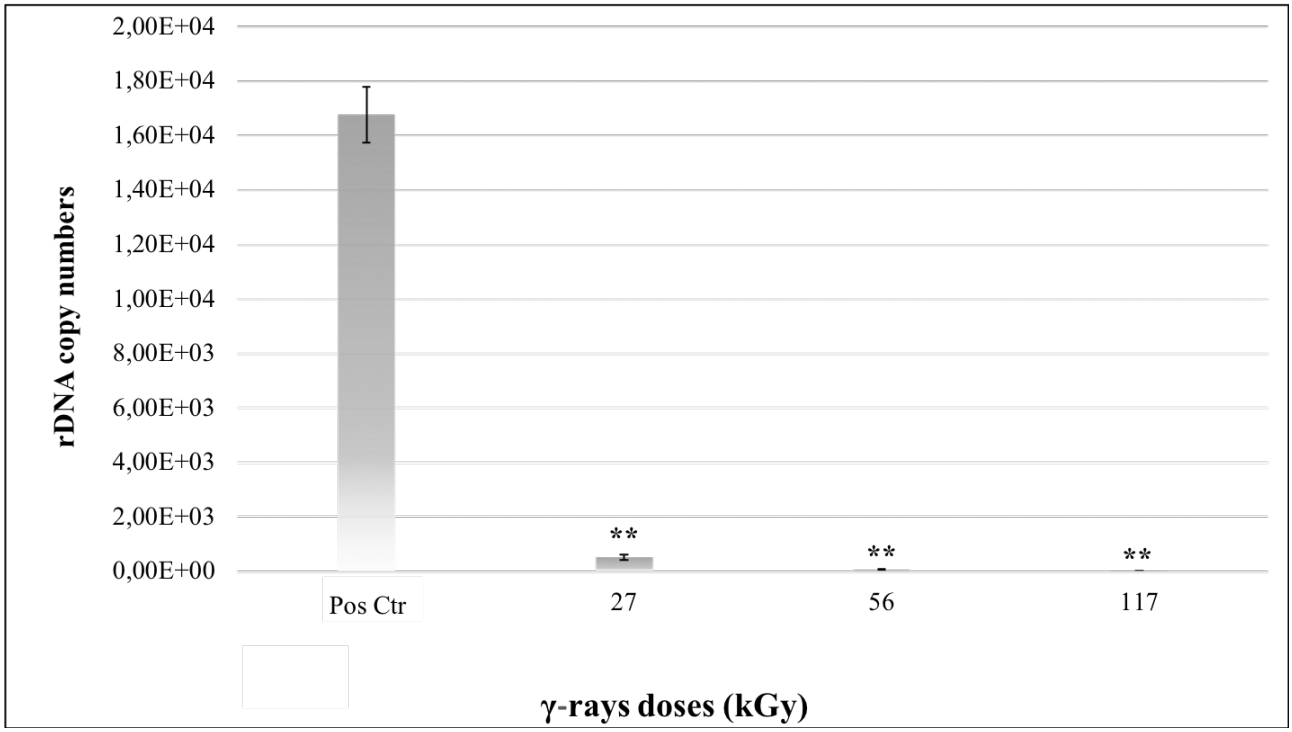

Figure 4. Quantitative PCR of a 939 bp target gene (LSU) of extracted *C. antarcticus* DNA after exposure to increased doses of γ-rays. The number of amplified copies on a logarithmic scale is shown on the y-axis, while treatments expressed in kGy on the x-axis. Pos Ctr= DNA from *C. antarcticus* colonies grown under physiological conditions. Significant differences were calculated by t test with * = $p < 0.05$ and ** = $p < 0.001$.

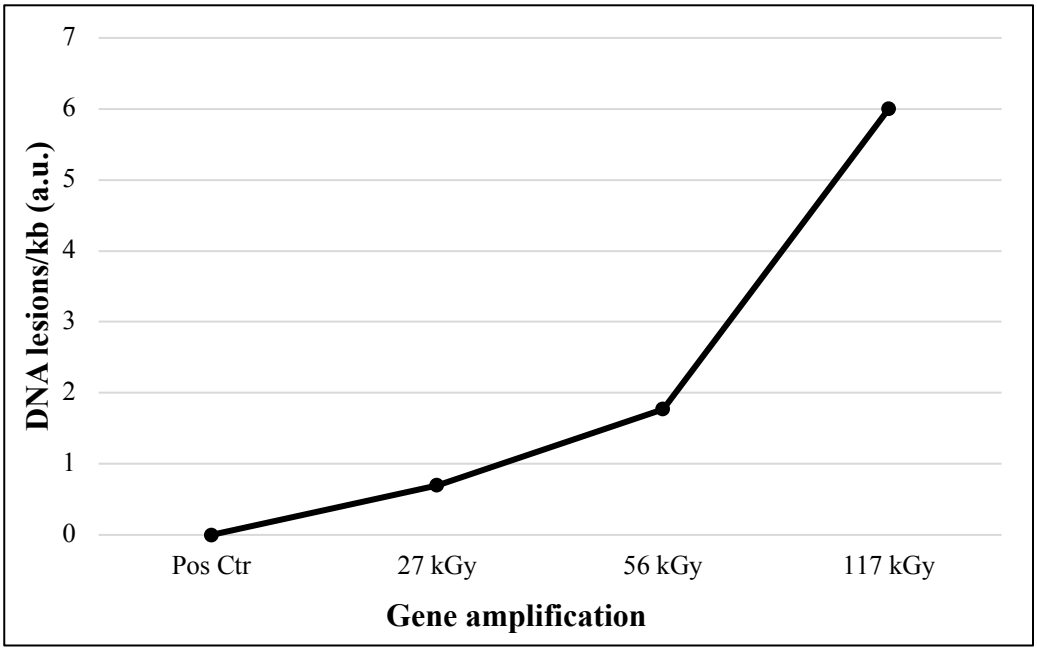

Figure S2. DNA lesions obtained after real-time PCR amplification of DNA extracted from samples exposed to increased doses of γ-rays.

Table S1. Representation of raw fluorescence values obtained after real-time PCR amplification of the LSU gene of DNA extracted from samples exposed to increased doses of γ-rays.

Samples	Mean	Final read	Relative amplification	Lesion frequency	Lesion/0.9 kb
Ctr	22.54	-11.78	1	0	0
27	28.91	-5.42	0.45967742	0.777230298	0.69950727
56	32.68	-1.65	0.13964346	1.968662794	1.77179651
117	34.31	-0.02	0.00127334	6.666108256	5.99949743

2.2.3.5 Nucleic acid integrity assessment

DNA integrity was investigated through amplification of the ITS-LSU target region of 700, 1600, and 2000 bp within the rRNA gene: amplicons were obtained using ITS5-ITS4A, ITS5-LR5, and ITS5-LR7 primers. Results revealed differences in DNA amplification according to the gene length and to the irradiation doses (Fig. S1). Figure S1A shows good amplification of the ITS region up to the dose of 56 kGy compared with Pos Ctr samples. On the contrary, the amplification of 1600 and 2000 bp genes did not occur for any of the irradiated samples (Fig. S1C).

Besides, the whole genome was investigated by a RAPD assay, which revealed no preserved profiles in all conditions tested (Fig. S1B) according to previous estimation of DNA lesions (Table 2); a modification of the *C. antarcticus* specific band pattern occurred even at the lowest irradiation dose (27 kGy; Fig. S1B).

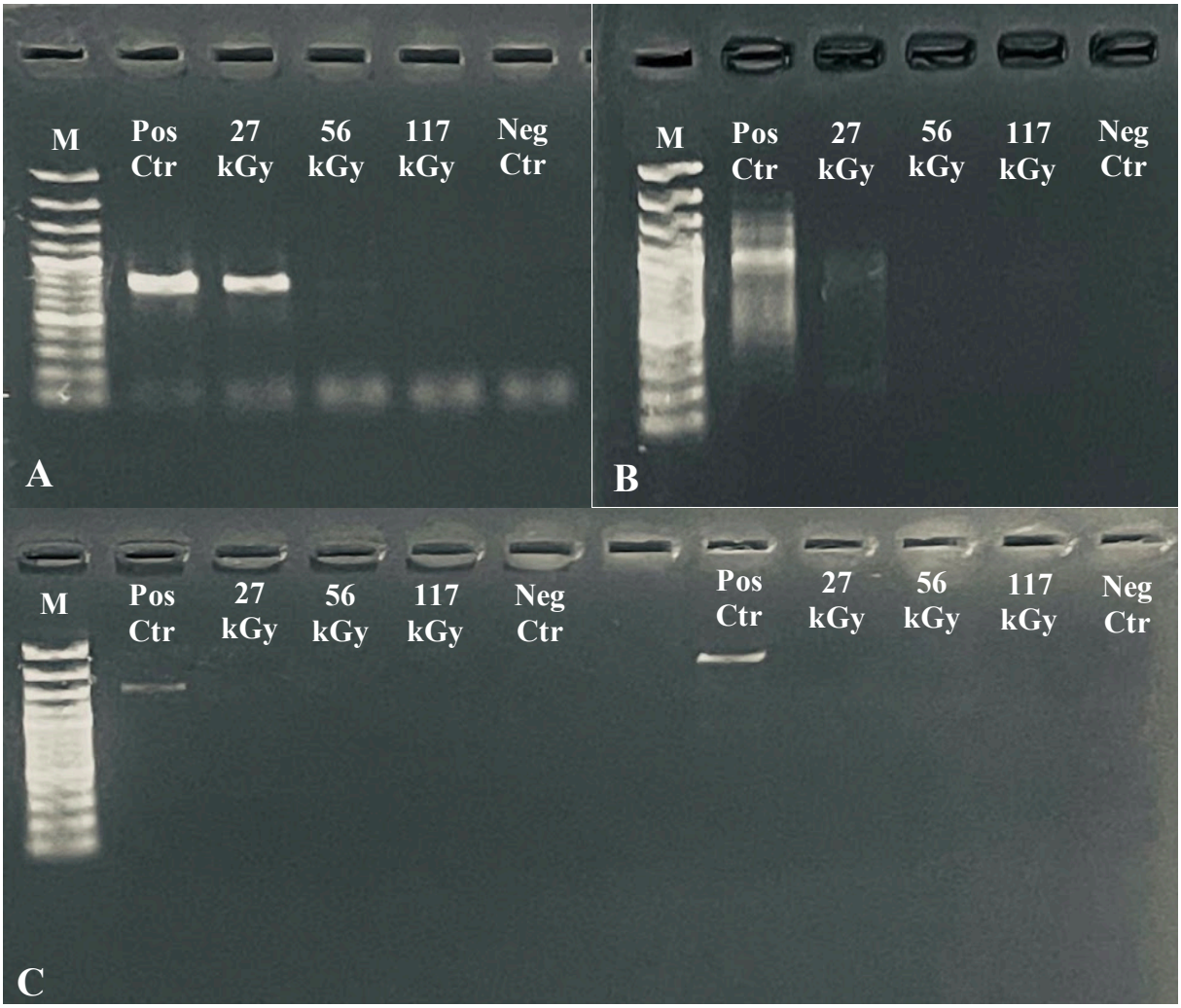

Figure S1. DNA amplification of **A**) ITS (700 bp) region; **B**) whole genome (RAPD assay); **C**) ITS-LSU (1600 bp (left) and 2000 bp (right)) regions. Pos Ctr= DNA from *C. antarcticus* colonies grown under physiological conditions.

2.2.4 Discussion

The search for life on Mars and the concept of habitability is strictly dependent on the availability of liquid water. It is assumed that the surface of Mars had a mild climate for the first 700-900 Myr (Carr, 1996; Fairen et al., 2010). The hypothesis is supported by geomorphological evidence that past constant water flow (Hynek et al., 2010), basins, lakes (Fassett et al., 2008), and hydrothermal systems (El Maarry et al., 2012; Osinski et al., 2013) existed on the planet. Until a few years ago, it was thought that water on Mars was only a past condition. The discovery of polar ice caps (Orosei et al., 2020) and Mg, Ca, Fe, and Na salts in martian regolith, which may retain water and form liquid

water brines (Chevrier et al., 2009), have changed the perspectives of habitability as well as the need for implementation of planetary protection protocols (Bhardwaj et al., 2019). These hygroscopic compounds may easily attract water vapor from the atmosphere, forming liquid solutions through the deliquescence process, providing liquid water for life even in a hyper arid environment like Mars. Although liquid water is the main factor driving the exploration of Mars, its interaction with ionizing radiation should be deeply investigated. Indeed, due to the thin Martian atmosphere and the lack of a global geomagnetic field (Acuña et al., 1998), solar and cosmic radiation particles are able to reach the surface. It is largely reported that ionizing radiations can cause effects on biological systems, such as the formation of reactive oxygen species (ROS), resulting in lipid peroxidation, denaturation of proteins and DNA damages, and contributing to several consequences on the microbial metabolism (Hansen et al., 2006). Considering these factors, a deep understanding of terrestrial living forms limits of life under radiation in aqueous environment is extremely important to i) support the search for life beyond Earth and to ii) expand the limit of habitability as we know it.

Here, in the frame of the "Life in space" project, we determined the survivability of metabolically active colonies of *C. antarcticus* after the exposure to increased doses of γ-rays. Contrary to our previous study on metabolically active fungal cells under Iron ions radiation (Pacelli et al., 2021a), this experiment reported damages in terms of cell survival after treatments. Survivability tests reported no microbial growth for samples exposed to γ-rays. Previous studies on the bacterium *Deinococcus radiodurans*, showed D_{10} values of approximately 5.5 kGy (for liquid samples) and 12.5 kGy (for dried cells) after the exposure to γ-rays (Bauermeister et al., 2011) while Pacelli et al. (2021a), reported high survivability (up to 2 kGy of iron ions) for the fungus *C. antarcticus*.

The metabolic activity results were obtained through a spectrophotometric assay, measuring the reduction of MTT in a water-insoluble blue formazan after 48 and 72 h of incubation. High metabolic activity was recorded for irradiated samples, even if no fungal growth was reported. Overall, the metabolic activity increases as the irradiation dose increases in comparison to control samples (Fig. 2). This condition could be attributed to an intense repair mechanism or to an elevated mitochondrial

biogenesis during the irradiation (Pacelli et al., 2021a; Rai et al., 2018). According to the survival analyses a high number of cells with damaged cell membranes is reported (Fig. 3). Nevertheless, 2% of cells with undamaged cell-membranes is reported at the dose of 117 kGy (Fig. 3); this percentage may explain the metabolic activity recovered at this dose. Similar result was reported for metabolically active colonies of *C. antarcticus* exposed to iron ions: a strong reduction of cells with undamaged cell- membranes (around 10%) at the dose of 1 kGy (Pacelli et al., 2021a). This may be due to the dangerous effects of high-energy iron particles compared to low LET γ-rays (Pouget and Mather, 2001).

These results are coherent with the evaluation of DNA damages. Effects of irradiation on DNA were investigated by PCR and quantitative PCR assay, amplifying different gene lengths. These analyses revealed highly damaged DNA. Indeed, our results reported a successful amplification for the ITS region only for samples irradiated with 27 and 56 kGy, according to DNA lesions estimation (less than 1 lesion per 1 Kbp, Table 2) while no amplicons were detected at the highest dose (117 kGy) (Fig. S1A). Accordingly, no amplicons were detected as the length of the amplified regions increased (1600 and 2000 bp, Fig. S1C). The whole genome amplification highlighted an altered fingerprinting profile at the dose of 27 kGy and the complete loss of the profile at the higher doses (Fig. S1B). On the contrary, as reported for *Chrococcidiopsis* 029 and 057 species, no change in amplicon profiles were reported (Verseux et al., 2017).

The same PCR analysis performed on dehydrated *C. antarcticus* colonies instead reported evident amplification bands even at the highest dose (117 kGy), despite the length of the amplified gene regions (Pacelli et al., 2017). At 117 kGy the bands showed a reduction in relative density for LSU amplification, while still remaining visible (Pacelli et al., 2017). Based on this result, we may hypothesize that dehydration state could preserve cells from ROS induced by radiation (Meßen et al., 2017). The fungus has already demonstrated to survive high doses of radiation in dehydrated conditions and subsequently retain metabolic activity upon cell re-activations. Even if the dehydration process cause itself severe damages to the organism at the membrane level and to proteins

(Anchordoguy et al., 1990; Potts, 1994), it is demonstrated that the down-regulation of metabolism reduces the production of free radicals and activates multiple scavenging mechanisms (Hoekstra et al., 2001). Contrary, metabolically active cells may activate repairing mechanisms that help to withstand the damages directly and indirectly caused by radiation (Brandt et al., 2017).

A quantitative PCR was performed based on the concept that any possible damage on the DNA sequence prevents the polymerase extension. As reported in Pacelli et al. (2021a), the amplification was not prevented even at high doses of irradiation (Fig. 4). Additionally, amplification data were useful to calculate the amount of DNA lesions applying the Poisson distribution. At the higher dose (117 kGy), a lesion of ~6/0.9 kb was reported (Fig. S2; Table S1). Comparing these results with those reported in Leuko and Rettberg (2017), the amplification of 16S rDNA of three bacterial and archaea species (*Halobacterium salinarum NRC-1*, *Halococcus hamelinensis*, and *Halococcus morrhuae*), showed a good amplification up to 78 kGy, while the irradiation at 112 kGy resulted in a 100% chance of a lesion within the gene. Instead, reduction of two orders of magnitude in the number of amplified copies was determined for liquid colonies of *Crococcidiopsis* 029 and 057 species exposed to γ-rays (113 kGy, Verseux et al., 2017). DNA fragmentation was reported for the cyanobacterium *Anabaena* sp. PCC 7120 after exposure to 3 kGy of γ-rays (Singh et al., 2013).

As further step, a comparison between irradiated and non-irradiated fungal colonies genomes would allow to discover any possible mutation in the whole genome sequence.

All the results demonstrated a weak survival of hydrated colonies of *C. antarcticus* exposed to of γ-rays: a complete loss of vitality and a high percentage of damaged cellular membranes were reported. An extended DNA damage was reported at lower irradiation doses (27 and 56 kGy) even through the amplification of a short rDNA region. Thus, the fungus not exhibits a great potential of survivability, allow us to define new limits of life.

These results are of high-impact if used in the context of Mars exploration. In fact the highest irradiation dose (117 kGy) tested in this experimentcorresponds to approximately 1.5 millions of years on the surface of Mars and 13 millions of years at 2 meters depth (extrapolated from Hassler et

al., 2014). Therefore, considering our results, we assumes that, if life ever evolved on Mars, putative fungal cells are not able to resist this scenario. However, it should be considered that in our experiment we have applied acute irradiation. In a real Martian scenario, hypothetical life forms would be exposed to chronic radiation; and this would have allowed the activation of adaptation mechanisms, not possible under an acute irradiation condition. For this reason, further experiments regarding the exposure of hydrated fungal colonies on chronic γ-rays will be necessary to understand whether microorganisms may cope with continuous damages by chronic radiation exposures.

Acknowledgements

This research was financially supported by the Italian Space Agency (ASI), ASI grant N. 2019-3-U.0, Life in Space). We acknowledge the ENEA-Casaccia research center team (Dr. Alessia Cemmi and Dr. Ilaria Di Sarcina) for handling the irradiation. We thank the PNRA (Italian National Program for Antarctic Research) for supporting sample collection in Antarctica and the Italian National Antarctic Museum "Felice Ippolito" for funding the MNA-CCFEE (Culture Collection of Fungi from Extreme Environments).

2.3 Fungal growth tolerance, metabolic activity recovery and ultrastructural damages in hypersaline substrata

Abstract

Evidences from recent Mars landers identified the presence of perchlorates salts at 1 wt % in regolith (Soudi et al., 2017) and their widespread distribution on the Martian surface (Li et al., 2015) that has been hypothesized as a critical chemical hazard for possible life forms. However, the hypersaline environment may also potentially preserve life and its biomolecules over geological timescales. The high concentration of natural perchlorates is scarcely reported on Earth, even if the presence of perchlorates in soil and ice has been recorded in some extreme environments such as the McMurdo Dry Valleys in Antarctica (Kounaves et al., 2010), which are considered one of the best terrestrial analogues for Mars (Friedmann, 1982; Wynn-Williams et al., 2000; Onofri et al., 2004; Bishop et al., 2014). In the frame of "Life in space", an Italian project of astrobiology, the polyextremophilic black fungus *Cryomyces antarcticus* CCFEE 515, a eukaryotic test organism isolated from Antarctic cryptoendolithic communities, has been tested for its resistance, when grown on different hypersaline substrates. In addition, *C. antarcticus* was grown on Martian relevant perchlorate soils (40% of $Mg(ClO_4)_2$ and 60% of $Ca(ClO_4)_2$).

Keywords: Perchlorates tolerance, deliquescence, growth, MTT, eukaryotic organism

Cassaro A., Pacelli C., Onofri S. Fungal growth tolerance, metabolic activity recovery and ultrastructural damages in hypersaline substrata. Prepared for the submission on "Frontiers in microbiology" (special issue: "Rising stars II").

2.3.1 Introduction

Since the 1970s, during the NASA Viking lander mission, the presence of oxidizers on Mars surface has been hypothesized from GC-MS data obtained by life detection instruments (Klein, 1978). While the distribution of chlorine was further confirmed by Mars Pathfinder (Gellert et al., 2004), Spirit and Opportunity rovers (Rieder et al., 2004) and Odyssey orbiter (Keller et al., 2006), its chemical form was established only with the launch of NASA Phoenix Mars and Mars Science Laboratory (MSL) landers on Mars (Quinn et al., 2013). The Phoenix's Wet Chemistry Laboratory analysis found that mostly of chlorine detected in Martian surface was in the form of perchlorate salts (Li et al., 2015), mainly present in regolith as mixture of $Ca(ClO_4)_2$ and $Mg(ClO_4)_2$ with a concentration of 0.4-0.6 wt% and a small amount of Na^+ and K^+ (Hecht et al., 2009). Recently, the Sample Analysis at Mars (SAM) instrument on the MSL lander discovered perchlorates in soil samples at Gale Crater (Glavin et al., 2013), the Rosalind Franklin rover landing site. The discovery of perchlorates occurred not only on Mars, but in several celestial bodies, including Moon and meteorite samples (Glavin et al., 2013; Jackson et al., 2015; Jaramillo et al., 2019). The finding of salts in Martian meteorite EETA79001 (Kounaves et al., 2014) confirms their broad presence on the planet.

The widespread presence of perchlorates on Mars surface represents a challenge for habitability and the detection of hypothetical life forms, since they can be harmful for life as we know it (Stern et al., 2015; Ming et al., 2014; Wadsworth and Cockell, 2017). The perchlorates in the first few centimeters of the Martian soil has important implications for the detection of habitability: perchlorates could both lower the freezing temperature of water (Möhlmann and Thomsen, 2011) and either form stable hydrated compounds and liquid solutions by absorbing atmospheric water vapor through deliquescence (Zorzano et al., 2009; Nuding et al., 2014). In fact, perchlorates are highly hygroscopic compounds (Soudi et al., 2017) and, at the appropriate range of temperature, they are able to absorb humidity and melt into the aqueous solution creating brines (Martin-Torres et al., 2015). The presence of an aqueous thin film could be important for a putative life-form on Mars, because water is essential for life as we known it (McKay, 2006). On other hands, perchlorates are known as toxic chemicals

and strong oxidants (Soudi et al., 2017) for cell membranes integrity (Urbansky, 1998), especially when combined with a highly radiation environment.

The search for life on Mars is mainly based on the knowledge of surface and subsurface conditions, but also on the survivability of Earth organisms in extreme environments and under Mars-like conditions (Cockell et al., 2016). Mars-like conditions can be found in extremely arid environment like deserts, where the natural occurrence of perchlorates has been generally found (Jackson et al., 2015; 2016). High concentration of chlorates and perchlorates has been detected at Lake Vida brines in McMurdo Dry Valleys (Antarctica) (Kounaves et al., 2010; Kenig et al., 2016) and in Atacama Desert (Chile) (Trumpolt et al., 2005; Catling et al., 2010), two of the closest terrestrial analogues to Mars past and present environments (Bishop et al., 2013).

Several terrestrial microorganisms survived when exposed to perchlorates and, based on their relationship with high salinity, they are divided into two groups: organisms that live in presence of perchlorates and organisms that need perchlorates for their metabolism (Beblo-Vranesevic et al., 2017). Several studies reported that different bacteria strains and only a few archaea organisms are able to metabolize perchlorates, producing chlorite (ClO_2^-) as a toxic end-product of (per)chlorate by nitrate reductase (Coates and Achenbach, 2004; Nerenberg, 2013).

The acidophilic iron sulfur bacterium *Acidithiobacillus ferrooxidans*, arrest its reproduction in the presence of 0.022 M (0.5%) and 0.044 M (1%) of $Mg(ClO_4)_2$ (Bauermeister et al., 2014), while spores of *Bacillus subtilis* are able to germinate up to 0.1 M of $NaClO_4$ (Nagler and Moeller, 2015).

As reported in Laye and DasSarma (2018), the cold-adapted halophilic Antarctic archaeon *Halorubrum lacusprofundi* demonstrates its ability to grow anaerobically on 0.04 M concentration of perchlorate, while the growth is halved at increased concentrations. *Planococcus halocryophilus* has been tested in presence of NaCl, $MgCl_2$, $CaCl_2$, $NaClO_4$, $Mg(ClO_4)_2$ and $Ca(ClO_4)_2$, showing a good growth rate (Heinz et al., 2019). Soudi et al. (2017) reported bacterial growth at concentrations of chlorate up to 2.75 M and at 1 M of perchlorate salts. Despite several studies on perchlorate tolerance are reported, the fungal survivability is poorly understood. Fungal survivability investigations are

mainly on chlorate species. *Hortaea werneckii* and *Phaeotheca triangularis* grow at up to 25% (w/v) NaCl, while *Aureobasidium pullulans* grows up to 10% (Turk et al., 2004). Recently, Heinz et al. (2021), reported the high survivability of *Debaryomyces hansenii* on $NaClO_4$.

In this context, Life in Space (Origin, presence and persistence of life in space: from molecules to extremophiles), an Italian Space Agency funded project, aims to understand the physiological responses of the cryptoendolithic black fungus *Cryomyces antarcticus* when grown in presence of perchlorate salts. The black fungus, isolated from the Antarctic cryptoendolithic communities, is considered as a eukaryotic test organism in astrobiological studies for its high resistance when exposed, in dehydrated conditions, to full solar radiation (including UV-A, UV-B, and UV-C) (Onofri et al., 2008; Pacelli et al., 2017a); to γ-rays up to 55.81 kGy (Pacelli et al., 2017b), deuterons (up to 1.5 kGy), and to space and Mars-like conditions in Low Earth Orbit (LEO) (Onofri et al., 2015; 2019); and in hydrated conditions up to 2000 Gy iron ions (Fe^{26+}) irradiation (Pacelli et al., 2021a) and to high dose of ionizing X-rays (up to 0.3 kGy, Pacelli et al., 2018).

Here, fungal colonies were grown on **i**) increasing concentrations of four perchlorate salts to test their tolerance to hypersaline environment and **ii**) Mars relevant perchlorate salts (0.4-0.6 wt%) cultivation medium to assess the possibility of survival in a Mars-like environment.

2.3.2 Materials and methods

2.3.2.1 Test-organism, perchlorates medium preparation and activity water measurement

The test organism is the black fungus *C. antarcticus* CCFEE 515, isolated by R. Ocampo-Friedmann from sandstone collected at Linnaeus Terrace in McMurdo Dry Valleys (Southern Victoria Land, Antarctica) by H. Vishniac, during the Antarctic expedition of 1980-1981 (Selbmann et al., 2005). Colonies of the fungus were grown at various concentrations (Table 1) of the following salts: K-perchlorate ($KClO_4$), Na-perchlorate ($NaClO_4$), Mg-perchlorate ($Mg(ClO_4)_2$), Ca-perchlorate ($Ca(ClO_4)_2$). The salts were cold dissolved in distilled water and then filtered with a filtration apparatus containing a filtration membrane with 0.2 μm pores, until the same molarity equivalent to

1M was obtained. Mars relevant salts medium containing 60% of $Ca(ClO_4)_2$ and 40% of $Mg(ClO_4)_2$ was prepared, with a final concentration of 72 mM and 48 mM, respectively. Due to the limited solubility of the $KClO_4$, concentration above 90 mM could not be tested. The activity water (a_w) of each medium was measured by using an HygroPalm (Rototronic, Bassersdorf, Germany) water activity meter (Decagon Devices, Inc., Pullman, WA). The instrument was run at room temperature, and providing 3 output data: percentage of water present in the slide with the pellet, ratio in g/Kg to the amount of water present, ambient temperature. Petri dishes were prepared by plating fungal colonies (fungal concentration 20000 CFU/mL) and spread on 2% Malt Extract Agar (MEA; malt extract, powdered 30 g/l; peptone 5 g/l; agar 15 g/l; Applichem GmbH, Darmstadt, DE) medium, with the addition of the different salt concentrations. For Mars relevant substrata, colonies were plated at fungal concentration of 40000 CFU/mL. Fungal colonies were grown at 15 °C that is the optimal grow temperature for 3 months; the experiment was performed in quadruplicates. After 3 months the grown colonies were counted for the survival analyses.

Table 1. Concentrations (*) and %wt for each tested perchlorate

$NaClO_4$	%wt/vol [w/v]	$KClO_4$	%wt/vol [w/v]	$Mg(ClO_4)_2$	%wt/vol [w/v]	$Ca(ClO_4)_2$	%wt/vol [w/v]
5	0.06	5	0.07	5	0.16	5	0.12
50	0.61	50	0.7	50	1.6	50	1.19
150	1.84	80	1.11	70	2.31	100	2.39
190	2.32	90	1.25	80	2.65	160	3.8
200	2.44			100	3.31	170	4.06
210	2.57			120	4	180	4.30
220	2.69			140	4.6	190	4.54
230	2.82			145	4.80	200	4.78
				150	5	210	5.02

*Concentrations are expressed in millimolarity (mM)

2.3.2.2 Metabolic activity estimation by MTT (3-(4,5-dimethylthiazol-2-yl)-2,5-diphenyltetrazolium) assay

For the metabolic activity analyses, a suspension containing 100 µL of fungal micro-colonies (3.5 x 10^5 cells/mL) and a solution of 0.5 mg/mL of MTT in Phosphate-Buffered Saline (PBS) was placed into 96-well microplates. After incubation at room temperature for 48 and 72 hours, MTT solution was removed with a multi-channel pipette and 100 µL of DMSO (DiMethyl SulfOxide) was added on each well. The absorbance of each samples was read at 595 nm with a microplates spectrophotometer (BMG NOVOstar microplate fluorometer, MTX Lab Systems), after time intervals of 10, 20 and 30 minutes, subtracting the absorbance relative to wells containing only MTT.

Results of the absorption were normalized by the number of cells per well and these values were normalized by dividing by the non-treated samples (Ctr).

2.3.2.3 Ultrastructural investigation

Transmission Electron Microscope (TEM)

Colonies grown on increased concentration of perchlorate cultivation medium were taken and prepared for microscopy analyses according to the protocol reported in Pacelli et al. (2017). TEM observations were performed with a JEOL 1200 EX II electron microscope at the Great Equipment Center, section of Electron of the University of Tuscia (Viterbo, Italy). Micrographs were acquired with an Olympus SIS VELETA CCD camera and iTEM software.

2.3.3 Results

2.3.3.1 Growth tolerance to perchlorate salts

The growth ability of *C. antarcticus* in presence of perchlorate salts was assessed by counting the colony-forming units (CFUs) after 3 months of incubation (Table 1).

Overall, a common trend in the fungal growth was detected: a decrease as the perchlorate concentration increases. However, *C. antarcticus* shows survivability up to 220 mM of Na-perchlorate (2% of survivors, Fig. 1A) and 145 mM of Mg-perchlorate (2% of survivors, Fig. 1C).

A concentration of 200 mM of Ca-perchlorate (3% of survivors) strongly affected the fungal growth ability (Fig. 1D). The solubility of the K-perchlorate, limited the survival analysis, however the fungus reported a good survival up to 90 mM (Fig. 1B).

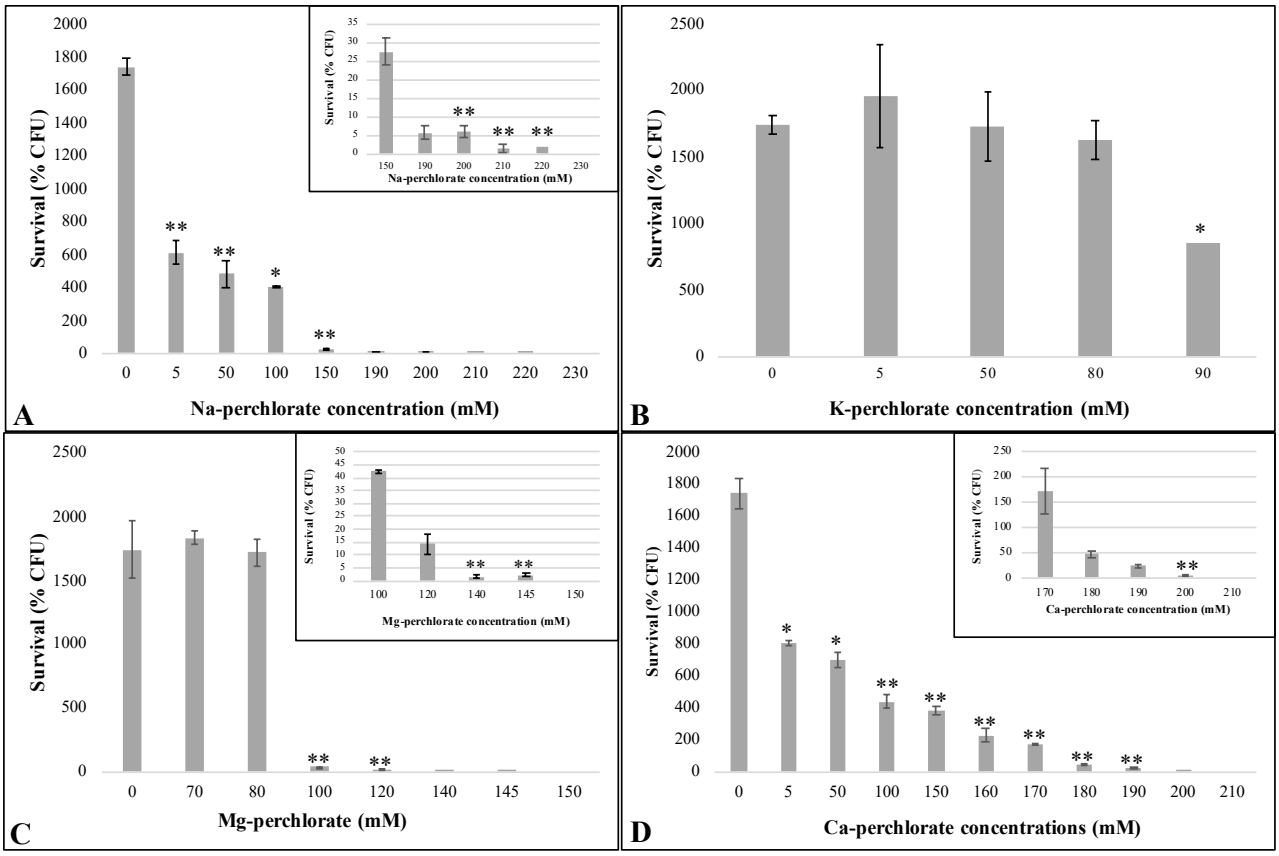

Figure 1. Survival ability of *C. antarcticus* colonies after growth on different perchlorates concentrations. A) Na-, B) K-, C) Mg-, and D) Ca-perchlorates. All concentrations are expressed in mM. Significant differences were calculated by *t test* with * = $p < 0.05$ and ** = $p < 0.001$.

2.3.3.2 Growth tolerance to Mars-relevant perchlorate salts

The growth ability of *C. antarcticus* in the presence of Mars-relevant perchlorate concentrations was investigated after incubation of fungal colonies in 2.4 mM ClO_4 cultivation medium (40% Mg- and 60% Ca-perchlorates mixture). An average of 80% of survivors have been detected (data not shown).

2.3.3.3 Water activity measurements

The activity of water is considered as a fundamental parameter for knowledge about the organization and habitability of Martian brines (Toner and Catling, 2016). The water activity is the equilibrium transience of water vapor over a solution (f) relative to the f transience of water vapor over pure water (f_0) ($aw = f/f_0$). This transition process could be approximated by partial vapor pressures (p and p_0) at low pressures. In this condition, a_w may be defined as similar to p/p_0 ratio, which is equivalent to the equilibrium relative humidity (RH) over a salt solution ($RH_{eq} = a_w$). The water activity measurements of our samples are reported in Table 2, and are in the range between 0.92 and 0.94.

Table 2. Water activitiy (a_w) values in perchlorates salt solutions

$NaClO_4$	a_w	$KClO_4$	a_w	$Mg(ClO_4)_2$	a_w	$Ca(ClO_4)_2$	a_w	T (°C)	g/Kg
5	0.928	5	0.934	5	0.936	5	0.932	17.6	24
50	0.929	50	0.932	50	0.934	50	0.933	17.6	24
150	0.929	80	0.93	70	0.934	100	0.934	17.6	24
190	0.933	90	0.927	80	0.937	160	0.932	17.6	24
200	0.933			100	0.94	170	0.925	17.6	24
210	0.932			120	0.94	180	0.931	17.6	24
220	0.933			130	0.94	190	0.934	17.6	24
230	0.935			140	0.937	200	0.932	17.6	24
				145	0.937	210	0.934	17.6	24
				150	0.936			17.6	24

*Concentrations are expressed in millimolarity (mM)

2.3.3.4 MTT assay

In this study, the MTT assay was performed in order to study changes in the metabolic activity of fungal colonies grown on perchlorate salts at different concentrations. MTT assay was performed

only on samples grown on the lower, the intermediated and the higher perchlorate concentration tested.

During the assay, the produced formazan is a clear indicator of the metabolic activity in a cell. The quantity of produced formazan was detected through spectrophotometric measurements, comparing treated and control cells. The metabolic activity was tested after 48 and 72 hours of DMSO addition, since no differences were reported among different incubation period, only the results after 72 hours of incubation were reported.

The results showed a decrease of metabolic activity as the perchlorate concentration increase (Fig. 2). For colonies grown on Ca-perchlorate, no statistical differences in metabolic activity were observed between Ctr, 50- and 150 mM concentration. A reduction in formazan production, and therefore in metabolic activity, was detected in samples grown on 200 mM (Fig. 2). Samples grown on Na-perchlorate showed no differences between Ctr and 50 mM samples, while a reduction in metabolic activity was revealed at 150 and 220 mM (Fig. 2). A similar trend - decreasing in metabolic activity as perchlorate concentration increases- was observed for samples grown on K- and Mg-perchlorates. Surprisingly, a decrement of metabolic activity was detected at 80 mM of Mg-perchlorate (Fig. 2).

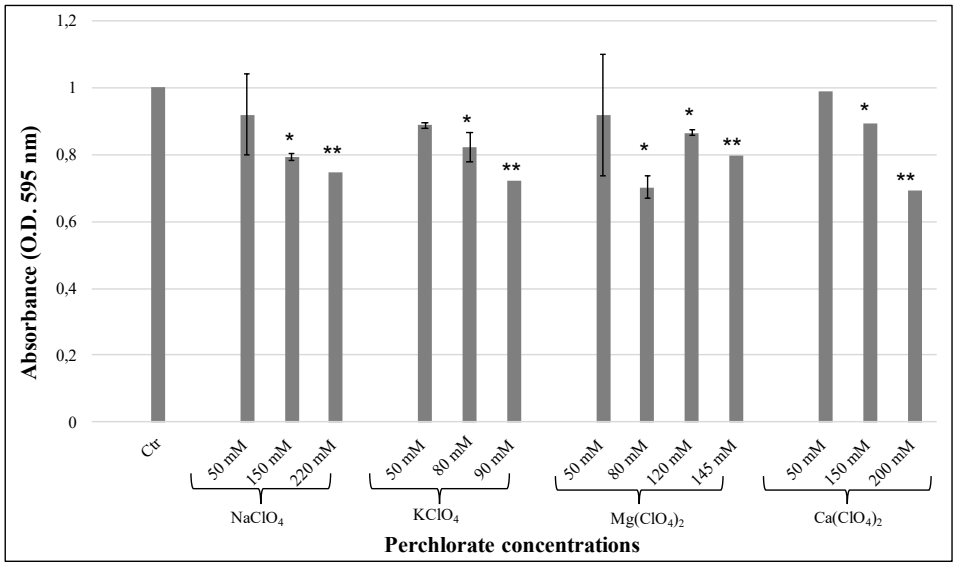

Figure 2. Effect of different perchlorate concentrations on the metabolic activity of *C. antarcticus* colonies. The results showed are after 72 hours of incubation with the DMSO. Concentrations are expressed in mM. Data were normalized against the control. Significant differences were calculated by *t test* with * = $p < 0.05$ and ** = $p < 0.001$.

2.3.3.5 Ultrastructural investigation: TEM observations

TEM observations (Figs. 3, 4 and S1) were performed only on samples grown at the lower, the intermediated and the higher perchlorate concentration, as for the metabolic activity assay. Control samples (Fig. 3A and B) showed a well-organized cells: a dense cytoplasm with well-visible cellular structures. Nucleus, mitochondrion and vacuoles are highly preserved. Lipids bodies are also visible (white arrow). A well-preserved cellular membranes and cell-walls have been reported (Fig. 3A and E, black arrow). Fungal colonies grown on Na-perchlorate (50, 150 and 220 mM, Fig. 3B, C and D; respectively) showed a well-preserved cellular membranes and cellular walls, even if a thinning of the cell walls has been reported for samples grown on 220 mM concentration (Fig. 3D, black arrow). The internal structures are scarcely distinguishable: vacuoles and lipid bodies are still visible unlike the nuclei and mitochondrion (Fig. 3B, C and D). Figure 3F, G and H reported TEM images of cells grown on increasing K-perchlorate concentrations. As reported for samples grown on Na-perchlorate, the only internal structure reported are lipid bodies (Fig. 3H, white arrow). Structures indicate with a black arrow correspond to damaged mitochondrion (Fig. 3F and G). In figure 3H, peculiar vacuolar structures, surrounded by melanin granules are reported (red arrows). Figure 4B, C and D shows TEM image of fungal cells grown Mg-perchlorate. Fig. 4B reported well-preserved cells grown on 50 mM of Mg-perchlorate with nucleus, mitochondrion (black arrow) and vacuoles (white arrow), compared to control sample (Fig. 4A). On the contrary, cells grown at higher concentration (120 and 145 mM, Fig. 4C and D; respectively) showed a not well-organized cytoplasm, with a high amount of melanin granules (white arrow). Cells at 145 mM of Mg-perchlorate showed a cell wall indentation (Fig. 4D, red arrow). Similarly to control sample (Fig. 4E), well-structured cells were reported for samples grown at 50 and 150 mM of Ca-perchlorate (Fig. 4F and G). Despite the increase in vacuoles size (Fig. 4G, white arrow), nuclei and mitochondrion are still distinguishable (Fig. 4G, black arrow).

A slack cytoplasm characterized by abundant melanin granules was reported for cells grown on 200 mM of Ca-perchlorate (Fig. 4H).

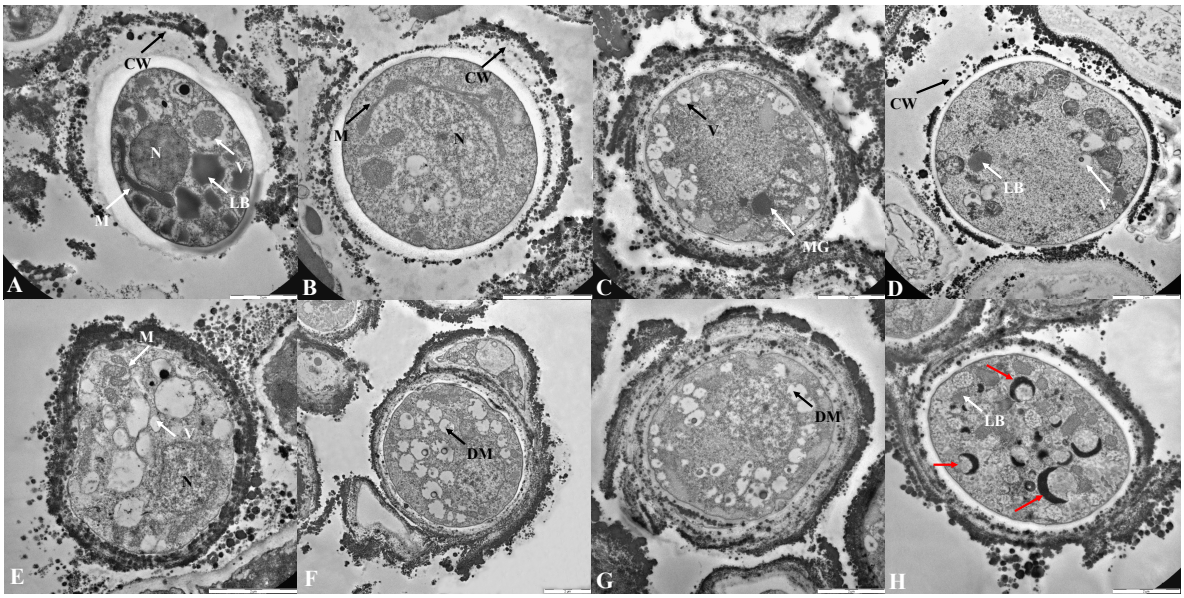

Figure 3. TEM images of *C. antarcticus* cells grown on A) MEA (no salt, control), B) 50 mM, C) 150 mM and D) 220 mM of Na-perchlorate; E) MEA (no salt, control), F) 50 mM, G) 80 mM and H) 90 mM of K-perchlorate. Scale bar: 2 µm. N: nucleus; M: mitochodrion; DM: damaged mitochodrion; CW: cell wall; LB: lipid body; V: vacuoles; MG: melanin granules; red arrow: cell wall indentation.

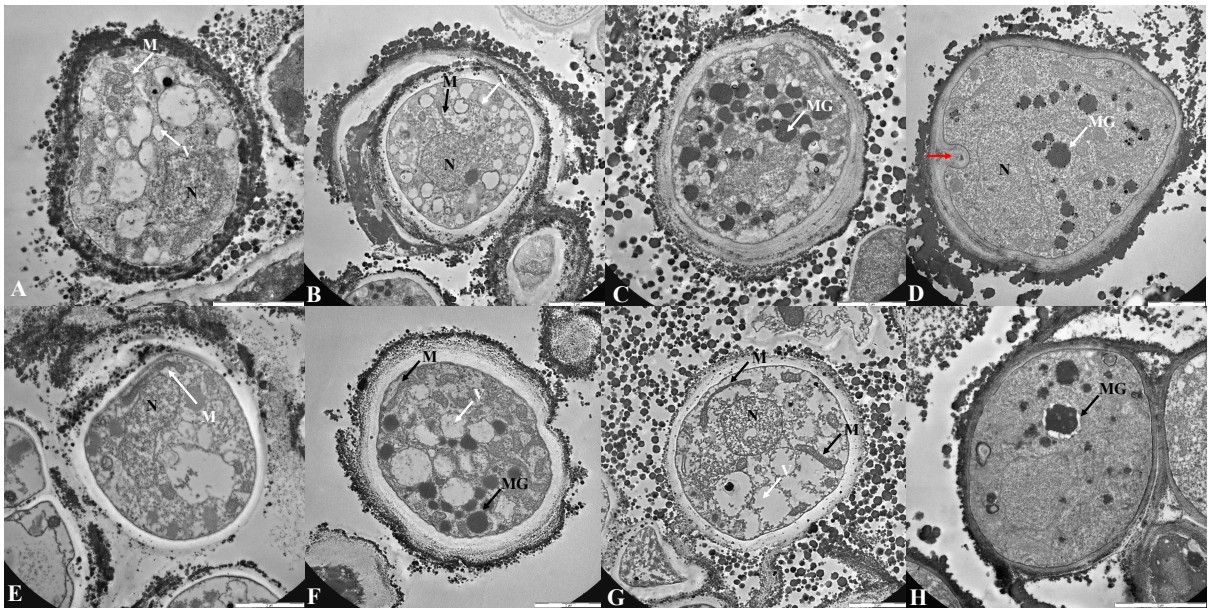

Figure 4. TEM images of *C. antarcticus* cells grown on A) MEA (no salt, control), B) 50 mM, C) 120 mM and D) 145 mM of Mg-perchlorate; E) MEA (no salt, control), F) 50 mM, G) 150 mM and H) 200 mM of Ca-perchlorate. Scale bar: 2 µm. N: nucleus; M: mitochodrion; DM: damaged mitochodrion; CW: cell wall; LB: lipid body; V: vacuoles; MG: melanin granules; red arrow: cell wall indentation.

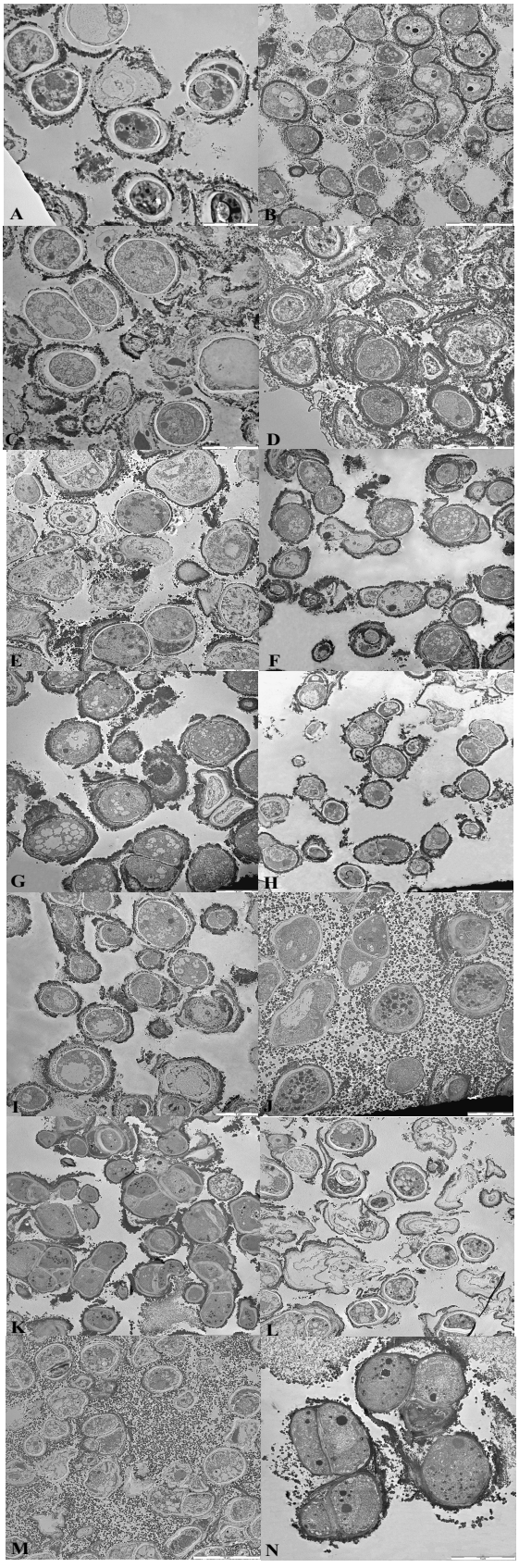

Figure S1. TEM images of *C. antarcticus* cells grown on A, B) MEA (no salts, controls), C) 50 mM, D) 150 mM and E) 220 mM of Na-perchlorate; F) 50 mM, G) 80 mM and H) 90 mM of K-perchlorate; I) 50 mM, J) 120 mM and K) 145 mM of Mg-perchlorate; L) 50 mM, M) 150 mM and N) 200 mM of Ca-perchlorate. Scale bar: 2 μm.

2.3.4 Discussions

The aim of this work was to investigate the survivability, metabolic activity recovery and the ultrastructural damages of the Antarctic cryptoendolithic black fungus *C. antarcticus* after grow in presence of perchlorates at different concentrations. The fungus was also tested in the presence of Mars-relevant perchlorate concentration, as 2.4 mM perchlorate ions (60 and 40% mixture of Mg- and Ca-perchlorate, respectively), as reported by the NASA's Phoenix Mars Lander (Hassler et al., 2014). The results might give insight for the concept of habitability beyond Earth, in particular on Mars. Perchlorate ions are known to damage the main functions of terrestrial living organisms; they interrupt a series of metabolic processes, and also act as oxidizing agents causing cell membrane damages (Urbansky, 1988). On Earth, the occurrence of perchlorates is limited only in certain arid environments (Trumpolt et al., 2005; Catling et al., 2010); while on Mars they have been detected in high concentrations at different location on the planet, determining the interest of the astrobiological community into the investigation of perchlorate microbial tolerance.

In addition, their importance is given by the fact that they favor the presence of transient liquid water on the Martian surface (one of the main factors to determine the habitability of a planet). Although liquid water is not a stable condition, geomorphological structures named Recurring Slope Lineae (RSL), have been detected on the planet in evidence of the seasonal presence of water. Perchlorates, in brines in the near surface, are able to maintain fluid state for several days under Martian environment conditions (Orosei et al., 2018; Chevrier et al., 2009; Hennings et al., 2013). The presence of perchlorates in Martian regolith may reduce the crystallization temperature of water, also allowing the activity of hypothetical microorganisms on Mars (Beblo-Vranesevic et al., 2020), and persisting in the first layer of regolith could support the preservation of cellular components (Primm et al., 2018).

In this context, the exposure of *C. antarcticus* cells to increasing perchlorate concentrations (Fig. 1) revealed that growth was: (i) not affected in 90 mM of K-, 80 mM of Mg-, 50 mM of Ca perchlorate; (ii) slightly reduced in 50 mM Ca-perchlorate; (iii) reduced in 100 mM of Na-, 160 mM of Ca-,

perchlorates; and (iv) completely inhibited in 230 mM Na- perchlorate, 150 mM Mg-perchlorate and 210 Ca-perchlorates (Fig. 1). We are not able to test the limit of growth in K-perchlorate due to its solubility limit. In addition, a good survivability was found for cultivation medium containing the perchlorates concentration finding at the Phoenix landing site (2.4 mM, data not shown). It has been hypothesized that meristematic grow, a peculiarity of black yeast, could enhance the ability to withstand this stressful condition (Wollenzien et al., 1995)

Similar concentrations were reported for the survivability of the cyanobacterium *Chroococcidiopsis* CCMEE 029 (Billi et al., 2021). A long-term exposure did not affect the survivability of the cyanobacterium up to 5 mM Na-, Mg- and Ca-perchlorates. A decrease with the increase of perchlorate concentration was reported: a slight reduction was observed in 50 mM Na-perchlorate and a complete loss was reported at 100 mM of Ca- and Mg-perchlorates (Billi et al., 2021). Contrary, a concentration of 100 mM of Na-perchlorate reduced the survivability of *C. antarcticus*.

Despite the good survivability recorded for *C. antarcticus*, the highest perchlorate tolerance was reported for the halotolerant yeast *D. hansenii* grown at 2.4 M of Na-perchlorate (Heinz et al., 2020). Several other studies reported the growth of non-fungal species in perchlorate solutions. The halophilic archaea *Halobacterium* strain NRC-1, *Hbt. salinarum* R1, *Haloferax volcanii*, *Hfx. mediterranei, Hfx. denitrificans, Hfx. gibbonsii, Haloarcula marismortui, and Har. vallismortis* demonstrated their ability to grow up to 0.4 M of Na-perchlorate (Oren et al., 2014). Al Soudi et al. (2016), recorded a robust grow of *Halomonas venusta* at 1 M of Na-perchlorate, while *Planococcus halocryophilus* survived up to 1.1 M of Na-perchlorate (Heinz et al., 2019). *Halorubrum lacusprofundi* showed a higher sensitivity to Mg-perchlorate than Na-perchlorate (50% inhibition at 0.3 M Na-perchlorate versus 0.1 M for Mg-perchlorate; Laye et al., 2018). Surprisingly, the tolerant bacterium *Hydrogenothermus marinus* resisted to an exposure of 5 min in 5 M Na-perchlorates at room temperature, reported not change in survivability, while a 96 h-exposure resulted in a reduced survivability (Beblo-Vranesevic et al., 2017). The water activity is known to be a major limiting factor for growth (Stevenson et al., 2015). Since the addition of salts to water may decrease the water

activity, this parameter was determined for each tested concentration. All the measurements are in a range between 0.92 and 0.94 (Table 2), significantly larger if compared to the limiting value of water activity ≈0.6 to support life. No differences are reported among perchlorate salts.

The survival results were further confirmed by the metabolic activity recovery. A decrease in metabolic activity with the increasing of perchlorate concentration was reported in all samples (Fig. 2). However, it should be taken into account that a good value of metabolic activity was reported even in samples where the growth ability was scarcely represented. Changes at ultrastructural level were detected with TEM observation. TEM images highlighted a slack cytoplasm in the cells grown on perchlorates, comparing with a dense cytoplasm of control cells. In control and low-perchlorate concentration, nuclei, mitochondrion, vacuoles and lipid bodies are well-preserved. Cells grown on Na-perchlorate (Fig. 3B, C and D), showed a cytoplasm with vacuoles and lipid bodies. At the concentration of 200 mM of Na-perchlorate, a decrease in cell wall thickness was observed (Fig. 3D). Similar results were obtained at the concentration of 150 and 200 mM of Ca-perchlorate (Fig. 4G and H). This condition is probably related to changes in the molecular composition: a branching degree of the polysaccharides, an elevated β-1,3-glucan level (Lesage et al., 2006), or the incorporation of proteins into the cell wall as a result of changed glucan synthesis (Smits et al., 2001), or elevated chitin levels (Pessoni et al., 2005). The decrease of cell wall thickness may be caused by the osmoadaptation processes; the mechanisms at the basis of will be elucidated in further studies. Colonies grown on K-perchlorate (Fig. 3F, G and H), showed the presence of damaged mitochondrion, compared to control sample (Fig. 3E) and at higher concentration, abundant vacuolar structures, surrounded by melanin granules are reported (Fig. 3H). Also, in samples grown on Mg- and Ca-perchlorates (Fig. 4B, C, D, F, G and H), lipid bodies and melanin granules are accumulated within the cytoplasm. It is demonstrated that pigmentation may protect cells from various stressors (Chung et al., 2003; Mandal et al., 2007). In this context, cells may act a protection strategy accumulating and secreting melanin granules. Similar structures were reported in TEM images of *H. werneckii* after growth on NaCl (Kogej et al., 2007). Melanin granules may limit the cell-wall

permeability by reducing the size of cell wall pores. A reduction pores size from 10.6 in non-melanized to 4 nm in melanized cell of *Cryptococcus neoformans*, was reported (Jacobson and Ikeda, 2005). In this context, a comparison with non-melanized *C. antarcticus* cells should be performed. In addition, an investigation of osmolytes production should be performed. As reported in Kogej et al. (2007), a combination of compatible solutes supported by a cell-wall melanization, was useful for the growth of *H. werneckii* on high NaCl concentrations.

In overall, the survivability of the fungus *C. antarcticus* to increased salinities are similar to that of halotolerant yeasts species. The current work is the first demonstration that a non-halophilic terrestrial eukaryotic organism can growth in hypersaline substrata, including Mars relevant perchlorate salts, potentially present near the surface of Mars or near the oceans of icy worlds. Further studies aiming at investigate the mechanisms at the basis of the fungal perchlorate tolerance will be performed, trying to identify the genes involved in the resistance. The identification of novel genes will elucidate the molecular strategies of microorganisms to withstand in presence of perchlorates. This could be exploited to create perchlorate-resistance strains to develop Bioregenerative Life Support Systems (BLSS) based on *in situ* resource utilization (ISRU) (e.g. to remove perchlorate in Martian soil). Also, the investigation of the combined effects of perchlorates and radiation (e.g. UV radiation) will be necessary to understand if conditions similar to those experienced on Martian surface might act as a fungicidal function.

2.3.5 Conclusions

The effects of perchlorates prevalent on the Martian surface are of significant interest to astrobiology from the perspective of the search of life on the planet. Perchlorates have been detected at many different locations on Mars surface and at different concentrations. The ubiquity presence of perchlorate salts on the planet could suggest the possibility of transient liquid water on the surface, thanks to the deliquescence of the salts. In this context, this study provide for the first time, insight about the resistance of the black fungus *C. antarcticus* to high concentration of different perchlorate

species, demonstrating the ability to grow at 0.4-0.6 wt% of $Mg(ClO_4)_2$ and $Ca(ClO_4)_2$ and up to 220 mM of Na-, 200 mM of Ca-, 145 mM of Mg- and 90 mM of K-perchlorates.

Acknowledgments

This work was supported by the Italian Space Agency by ASI grant (ASI N. 2019-3-U.0, Life in Space). The Italian National Program of Antarctic Researches (PNRA) and the Italian National Antarctic Museum "Felice Ippolito" (MNA) are also acknowledged for funding the collection of Antarctic samples CCFEE. Authors would also to acknowledge the Dr. Annarita Taddei for supporting TEM analyses.

3. Insights into the biosignatures detection

3.1 The ground-based BIOMEX Experiment Verification Tests for life detection on Mars

Abstract

The success of an astrobiological search for life campaign on Mars, or other planetary bodies in the Solar System, relies on the detectability of past or present microbial life traces, namely biosignatures. Spectroscopic methods require little or no sample preparation, can be repeated essentially endlessly, and can be performed in contact or even remotely. Such methods are therefore ideally suited to use for the detection of biosignatures, which can be confirmed with supporting instrumentation. Here, we discuss the use of Raman and Fourier Transform InfraRed (FT-IR) spectroscopies for the detection and characterization of biosignatures from colonies of the fungus *Cryomyces antarcticus*, grown on Martian analogues and exposed to increasing doses of UV irradiation under dried conditions. Results reported significant UV-induced DNA damage but still within thresholds for allowing DNA amplification and detection, while spectral properties of the fungal melanin resulted unaltered, and the pigment detection and identification was achieved via complementary analytical techniques. Finally, this work found that fungal cell wall compounds, likely chitin, were not degraded and still detectable even after high UV irradiation doses. Implications for the preservation and detection of biosignatures in extraterrestrial environments are discussed.

Keywords: biosignature; dark pigments; polysaccharides; polychromatic radiation; simulated conditions; Mars; life-detection

Pacelli, C., **Cassaro, A.**, Catanzaro, I., Baqué, M., Maturilli, A., Böttger, U., Rabbow, E., de Vera, J.-P. P. and Onofri, S. (2021b). The Ground-Based BIOMEX Experiment Verification Tests for Life Detection on Mars. Life, 11(11), 1212.

3.1.1 Introduction

The detection of biosignatures on Mars is of outstanding interest in the current field of astrobiology and drives various fields of research, ranging from new sample collection strategies to the development of more sensitive detection techniques. The effects of radiation on the stability of biosignatures are essential to be investigated. On Earth, the preservation of organic biosignatures is principally influenced by the rate of biological records production and by that of alteration from biological recycling and abiotic factors (e.g., radiation), which must not exceed the former one. Some types of biosignatures have been found to be more resistant to certain degradation processes, while some environments may be more favorable in preserving some types rather than others (Cockell et al., 2005; Dartnell et al., 2012; Dartnell and Patel, 2014; Poch et al., 2013). Research on these issues is a driving factor in designing explorative strategies for life-detection missions throughout the Solar System.

Ultraviolet (UV) radiation, especially shorter wavelength UVC radiation, is known to be a damaging factor to organisms and potential organic biosignatures. On Mars, for example, the exposure to the surface UV radiation can degrade common biologically relevant organic molecules to simple organics that may confound the identification of biosignatures even on relatively recently exposed surfaces (Ehlmann et al., 2011; Thomas et al., 2017; Travis et al., 2003; Dartnell et al., 2007). On Earth, the interiors of rocks provide a protected environment for extant life in some of the most inhospitable terrestrial environments, including the Antarctic Dry Valleys. The endolithic habitat provides thermal buffering, physical stability, and protection from incident UV, solar radiation, and dryness (Friedmann and Ocampo-Friedmann, 1984). Microorganisms can be found at depths of a few to tens of millimeters in rock interiors inhabiting these protected environments; they are the so-called cryptoendolithic organisms.

The UV environment on Mars differs significantly from that on present-day Earth, and it can significantly influence how biosignatures may persist. The Martian atmosphere (primarily composed

of CO_2) effectively absorbs all UV radiation below 190 nm and has a modest absorbing effect from 190-200 nm, but atmospheric absorbance at longer wavelengths is negligible, and therefore UV with wavelengths >200 nm interacts with the surface (Patel et al., 2002). On Earth most of the UVB (280-315 nm) and UVC (200-280 nm) radiation is absorbed by ozone (O_3); conversely this molecule is in low concentrations in the current Martian atmosphere (Vago et al., 2015). The actual UV flux reaching the surface of Mars is influenced by various factors as latitude, season, and orbital position of the planet, and can also fluctuate due to small seasonal build-ups of O_3, as well as dust load in the atmosphere (Gómez-Elvira et al., 2014; Patel et al., 2002). The average UV irradiance (200-400 nm) at the Martian surface has been modelled to be ~50 J/(s·m^2) (Kuhn and Atreya, 1979; Schuerger et al., 2003). The UVB and UVC represent the UV Mars incident radiation wavelengths that are extremely harmful to DNA and other common biological molecules (Cockell et al., 2005; Dartnell et al., 2012; Poch et al., 2013; Stalport et al., 2009). Several direct measurements of UV irradiance have been made by the Curiosity rover, showing that the maximum total UV flux at Gale Crater may be closer to 20 J/(s·m^2), which is less severe than the typical modelled irradiance but still not favorable for surface habitability (Gómez-Elvira et al., 2014). Additional factors such as ionizing radiation, presence of oxidants or other reactive species in the atmosphere and regolith on Mars would appear to make long-term survival of organisms or organic biosignatures on the surface highly unlikely (Carrier and Kounaves, 2015; Encrenaz et al., 2012; Glavin et al., 2013; Ming et al., 2014; Quinn et al., 2013).

Considering that few works have dealt with the interactions of incident UV flux with minerals and rocks (Patel, 2002, 2003; Moores et al., 2007; Schuerger et al., 2012), even in preparation for *in situ* missions to Mars such as ExoMars and Mars 2020 (Lopez-Reyes et al., 2020; Kinch et al., 2020), the question is not yet well understood and therefore a further necessary step is to identify the extent to which rocks and minerals can provide effective shielding against UV radiation.

The present study was performed in the frame of the BIOlogy and Mars Experiment (BIOMEX), part of the EXPOSE-R2 mission of the European Space Agency (ESA) along with three other

astrobiological experiments, which allowed a 16-month exposure on the outer side of the International Space Station (ISS) from August 2014 to February 2016 (de Vera et al., 2019; Rabbow et al., 2017). The aim of the study was to investigate the resistance and stability of biomolecules to UV irradiation performed during the Experiments Verification Test (EVT) ground-based experiments in preparation for the space-exposure BIOMEX project, as support for the ongoing life-detection missions on Mars (e.g., ExoMars' Rosalind Franklin mission). They included the exposure of *C. antarcticus* MNA-CCFEE 515, a cryptoendolithic black fungus isolated from Antarctic rocks, to increasing doses of polychromatic UV (200-400 nm) irradiation (up to 5.5×10^5 kJ/m^2). Samples were grown on Martian mineral analogues (Phyllosilicatic and Sulfatic Mars Regolith Simulants) and dried before the irradiation treatment. The stability of fungal biomolecules within Martian analogue minerals was investigated through quantitative PCR (qPCR), UV-Visible (UV-Vis) spectrophotometry, and Raman and FT-IR spectroscopies.

3.1.2 Materials and Methods

3.1.2.1 Sample preparation and cultivation conditions

The cryptoendolithic black fungus *C. antarcticus* MNA-CCFEE 515 of the Mycological Section of the University of Tuscia (Viterbo, Italy) was isolated by R. Ocampo-Friedmann from sandstone collected by H. Vishniac at Linnaeus Terrace in McMurdo Dry Valleys (Southern Victoria Land, AQ) during the 1980-1981 Antarctic expedition (Selbmann et al., 2005).

Fungal cell suspension was spread on Malt Extract Agar (MEA) medium (malt extract, powdered: 30 g/L; peptone: 5 g/L; agar: 15 g/L; Applichem GmbH) in Petri dishes and mixed with three separate substrates: Antarctic sandstone (15 g/L) and two Martian regolith analogues (10 g/L). Antarctic sandstone was the Original Substrate (OS) where the fungus occurs naturally, while the Phyllosilicatic Mars Regolith Simulant (P-MRS) and the Sulfatic Mars Regolith Simulant (S-MRS) mimicked regolith of phyllosilicate deposits formed mainly on early Mars and regolith of sulphate deposits

currently observed on Mars, respectively. The mineralogical composition of both Martian analogues was provided by Böttger et al. (2012). These Martian regolith analogues have been chosen to evaluate if they may interfere with the fungal biomolecule detection.

All samples were incubated for 3 months at 15 °C; once fungal colonies were grown, circular portions were cut to fit within the diameter wells (12 mm) of the exposure carrier and then dehydrated in a sterile hood at room temperature overnight.

3.1.2.2 Test facilities and exposure conditions

In the frame of the BIOMEX project, ground-based environmental and space simulations were performed using the Planetary and Space Simulation facilities (PSI) at the Institute of Aerospace Medicine (German Aerospace Center, DLR, Köln, DE). Exposure conditions of the two parts of the EVTs (Experiment Verification Test part 1: performed to simulate several space and Mars-like parameters; Experiment Verification Test part 2: performed to simulate the UV irradiance of 1271 J/(s·m^2) as expected during a 12-month mission in Low Earth Orbit) were reported by de Vera et al. (2019).

All tests were performed in triplicate and untreated samples, kept in the dark at room temperature, were used as laboratory controls (CTRs). Samples of each substrate were either not irradiated or irradiated with one of the fluences from 5.5 × 10^2 kJ/m^2 up to 5.5 × 10^5 kJ/m^2 in the respective irradiation times using a Solar Simulator at 1271 J/s·m^2 as listed in Table 1. For each substrate (OS, P-MRS, S-MRS), we investigated pivotal samples from the EVT2 treatment (i.e., CTRs, 5.5 × 10^2 kJ/m^2, and 5.5 × 10^5 kJ/m^2 samples; Table 1); moreover, *C. antarcticus* colonies grown under physiological conditions on MEA without substrate mixing were used as positive controls (POS CTRs).

Table 1. Sample exposure conditions during the UV irradiation treatment of the EXPOSE-R2 Experiment Verification Tests part 2 (EVT2) from the BIOMEX project. Samples for which results are available and included in the study are highlighted in grey.

Polychromatic UV irradiance with SOL2000 (200–400 nm)	**Irradiation time / sample**	**Resulting fluence / sample[1]**	**Simulated Martian days[2]**	**Sample set substrate**
0 J/(s·m^2) → CTR (laboratory control)	0 s	0 kJ/m^2	-	MEA + OS/ MEA + P-MRS/ MEA + S-MRS
0 J/(s·m^2) → Dark (transport control)	0 s	0 kJ/m^2	-	
1271 J/(s·m^2)	7 min, 12 s	5.5 × 10^2 kJ/m^2 (0.1% ND[3])	0.37	
1271 J/(s·m^2)	1 h, 12 min	5.5 × 10^3 kJ/m^2 (1.0% ND[3])	3.70	
1271 J/(s·m^2)	30 h	1.4 × 10^5 kJ/m^2	94.15	
1271 J/(s·m^2)	60 h	2.7 × 10^5 kJ/m^2	181.57	
1271 J/(s·m^2)	120 h	5.5 × 10^5 kJ/m^2	369.87	
Physiological conditions → POS CTR (positive control)	0 s	0 kJ/m^2	-	MEA

[1] Each set of samples was irradiated with one of the applied fluences (from 5.5 × 10^2 kJ/m^2 up to 5.5 × 10^5 kJ/m^2) in the respective irradiation times, using a Solar Simulator with 1271 J/s·m^2 as listed in the table.

[2] Calculated from Cockell et al. (2000).

[3] ND: neutral density filter. Modified from Vera et al. (2012).

3.1.2.3 DNA integrity assay

3.1.2.3.1 DNA extraction and quantification

Genomic DNA was extracted from the selected EVT2 and POS CTR samples using NucleoSpin Plant II Kit/2011 (MACHEREY-NAGEL GmbH & Co. KG) and following the protocol optimized for fungi (Selbmann et al., 2005).

Samples were quantified using the Qubit Fluorometer (Invitrogen) and the Qubit dsDNA High Sensitivity (HS) Assay Kit (Invitrogen). The assay was performed at room temperature, and three readings for each sample were performed. Dilution factors were calculated after achieving sample concentrations, and DNA samples were diluted up to the same concentration (0.018 ng/µL) before running the qPCR analysis.

3.1.2.3.2 DNA amplification

A real-time qPCR was conducted to quantify the number of fungal Large Subunit (LSU) ribosomal DNA restricted fragments (~330 bp) by using LR3R (GTC TTG AAA CAC GGA CC; Vilgalys and Hester, 1990) and LR5 (TCC TGA GGG AAA CTT CG; Hopple and Vilgalys, 1999) primers. The qPCR reactions were performed in the Bio Rad CFX96 Real-Time PCR Detection System, whereas the Bio Rad CFX Manager software processed results in graphs. Reactions were carried out in triplicate in the 96-well plate with a solution containing: 7.5 µL iQ SYBR Green Supermix (Bio Rad, Milan, IT), 1.0 µL each primer solution (5 pmol/µL), 5.5 ng DNA template in a final volume of 15 µL; for the No Template Control (NTC) sample, 5.5 µL sterile deionized water were added instead of DNA template.

The amplification conditions of the LSU region were retrieved from Selbmann et al. (2011). Fluorescence measurements were performed at the end of each annealing cycle. A melt curve analysis was made by raising the temperature from 65 to 95 °C in 0.5 °C steps for 5 s each. To enable the quantification of PCR products, standard curves based on threshold cycles were produced by re-amplifying tenfold dilution series of PCR products from genomic DNA. Aliquots of each dilution

(equivalent to 1×10^2–1×10^8 LSU copies) in triplicate were used as templates in qPCR. Means and standard deviations were calculated for qPCR products.

3.1.2.3.3 Statistical analysis

The One-way analysis of variance (ANOVA) and the pairwise multiple comparison procedures (Tukey's HSD post-hoc test) were performed on log-transformed data by using RStudio software (R Core Team, 2018; RStudio Team, 2016).

3.1.2.4 Fungal melanin assay

3.1.2.4.1 Pigment extraction and quantification

Melanin was extracted from the previous EVT2 and POS CTR samples following the optimized protocol for black fungi (Pacelli et al., 2020a). After the extraction, serial dilutions of purified pigments (1:5, 1:10, 1:20, 1:50 to 1:100) were made allowing dissolution in an aqueous substrate (NaOH 1 M). To define the correlation between absorbance and wavelength, spectral measurements of all sample solutions were recorded by a UV-Vis spectrophotometry as described in Pacelli et al. (2020a).

To determine the concentration of extracted melanin samples, synthetic DHN (1,8-DiHydroxyNaphthalene) melanin (Sigma-Aldrich) was prepared in NaOH 1 M at concentration of 500 mg/mL, and a standard curve at 650 nm (A_{650}) was obtained as reported in Raman and Ramasamy (2017). Dilutions at 1:5 for the OS and S-MRS samples and at 1:50 for the P-MRS samples were selected for measuring the A_{650}.

3.1.2.4.2 Pigment detection

Raman spectroscopic analysis was performed directly on the previous EVT2 samples at the Raman Laboratory of German Aerospace Center (DLR) in Berlin with an alpha300 R Confocal Raman microscope (WITec) at room temperature and under ambient atmospheric conditions, according to the optimized protocol by Böttger et al. (2012).

The Raman laser excitation wavelength was 532 nm, and the spectral resolution was 4-5 cm^{-1}. A Nikon 10× objective with a 0.25 numerical aperture was used to focus the laser on a 1.5 μm spot. Before the analysis, spectral calibration was performed with pure silicon and paracetamol test samples. As for spectral data acquisitions, image scans were collected following the protocol reported by Pacelli et al. (2021) in order to remove the background noise, while spectral data evaluation and processing were performed with WITec Project FOUR software.

3.1.2.5 Fungal organic compound detection

FT-IR spectroscopic analysis was performed directly on the previous EVT2 samples at the Planetary Emissivity Laboratory of DLR in Berlin.

Spectra were recorded in triplicate on the Vertex 80v FT-IR Spectrometer (Bruker) in reflectance mode and read at a resolution of 4 cm^{-1} in the wavenumber region of 400–10000 cm^{-1} with Spectragryph software (Menges, 2019). Measurements have been performed under evacuated atmosphere to remove atmospheric features from the spectra.

For analyzing the presence of specific organic molecules, the region of interest 600–4000 cm^{-1} was cropped.

3.1.3 Results

3.1.3.1 DNA damage assessment

The integrity of genomic DNA samples was tested by assessing its ability to serve as a PCR template after the polychromatic UV irradiation treatment.

Results showed reduced gene target amplifications while increasing the irradiation dose for all tested samples (Figure 1). Overall, an average of $\sim 3 \cdot 10^5$ copies were amplified in the POS CTR, whereas an average of $\sim 2 \cdot 10^5$ copies were amplified in the non-irradiated (i.e., CTR) samples, $\sim 1.7 \cdot 10^4$ in the

low-irradiated (i.e., 5.5 × 10^2 kJ/m^2) samples, and ~1·10^4 in the high-irradiated (i.e., 5.5 × 10^5 kJ/m^2) samples. Particularly, both OS 5.5 × 10^2 and OS 5.5 × 10^5 showed significantly less amplified copies than OS CTR (14% and 11%, respectively), as well as P-MRS 5.5 × 10^2 kJ/m^2 and P-MRS 5.5 × 10^5 kJ/m^2 with P-MRS CTR (2% and 0.02%, respectively), and S-MRS 5.5 × 10^2 kJ/m^2 and S-MRS 5.5 × 10^5 kJ/m^2 with S-MRS CTR (6% and 1%, respectively).

To summarize, the amplification was successful in all OS, P-MRS, and S-MRS samples, even in the high-irradiated P-MRS (5.5 × 10^5 kJ/m^2) sample, which reported less than 100 copies.

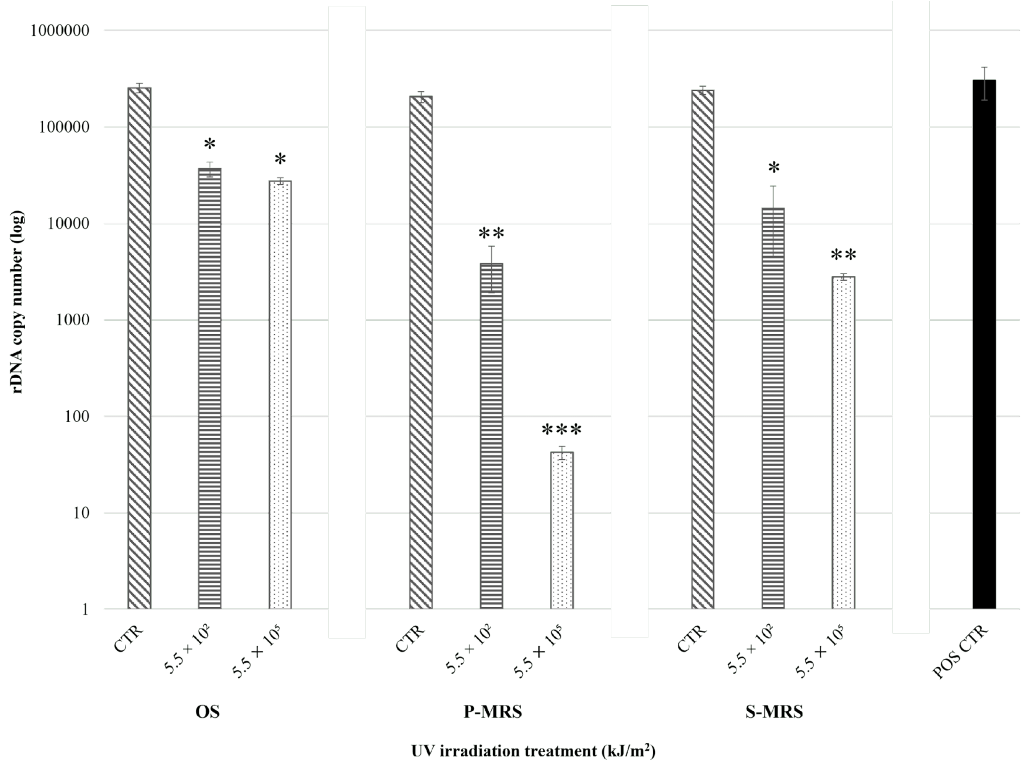

Figure 1. Real-time qPCR of an LSU gene fragment (~330 bp) from *C. antarcticus* after irradiation treatment within EVT2 simulations. On x-axis, increasing polychromatic UV irradiation doses (CTR: non-irradiated sample; 5.5 × 10^2 kJ/m^2 and 5.5 × 10^5 kJ/m^2: irradiated samples) for each substrate (OS: Antarctic sandstone; P-MRS: Phyllosilicatic Mars Regolith Simulant; S-MRS: Sulfatic Mars Regolith Simulant); on y-axis, the number of amplified target gene copies (in logarithmic scale). Irradiation treatments were compared within analogues, whereas the positive control (POS CTR: *C. antarcticus* grown on MEA under physiological conditions) is shown for reference purpose. Statistically significant difference within substrate samples was calculated with Tukey's test (* < 0.05; ** < 0.001; *** < 0.0001); no significant differences were reported between each CTR and the POS CTR (p-value < 0.05).

3.1.3.2 Pigment characterization by UV-Vis spectrophotometry

Due to its dark color, only melanin among all biological pigments absorbs all visible wavelengths (Bell and Wheeler, 1986). The nature of the purified pigments was thus confirmed by their spectral properties (Figure 2). Sample solutions were scanned from the UV to visible wavelength range (200 to 800 nm). Overall, every spectrum showed a strong absorbance in the UV region, reaching maximum values at ~230 nm and progressively decreasing as the wavelength increased. This property is due to the presence of a complex polymeric structure in the melanin molecule (Cockell and Knowland, 1999). Particularly, when referred to the POS CTR spectrum, all P-MRS and S-MRS spectra showed similar spectral profiles but with wider and narrower absorption peaks in the UV region, respectively. To quantify sample purified pigments, their concentration was estimated by comparing the absorbance values at 650 nm of each sample with the A_{650} standard curve of the synthetic DHN melanin (Figure 1S). Mean and standard deviation values for melanin concentrations (in mg/mL) and maximum absorbance wavelengths (in nm) are reported in Table 2.

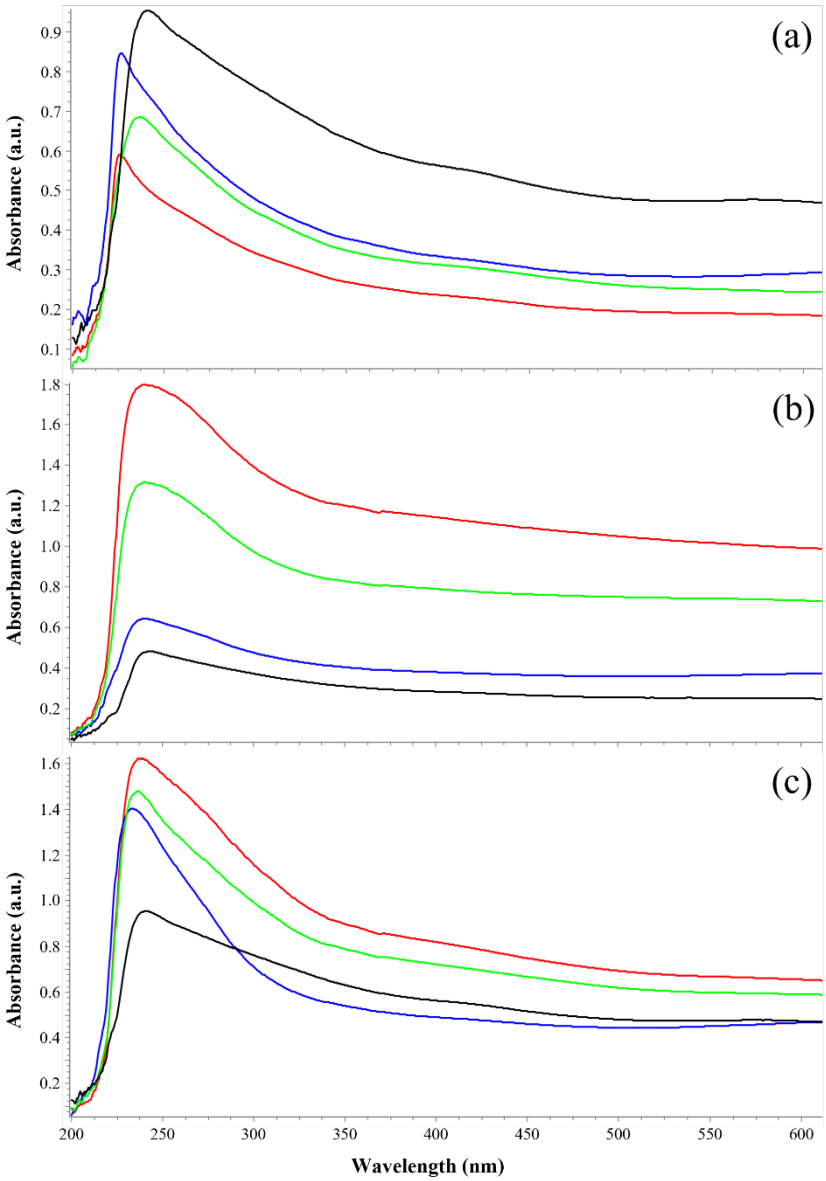

Figure 2. Ultraviolet-Visible (UV-Vis) spectra of extracted melanin pigments from *C. antarcticus* dried colonies mixed with (**a**) OS: Antarctic sandstone; (**b**) P-MRS: Phyllosilicatic Mars Regolith Simulant; (**c**) S-MRS: Sulfatic Mars Regolith Simulant, after exposure to increasing polychromatic UV irradiation doses (CTR: red line; 5.5×10^2 kJ/m^2: blue line; 5.5×10^5 kJ/m^2: green line). On x-axis, increasing wavelengths (in nm); on y-axis, absorbance values (in absorbance units). Spectral profiles were compared within analogues, while the positive control (POS CTR: *C. antarcticus* grown on MEA under physiological conditions) is shown as the melanin spectrum reference (black line).

Table 2. Mean (± S.D.) values of the melanin concentration (in mg/mL) and the maximum UV absorbance wavelength (in nm) of purified pigments from the selected EVT2 and POS CTR samples.

Sample	Concentration (mg/mL)	Absorption peak (nm)
OS CTR	5.271 (± 2.705)	228 (± 4)
OS 5.5 × 10^2 kJ/m^2	12.116 (± 3.708)	230 (± 6)
OS 5.5 × 10^5 kJ/m^2	6.758 (± 7.760)	233 (± 7)
P-MRS CTR	322.409 (± 103.428)	234 (± 9)
P-MRS 5.5 × 10^2 kJ/m^2	100.973 (± 22.709)	236 (± 6)
P-MRS 5.5 × 10^5 kJ/m^2	237.980 (± 134.799)	234 (± 9)
S-MRS CTR	24.005 (± 15.427)	234 (± 6)
S-MRS 5.5 × 10^2 kJ/m^2	19.811 (± 3.545)	232 (± 7)
S-MRS 5.5 × 10^5 kJ/m^2	22.096 (± 14.595)	233 (± 6)
POS CTR	20.136 (± 5.752)	233 (± 6)

OS: Antarctic sandstone; P-MRS: Phyllosilicatic Mars Regolith Simulant; S-MRS: Sulfatic Mars Regolith Simulant; CTR: non-irradiated sample; 5.5 × 10^2 kJ/m^2 and 5.5 × 10^5 kJ/m^2: irradiated samples; POS CTR: *C. antarcticus* grown on MEA under physiological conditions.

3.1.3.3 Pigment characterization by Raman spectroscopy

The Raman signal was obtained by focusing the exciting laser onto *C. antarcticus* dried colonies of the EVT2 samples without any previous preparation. All the acquired Raman spectra showed two clearly distinguishable broad peaks, located at 1323-1345 cm^{-1} and at 1565-1598 cm^{-1} (Figure 3). The Raman spectra obtained share key features with those reported in the literature for melanin pigments (Pacelli et al., 2021; Centeno and Shamir, 2008; Culka et al., 2017).

However, the definite assignment of the two melanin bands is not entirely agreed upon. Some authors ascribe both bands to the C–C stretching bonds within the aromatic rings, whereas others mark a contribution of the aromatic C–N and C–H deformation bonds towards the 1400 cm^{-1} region (De Gussem et al., 2005; Huang et al., 2004; Maquelin et al., 2006; Movasaghi et al., 2007; Rösch et al.,

2006; Samokhvalov et al., 2004; Saif et al., 2020). According to Culka et al. (2017), this uncertainty is probably due to the vibrations of the constituent monomers resulting in many overlapping Raman bands.

The specific position of main peaks served as a proof that the samples did not undergo thermal degradation and the signal acquired is of melanin and not burnt organic matter (or amorphous carbon), according to Pacelli et al. (2021). Furthermore, the presence of the peak around 1425 cm^{-1} is a clear

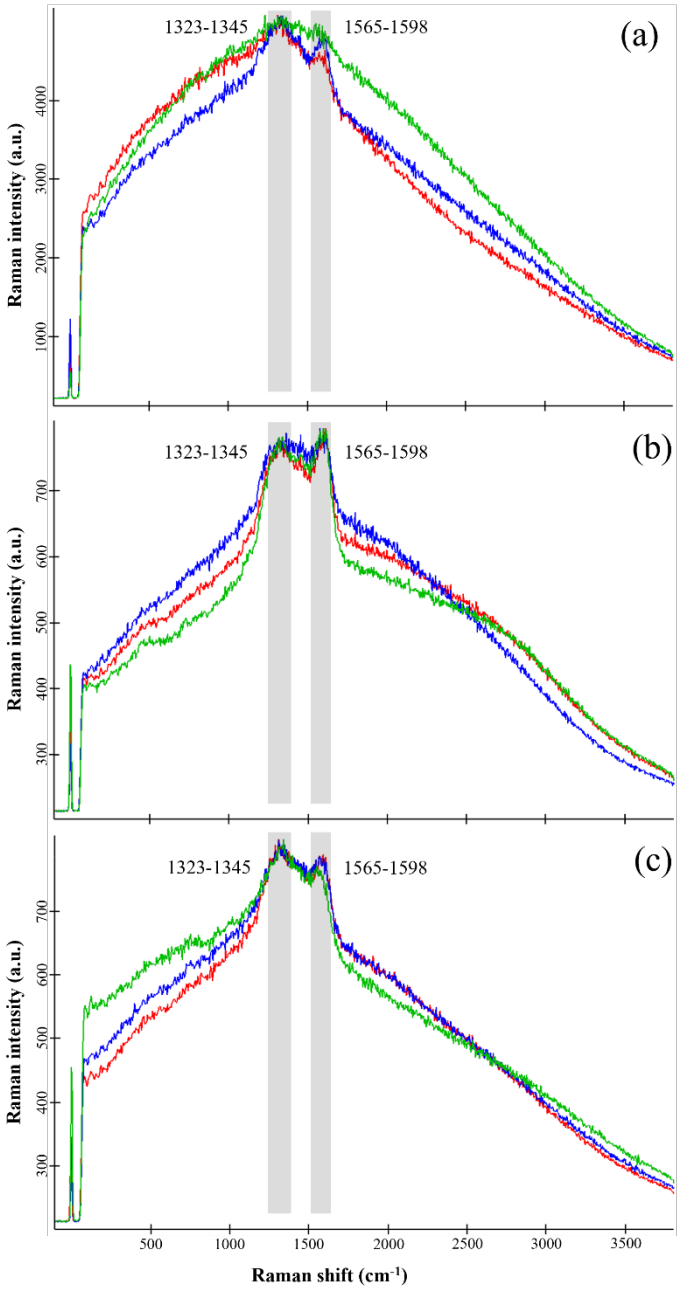

sign of the *C. antarcticus* melanin (Pacelli et al., 2021).

Figure 3. Raman spectra of *C. antarcticus* dried colonies mixed with (**a**) OS: Antarctic sandstone; (**b**) P-MRS: Phyllosilicatic Mars Regolith Simulant; (**c**) S-MRS: Sulfatic Mars Regolith Simulant, after exposure to polychromatic

UV irradiation (CTR: red line; 5.5×10^2 kJ/m^2: blue line; 5.5×10^5 kJ/m^2: green line). On x-axis, Raman shift (in cm^{-1}); on y-axis, Raman intensity of the scattered light (in arbitrary units). Shared peaks are highlighted within grey squares.

3.1.3.4 Organic compounds characterization by FT-IR spectroscopy

FT-IR spectroscopy was used to confirm the melanic nature of the *C. antarcticus* pigment, and to verify the possible presence of further organic compounds after exposure to the UV irradiation treatment. Spectra were obtained directly from dried fungal colonies of the EVT2 samples without any previous preparation. All the acquired FT-IR spectra (Figure 4) revealed a strong, broad band at 3461-3372 cm^{-1}, which was attributed to the O–H groups linked by the NH_2 groups of phenolic and aromatic amino functions present in pyrrolic and indolic molecules (Hou et al., 2019; Jones, 1970; Magarelli et al., 2010). Instead, the band duplet at 2931-2926 cm^{-1} and 2858-2851 cm^{-1} was ascribed to the CH stretching of saturated aliphatic hydrocarbons (Maquelin et al., 2006; Movasaghi et al., 2008; Safar et al, 1994). The small bands occurring between 1669 and 1632 cm^{-1} can be assigned to the alkenyl C=C as well as C=O stretching of carboxylic or amide functions present in proteins (Coates, 2000; Magarelli et al., 2010; Schulz and Baranska, 2007; Stuart, 2004). The broad spectral region between 1250 and 1000 cm^{-1} can be related to phosphate groups as well as C–O, C–N, and C–O–C absorption peaks of carbohydrates or lipids Kosa et al., 2017; Maquelin et al., 2006; Salman et al., 2014; Schulz and Baranska, 2007). Below 1000 cm^{-1}, the absorption bands were usually weak and mostly assigned to aromatic C–H and O–H out-of-plane deformations (Magarelli et al., 2010;

Schulz and Baranska, 2007; Stuart, 2004). Other specific absorption bands have been identified in Table 3.

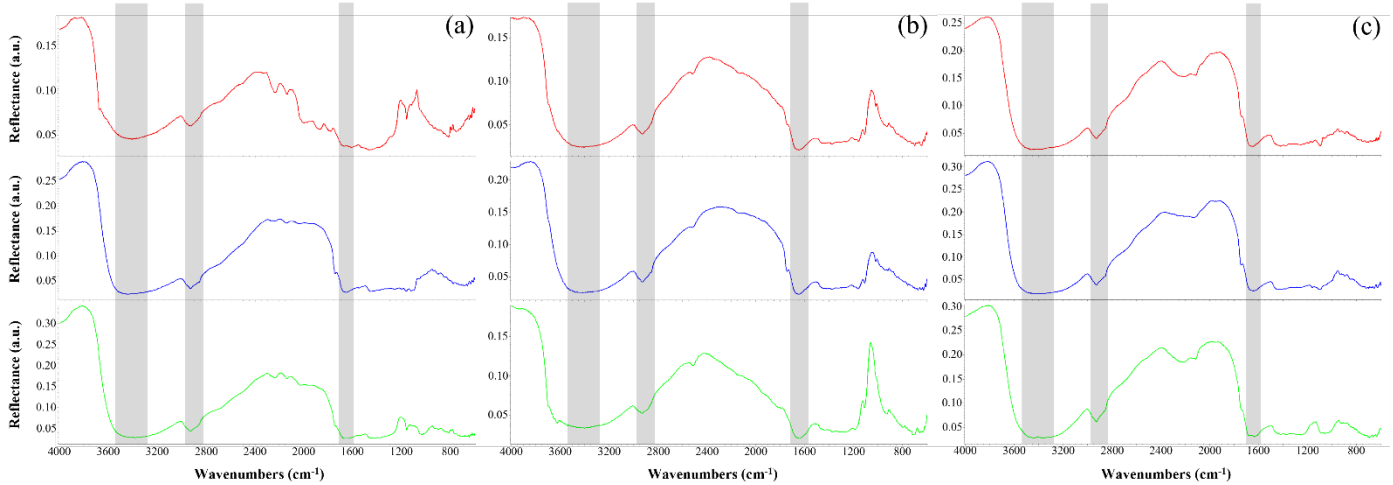

Figure 4. Fourier Transform InfraRed (FT-IR) spectra of *C. antarcticus* dried colonies mixed with (**a**) OS: Antarctic sandstone; (**b**) P-MRS: Phyllosilicatic Mars Regolith Simulant; (**c**) S-MRS: Sulfatic Mars Regolith Simulant, after exposure to the polychromatic UV irradiation treatment (CTR: red line; 5.5×10^2 kJ/m^2: blue line; 5.5×10^5 kJ/m^2: green line). On x-axis, decreasing wavenumbers (in cm^{-1}); on y-axis, reflectance values (in arbitrary units). Shared peaks are highlighted within grey squares.

Table 3. Absorption bands (in cm^{-1}) observed in the EVT2 FT-IR spectra and their possible molecular bonding interpretation.

Wavenumber (cm^{-1})	Molecular bond interpretation	References
3461-3372	NH_2/OH stretching of phenols and aromatic amines in indolic and pyrrolic systems	Magarelli et al., 2010
2931-2926	CH_2 asymmetric stretching of saturated aliphatic groups in fatty acids	Coates, 2000; Safar et al. 1994
2858-2851	CH_2 symmetric stretching of saturated aliphatic groups in fatty acids	Coates, 2000; Safar et al, 1994
2515-2511	OH stretching in carboxylic acids	Shurvell, 2006; Stuart, 2004
2249	Acetylenic C≡C/aliphatic nitrile C≡N stretching	Coates, 2000; Stuart, 2004

2233-2211	Acetylenic C≡C/aromatic nitrile C≡N stretching	Coates, 2000; Stuart, 2004
2136-2114	Acetylenic C≡C/aliphatic isonitrile N≡C stretching	Coates, 2000; Stuart, 2004
2037-1788	Several vibrations from overtones and combinations of substituted benzene rings	Shurvell, 2006
1743-1738	C=O stretching of aliphatic esters in triglycerides	Guillén and Cabo, 1999; Stuart, 2004
1669-1632	Alkenyl C=C/C=O/C=N stretching of amide I in proteins	Coates, 2000; Stuart, 2004
1462-1445	CH_2 scissoring/CH_3 asymmetric bending of aliphatic compounds in proteins or fatty acids	Irudayaraj et al., 2001; Stuart, 2004
1422-1415	OH in-plane bending in carboxylic acids	Shurvell, 2006
1380-1374	CH_3 symmetric bending of aliphatic compounds in proteins or fatty acids	Irudayaraj et al., 2001; Stuart, 2004
1254-1252	P=O asymmetric/CO stretching of aliphatic phosphorus compounds, aromatic ethers and esters in carbohydrates or lipids	Kosa et al., 2017; Stuart, 2004
1193-1190	PO/CN/CO stretching of aromatic amines, phosphates, and phenols in carbohydrates or lipids	Shurvell, 2006; Stuart, 2004
1164-1158	CO stretching of aliphatic ethers, esters, and alcohols in carbohydrates	Shurvell, 2006; Stuart, 2004
1122-1085	CN/COC asymmetric/CO stretching of aliphatic amines, ethers, esters, and alcohols in carbohydrates	Schulz and Baranska, 2007; Shurvell, 2006
1061-1018	POC asymmetric/CO stretching of aliphatic phosphorus compounds, ethers, and alcohols in carbohydrates	Schulz and Baranska, 2007; Stuart, 2004
928-921	COH out-of-plane bending in carboxylic acids	Stuart, 2004
901-814	CH out-of-plane bending of benzenes	Schulz and Baranska, 2007; Shurvell, 2006

721-712	$-(CH_2)_n-$ rocking of methylene chains in hydrocarbons	Irudayaraj et al., 2001 Stuart, 2004
700-687	Olefinic *cis*-CH/phenolic OH out-of-plane bending	Shurvell, 2006
675-642	Acetylenic C=CH bending	Coates, 2000

3.1.4 Discussion

In this work, we investigated the stability of biomolecules in the black fungus *C. antarcticus* after exposure to the ground-based simulations performed in preparation for the space-exposure BIOMEX project and in support to the biosignature detection planned for the explorative mission on Mars.

The search for life on Mars is necessarily informed by terrestrial biomolecules, the only form of life that we know; furthermore, it is reasonable that life on Mars could be related to life on Earth due to the massive meteoritic exchange between Earth and Mars (Melosh, 1988; Mileikowsly et al., 2000; Pavlov et al., 2012). In addition, several papers demonstrated that terrestrial life, if landed on Mars, would be able to resist and live on Mars when protected by regolith from the harsh radiation environment of the Martian surface.

A prime consideration for the detection of organic biosignatures on Mars is their long-term preservation on the surface, where the presence of UV and ionizing radiations are one of the main damaging factors. Although preservation of complex organic molecules in the shallow subsurface (~10 cm) of Martian rocks drops 1000-fold due to ionizing radiation (Hays et al., 2017), there are recent indications that rapid burial of organic molecules, short surface exposure ages thanks to slower weathering rates, and the characteristics of certain mineral depositions are key factors to enhance biosignature preservation in the subsurface of Mars (Williams and Lynch, 2017; National Research Council, 2007). Therefore, we exposed dried fungal colonies, once grown on Martian rock analogues, to increasing doses of Mars-relevant polychromatic UV irradiation (200-400 nm) up to 5.5×10^5 kJ/m^2, which simulate 369.87 days on the Martian surface (Cockell et al., 2000). Here, we investigate

the stability of the fungus itself and its related biomolecules in relation to the potential detectability of Martian biosignatures.

C. antarcticus DNA was showed to be resistant to the increasing UV doses, since its detection and amplification was achieved in all samples, even in those highly irradiated (5.5×10^5 kJ/m^2) and using very low DNA concentration (0.018 ng/μL) (Figure 1). Although further data are required to confirm any potential role of the different substrates in providing protection against UV radiation, higher damages were reported for samples grown on Martian analogues. Although nucleic acids are organic compounds highly sensitive to degradation over geological timescales (Aerts et al., 2014) and their preservation may be precluded (Summons et al., 2011), labile/polar compounds of these types are of utility to assess whether life processes are currently active or were active in recent geological times (Simoneit et al., 1998; Maggiori et al., 2020). Hence, we corroborate the possibility of using DNA as a potential biosignature in the search for extant or recently extinct life forms on Mars, considering its unambiguous biological origin. Since the Viking missions in the '70s, nucleic acid detection instruments have not been included onboard life-detection rovers; however, the miniaturization of PCR devices could allow their integration in future missions. Indeed, the development of e.g., the MinION device (Oxford Nanopore Technologies), a portable nanopore real-time sequencer that requires just small DNA or RNA amounts, would be able to clearly detect signs of life (Pacelli et al., 2017).

Among the other potential biosignatures investigated, we have focused on melanin pigments (present in all domains of terrestrial life) as they are part of those biomolecule classes (i.e., lipids and biopolymers) that exhibit the highest molecular stability and potential preservation among all organic compounds on Earth - i.e., over timescales of billion-years (Engel et al., 1993; Simoneit et al., 1998), while also abundant in *C. antarcticus* cell-walls (Bottger et al., 2012) and well-known to be involved in photoprotection (De Gussem et al., 2005; Pacelli et al., 2020; Messen et al., 2013). We used three different approaches to detect the pigments: (**i**) UV-Vis spectrophotometry; (**ii**) Raman spectroscopy; (**iii**) FT-IR spectroscopy.

(**i**) Since dark melanin pigments act as a blackbody, they absorb radiation at all visible wavelengths; the percentage of absorption is generally greater in the UV region and decreases progressively as the wavelength is increased to the far-red region (Cockell and Knowland, 1999). UV-Vis results of the purified pigments reported the typical spectral profile of fungal melanins (Pacelli et al., 2021; Pal et al., 2013; Suryanarayanan et al., 2004; Yuan et al., 2007) in OS, P-MRS, and S-MRS spectra of all three irradiation treatments (Figure 2), showing the maximum absorbance peak at around 230 nm (Table 2). The higher absorption in the UV region is a property of aromatic organic compounds (Mach et al., 1995), and this absorbance peak suggests the detectability of melanin only: if proteins and nucleic acids were present, the peak would be shifted to the wavelength region between 250 and 320 nm (Baqué et al., 2018).

Melanin has proved to be well detectable and quantifiable (Table 2). Nevertheless, it has been noted that the P-MRS analogue because it contains phyllosilicatic minerals or clays, presents high adsorption/absorption properties, with respect to the other substrates. It is likely that some minerals were still present in the purified melanin pigments interfering with the UV-Vis analysis, as reported in Pacelli et al. (2017), the presence of minerals may have altered melanin absorbance values at 650 nm – thus explaining the unusual spectral profile with a second large peak around 245 nm. In the frame of searching for traces of extinct or extant life on Mars, the melanin concentration results from both P-MRS and S-MRS samples (Table 2) led us to assume that, although the estimation of melanin concentration from fungal colonies in Martian analogues regolith can be altered by the presence of the soil itself, it is still possible to clearly detect the absorbance of purified melanin pigments even with both the presence of mineral compounds and from irradiated samples (up to 5.5×10^5 kJ/m^2).

(**ii**) The UV-Vis results about melanin pigment identification are supported by data from Raman and FT-IR analyses (Figures 3, 4). Sample spectra clearly showed the presence of unaltered melanin pigments even in samples exposed at the dose of 5.5×10^5 kJ/m^2. The specific peaks position, and the presence of the intermediate peak at 1425 cm^{-1} allows to discriminate melanin pigments from organic or inorganic carbon, which have similar features in the Raman spectrum, according to our

previous study (Pacelli et al., 2021). Neither the UV irradiation treatment nor dried conditions altered the melanin spectral properties, and thus melanin was successfully detected in all samples. Previous works have reported the degradative effect of UV and ionizing radiation on photosynthetic pigments (e.g., carotenoids) with significant diminishment of spectral peak intensity and fluorescence (Dartnell et al., 2011, 2012; Bibring et al, 2017). Our results showed the absence of the phenomenon on melanin pigments, demonstrating a successful detection even from samples irradiated with high UV doses (i.e., 5.5×10^5 kJ/m^2). This corroborates the initial proposal of using melanin as a potential biosignature due to its remarkable detectability in highly UV irradiated environments.

(**iii**) Considering that two IR instruments are among the ExoMars payloads (De Sanctis et al., 2017; Rull et al., 2017; Vago et al., 2017; Kendall et al., 2009), along with a Raman Laser Spectrometer, it is important to study biomolecules with a spectroscopic approach. FT-IR spectroscopy is an absorption-based optical analytical technique. Major benefits of using the FT-IR imaging over traditional methods are that it is non-disruptive, label-free, and requires a very limited amount of samples. Through the acquisition of a biochemical fingerprint, FT-IR can provide information about content, structure, and chemical modification of major biomolecules present in the investigated sample (McCreery, 2001). Raman and FT-IR spectroscopies are related techniques with their respective complementary spectra (Bonner and Duncan, 1962). The synergy of both techniques is a powerful tool when performing organic and inorganic compounds characterization.

Results obtained by FT-IR spectroscopy revealed the presence of some main functional groups in all EVT2 spectra (Figure 4), and their presence was related to common organic compounds (Table 3). For instance, the ubiquitous presence of peaks at 3461-3372 cm^{-1}, 2931-2926 cm^{-1}, 2858-2851 cm^{-1}, and 1669-1632 cm^{-1}, along with the narrow one at 1061-1018 cm^{-1} was related to the *C. antarcticus* melanin pigments (Raman and Ramasamy, 2017). Particularly, peaks at 3461-3372 cm^{-1} and 1669-1632 cm^{-1} are generally attributed to melanin pigments (Movasaghi et al., 2008; Kannan and Ganjewala, 2009; Sajjan et al., 2010; Paim et al., 1990), while additional peaks at 2931-2926 cm^{-1}, 2858-2851 cm^{-1} and 1061-1018 cm^{-1} are typically attributed to fungal melanins (Pacelli et al., 2021;

Suryanarayanan et al., 2004; Sun et al., 2016; Forfang et al., 2017). Besides, peaks observed in the fingerprint region of all spectra could be eventually identified as phenolic compounds, whose presence could be correlated to that of fungal melanins or other secondary metabolites (Culka et al., 2017; Stuart, 2004).

As for the detection of fungal biomolecules other than melanin pigments, many narrow peaks between 1254 and 1018 cm^{-1} related to carbohydrates as well as to amino and phosphate compounds could be associated with polysaccharides of the fungal cell wall (e.g., chitosan, β-glucan, mannan, etc.) (Movasaghi, 2007; Salman et al., 2014 Shurvell, 2006; Ivshin et al., 2007). Furthermore, peaks observed in relation to the amide I band (1669-1632 cm^{-1}), the CH_2 bending signal (1462-1445 cm^{-1}), and the CO stretching (1164-1158 cm^{-1}) suggest the detection of chitin characteristic vibrations (Shurvell, 2006; Ivshin et al., 2007; Rinaudo, 2006; Bottger et al., 2012). To conclude, FT-IR results confirmed the presence of melanin pigments in all EVT2 samples; this evidence corroborates the suggestion to use the biomolecule as biosignature, since it results highly detectable by different analytical techniques. Furthermore, all these results showed the importance of using multiple and interconnected analytical techniques in the search for life, since they can provide complementary and useful information for detecting and characterizing biosignatures.

Moreover, our outcomes have identified chitin, the main component of the fungal cell wall, as a resistant biomolecule to UV irradiation. So far, it has also been reported in the frame of the BIOMEX experiments by the Raman analysis of the *Circinaria gyrosa*'s fungal symbiont (Briggs et al., 2014). Chitin is known as one of the few biosignatures specific for fungi, and it has been reported in organically preserved fossils (Ivarsson et al., 2011). Nevertheless, the detection of chitin in geological materials is a difficult task: its occurrence in 25-million-year-old fossils has shown that the primary criterion for chitin preservation is not geological time, but rather the conditions of depositional environment and the absence of diagenetic processes such as alteration and decomposition (Cockell et al., 2014). Following the previous interpretation of FT-IR results, we consider the possibility of using chitin as a potential, stable biosignature, since it is detectable in fungal samples even after

exposure to high UV irradiation (i.e., 5.5×10^5 kJ/m^2 dose) and is intrinsically related to terrestrial life.

3.1.5 Conclusions

In the light of previous investigations (Raman and Ramasamy, 2017; De Gussem et al., 2005; Pacelli et al., 2021; Messen et al., 2013), we confirm the relevance of using melanin pigments as a possible biosignature and propose the further study of the chitin molecule as a possible new one, because both are highly stable biosynthesized molecules that could still be detected if exposed to extreme UV radiation – an extreme environmental condition that normally occurs on the Martian surface.

Even if the Martian subsurface offers protection against solar UV radiation and those oxidizing conditions found at the surface (only a few millimeters of dust coverage is required to shield the harmful UV radiation to survivable levels, in contrast to shorter-wavelength ionizing radiation that could penetrate up to 1.5 meters beneath the surface), this work may regard the case of recently surface-exposed rocks where photolytic destruction of organic compounds can rapidly occur. Therefore, this work can help broaden our knowledge on those terrestrial biomolecules that could be searched for in upcoming life-detection missions.

Acknowledgments: The Italian National Antarctic Research Program (PNRA) and the Italian National Antarctic Museum "Felice Ippolito" (MNA) are also acknowledged for funding the collection of MNA-CCFEE Antarctic samples. M.B. acknowledges the support of the Deutsche Forschungsgemeinschaft (DFG – German Research Foundation) for the project "Raman Biosignatures for Astrobiology Research" (RaBioFAM; project number: 426601242).

3.2 Fungal biomarkers stability in Mars regolith analogues after simulated space and Mars-like conditions

Abstract

The discovery of life on other planets and moons in our Solar System is one of the most important challenges of this era. The second ExoMars mission will look for traces of extant or extinct life on Mars. The instruments on board the rover will be able to reach samples with eventual biomarkers until 2 meters of depth under the planet's surface. This exploration capacity offers the best chance to detect biomarkers which would be mainly preserved compared to samples on the surface which are directly exposed to harmful environmental conditions. Starting with the studies of the endolithic meristematic black fungus *Cryomyces antarcticus*, which has proved its high resistance under extreme conditions, we analyzed the stability and the resistance of fungal biomarkers after exposure to simulated space and Mars-like conditions, with Raman and Gas Chromatography-Mass Spectrometry, two of the scientific payload instruments on board the rover.

Keywords: spectroscopy, Mars exploration, life-detection, pigments, nucleic acids.

Cassaro, A., Pacelli, C., Baqué, M., de Vera, J. P. P., Böttger, U., Botta, L., Saladino, S., Rabbow, E. and Onofri, S. (2021). Fungal Biomarkers Stability in Mars Regolith Analogues after Simulated Space and Mars-like Conditions. Journal of Fungi, 7(10), 859.

3.2.1 Introduction

In the next few years, *in situ* space exploration missions will be devoted to the detection of biogenic signatures of extinct or extant life on Mars. The driver for searching for life on Mars is the findings supporting that ancient environments on Mars could have supported microbial life (Grotzinger et al., 2013). One of the primary issues in the search for life is that the present-day Martian surface presents a very inhospitable habitat for life as we know it because of the intense radiation, highly oxidizing conditions, concentrated evaporative salts, and extremely low water activity (Davila et al., 2010). Despite the Martian surface having been cold and predominantly dry for at least the last three billion years (i.e., the Amazonian Period, immediately following the Hesperian), the subsurface could have sustained stable reservoirs of geothermally heated liquid water for the majority of this time. These conditions could represent a long-lived habitat that have maintained hypothetical living cells (Clifford et al., 2010; Ehlmann et al., 2011; Thomas et al., 2017; Travis et al., 2003). For these reasons, the next planetary mission, ESA-Roscosmos ExoMars Rosalind Franklin, will collect and analyze samples in the subsurface, up to 2 meters depth (Dartnell et al., 2007, 2012; Hassler et al., 2013), to access places where organic molecules may be well preserved even after billions of years (Vago et al., 2015).

In this context, our best chance to find traces of extant or recently extinct life on Mars is to look for biomarkers (Westall et al., 2015). A molecular biomarker is defined as a pattern, distribution of molecules or molecular structures that in nature derives uniquely from past or present biological processes (Summons et al., 2011; Vago et al., 2013). Indeed, we consider as a possible biomarker a range of molecules indicative for life as we know it, such as DNA, amino acids, lipids, carbohydrates, pigments, intermediary metabolites (Vago et al., 2017), their degradation products and their general characteristics as preservation potential, specificity and extractability (Aerts et al., 2014). Assuming that hypothetical Martian life is similar to that on Earth, the identification of these compounds would be diagnostic of extant or recently extinct life because they are the indispensable biological components of the organisms as we know it. Any extinct or existing forms of microbial life on Mars

may have produced biomolecules that may still be preserved and detectable in Martian rocks. In fact, minerals and organic molecules are strictly linked: minerals provide surfaces to support, concentrate, and preserve organic molecules. In support of this, organic matter was recently found within the 3 billion-year-old mudstones of Gale Crater (Eigenbrode et al., 2018).

Due to the capability to detect biomolecules or their alteration products within mineral grains, Raman spectroscopy is part of the analytical instrumentation in the payloads of the rovers. This technique, on top of its main goal to provide mineralogical identification of the samples, can also detect a wide range of potential biomarkers in the rock substrate. It has been chosen for its non-destructive properties, for its sensibility during the detection of microbial life closed in their niches, and for its efficiency for the *in-situ* analyses also in presence of mineral rocks (Ellery and Wynn-Williams, 2003).

The Mars Organic Molecule Analyzer (MOMA), among various instruments, will operate with Pyrolysis-Gas Chromatography-Mass Spectrometry (Pyr-GCMS) in order to analyze volatile compounds in the Martian subsurface. In this context, it is important to understand the interaction effect of high temperatures with regolith and organic matter. In extreme environments life could find refuge inside rocks, as in terrestrial analogs environment, where in harsh conditions, extremophilic microorganisms dwelling inside the subsurface produce characteristic compounds protecting themselves from stressed conditions (Wynn-Williams and Edwards, 2000; Onofri et al., 2004), among which are carotenoids and melanin pigments. Organic, metabolic and morphological structure or compounds of the organisms could persist in mineral structures, and are considered good biomarkers of microorganisms' presence. On Earth, biological matter can be preserved in sedimentary rocks as carbonaceous macromolecules (Summons et al., 2011) and maybe, if life exists or existed on Mars, its rocks could preserve organic deposits: organic components may be preserved either as degraded molecules within mineral structures or as disseminated molecules chemically bonded to mineral particles of rocks, such as phyllosilicates (Preston et al., 2019).

In this context, the BIOMEX (BIOlogy and Mars EXperiment) project, aimed at investigating the endurance of extremophiles and the stability of biomolecules under space and Mars-like conditions in the presence of Martian regolith analogs (de Vera et al., 2012). This experiment involved 16 months of real space and a close approach to Mars-like conditions exposure outside the International Space Station (ISS). The experiment was placed externally aboard the EXPOSE-R2 exposure payload and comprised a series of ground-based simulation tests, including Experiment Verification Test (EVT) and Science Verification Tests (SVTs), carried out before the flight. In the frame of ground-based tests, the stability/degradation of biomolecules of the extremotolerant microorganism *Cryomyces antarcticus* was investigated; the fungus, isolated from the McMurdo Dry Valleys (South Victoria Land, Antarctica), was chosen for its widely proved ability to withstand stressors similar to the ones encountered in space and Mars-like environments (e.g. ionizing and no ionizing radiation, vacuum or Martian atmosphere, temperature cycles) (Onofri et al., 2012, 2015).

In total, fungal colony samples were investigated after exposure to simulated space and Mars-like conditions during the ground-based experiments before flight. Fungal colonies where spread on three different cultivation media consisting of Malt Extract Agar (MEA) and three different regoliths: the Original Substrate (i.e. Antarctic sandstone, OS), the Phyllosilicatic Mars Regolith Simulant (P-MRS) analogue and the Sulfatic Mars Regolith Simulant (S-MRS) analogue. The P-MRS simulates igneous rocks altered by hydrous fluids (neutral to basic) while the S-MRS mimics a more acidic environment with sulfate deposits (Bottger et al., 2012). The objectives of this study were to identify potential fungal biomolecules to be accounted as biomarkers, and to understand if and how simulated space and Mars environment could modify them. As the primary goal of this study was the detection of microbial signatures within the Martian regolith analogues, the same methodology, as Raman spectroscopy and Gas Chromatography-Mass Spectrometry (GC-MS), planned for the ExoMars Rosalind Franklin mission, were used. In addition, extracted melanin pigments and nucleic acids were analyzed by using UV-Vis spectrophotometry and by quantitative Polymerase Chain Reaction

(qPCR) technique, respectively, to detect any changes in structure after simulated space and Mars exposure.

3.2.2 Materials and Methods

3.2.2.1 Science Verification Tests (SVTs)

The SVTs were performed at the Planetary and Space Simulation facilities (PSI) at the Institute of Aerospace Medicine (German Aerospace Center, DLR, Koln, Germany). SVTs are designed to ensure that all samples are appropriately prepared to successfully withstand hardware integration, conditions experienced during the mission, and post flight de-integration. The application of mission-equivalent space parameters allows for testing the resilience of samples toward the extreme environmental conditions of space and simulated Mars exposure on the ISS. Samples were accommodated in wells with a diameter of 12 mm, within square aluminum alloy carriers, 76 mm side. Following the accommodation plan scheduled for the EXPOSE-R2 mission, SVTs allowed only one replicate per sample (de vera et al., 2012). To simulate space-like test conditions, the sample that was grown on OS analogue was exposed to vacuum (10^{-5} Pa) and cycling temperatures between -25 °C (16 h in the dark) and +10 °C (8 h during irradiation), alone (Bottom samples) or in combination with polychromatic UV (200-400 nm) radiation produced by the solar simulator SOL2000 (Top samples). The dose of 570 MJ/m^2 was reached by running the solar simulator (SOL2000; Dr. Hönle GmbH, Germany, Rabbow et al., 2017) for 125 h at 1271.2 W/m^2. In parallel, Mars test parameters were simulated by low temperature (-25 °C), Mars-like atmosphere (95.55% CO_2, 2.70% N_2, 1.60% Ar, 0.15% O_2, *370 ppm H_2O; Praxair Deutschland GmbH), and Mars-like pressure of 10^3 Pa for S-MRS and P-MRS analogues, alone or in combination (Top samples) with the same radiation as described above. Neutral density filters (0.1%) were used to attenuate radiation in all tests performed; all conditions were simulated for a period of 28 days. The applied fluency corresponds to the long-term space experiment of 1 year of exposure outside the ISS, as estimated from previous EXPOSE data and simulations (Rabbow et al., 2012, 2014). It should be noted that space parameters cannot be

fully mimicked in the laboratory (space vacuum and complex radiation environment): for example, deep UV, that is, solar UV radiation below 200 nm. Below the irradiated samples, an identical set of samples (space dark samples and Mars dark samples / bottom samples) was kept in the dark and experienced all simulation parameters except UV radiation exposure. Controls (Ctr) were kept at DLR in the dark at room temperature. The exposure conditions are summarized in Table 1.

Table 1. Exposure conditions during the Scientific Verification Tests (SVTs)**.**

Test parameters	Duration
Vacuum (2 x 10^{-4} Pa) + polychromatic UV irradiation (200-400 nm), with SOL2000 at 1271.2 W/m^2, attenuated with 0.1 % neutral density filter.	28 days SOL2000 125 hours
Simulated CO_2 Mars atmosphere 10^3 Pa + UV irradiation, polychromatic (200-400 nm), with SOL2000 at 1271.2 W/m^2, attenuated with 0.1 % neutral density filter.	28 days SOL2000 125 hours
Control experiment, 1 atm air, dark, room temperature	28 days

SOL=Solar simulator

3.2.2.2 Fungal melanin extraction

Melanin was extracted from dried colonies of *C. antarcticus* grown on different substrata, optimizing the protocol reported by (Rosas et al., 2000). Fungal cells were collected by centrifugation at 16100 rcf for 20 min, washed with phosphate-buffered saline (PBS) (pH 7.4). Cells were suspended in 20 µl of a buffer composed by 0.25 µl of enzyme from *Trichoderma harzarium* (Sigma #L1412), 50 µl of 0.2 M sodium citrate (pH 5.5), 15 µl of 0.2 M citric acid and 18.2 g of sorbitol, up to the final volume of 500 µl.

Samples were incubated overnight at 30 °C, shaken at 50 rpm, washed with PBS two times and collected by centrifugation (10 minutes at 16100 rcf). The supernatant was removed by adding 1 ml of 4M guanidine thiocyanate (VWR International srl) and samples were incubated overnight on stirrer. Samples were washed with PBS and centrifuged for 15 minutes at 16100 rcf for two times. 1 mg/ml of Proteinase K, previously dissolved in the reaction buffer (4 µl of TRIS HCl, 1 µl of $CaCl_2$

and 1 ml of SDS, up the final volume of 20 ml) was added to the samples; they were incubated at 37 °C for 4h and after centrifuged for 5 minutes at 16100 rcf. Samples were washed two times by adding 1 ml of PBS 4X, and three times by adding 1 ml of chloroform.

A volume of 2 ml of a 6M HCl solution was added to the samples and they were boiled for 1 h. Samples were transferred in dialysis membrane (SnakeSkin Dialysis Tubing, 3.5K MWCO-Thermo Scientific) in sterile water for 3 days, changing the water every day. Finally, samples were lyophilized overnight with the Lyophilizer FreeZone 2.5 Liter (Freeze Dry Systems, LabConco) and then used for the analyses.

3.2.2.3 Spectrophotometric analysis

After the extraction, purified pigments were dissolved in 500 µl of NaOH 1M and its UV-Visible spectrum was measured in a UV spectrophotometer (UV 1600 PC Spectrophotometer, VWR International) by using M.Wave professional 2.0. A standard graph for estimation was used and was made using synthetic melanin. NaOH 1M was used as a blank and the instrument was set in a range of 200-800 nm for the analysis. The correlation between absorbance and wavelength was defined. To determine the concentration of extracted melanin, synthetic DHN (1,8-DiHydroxyNaphthalene) melanin (Thermo-Fisher scientific) was prepared in 1M NaOH at concentrations of 500 mg/ml and as reported in (Raman and Ramasamy, 2017), a standard curve at 650 nm was obtained.

3.2.2.4 Confocal Raman spectroscopy analyses

Raman spectroscopy was performed at German Aerospace Center in Berlin, using a 532 nm excitation laser, with a Confocal Raman microscope (WITec alpha300), at room temperature, under ambient atmospheric conditions. The spectral resolution of the spectrometer is 4-5 cm^{-1}. Before the analyses, the spectrometer was calibrated with pure silicon and paracetamol test samples. A 10X Nikon objective, with a 0.25 numerical aperture, was used to focus the laser on a 1.5 µm spot. For single spectra, all measurements were performed at 0.1 mW laser power with 10s integration and 50

accumulations. Image scans were done at 0.7 mW with 1s and 1 accumulation (to avoid signal saturation or damaging effects) on three distinct areas up to 100 µm × 100 µm and up to 500 image points, thus collecting a minimum of 1000 measurements per sample.

All data analyzes were performed with the WITec Project FIVE software. Parameters used for analysis were the value of signal coverage on random zones on the samples, to show the presence/absence of the signal defined as spectra having Signal to Noise Ratio (SNR) values superior to 5 and the value of SNR. To analyze the presence of the signal, the region of interest between 200 and 2000 cm^{-1} was cropped, then a fifth-order polynomial function was applied for background subtraction; and finally, SNR masks were applied. As previously described in (Baqué et al., 2018) for carotenoid pigments, the SNR was defined as the height of the 1600 cm^{-1} peak divided by the noise represented by the standard deviation of a spectral region without features (1750 to 1950 cm^{-1}). The position of the 1600 cm^{-1} peak was also derived from masks available in the WITec Project FIVE software.

3.2.2.5 Nucleic acid analysis

3.2.2.5.1 Nucleic acid Extractions from synthetic Mars and terrestrial soils

DNA was extracted from colonies, using the Nucleospin Plant kit (Macherey-Nagel, Düren, Germany) following the protocol optimized for black fungi as reported in (Selbmann et al., 2005). Before amplification, DNA was quantified using QUBIT system and diluted at the concentration of 0.1 ng/µl for the following analyses.

3.2.2.5.2 Acid nucleic detection through quantitative real-time PCR (qPCR)

Three different target genes were amplified with qPCR approach to investigate the differences in acid nucleic detection: a long-repeated fragment (Large Sub-Units, LSU gene of 939 bp), a short-repeated fragment of the same gene (LSU gene of 330 bp) and a small but non-repeated fragment in the genome (β-actin gene of 330 bp). qPCR was performed with a BioRad CFX96 real time PCR detection system

(BioRad, Hercules, CA) using primers targeting the fungal LSU rRNA gene and the β-actin gene: LR0R (ACCCGCTGAACTTAAGC, Cubeta et al., 1991) and LR5 (TCCTGAGGGAAACTTC, Vilgalys and Hester, 1990), and ACT512-F (ATGTGCAAGGCCGGTTTCGC3) and ACT783-R (TACGAGTCCTTCTGGCCCAT, Carbone and Kohn, 1999), respectively, each at 5 pmol final concentration.

The primers LR0R-LR5 and LR0R-LR3 are used to amplify a 939 bp and 300 bp products, respectively, spanning the LSU region of rRNA encoding genes. The standard qPCR cycling protocol for both products, consisting of a denaturation step at 94 °C for 5 min, followed by 35 cycles of denaturing at 94 °C for 45 s, annealing at 52 °C for 30 s, and elongation at 72 °C for 2 min, was performed. The primers ACT512-F and ACT783-R are used to amplify a 330 bp product spanning the β-actin gene. The standard qPCR cycling protocol, consisting of a denaturation step at 95 °C for 10 min, followed by 35 cycles of denaturation at 95 °C for 15 s, annealing at 61 °C for 20 s, and elongation at 72 °C for 15 s, was performed. Fluorescence measurements were recorded at the end of each annealing step. After 35 cycles, a melt curve analysis was performed by recording changes in fluorescence as a function of raising the temperature from 60-90 °C in 0.5 °C per increments. All tests were performed in triplicate.

3.2.2.6 Statistical analyses

For multiple data points, mean and standard deviation were calculated. Statistical analyses were performed by one-way analysis of variance (Anova) and pair wise multiple comparison procedure (t test), carried out using the statistical software SigmaStat 2.0 (Jandel, USA).

3.2.2.7 Organic compounds detection by Gas Chromatography-Mass Spectrometry

Gas-chromatography associated to mass spectroscopy has been selected for the analysis of samples onboard of the rover of the ESA-ExoMars mission (Holland et al., 2003). Each sample (pellet), was grinded in agate mortar and then suspended in 2 ml of ethyl acetate. The mixture was left 4 h under

magnetic stirring at room temperature. After this time, the suspension was filtered to remove the solid, and the solution obtained was concentrated under reduced pressure. After the extraction and fractionation of the samples with *N*,*N*-bis-trimethylsilyl trifluoroacetamide in pyridine (620 µl) at 60 °C for 4 h in the presence of betulinic acid [3β -hydroxy-20(29)-lupaene-oic acid] as the internal standard (0.2 mg), the Gas Chromatography-Mass Spectrometry was performed. Mass spectrometry was carried out through the following program: injection temperature 280 °C, detector temperature 280 °C, gradient 100 °C for 2 min, and 10 °C for 60 min. To identify the structure of the products, two strategies were followed. First, the spectra were compared with commercially available electron mass spectra libraries such as NIST (Fison, Manchester, UK). Second, GC-MS analysis was repeated with standard compounds. All products have been recognized with a similarity index (SI) greater than 98% compared with that of the reference standards. The analysis was limited to products of ≥1 ng/ml quantity, and the yield was calculated as micrograms of isolated product.

3.2.3 Results

3.2.3.1 Detection of pigments by spectrophotometric analyses

Spectrophotometric analyses were performed on fungal melanin extracted from *C. antarcticus* colonies after exposure to simulated space conditions (OS) and Mars-like conditions (P-MRS and S-MRS). The wavelength of maximum absorbance was scanned at a range of 200 to 800 nm. The UV-visible absorbance spectrum of the purified pigments showed a strong absorbance in the UV region, and a characteristic absorption peak was observed at 230 nm corresponding to typical melanin UV absorption. The strong absorption in the UV region with a progressive decrease at high wavelength is due to the presence of complex conjugated structures in the melanin molecule (Bell and Wheeler, 1986; Cockell and Knowland, 1999). The decrease in the absorption with increasing wavelength is linear in the case of melanin.

Figure 1 shows the melanin spectra extracted from samples exposed to simulated space UV radiation (OS Top; red line), vacuum (OS Bottom; blue line), to Mars-like UV radiation (P-MRS and S-MRS Top; red line) and Mars-like atmosphere (P-MRS and S-MRS Bottom; blue line) compared with relative control (black line). No change in melanin absorbance at 230 nm has been reported in all the experimental conditions (Top, Bottom and Control); compared with those reported in (Pacelli et al., 2021) for extracted melanin pigments from *C. antarcticus*. In addition, UV-Vis analyses of melanin pigments extracted for P-MRS and S-MRS analogues, revealed a bulge at ~300 nm, not show in OS spectra, probably due to the presence of regolith during the detection process.

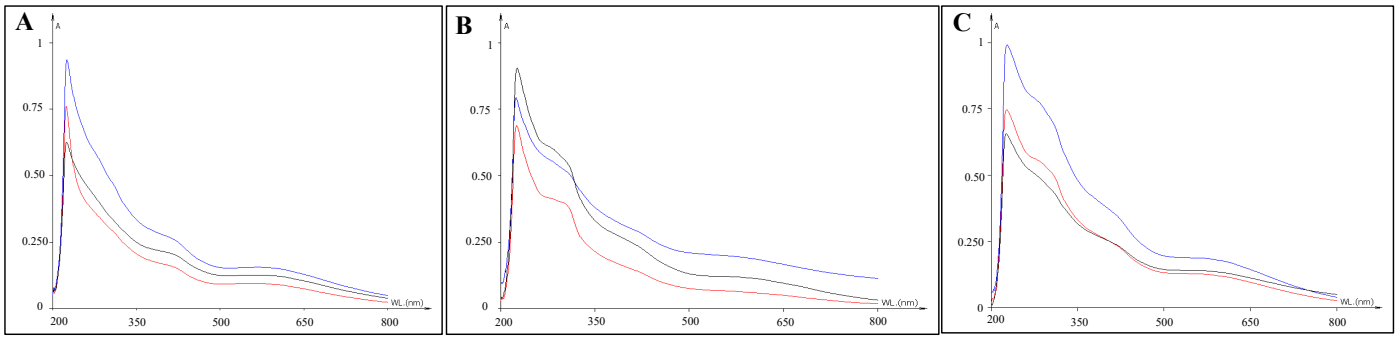

Figure 1. UV/VIS-spectra of melanin pigment extracted from *C. antarcticus* colonies grown on A) OS exposed to simulated space conditions; B) P-MRS and C) S-MRS exposed to Mars-like conditions on different layers: Top (exposed to sun light with 0.1% Neutral Density filters) =red spectrum, Bottom (dark control in space, not exposed to space radiation) =blue spectrum and CTR (sample kept in the lab, in the dark at room temperature) =black spectrum. OS=Original Substrate, P-MRS= Phyllosilicatic Mars Regolith Simulant, S-MRS=Sulfatic Mars Regolith Simulant.

3.2.3.2 Detection of pigments by Confocal Raman spectroscopy

Colonies of *C. antarcticus* grown on different analogues were analyzed by Confocal Raman spectroscopy after exposure to simulated space and Mars-like conditions. The results of Raman analyses identified the melanin spectra with two main peaks, according to Culka et al. (2017): an intense and broad peak at 1590-1605 cm^{-1} and a second peak at lower wavenumber at 1340 cm^{-1} (Fig. 2). The presence of these peaks is probably due to the aromatic C-N bonds for the first peak (Samokhvalov et al., 2007), and to the stretching of the C-C bonds within the rings of the aromatic melanin monomers for the second peak (Galvan et al., 2013). The presence of other peaks and

shoulders in all spectra, with the most prominent one around 1425 cm^{-1}, served as a proof that the samples did not undergo thermal degradation and that the signal acquired is of melanin and not burnt organic matter (or amorphous carbon). Figure S1 shows the signal coverage for the image scan analyses, calculated from the application of a SNR superior to 5; results were normalized to the corresponding SNR of the non-irradiated sample (Ctr) for each analogue.

No significant melanin changes are reported in all the collected spectra; similar peak positions (1602-1604 cm^{-1}) were detected in samples exposed to simulated space conditions (OS) and in samples exposed to Mars-like conditions (P-MRS and S-MRS), both in Bottom and Top conditions, in comparison with the respective Control samples (Fig. S2A and B).

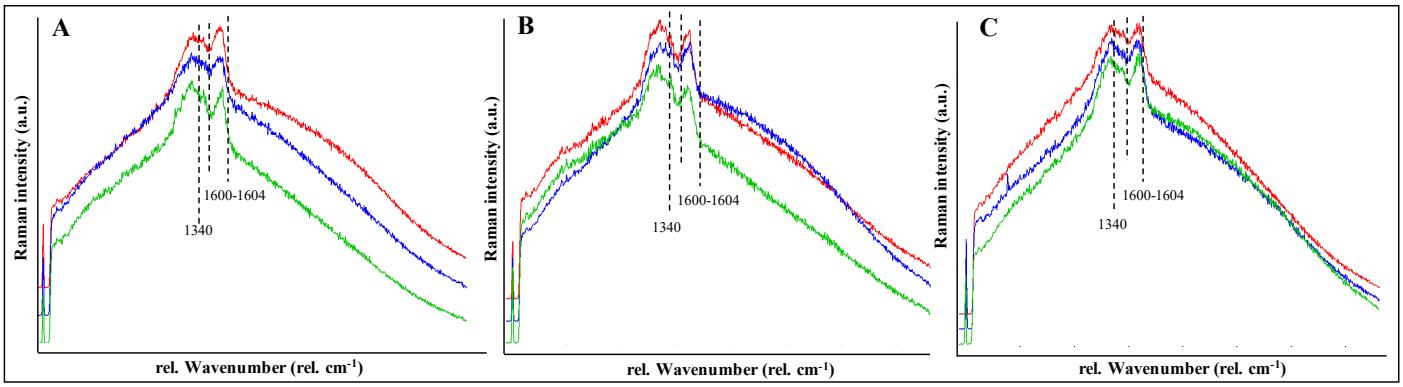

Figure 2. Raman spectra of melanin pigments of *C. antarcticus* grown on **A**) OS exposed to space simulated conditions; B) P-MRS and **C**) S-MRS exposed Mars-like conditions on different layers: Top (exposed to sun light with 0.1% Neutral Density filters) =red spectrum, Bottom (dark control in space, not exposed to space radiation) =blue spectrum and Control (sample kept in the lab, in the dark at room temperature) =green spectrum. OS=Original Substrate, P-MRS= Phyllosilicatic Mars Regolith Simulant, S-MRS=Sulfatic Mars Regolith Simulant.

3.2.3.3 Detection of nucleic acids through amplification method

Although a thermocycler instrument is not one of the equipment foreseen for the imminent exploration missions to Mars, it is a good candidate instrument to search for Earth-like life beyond Earth (Thiel et al., 2012). It is specific and sensitive, detecting even a single DNA molecule in a

sample. The persistence of intact DNA has been tested on samples after ground-based experiment simulating 16 months of exposure to space and Mars-like conditions outside the ISS. First, two different gene lengths, of 939 bp and 330 bp, spanning the ribosomal LSU, have been targeted to be quantitatively amplified by qPCR based on the principle that damaged DNA is not amplifiable. Then, since the ribosomal genes occur in multiple copies in the genomes, we decided to amplify a region of 330 bp of the housekeeping gene β-actin, which is present in a single copy in the genome, to compare the level of detection based on the different gene length and number of copies in the genome.

In Figure 3, we reported the amplification of nucleic acids amplifying 939 bp and 330 bp of LSU gene, and 330 bp of β-actin; the results showed a high amount of amplified DNA in all the experimental condition tested and despite the gene type amplified: 13170 DNA copies on average and never less than 10^2 copies were amplified. The test highlighted a common trend for all the samples, i.e. a lower amount of amplified DNA for samples exposed to UV radiation and vacuum (Top), and a higher copy number for samples exposed to vacuum but no radiation (Bottom) and in the control samples.

To conclude, all the gene amplifications worked out and the number of amplified DNA copy was never under the amplification limit (one copy of a target sequence in genomic DNA), even when we decided to use the single copy gene β-actin.

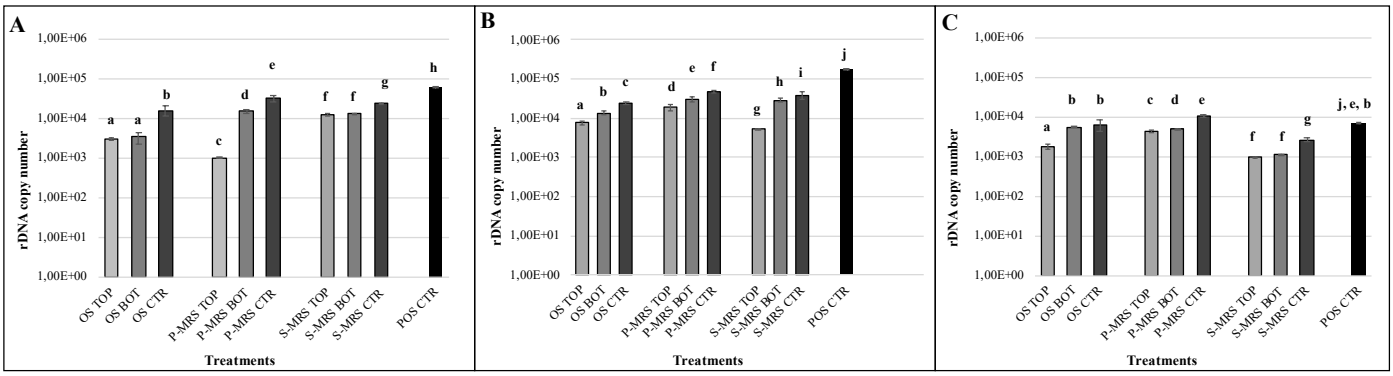

Figure 3. A) Quantitative PCR (qPCR) of a 939 bp target LSU (Large SubUnit) gene; B) a 330 bp target gene (LSU) and C) a 330 bp target gene (actin) of *C. antarcticus* DNA, after exposure to SVT treatments. On the axis of the ordinates the number of amplified copies on a logarithmic scale is shown; on the abscissa axis the treatments are as follow: DNA from samples exposed to space simulated conditions (OS) and samples exposed to Mars-like conditions (P-MRS and S-MRS).

OS= Original Substrate (sandstone); P-MRS= Phyllosilicatic Mars Regolith Stimulant; S-MRS= Sulfatic Mars Regolith Stimulant. Top (exposed to sun light with 0.1% Neutral Density filters), Bottom (dark control in space, not exposed to space radiation) and CTR (sample kept in the lab, in the dark at room temperature); POS CTR= DNA of *C. antarcticus* colony growth in physiological conditions (cultivated on MEA and incubated at 15 °C). The same letters above the bars indicate that the values are not statistically significant according to the *t* test ($p \leq 0.05$). OS=Original Substrate, P-MRS= Phyllosilicatic Mars Regolith Simulant, S-MRS=Sulfatic Mars Regolith Simulant.

3.2.3.3.1 Organic compounds detection by Gas Chromatography associated to Mass Spectrometry

The Mars Organic Molecule Analyzer instrument onboard the ExoMars rover will employ thermal extraction protocols (Goesmann et al., 2017). The characterization of thermal extracts will be carried out by GC-MS detection (Mahaffy et al, 2012). This analysis was performed only on a selection of samples, control and samples exposed to simulated space and Mars-like conditions (Top condition). The GC-MS analysis revealed the presence of several compounds using mass-to-charge ratios (m/z): azelaic acid (1,7-epta-didecanoic acid), myristic acid (1-tetradecanoic acid), pyruvic acid (2-Oxopropanoic acid), glucose, fructose, glucitol, glycerol (1,2,3-tri-hydroxy propane), and ethylene glycol (1,2-dihydroxy ethane). The identified compounds are shown in Table 2; the *m/z* fragmentation spectra of each identified compounds are reported in Table 3. Particularly, the results of pyrolysis analyses showed the presence of low-molecular-weight saturated carboxylic acids. Dicarboxylic acids, such as azelaic acid, were detected in Control and Top samples in OS, P-MRS, and S-MRS analogues (Table 2). In particular, azelaic acid was found in all examined samples, allowing to consider this molecule as a distinctive biomarker for the presence of *C. antarcticus*. Myristic acid was detected only in S-MRS samples exposed to Top conditions and in the relative Control (Table 2). Surprisingly, the amount of azelaic and myristic acids increased after the treatments. A low amount of pyruvic acid was found only in S-MRS control samples; no amount was shown in exposed samples, probably due to the effect of radiation. These results are similar to those reported for ethylene glycol, detected only in the case of S-MRS and P-MRS Top samples.

Table 2. Abundance of main compounds detected with Gas Chromatography-Mass Spectrometry analysis after ground-based simulation.

Compounds[a]	OS Top	OS Control	P-MRS Top	P-MRS Control	S-MRS Top	S-MRS Control
Azelaic acid	0.99	0.13	0.69	0.45	0.30	0.02
Myristic acid	nd	nd	nd	nd	0.48	0.42
Pyruvic acid	nd	nd	nd	nd	nd	0.17
Glucose	3.14	2.78	nd	nd	0.68	13.87
Fructose	0.64	7.53	nd	nd	nd	4.50
Glucitol	nd	3.58	nd	nd	0.88	2.50
Glycerol	nd	nd	nd	nd	nd	nd
Ethylene glycol	nd	nd	1.73	nd	0.41	nd

[a] The analyses was performed after silylation with *N*,*N*-bis-trimethylsilyl trifluoroacetamide in pyridine (620 µl) at 60 °C for 4 h in the presence of betulinic acid [3b-hydroxy-20(29)-lupaene-oic acid] as the internal standard (0.2 mg). All quantities are expressed in μg. GC-MS analysis of OS, P-MRS, and S-MRS samples. Original substrate (OS), Phyllosilicatic Mars Regolith Simulant (P-MRS), and the Sulfatic Mars Regolith Simulant Phyllosilicate (S-MRS). Top samples exposed in the Top of the payload in comparison with Control samples, not exposed to treatments. Nd: not determined.

Table 3. Mass-to-charge ratio (*m/z*) value and the abundance of peaks of identified compounds.

Products[a]	*m/z* (%)
Azelaic Acid[c]	317 (25) [M-CH_3], 302 (3) [M-2xCH_3], 243 (2) [M-OSi(CH_3)$_3$], 201 (15) [M-Si(CH_3)$_3$-CO_2-CH_3], 186 (3) [M-2xSi(CH_3)$_3$], 170 (4) [M-OSi(CH_3)$_3$- Si(CH_3)$_3$], 73 (100).
Myristic Acid[b]	300 (10) [M], 285 (95) [M-CH_3], 257 (3) [M-2xCH_3], 73 (100).
Pyruvic acid[b]	160 (10) [M], 145 (7) [M-CH_3], 88 (14) [M-Si(CH_3)$_3$], 71 (12) [M-Si(CH_3)$_3$-OH], 43 (100) [M-HSi(CH_3)$_3$- CO_2].
Glucose[d]	437 (5) [M-Si(CH_3)$_3$-2xCH_3], 394 (4) [M-2xSi(CH_3)$_3$], 305 (5) [M-OSi(CH_3)$_3$-2xSi(CH_3)$_3$], 217[h] (30), 204[h] (100), 191[h] (75).
Fructose[d]	437 (5) [M-Si(CH_3)$_3$-2xCH_3], 217[h] (30), 204[h] (100), 146 (75).
Glucitol[c]	319 (60) [M], 297 (94) [M-CH_3], 282 (30) [M-2xCH_3], 267 (40) [M-3xCH_3]; 217[h] (90), 204[h] (80); 147 (40).
Glycerol[d]	293 (3) [M-CH_3], 263 (2) [M-3xCH_3], 218 (20) [M-OSi(CH_3)$_3$], 205 (60) [M-OSi(CH3)$_3$-CH_3], 191 (3) [M-OSi(CH_3)$_3$-2xCH_3], 171 (4) [M-OSi(CH_3)$_3$-3xCH_3].
Ethylene Glycol[c]	191 (25) [M-CH_3], 147 (100) [M-4xCH_3], 133 (5) [M-Si(CH_3)$_3$], 103 (20) [M-Si(CH_3)$_3$-2xCH_3].

[a] Mass spectroscopy was performed by using a GC-MS Varian 410 GC-320 MS. The peak abundance is reported in parenthesis [b] Product analysed as the monosilyl derivative; [c] Product analysed as the bis-silyl derivative; [d] Product analysed as the tris-silyl derivative; [e] Product analysed as the tetra-silyl derivative; [f] Product analysed as the penta-silyl derivative; [g] Product analysed as the hexa-silyl derivative; [h] Ions characteristic for EI/MS sugar degradation: m/z 217 [(CH_3)$_3$SiOCH=CH-CH=OSi(CH_3)$_3$]$^+$, m/z 204 [(CH_3)$_3$SiOCH=CHOSi(CH_3)$_3$]$^{+\bullet}$, m/z 191 [(CH_3)$_3$SiOCH=OSi(CH_3)$_3$]$^+$.

3.2.4 Discussion

The detection of biomolecular markers in the subsurface regolith of Mars is a primary goal for astrobiology. Investigation on the stability or degradation-rate of any biomarker after exposure to simulated or real space conditions is of high interest for space exploration. The stability of any biomarker is dependent on its initial form, the matrix in which it is hosted, and the chemical and physical processes it is subjected to over time (Preston et al., 2019).

In this paper, we aimed at investigating the biomarkers associated with fungal colonies in Martian regolith analogues under simulated space and Mars-like conditions, tested during the Scientific Verification Test of the BIOMEX project, with the same techniques planned for the robotic exploration of Mars. Assuming that life on Mars evolved with the same characteristics than those on Earth, or that there was an exchange of material inside meteorites between Earth and Mars (Melosh, 2003) it is reasonable to search for traces of Earth-like life on Mars. Among biomarkers, we first focused on pigments. The black fungus *C. antarcticus,* can withstand the hyper-arid and extremely cold conditions of McMurdo Dry Valleys in Antarctica, thanks to its strongly melanized cell wall that help to protect the fungus from the environmental stressors of these remote areas. It is known that the fungus is able to survive in different stressor conditions, such as ionizing radiation (Pacelli et al., 2021), heavy ions in hydrated and de-hydrated conditions (Pacelli et al., 2020; Aureli et al., 2020).

Melanins are known to be involved in cellular resistance against a multitude of factors, such as toxic metals, hyperosmotic conditions, pH variations (Eisenman and casadevall, 2011), but also extreme temperatures, desiccation and radiation, such as ultraviolet (UV) light, oxidizing agents and even ionizing radiation (Bhartia et al., 2015). We aimed at detecting the presence of melanin pigments in samples subjected to simulated space and Mars-like exposure with different methods. Spectral analyses were used to confirm the presence and the possible alteration of melanin pigments after treatments. UV spectrum (Fig. 1) was characterized by unaltered typical absorption profile of *C. antarcticus* melanin pigments (Pacelli et al., 2021). It shows a strong absorption in the UV region (230 nm) with a progressive reduction as the wavelength increased, due to the presence of many

complex conjugated structures in the melanin molecule (Bell and Wheeler, 1986; Cockell and Knowland, 1999). This kind of analyses is relevant for the upcoming NASA Mars 2020 exploration rover Perseverance, which has onboard the SHERLOC (Scanning Habitable Environments with Raman and Luminescence for Organics and Chemicals) instrument, a deep UV laser with emission wavelengths below 250 nm that will provide an integrative analysis to avoid the fluorescence background during Raman measurements (Samokhvalov et al., 2004). The importance of using a multiple technique approach to characterize melanic pigments is due to its absorption wavelength, which is similar to other compounds (e.g. amorphous carbon), making its detection more challenging. Indeed, to further investigate the state of preservation and characterize the fungal melanin we performed Raman spectroscopy analysis. The Raman spectra were dominated by two main peaks around 1340 cm^{-1} and 1600 cm^{-1} and one smaller at 1425 cm^{-1} (Fig. 2). According to the literature, the presence of the main peak at 1600 cm^{-1} is due to the stretching vibration of the aromatic C=C stretching modes and the 1340 cm^{-1} peak to the C-N stretching band of indole (Pacelli et al., 2018): these peaks together with the smaller peak at 1425 cm^{-1} are attributed to the presence of melanin pigments and, hence, to the fungal colonies.

It is well known that melanin pigments contribute to protect microorganisms against the effect of radiation, which are abundant in space. Melanin pigments may have helped potential Earth-like life to survive in the harsh and highly irradiated environment of Mars, as it occurs in some extreme environments on Earth, where microorganisms have adopted this survival strategy. This assumption is supported by previous studies on the black fungus *C. antarcticus*; the melanized strain survived better the exposure to increasing doses of ionizing radiation compared to the non-melanized counterpart (Pacelli et al., 2017a), confirming the protective role of melanin against ionizing radiation.

Furthermore, the ExoMars rover is equipped with a pyrolysis gas chromatography-mass spectrometry device with the aim to detect organic molecules such as carboxylic acids in Martian subsurface materials (Goesmann et al., 2017; Reinhardt et al., 2020). Assessing the possible thermal destruction

and transformation of organic matter induced by pyrolysis is of utmost importance, for the next rover missions. Indeed, pyrolysis, may alter and transform organic matter (Faure et al., 2006; Moldoveanu, 2010), hiding the presence of organic signatures from samples. For example, organosulfur compounds that were detected by the Sample Analysis at Mars (SAM) instrument onboard the Curiosity rover may derive from artificial secondary reactions of sulfur (from decomposition of sulfates) with organic radicals (Eigenbrode et al., 2018), due to the high temperature of pyrolysis processes. In this context, the main question is: do potential fungal biomarkers remain unaltered during pyrolysis processes? Our study reports that pyrolysis GC-MS is able to detect fungal signals, even when the biomarkers are present in low amounts. Indeed, our data highlighted the presence of low molecular weight carboxylic acids, such as pyruvic acid (only in S-MRS Control samples) and myristic acid (only in S-MRS Top and Control samples). Although pyruvic acid is a key intermediate in several metabolic pathways throughout the cell, it cannot be accounted as a biomarker since it has been found in carbonaceous meteorites and it can be produced through the chemistry of interstellar nitriles, HCN/CN, and ketene (Dorn et al., 2011). Conversely, myristic acid, which can be part of the phospholipid bilayer of the plasma membrane of the eukaryotic cell, can be considered as biomarker. Nevertheless, in our study it has been found only in Top and Control S-MRS samples. Interestingly, azelaic acid, which is a saturated dicarboxylic acid involved in stress resistance, was found in all tested samples, without any alteration in GC-MS profiles (Table 2). In this framework, we can define this dicarboxylic acid directly related to the presence of fungal colonies and we can define it as a good biomarker for the search of Earth-like life elsewhere. Although they can be generated by both biotic and abiotic synthesis (Fischer-Tropsch reactions), in the latter carbons are added one at a time. In most microorganisms, fatty acids are generated biochemically by the addition of two carbon atoms at a time (McKay, 2004). This can help discriminating biotic and abiotic origins of the molecules and, therefore, it allows to considering fatty acids with an odd C number as a potential biomarker. The other detected compounds in our experiment, such as carbohydrates components (glucose and fructose) may derive from the malt extract used for the cultivation of *C. antarcticus*. The low amount

of ethylene glycol detected only in S-MRS and P-MRS irradiated samples most probably derived from the degradation of more complex substances. Even if we can correlate the presence of the colony with the detection of azelaic acid through the GC-MS analyses, the compound was detected in very small amount; this has to be taken into account in future space exploration missions, in order to avoid negative outcomes. One of the restrictions of this technique is the undetectability of high molecular weight compounds. Indeed, one of the main features of the black fungus, the melanin pigments, was not detected using GC-MS instrumentation, showing the importance to use multiple and connected techniques to avoid false negative results.

Then, we investigated the possibility to detect fungal DNA after the exposure through quantitative PCR. Nucleic acids are an ideal target biomarker for its unambiguity, non-specificity and mainly for the impossibility of generation in the absence of life (Mustard et al., 2013; Neveu et al., 2018). DNA potentially preserved in Martian soil may be destroyed by the effects of UV, cosmic ray exposure, and radioactive decay on nucleic acids (Kminek and Bada, 2006; Dabney et al., 2013). Ancient DNA is prone to damage (e.g., hydrolysis, depurination) and fragmentation (Millar and lambert, 2013; Alvarez et al., 1998) once it is no longer actively repaired in a biological system. However, as previously reported in Haberle et al. (2018) and in Castro-Wallace et al. (2017), DNA showed to be still detectable in environmental samples by PCR and stable in Mars-like conditions (Isenbarger et al., 2018). In addition, the bound between DNA and minerals may have facilitated the preservation on different geological timescales, even more in cold and dry environments, such as the Gale Crater on Mars with an average temperature of -48 °C (Fajardo-Cavazos, 2010). In the framework on planetary exploration, the implementation of techniques, such as the qPCR that allows to amplify fragments of a DNA molecule, would detect even minimal traces of DNA, even after partial degradation. Such kind of instrumentation are also very easy to miniaturize. It is already used in field campaigns with the MinION device (Maggiori et al., 2020). This miniaturized technology was used for the first time in 2016 in the frame of Biomolecule Sequencer project (Maggiori et al., 2020) with the aim to detect unambiguous signs of life through nucleic acids sequencing, starting from a small

amount of sample. The advantage of the *in-situ* DNA detection with a miniaturized tool, also allows minimizing any eventual contamination from terrestrial microorganisms (Maggiori et al., 2020). Accordingly, our results suggested that, in spite of the treatments, the nucleic acids are still detectable by qPCR technique. In particular, we found no differences in the amplified region: an average of ~ 13000 DNA copy number were detected. The advantage of the amplification of long-repeated LSU gene, allows detecting any modification at the genomic level in an extended region. On the other hand, these results may give a false outcome, disguising possible radiation damage on DNA, due to the repetition of the gene in the whole genome. Indeed, the choice of β-actin gene amplification permits to amplify a small non-repeated gene region, with the objective to identify nucleic acid damage in a single copy gene. Therefore, we recommend that space agencies should investigate the utility of establishing and promoting a miniaturized PCR instrument (e.g. MinION) to promote the detection of nucleic acids beyond Earth. Specific primers should be used for each of the three domains: bacteria, archaea, and eukarya. In order to identify microorganisms by their sequence, an automated sequencer needs be included in addition to the thermocycler apparatus. Our results showed that, even when using instrumentation already planned for future missions, each analytical technique has constraints that limit the set of information produced. Further improvements in technique and instrumentation, as well as cross comparisons in varying approaches, will be required to optimize data interpretation for the upcoming missions to Mars.

3.2.5 Conclusions

The final aim of this work was to find a good approach to detect fungal biomarkers and to evaluate their detectability after exposure to simulated space and Mars-like conditions as well as to test instrumentation applicability for *in situ* analyses. Additionally, this work is useful to outline a database of biomarker of Earth microbial life, to improve the detection of biomarkers at Mars and to eliminate false-positives or negative detections (Javaux, 2006). In this context, we may consider melanin pigments as a fungal biomarker, owing to its high stability when detected in Martian regolith

analogues after simulated space and Mars-like exposure. In addition, the detection of fatty acids through a GC-MS approach is of utmost importance since these molecules are found in the membranes of all living organisms and then, considered as potential biomarkers for life. Finally, although nucleic acids represent a controversial issue in the context of biomarkers, due to their lower stability and preservation over the time, our results demonstrate a good amplification and stability after the exposure to simulated space and Martian conditions. The results of this work are very appropriate given that the ExoMars Rosalind Franklin rover includes within its payload a Raman Laser Spectrometer and a Gas Chromatograph-Mass Spectrometry instrument.

Acknowledgments: The Italian National Program of Antarctic Researches (PNRA) and the Italian National Antarctic Museum "Felice Ippolito" (MNA) are also acknowledged for funding the collection of Antarctic samples CCFEE. Special acknowledgments also to Timm Roegler and its DLR-department Programmatics in Space Research and Technology and to the Ministry of Economics and Energy for supporting these studies within BIOMEX and BioSigN.

3.3 Fungal biomarkers are detectable in Martian rock-analogues after space exposure: implications for the search of life on Mars

Abstract

Mars is a primary target of astrobiological interest: its past environmental conditions may have been favorable to the emergence of a prebiotic chemistry and, potentially, biological activity. In situ exploration is currently underway at the Mars surface, and the subsurface (2-meter depth) will be explored in the future ESA ExoMars mission. In this context, BIOlogy and Mars EXperiment was performed to evaluate the stability and detectability of organic biomarkers under space and Mars-like conditions. Our data suggested that some target molecules, namely melanin, azelaic acid, and nucleic acids, can be detected even after 16 months exposure to Low Earth Orbit conditions by multidisciplinary approaches. We used the same techniques as onboard the ExoMars rover, as Raman and infrared spectroscopies and Gas Chromatograph-Mass Spectrometer, and polymerase chain reaction even if this is not planned for the imminent mission to Mars. These results should be taken into account for future Mars exploration.

Keywords: life detection, spectroscopy, pigments, biomarkers, Mars, exploration missions.

Pacelli, C., **Cassaro, A.**, Baqué, M., Selbmann, L., Zucconi, L., Maturilli, A., Botta, L., Saladino, R., Bottger, U., Demets, R., Rabbow, E., de Vera, J.-P. P. and Onofri, S. (2021c). Fungal biomarkers are detectable in Martian rock-analogues after space exposure: Implications for the search of life on Mars. International Journal of Astrobiology, 20(5), 345-358.

3.3.1 Introduction

The question of whether Mars ever hosted life remains unanswered. Theoretically, various kinds of metabolisms could have been supported there (Stamenković *et al.,* 2018), especially in the Noachian when conditions were supposedly more favorable to life. If life ever evolved on Mars, nowadays it could still develop underground, given the harsh irradiation conditions on the surface (Cockell, 2014). The upcoming missions to Mars aim to detect traces of extant or recently extinct life, namely biomarkers. A biomarker definition is still under development and debate; but it should be considered as a fingerprint of past or present biological activity (McMahon, 2021) and thus, be strictly biogenic (not found in the abiotic organics in nature). Indeed, it should be an integral component of any water-based life form, and should possess universal chemical and physical properties required for any form of life as we know it. Diverse organic biomarkers have been classified based on the biological features that belong to all known life-forms on Earth, such as a compartmentalized shape, energy-producing and storage mechanisms, and the use of biomolecules to store hereditary information (Summons *et al.,* 2008; Parnell *et al.,* 2007). These biomarkers are made of simple monomers that constitute the building blocks of cells, such as amino acids, sugars, pigments, and lipids, as well as more complex biopolymers such as nucleic acids. A critical consideration in biomarker detection is the compound's resiliency. For example, the persistence of possible biomarkers on the surface of Mars could be affected by the current hostile environmental conditions, such as the unshielded flux of UV and ionizing radiation (Dartnell *et al.,* 2007, 2012a) and strongly oxidizing conditions.

In this framework and with the aim of achieving a list of biomarkers to serve as reference in the ExoMars mission, the BIOlogy and Mars EXperiment (BIOMEX) has exposed for 16 months extremophiles and molecules outside the ISS (de Vera *et al.,* 2019) to investigate their resistance and stability. Among them, the cryptoendolithic fungus *Cryomyces antarcticus*, living in the McMurdo Dry Valleys rocks, Antarctica, is a relevant test organism (Onofri *et al*., 2019). Endolithic black fungi find refuge in the rock's subsurface, where they receive protection from the extreme conditions on the surface, and it has been speculated that a hypothetical form of life may have adopted the same

strategy on Mars (Friedmann, 1986). Here, colonies of *C. antarcticus* were grown on two Martian rock-analogues: the Phyllosilicatic Mars Regolith Simulant (P-MRS) that resembles altered igneous rocks to clays and the Sulfatic Mars Regolith Simulant (S-MRS) mimicking a more acidic environment with sulfate deposits. Samples were grown also on the Original Substrate (OS), the Antarctic sandstone, as a comparison. Once grown, colonies were dried and exposed outside the ISS onboard the exposure facility EXPOSE-R2 (Fig. 1A). During the mission, samples in Tray 1 (space vacuum and solar radiation, from $\lambda \approx 110$ nm) and Tray 2 (Mars-like UV flux, $\lambda > 200$ nm and Mars-like atmosphere) received total UV (200–400 nm) fluencies of about 2.73-3.26×10^2 kJ/m^2 and 3.13-3.63 × 10^2 kJ/m^2, respectively, and 0.5 Gy of cosmic ionizing radiation (Rabbow et al., 2017). Samples in Tray 1 were the ones grown on the OS, samples in Tray 2 were the ones grown on P-MRS and S-MRS analogues (Fig. 1B).

We studied three treatments: i) samples exposed to the whole conditions experienced in space (OS) or Mars-like (P-MRS and S-MRS), including UV radiation (Top), ii) samples maintained in darkness (shielded from UV radiation, Bottom) and iii) samples maintained in the laboratory at room conditions (Control) (detailed description in the section "*Exposure conditions aboard the ISS*"). By using instruments analogous to those carried by Perseverance and Rosalind Franklin rovers (Raman and infrared spectroscopy and gas chromatography-mass spectrometry), we determined if fungal molecules are stable and can be detected in samples similar to those that would be explored by the rovers in the near future. Our goals were to optimize the detection of fungal biomarkers after exposure to simulate the detection of possible traces of life on Mars, as well as to highlight some current limitations and challenges of analytical techniques used in life detection missions.

3.3.2 Materials and Methods

3.3.2.1 Test organism

The test-organism used in the experiment is the cryptoendolithic black yeast-like fungus *C. antarcticus* MNA-CCFEE (Italian National Antarctic Museum's Culture Collection of Fungi from Extreme Environment) 515 that was isolated by R. Ocampo-Friedmann from sandstone collected at Linnaeus Terrace in the Antarctic McMurdo Dry Valleys (Southern Victoria Land) by H. Vishniac, in the expedition 1980-1981 (Selbmann *et al.,* 2005). The fungus was grown on original substrate (sandstone) and Mars Regolith Simulants (MRS). Substrata were prepared as follow: 2% of Malt Extract Agar (MEA) was mixed with 1.5g of Antarctic sandstones, 1g of P-MRS or S-MRS analogues, as described in the following section ("*Mars analogues composition and preparation")*. After growth, each substratum with fungal colonies was de-hydrated under sterile conditions and then cut in a 12 mm-diameter disk to fit within the wells of exposure facility.

3.3.2.2 Mars analogues composition and preparation

Two MRS were used as reported in de Vera *et al*. (2012): two specific Martian mineral analogue mixtures were developed in the frame of the BIOMEX project to simulate early acidic and late basic Mars surface lithosphere composition. The MRS composition was developed and produced by the Naturkundemuseum Berlin according to the data of Mars missions (Bibring *et al*., 2006; Chevrier *et al*., 2007; McCollom and Hynek, 2005). The use of two different mixtures derives from the observation that phyllosilicate deposits do not occur together with sulphate deposits (Poulet *et al*., 2005). Both mixtures are composed of igneous rocks with a mineral composition similar to those of Martian meteorites (composed mainly of pyroxene and plagioclase (gabbro), and olivine). Quartz and anhydrous iron oxide hematite (Fe_2O_3) were added to both mixtures (Böttger *et al*., 2012). The phyllosilicatic MRS resembles igneous rocks altered by pH neutral hydrous fluids to clays of the smectite group, including montmorillonite [$(Na,Ca)_{0.3}$ (Al, $Mg)_2Si_4O_{10}(OH)_2 + H_2O$] and chamosite [$(Fe^{2+},Mg,Fe^{3+})_5Al(Si_3Al)O_{10}(OH,O)_8$] (Poulet *et al.,* 2005), and the clay mineral kaolinite

[$Al_2Si_2O_5(OH)_4$] (Mustard *et al*., 2009). Siderite [$FeCO_3$] and hydromagnesite [$Mg_5(CO_3)_4(OH)_2 + 4H_2O$] are included to account for carbonates formed by either precipitation or interaction between a primitive CO_2-rich atmosphere/hydrosphere and the basaltic subsurface rocks (Chevrier and Mathé, 2007; Morris *et al*., 2010). The sulfatic S-MRS serves as an analogue for a more acidic environment with sulphate deposits: it includes igneous rocks, anhydrous iron oxides, goethite [a-FeOOH] and gypsum [$CaSO_4 + 2H_2O$]. Minerals were mechanically crushed and only fragments smaller than 1 mm were used for the mineral mixtures (Böttger *et al*., 2012). As comparison, the original substratum of the fungus, namely sandstone (composed mainly of quartz) from Beacon Valley in Antarctica, was used.

3.3.2.3 Exposure conditions aboard the ISS

Samples, in the EXPOSE-R2 facility (Fig. 1A and B), were exposed to different conditions:

- to space condition for 16 months outside the International Space Station, in two layers on the Top (exposed to sun light with 0.1% Neutral Density filters) and Bottom (dark control in space) positions of the two-layer stacked sample carrier of EXPOSE-R2 (Fig. 1A).
- Tray 1 (Space conditions), was used to expose samples grown on OS to space vacuum (ranging from $1.33x10^{-3}$ to $1.33x10^{-4}$ Pa), while Tray 2 (Mars-like conditions), to expose samples grown on P-MRS and S-MRS to Mars-like gas mixture composed of 95.55% CO_2, 2.70% N_2, 1.60% Ar, 0.15% O_2, ~ 370 ppm H_2O, at a pressure of 980 Pa. Samples in Tray 1 were exposed to solar UV spectrum >110nm below MgF_2 windows; a Mars-like spectrum >200nm for Tray 2 samples was achieved by respective cut-off filters. (Fig. 1A).

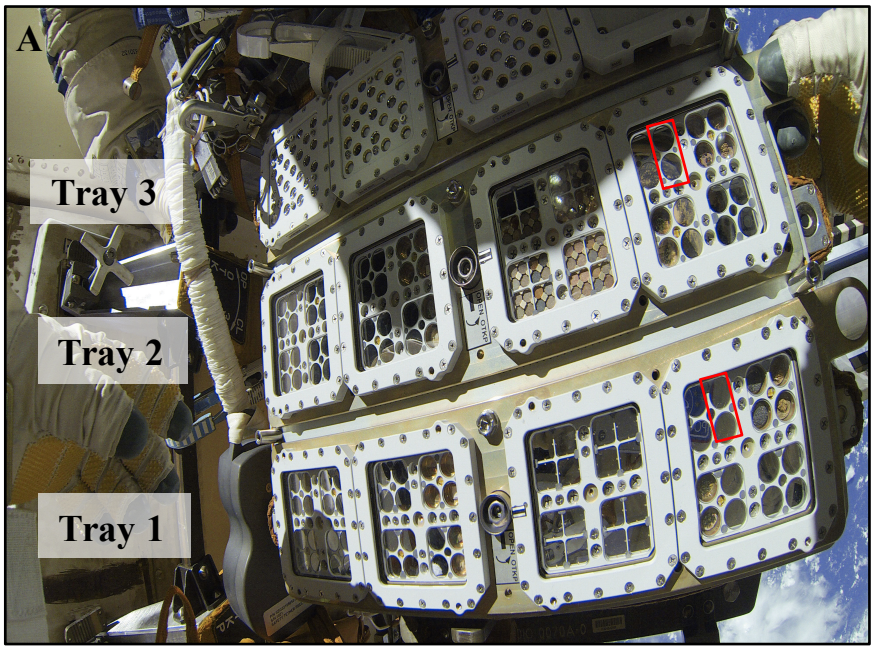

B

Treatments	Tray 1 Space conditions	Tray 2 Mars-like conditions	
	OS	P-MRS	S-MRS
Top Samples exposed to vacuum or Mars-like conditions and irradiation		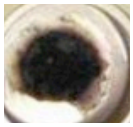	
Bottom Samples exposed to vacuum or Mars-like conditions, not irradiated			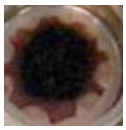
Control Samples maintained in the lab at room conditions			

Figure 1. Exposure setup. (A) EXPOSE-R2 facility during exposure outside the ISS, red squares indicate *C. antarcticus* samples accommodation. **(B)** Set of samples: for each sample (OS = Original Substrate, P-MRS = Phyllosilicatic Mars Regolith Simulant, S-MRS = Sulfatic Mars Regolith Simulant), one disk was exposed in the Top and one in the Bottom position of the two-layer sample carrier. In the top-layer carrier of Tray 1, samples were exposed to space condition and UV irradiation (Top samples), in the bottom layer to space condition only (Bottom samples, dark in-flight control). In the top-layer carrier of Tray 2, samples were exposed to a Mars-like UV flux and Mars-like atmosphere (Top samples); in the bottom-layer carrier only to Mars-like atmosphere (Bottom samples, dark in-flight control). A set of control samples was kept in the laboratory in the dark and at room temperature (control samples). All samples were dried before the

exposure. All details for exposure conditions are reported in "*Exposure conditions aboard the ISS"* section. Photo credits: (A) Cosmonauts Maksim Surayev and Aleksandr Samokutyaev, (B) Elke Rabbow.

3.3.2.4 Timing and conditions of space exposure

Four identical sample sets were subjected to different environmental conditions:

Set 1 was exposed to space vacuum and full-spectrum solar light (OS Top),

Set 2 was exposed to space vacuum but shielded against the Sun (OS Bottom),

Set 3 was kept in a Mars-like atmosphere and solar wavelength spectrum (P-MRS and S-MRS Top),

Set 4 was kept in a Mars-like atmosphere but shielded against the Sun (P-MRS and S-MRS Bottom).

3.3.2.5 Pressure

Sets 1 and 2 were placed in the same sample compartment and therefore shared the same pressure history. Before launch, their compartment was filled with nitrogen at 10^5 Pa (= 1 atm = 760 mm Hg). Once the EXPOSE facility was deployed outside the ISS, this compartment was evacuated by the opening of a valve. The pressure dropped down to near-vacuum, which ranged between 1.33×10^{-3} Pa and 1.33×10^{-4} Pa. The valve was closed again before EXPOSE was moved back into the ISS, leaving the near-vacuum intact until the samples were removed after landing. Sets 3 and 4 were placed in the same sample compartment and therefore shared the same pressure history. Before launch, this compartment was filled with 'Martian air' at 980 Pa. Mars-like pressure was retained until the samples were removed after landing.

3.3.2.6 Solar irradiation

Set 1 was covered by an optical window made of MgF_2 (transmission: $\lambda > 110$ nm), and a 0.1% Neutral Density filter. The total solar dose received by Set 1 ranged between 4750 and 5450 kJ/m^2. Set 2, sharing the same sample compartment, was maintained in darkness for reference.

Set 3 was covered by a window made of quartz (transmission: $\lambda > 170$ nm), a cut-off filter (transmission: $\lambda > 200$ nm) to approach the solar wavelength spectrum at the surface of Mars, and a

0.1% Neutral Density filter. The total solar dose received by Set 3 ranged between 4260 and 4750 kJ/m^2. Set 4, sharing the same sample compartment, was maintained in darkness for reference.

3.3.2.7 Temperature

Sets 1, 2, 3 and 4 experienced a similar temperature history. The highest recorded temperature was +47°C, the lowest -15.0°C, and the average +18.5°C (Rabbow et al., 2017). The strong temperature variations were caused by the constantly changing attitude of the orbiting EXPOSE facility towards the Sun.

3.3.2.8 Cosmic radiation

The total mission dose of the BIOMEX samples was 200-230 mGy. With a mission duration of 696 days, this translated into a daily dose of 290–330 μGy. Inside the ISS (the Columbus module), daily doses of 210–300 μGy were measured. The similarity of the radiation doses recorded outside the ISS (in Expose) and inside (in Columbus) are due to the fact that EXPOSE provided its samples with ≥ 2.2 g/cm^2 of mass shielding by its metal structure, windows and optical filters. This was enough to stop the low-energy cosmic particles, i.e. electrons and most of the protons (Berger *et al.,* 2013).

3.3.2.9 Mission timeline

BIOMEX spent 696 days in space (from launch until landing), 531 of them externally exposed.

12.06.2014 Sample integration completed at MUSC/DLR, Cologne

23.07.2014 Launch

20.08.2014 EXPOSE placed outside the ISS; evacuation of Sets 1 and 2

22.10.2014 Sun shield removed; start of solar exposure Sets 1 and 3

03.02.2016 EXPOSE moved back into the ISS

18.06.2016 Landing

24.06.2016 Sample de-integration at MUSC/DLR, Cologne

3.3.2.10 Raman spectroscopy analyses

Raman spectroscopy was performed at the German Aerospace Center (DLR) in Berlin, using a 532-nm excitation laser, with a WITec alpha300 Confocal Raman microscope, at room temperature, under ambient atmospheric conditions. The spectral resolution of the spectrometer is 4-5 cm^{-1}, a Nikon 10X objective with a 0.25 numerical aperture was used to focus the laser on a 1.5 μm spot. Before the analyses, a spectral calibration was performed with a pure silicon and paracetamol test samples. For single spectra, all measurements were performed at 0.1 mW laser power with 10s integration and 50 accumulation. *Image scans* were done at 0.7 mW with 1s and 1 accumulation (to avoid signal saturation or damaging effects) on three distinct areas up to 100 μm × 100 μm and up to 500 image points, thus collecting a minimum of 1000 measurements per sample. The optimization of Raman measurements is of utmost importance for the discernibility of melanin and amorphous carbon spectra. Therefore, to avoid melanin degradation and thus noticeable shifts in band positions at higher laser powers, the laser power was kept below 0.7 mW with 1s integration time and 1s accumulation for *image scans*, and 0.1 mW with 10s integration time and 50 accumulations for single spectra acquisitions. All data analyses were performed with the WITec Project FOUR software. Parameters used for analysis were the value of signal coverage, to show the presence/absence of the signal, and the value of signal to noise ratio (SNR), defined as spectra having SNR>5. To analyse the presence of the signal, the region of interest (between 200 and 2000 cm^{-1}) was cropped, then a fifth order polynomial function was applied for background subtraction, and finally SNR masks were applied. The SNR is defined here as the height of the 1600 cm^{-1} band divided by the noise represented as the standard deviation of the spectral region (1750 to 1950 cm^{-1}), as previously applied to carotenoids in (Baqué *et al.,* 2018). The typical Raman signal expected from *C. antarcticus* consists of two main melanin bands with a higher intensity band that is located in the region 1590–1605 cm^{-1} and a second

band around 1350 cm^{-1}. Since the exact pigment composition of the fungus is not completely defined (Pacelli *et al.,* 2020), we compared the fungus Raman spectra with the spectra of two synthetic melanins: DOPA (3,4-DiOxyPhenylAlanine) and DHN-melanin (1,8-DiHydroxyNaphthalene), which were bought at Sigma-Aldrich and Thermo-Fisher scientific, respectively. Detailed description of two synthetic melanins used as control is reported in Supplementary Section 1 "*Material and Methods"*. As additional comparison, the spectra acquired from colonies were compared with the spectrum of melanin extracted from the fungus.

Melanin was extracted from dried colonies of *C. antarcticus*, optimizing the protocol reported by Rosas *et al*. (2000). Fungal cells were collected by centrifugation at 16100 rcf for 20 min, washed with phosphate-buffered saline (PBS) (pH 7.4). Cells were suspended in 20 µl of a buffer composed by 0.25 µl of *Trichoderma harzianum* (Sigma #L1412), 50 µl of 0.2 M sodium citrate (pH 5.5), 15 µl of 0.2 M citric acid and 18.2 g of sorbitol, up to the final volume of 500 µl.

Samples were incubated overnight at 30°C, shaken at 50 rpm; samples were washed with PBS two times and collected by centrifugation (10 minutes at 16100 rcf). The supernatant was removed by adding 1 ml of 4M guanidine thiocyanate (VWR International s.r.l.) and samples were incubated overnight on stirrer. Samples were washed with PBS and centrifuged for 15 minutes at 16100 rcf for two times. 1 mg/ml of Proteinase K, previously dissolved in the reaction buffer (4 µl of TRIS HCl, 1 µl of $CaCl_2$ and 1 ml of SDS, up the final volume of 20 ml) was added to the samples; they were incubated at 37°C for 4h and after centrifuged for 5 minutes at 16100 rcf. Samples were washed two times by adding 1 ml of PBS 4X, and three times by adding 1 ml of chloroform.

2 ml of HCl 6M were added to the samples and they were boiled for 1 h. Samples were transferred in dialysis membrane (SnakeSkin Dialysis Tubing, 3.5K MWCO-Thermo Scientific) in sterile water for 3 days, changing the water every day. Finally, samples were lyophilized overnight with the Lyophilizer FreeZone 2.5 Liter Freeze Dry Systems, LabConco and then used for the analyses.

3.3.2.11 Fourier-transform infrared spectroscopy

Mid infrared spectra were obtained with an Infrared spectrometer Bruker Vertex80V, at the Planetary Emissivity Laboratory (DLR), Berlin at room temperature, operating under vacuum conditions to remove atmospheric features from the spectra. Reflectance measurements (showed as transmittance units) performed on fungal colonies grown on each medium mixed with the respective regolith analogue after exposure, were obtained over a spectral range of 600–4000 cm^{-1} at a resolution of 4 cm^{-1}. Smoothing and Fourier self-deconvolution were used to make the spectra. To enhance those specific absorptions and enable better comparisons and interpretations, quadratic polynomials were used to baseline these spectra in those ranges. Three analyses were performed for each sample. Band assignments were performed with 5% of threshold and 2 of prominence.

3.3.2.12 Lipid extraction and fractionation and gas chromatography-mass spectrometry analysis

Solvents and reagents for the extraction and fractionation and for gas chromatography-mass spectrometry (GC-MS) analysis were purchased from Sigma Aldrich. GC-MS was recorded on a Varian 410 GC-320 MS (Palo Alto, CA, USA) using a VF-5 ms column (30 m, 0.25 mm, 0.25 m), and an electron beam of 70 eV. All experiments were performed in triplicate.

The fungal colonies grown on each medium mixed with the respective regolith analogue after exposure, were grinded in agate mortar and then suspended in 2 ml of ethyl acetate. The mixture was left 4 h under magnetical stirring at room temperature. After this time, the suspension was filtered through celite to remove the solid and the solution obtained was concentrated under reduced pressure obtaining a mixture. The mixture obtained with the extraction and fractionation processes was analyzed by GC-MS after silylation with *N*,*N*-bis-trimethylsilyl trifluoroacetamide in pyridine (620 µl) at 60°C for 4 h and addition of a betulinic acid [3β -hydroxy-20(29)-lupaene-oic acid] internal standard (0.2 mg). Mass spectrometry was performed through the following program: injection temperature 280°C, detector temperature 280°C, gradient 100°C for 2 min, and 10°C·min^{-1} for 60

min. To identify the structure of the products, two strategies were followed. First, the spectra were compared with commercially available electron mass spectra libraries such as NIST (Fison, Manchester, UK). Second, GC-MS analysis was repeated with standard compounds. All products were recognized with a similarity index (SI) greater than 98% compared with that of the reference standards. The analysis was limited to products of > 1 $ng \cdot ml^{-1}$, and the yield was calculated as micrograms of isolated products. Mass-charge ratio (*m/z*) values and the abundance of mass spectra peaks of compounds identified are showed in Table S1 (Supplementary Section 2 "*Results*").

3.3.2.13 Nucleic acids extraction and quantitative PCR

DNA was extracted from colonies, using Nucleospin Plant kit (Macherey-Nagel, Düren, Germany) following the protocol optimized for black fungi as reported in Selbmann *et al*. (2005). Before amplification, DNA was quantified using QUBIT system and diluted at the same concentration (0.1 ng/µl). Two different target genes were amplified with qPCR approach to investigate the differences in acid nucleic detection: a small but non-repeated fragment in the genome (β-actin gene of 330 bp) and a long-repeated fragment (LSU gene of 939 bp). qPCR was performed with a BioRad CFX96 real time PCR detection system (BioRad, Hercules, CA) using primers targeting the fungal LSU rRNA gene and the β-actin gene: LR0R [ACCCGCTGAACTTAAGC, (Cubeta *et al*., 1991)] and LR5 [TCCTGAGGGAAACTTC, (Vilgalys and Hester, 1990)], and ACT512-F (ATGTGCAAGGCCGGTTTCGC) and ACT783-R (TACGAGTCCTTCTGGCCCAT) (Carbone and Kohn, 1999) respectively, each at 5 pmol final concentration.

The primers LR0R and LR5 were used to amplify a 939 bp product spanning the LSU region of rRNA encoding genes. The standard qPCR cycling protocol, consisting of a denaturation step at 94°C for 5 min, followed by 35 cycles of denaturing at 94°C for 45s, annealing at 52°C for 30s, and elongation steps at 72°C for 2 min, was performed.

The primers ACT512-F and ACT783-R were used to amplify a 330 bp product. The standard qPCR cycling protocol, consisting of a denaturation step at 95°C for 10 min, followed by 35 cycles of denaturing at 95°C for 15s, annealing at 61°C for 20s, and elongation steps at 72°C for 15s, was performed. Fluorescence measurements were recorded at the end of each annealing step. After 35 cycles, a melt curve analysis was performed by recording changes in fluorescence as a function of raising the temperature from 60-90°C in 0.5°C per increments. All tests were performed in triplicate. For multiple data points, the calculation of the mean and standard deviations was performed. Statistical analyses were performed by one-way analysis of variance (Anova) and pair wise multiple comparison procedure (*t* test), carried out using the statistical software SigmaStat 2.0 (Jandel, USA).

3.3.3 Results

3.3.3.1 Raman spectroscopy analyses

Raman spectroscopy is one of the analytical techniques in future missions potentially capable of detecting traces of life on Mars. Nevertheless, what is the potential of a Raman spectrometer to detect microbial life signatures in Martian rock-analogues? Specifically, in our case, which are the main spectral features from *C. antarcticus*, and are they stable after 16 months of space exposure? Raman mapping was performed on colonies of *C. antarcticus* that have been exposed for 16 months to space and Mars-like conditions. Raman spectra of the substrata identified component minerals (Fig. S1) (Supplementary Section 2 "*Results*").

3.3.3.2 Pigments detection by Raman spectroscopy

The main spectra acquired from fungal colonies correspond to the melanin spectrum. According to Culka *et al.* (2017), the melanin signature consists of two broad bands that can be clearly distinguished: a higher intensity band in the region 1590–1605 cm^{-1} and a second lower intensity band around 1340 cm^{-1}. Recently, it has been demonstrated that *C. antarcticus* possesses a mixture

of two different melanins, L-DOPA and DHN (Pacelli *et al.,* 2020). Therefore, we compared the Raman spectra of the fungal colony (Fig. 2, black line), with the spectra of two synthetic melanins, L-DOPA and DHN (Fig. 2, blue and red lines, respectively). In addition, the spectrum of melanin extracted from the fungal colonies was used as a reference (Fig. 2, green line).

3.3.3.3 Melanin pigments vs amorphous carbon detection

It was an open question whether melanin detected by Raman spectroscopy can be accounted as a biomarker due to its high similarity with the amorphous carbon spectrum. Indeed, the presence of amorphous carbon in the P-MRS analogue (Böttger *et al.,* 2012) represents a challenge for the unambiguous detection of melanin, as demonstrated by the recorded spectrum of amorphous carbon in P-MRS (Fig. 2, turquoise line). However, we pointed out that the melanin and amorphous carbon spectra are different: i) the positions of the D ("disorder" or "defect") and G (graphite) bands of amorphous carbon differ from the recorded melanin spectra with a higher shift for each feature (1350 cm^{-1} for D and 1612 cm^{-1} for G, see Fig. 2), and ii) an additional band around 1457 cm^{-1} was found only in the spectra from the fungal colony and the extracted melanin, highlighted by a grey box in Fig. 2. In addition, the band around 1600 cm^{-1} in the amorphous carbon in P-MRS is shifted and thinner than the broader bands shown in the melanin spectra, as similarly reported in Ferrari *et al.* (2003). The optimization of Raman measurements is of utmost importance for the discernibility of melanin and amorphous carbon spectra.

3.3.3.4 Raman analyses interpretation

As previously applied to the preservation of carotenoids in cyanobacteria (Baqué *et al.,* 2018), we defined the signal coverage as a criterion for quantifying the melanin in the exposed samples. In Figure S2 (Supplementary Section 2 "*Results*"), we defined the Signal to Noise Ratio (SNR) for the melanin' spectra as the height of the 1604 cm^{-1} band divided by the noise represented as the standard deviation of the spectral region 1750-1950 cm^{-1} near the Raman bands. SNR intensity masks were

then derived for each image scan containing 400 spectra on a 100 x 100 µm area, as shown in Fig. S2B (Supplementary Section 2 "*Results*"). The band positions were recorded for each measurement series and did not vary significantly for Top, Bottom, and Control samples (1603-1604 cm^{-1}), regardless of the substratum (Fig. S3; Supplementary Section 2 "*Results*"). The presence of signal, expressed as signal coverage for the image scans, was then defined by a mask with a SNR superior to 5 and was considered as 100% for the control of each substratum (Fig. 3). No significant differences were recorded between the exposure conditions (Top, Bottom, and Control): melanin spectra were present at the same level as non-exposed controls even on Top samples (Fig. 3A). Exposure to Mars-like conditions on the P-MRS and S-MRS analogues (Tray 2) did not show significant difference either between the controls and the exposed samples. However, a higher and more heterogeneous fluorescent background was recorded around the melanin bands (1607 cm^{-1}) in the presence of the P-MRS analogue, as shown in Fig. 3B. The presence of fluorescence was already highlighted in the preparation and first characterization of the P-MRS analogue by Raman spectroscopy (Böttger *et al.,* 2012) and it is shown here to be more problematic when exposed to simulated Martian conditions in space, either in Top or Bottom samples. Single spectra recorded on three different spots on each sample, all showed the unequivocal presence of the melanin signal in all tested conditions (Top, Bottom, and Control) for each substratum (Fig. 4A, B, C). The two main bands recorded on fungal colonies, synthetic melanins, and extracted melanin at around 1340 and 1604 cm^{-1}, as well as the additional band around 1457 cm^{-1} found only on fungal colonies and extracted melanin, could be identified. As stated above, only the spectra recorded in the presence of the P-MRS analogue proved to be altered due to the higher fluorescent background (Fig. 3B). No changes were recorded in the melanin spectra related to the different conditions of exposure (Fig. 4A, B, C). To further confirm the presence of unaltered melanin fingerprint in all experimental conditions, we reported in figure S3 a histogram with the bands position, showing no differences among all tested samples. The highest

recorded shift for the ~1600 cm^{-1} melanin band was 1605 cm^{-1} which is significantly lower than the G band of amorphous carbon given our instrument resolution (1612 cm^{-1}).

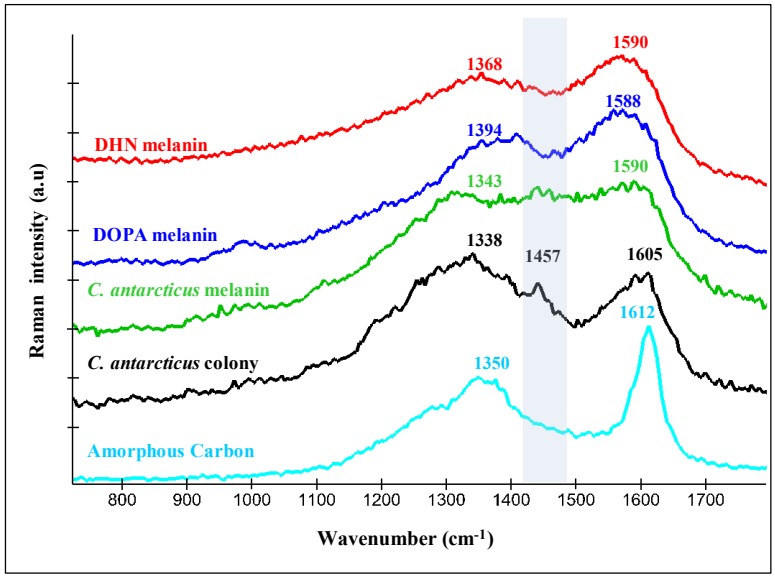

Figure 2. Raman spectra for each exposure condition (Top, Bottom, and Control) and substratum (original substrate: OS, P-MRS, and S-MRS). Raman spectra of the melanin extracted from the fungus (green line), fungal colony (black line), compared with the spectra of two synthetic melanins: L-DOPA and DHN melanins (blue and red line, respectively). Amorphous carbon spectrum from P-MRS analogues was reported as comparison (turquoise line).

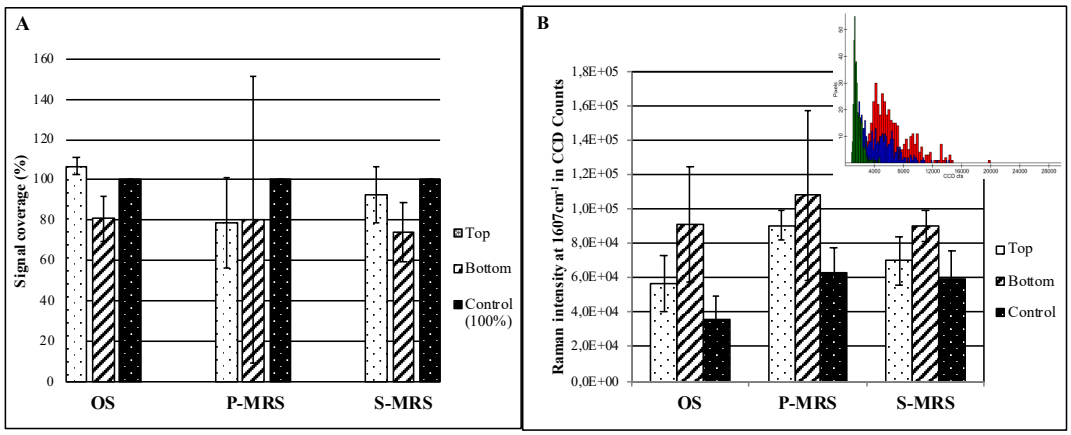

Figure 3. A) Signal coverage (%) calculated by applying a SNR mask superior to 5. **B)** Average value of fluorescent background around 1607 cm^{-1} on image scans for each exposure conditions and substratum, and example of a histogram highlighting the distribution of the fluorescent background in Charge-Coupled Devices counts per pixels on Image scans of the Bottom P-MRS analogue sample (colors as in Fig. 4)

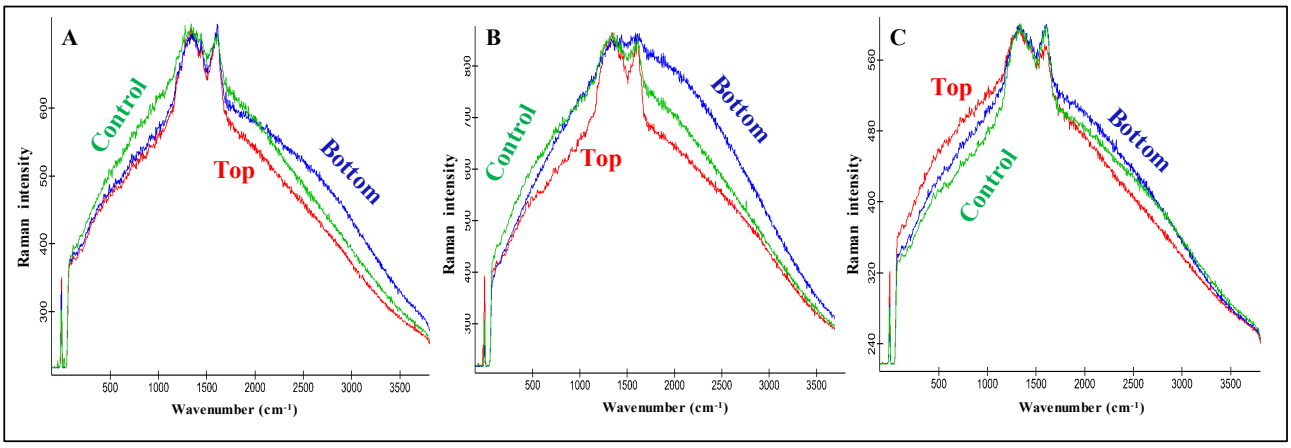

Figure 4. Raman spectra of *C. antarcticus* grown on (**A**) OS (Antarctic sandstone), (**B**) P-MRS and (**C**) S-MRS analogues, after exposure to different conditions: Top (exposed to vacuum or Mars-like conditions and irradiation): red spectrum, Bottom (exposed to vacuum or Mars-like conditions, not irradiated): blue spectrum and control (kept in the lab, in the dark at room temperature): green spectrum.

3.3.3.5 Organic compounds detection by Fourier Transform Infrared Resonance (FTIR) spectroscopy

Among spectroscopy techniques, FTIR spectroscopy has been the preferred one to analyse spectral composition assignments of functional groups by associating them to their respective absorption bands (Centeno and Shamir, 2008). This technique has the advantage to be rapid, requires only a small amount of sample, and has been used successfully for the identification of microorganisms and microscopic biological structures (Preston *et al.,* 2015). FTIR spectroscopy is a technique well proven in space studies and expected to be even more valuable and precise at the local scale within ExoMars instrumentations (Korablev *et al.,* 2017). Mid-infrared (MIR) spectra of the original substrate, P-MRS and S-MRS analogues without colony, used as reference for mineralogical absorbance, are reported in figure S4 (Supplementary Section 2 "*Results*"). Figure 5 shows the IR spectra of OS, P-MRS, and S-MRS samples (Fig. 5A, B, and C, respectively). Several organic functional groups were identified in the spectra. The IR spectra of OS samples (Fig. 5A) Control, Bottom, and Top (green, blue and red lines, respectively) show the characteristic bands of quartz around 1000 cm^{-1}, identified in figure S4A (Supplementary Section 2 "*Results*") and, in addition to gypsum, there are also vibrational modes indicative of carbonate ions (CO_3^{2-}) around 1080 cm^{-1}. Some organic functional groups can be

identified; we report the presence of carboxylic acids with the bands around 3000 cm^{-1} (= C-H stretch) and 1740 cm^{-1} (C = O stretching in esters), as well as the presence of amides around 1535 cm^{-1} (Dovbeshko *et al*., 2000). The presence of melanin bands (3422, 2917, 2843, 1621 and 1024 cm^{-1}) can be highlighted. Figure 5B shows the IR spectra of P-MRS samples Control, Bottom, and Top. The main bands for carboxylic acids [3001, 1732, 739 cm^{-1} (Forfang *et al*., 2017)] are evident in the spectra. The presence of carboxylic acids is more evident in S-MRS samples (Fig. 5C); bands related to C-H stretching vibrations (= C-H stretch at 3011 cm^{-1}, C-H stretching in CH_3 and CH_2 at around 2928 cm^{-1}), C-O-C stretching in esters (1070 and 1250 cm^{-1}), and CH_2 rocking [729 cm^{-1}, (Shurvell, 2006)] are showed. The presence of amides I and II [1610 and 1502 cm^{-1} (Movasaghi *et al*., 2008)] are also reported. Our previous study of *C. antarcticus* melanin characterization by FTIR spectroscopy (Pacelli *et al*., 2020) reported the following bands as characteristic for fungal melanin: broad absorption bands at 3360-3000 cm^{-1} and 2920-2850 cm^{-1}, indicative of stretching vibration of OH groups and NH, respectively, a band at 1633 cm^{-1} (vibration of the aromatic groups C=C or C=O), and a band around 1024 cm^{-1} (for the aromatic ring CH stretching) (Dovbeshko *et al*., 2000). In particular, the two distinct bands of extracted pigments at 2917 and 2843 cm^{-1} were reported as distinctive of IR spectra of the melanin of *C. antarcticus*. Although the presence of melanin can be related to the bands at 1632 and 1032 cm^{-1}, the bands around 2921 and 2835 cm^{-1} are in common with those reported for carboxylic acids [due to C-H stretching vibration in CH_2 (Shurvell, 2006)], and therefore it is difficult to unequivocally assign the molecules. In general, the FTIR analyses revealed the presence of functional groups related to carboxylic acids, amides and melanin pigments. Overall, we found a similar trend for the IR spectra regardless of the substrata: i) no significant differences were found between Top, Bottom, and Control samples (Fig. 5, red, blue, and green lines,

respectively); ii) some bands of mineral and organic compounds overlap and it is not always possible to unequivocally discern their presence.

Figure 5. MID Infrared spectra of fungal colonies growth on different substrata after space exposure. Spectra of *C. antarcticus* grown on (**A**) OS = Original Substrate (Antarctic sandstone), (**B**) P-MRS and (**C**) S-MRS analogues, after exposure to different conditions: Top (exposed to vacuum or Mars-like conditions and irradiation): red spectrum, Bottom (exposed to vacuum or Mars-like conditions, not irradiated): blue spectrum and control (kept in the lab, in the dark at room temperature): green spectrum. Absorbance is expressed as arbitrary unit.

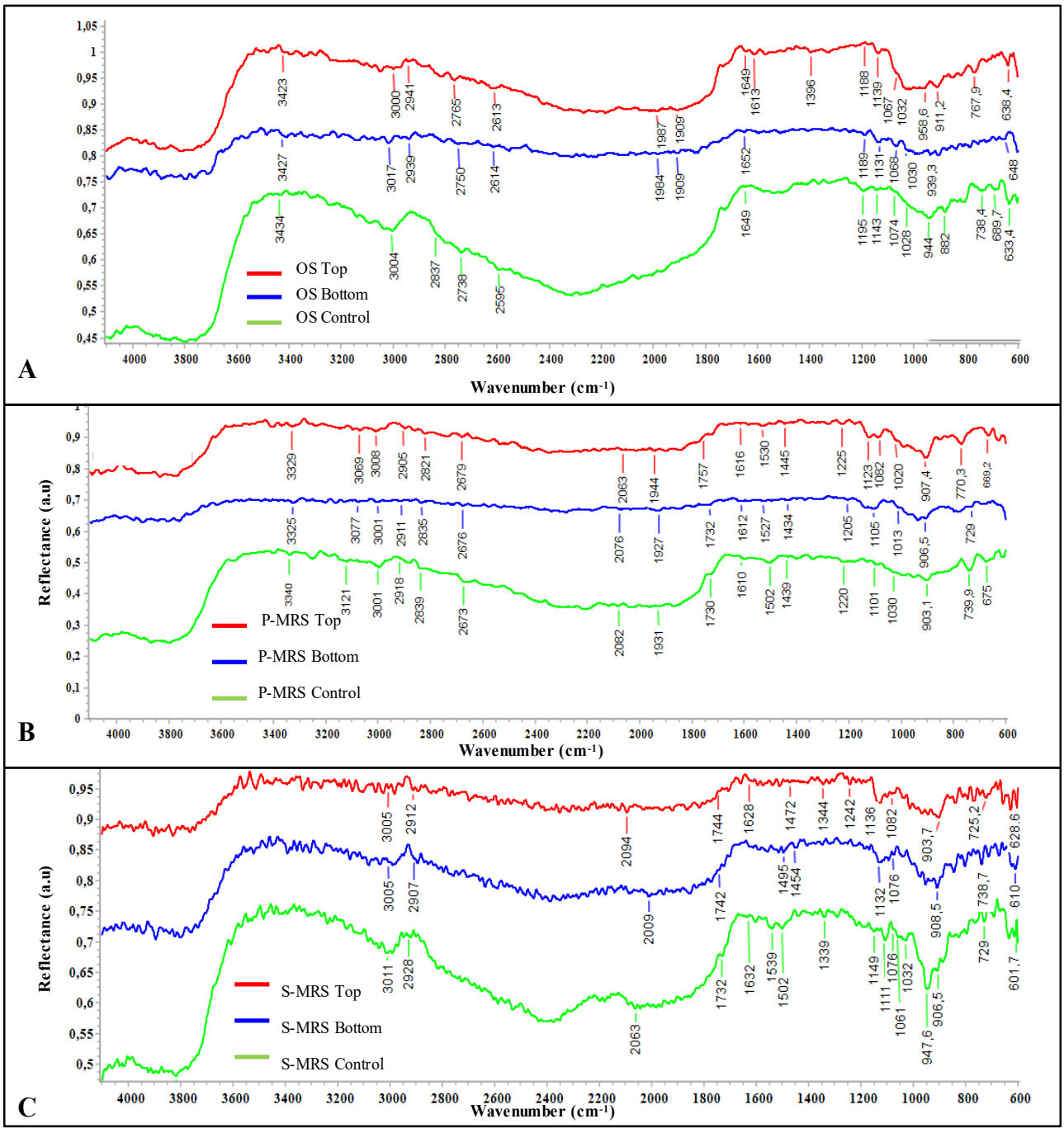

3.3.3.6 Organic compounds detection by gas chromatography associated to mass spectrometry

Gas-chromatography associated to mass spectrometry has been selected for the analysis of samples onboard of the ESA-ExoMars rover (Holland *et al*., 2003) and has a long history of successful use on space missions (Biemann, 2007; Mahaffy, 2008). In order to distinguish which organic compounds are directly related to the presence of the fungus and which are related to the growth medium (rock analogues with MEA), a subset of samples, consisting of substrata without fungal colony, was investigated with this technique. They did not show organic compounds in appreciable amount, except for sugar derivates as glucose and fructose (results not shown). The identification of compounds was performed by using commercially available electron mass spectra libraries such as NIST (Fison, Manchester, UK) and by comparison with standard compounds (Supplementary Section 2, "*Results*"). The results of the GC-MS analyses of the samples exposed outside the ISS for 16 months are reported in Table 1, showing the identified compounds (and the respective amount) for each substratum and treatment. A selected chromatogram is showed as example (Fig. S5; Supplementary Section 2 "*Results*"). The m/z values and the abundance of peaks of the identified compounds are reported in Table S1. The following compounds were identified: azelaic acid (1,7-epta-didecanoic acid), myristic acid (1-tetradecanoic acid), palmitic acid (1-hexadecanoic acid), stearic acid (1-octadecanoic acid), lactic acid, pyruvic acid, glucose, fructose, glucitol, glycerol (1,2,3-tri-hydroxy propane), and ethylene glycol (1,2-dihydroxy ethane) (Table 1). Note that sugar derivatives (glucose and fructose) most probably derived from the malt extract used as cultivation medium of *C. antarcticus*. The samples exposed in the Top and the Bottom position of EXPOSE-R2's carriers on the ISS showed a composition of organic compounds similar to that of the respective Control samples (Table 1, Fig. S6), with some exceptions. Myristic acid, absent in the Control samples, was detected in OS, P-MRS and S-MRS Top samples, while palmitic acid was detected only in OS Bottom and Top samples. Glycerol was observed in Bottom and Top samples, but never in the Control sample. Among the samples, OS samples were characterized by the largest panel of carboxylic acid derivatives, including palmitic acid, stearic acid, and lactic acid. Irrespective of the

analyzed sample, azelaic acid was detected in all the conditions tested (and not detected in the samples without colony) and therefore can be considered distinctive for the presence of fungal colony. To the best of our knowledge, this is the first time that azelaic acid shows the potential to be used as a biomarker.

Table 1. GC-MS analyses of samples after 16 months exposure outside the ISS.

Compound[a]	OS Top	OS Bottom	OS Ctr	P-MRS Top	P-MRS Bottom	P-MRS Ctr	S-MRS Top	S-MRS Bottom	S-MRS Ctr
Azelaic acid	0.13	traces	0.13	0.10	0.01	0.09	0.11	traces	0.45
Myristic acid	0.2	nd	nd	0.7	nd	nd	0.1	nd	nd
Palmitic acid	0.80	0.90	nd	nd	nd	nd	nd	nd	nd
Stearic acid	2.57	1.71	2.46	nd	nd	nd	nd	nd	nd
Lactic acid	nd	0.15	0.35	nd	nd	nd	0.17	0.03	nd
Piruvic acid	nd	nd	nd	nd	nd	nd	nd	nd	nd
Glucose	nd	1.09	0.31	2.31	nd	nd	nd	nd	4.39
Fructose	nd	nd	10.03	0.12	0.54	0.06	nd	nd	0.28
Glucitol	4.24	1.07	1.04	nd	nd	0.85	nd	nd	4.41
Glycerol	nd	0.18	nd	0.52	0.19	nd	0.3	0.45	nd
Ethylen glycol	nd	0.22	0.35	2.22	0.25	0.39	0.09	nd	nd

[a]The analysis was performed after silylation with *N*,*N*-bis-trimethylsilyl trifluoroacetamide in pyridine (620 µl) at 60°C for 4 hrs, followed by addition of betulinic acid [3β-hydroxy-20(29)-lupaene-oic acid] as internal standard. Values are expressed as micrograms (µg) of identified compound. Nd: not determined. Samples reference: OS=original substrate (Antarctic sandstone), P-MRS and S-MRS analogue, after exposure to different conditions: Top (exposed to vacuum or Mars-like conditions and irradiation), Bottom (exposed to vacuum or Mars-like conditions, not irradiated) and control (kept in the lab, in the dark at room temperature).

3.3.3.7 Nucleic acids detection by quantitative Polymerase Chain Reaction (qPCR)

Nucleic acids detection methods like PCR are highly specific and sensitive, able to detect even a single DNA molecule in a sample. The persistence and the detection of fungal DNA were analysed on samples after 16 months exposure to space and Mars-like conditions outside the ISS. Two different target genes were amplified with a qPCR approach to investigate the differences in nucleic acid detection: a long-repeated fragment [Long SubUnit (LSU) gene of 939 bp] and a small but non-repeated fragment in the genome (β-actin gene of 330 bp). Figure 6 shows the results of the LSU and β-actin genes amplification; the DNA was detectable in all the experimental conditions: 5400 DNA copies on average and never less than 300 copies were amplified. The test of LSU amplification highlighted a common trend for all the samples, i.e. a lower amount of amplified DNA for samples exposed to UV radiation and vacuum (Top), a higher copy number for samples exposed to vacuum but no radiation (Bottom) and a further increase in the control samples (up to 10^5 DNA copies, Fig. 6A). The β-actin gene amplification reported a lower number of amplified DNA copies (2700 bp on average). Top samples, in general, showed a lower copy number, which confirms that their DNA was more damaged than the other samples (Fig. 6B), but still amplifiable. To conclude, both LSU and β-actin genes amplification were successful, the number of amplified DNA copy was never under the amplification limit, despite the treatments.

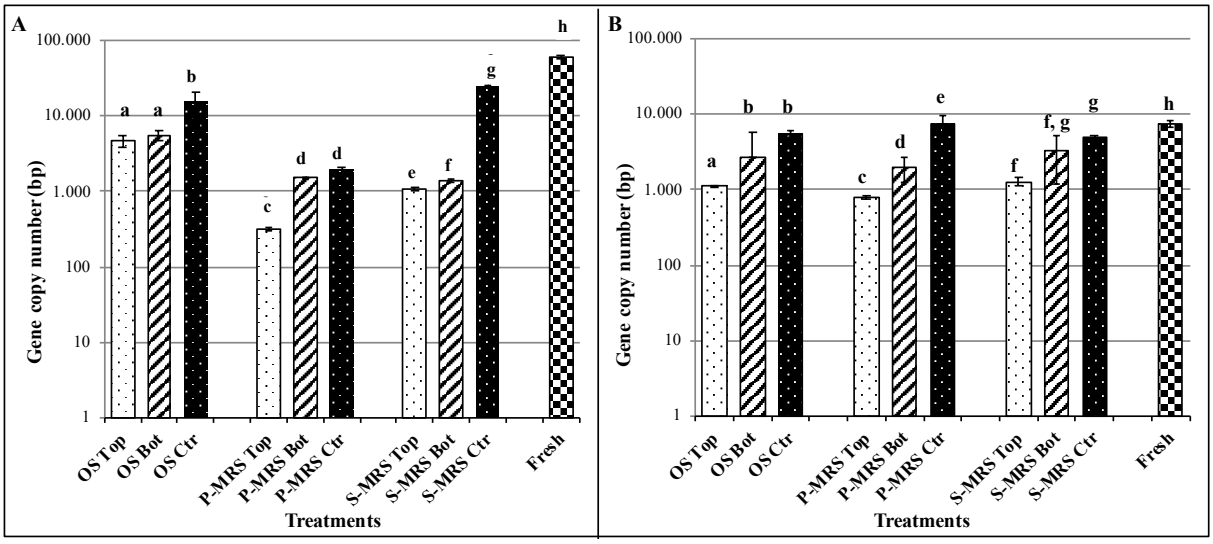

Figure 6. Histogram of Real-time qPCR. Amplification comparison between (**A**) a 939 bp target gene (LSU) and (**B**) a 330 bp target gene (β-actin) of *C. antarcticus* DNA, after 16 months exposure outside the ISS. On the y-axis is the number of amplified copies on a logarithmic scale. On the x-axis the treatments are reported as follow: DNA from samples grown on OS=original substrate (Antarctic sandstone), P-MRS analogue, and S-MRS analogue, and exposed to different conditions: Top (exposed to vacuum or Mars-like conditions and irradiation), Bottom (exposed to vacuum or Mars-like conditions, not irradiated) and control (kept in the lab, in the dark at room temperature). Fresh= positive control: DNA extracted from fungal colony in physiological condition (not dried). The same letters above the bars indicate that the values are not statistically significant according to the *t* test ($p \leq 0.05$).

3.3.4 Discussion

In the context of planetary exploration, this paper reports the first investigation on biomarkers stability in the black fungus *C. antarcticus*, isolated from the Antarctic desert ecosystems of the McMurdo Dry Valleys that have close analogies with Mars, after 16 months exposure in space and Mars-like conditions. Raman and infrared spectroscopies, and GC-MS were chosen to check the stability of pigments and organic compounds, because they are among the selected instrumentations onboard the upcoming missions to Mars (Vago *et al.,* 2015). The aim was to answer the following questions: are the distinctive Raman and infrared fingerprints of the fungus affected by space and Mars-like conditions exposure? Are the fungal compounds modified or distorted by radiation-induced breakdown, and therefore difficult to be detected in highly irradiated Martian surface environment? Raman spectroscopy is a recent addition to astrobiological missions, and is included both on ESA ExoMars and NASA Mars missions, to analyse subsurface samples of Martian soil retrieved by the rover's drill system in the case of the ExoMars rover (Rull *et al*., 2017). Since Raman is a non-destructive technique and does not require reagents or sample preparation, it is a very promising tool for *in situ* diagnosis of biomolecules during life detection missions; it is also sensitive to mineralogy, so it can provide information on the geochemistry of the soil. In addition, Raman instruments allow to detect a low concentration of organic molecules and have the potential to be miniaturized and used aboard the planetary exploration rovers (Edwards et al., 2021).

To gain insight into the preservation of fungal pigments in exposed samples, Raman spectra were recorded. They show the typical melanin signal: two main bands around 1600 cm^{-1} and 1340 cm^{-1}. The assignment of these two bands is not entirely agreed upon; some authors have attributed both bands to the stretching of the C-C bonds within the rings of the aromatic monomers (Galván *et al.,* 2013). Others assigned the contribution of the 1600 cm^{-1} band to the vibration of the aromatic C=C stretching modes and the 1340 cm^{-1} band to the C-N stretching band of indole (Dhole *et al.,* 2016). It is likely that the broad features of melanin are composed of many overlapping Raman bands because of the vibrations of the constituent monomers; furthermore, it is important to highlight that even if some authors pointed out a marked resemblance of the melanin bands to the bands of amorphous carbon (Capozzi *et al.,* 2005), we demonstrated that spectra are discernable. Figure 2 reports the melanin and amorphous carbon spectra: the amorphous carbon spectrum in P-MRS does not have the intermediate band characteristic for fungal melanin (around 1450 cm^{-1}) and the entire spectrum is slightly shifted (1350 cm^{-1}, 1612 cm^{-1}) compared to the melanin one. In general, the intermediate band around 1450 cm^{-1}, is only in the spectra from *C. antarcticus* colonies and from their extracted melanin. According to the study of Culka *et al*. (2017), this can be due to the CH deformation vibrations from compounds such as lipids, polysaccharides and proteins that form the fungal biomass, mainly the cell walls, and this is a distinctive signature of the fungal melanin. The main outcomes of our Raman investigations are that fungal melanin is always detectable through Raman spectroscopy in all experimental conditions and it could be considered as a suitable biomarker (Fig. 4A, B, C). To our knowledge, this is the first study reporting the persistence of fungal melanin in Martian rock-analogues after space and Mars-like conditions exposure. This is even more noteworthy if we consider that, due to the presence of harmful ultraviolet and cosmic radiation on the Martian surface, it can be expected that microbial life, if it ever existed on Mars, would have produced UV-protecting pigments, as part of its survival strategy. The remarkable protective role of melanin has already been widely reported; melanins act as powerful protectors against a broad range of stressors, such as UV and ionizing radiation, extremes of temperature, oxidizing agents and antibiotics, hypersaline and

desiccation conditions (Eisenman and Casadevall, 2012). In particular, the presence of a thicker cell wall and consequent denser incrustation of melanin have previously been demonstrated to enhance the resistance to acute and chronic ionizing radiation of *C. antarcticus*, if compared to its non-melanized counterpart (Pacelli *et al*., 2017, 2018) and to a different species of the same *Cryomyc*es genus, namely *C. minteri*, after 18 months of space and Mars-like exposure (Onofri *et al*., 2012, 2015, 2019). In addition, due to the melanins' wide distribution in all kingdoms of life, they are considered ancient molecules (Blois, 1965). Moreover, melanin is exceptionally preserved in fossils; Glass *et al*. (2012) have demonstrated the preservation of eumelanin in fossil records older than 160 Ma. Therefore, it is plausible that melanization represents an important adaptation mechanism to Earth's climate history and eukaryotic evolution (Pinkert and Zeuss, 2018). Nevertheless, highly energetic UV and ionizing radiations, as present on the early Earth, and present-day Mars, are reported to be the major unresolved issue in the search for biomarkers of past or present microbial life on the Martian surface (Dartnell *et al*., 2007). Dartnell *et al*. (2012b) pointed out the effect of long-term irradiation, especially ionizing radiation, on the preservation of biomolecules, namely deinoxanthin in *Deinococcus radiodurans* and β-carotene in *Synechocystis*. However, recent findings demonstrated that the carotenoids were quickly destroyed by gamma rays only on cells irradiated alone, but they were totally preserved if protected by two Martian mineral analogues, up to the dose of 117 kGy of ionizing radiation (Baqué *et al*., 2018). Differently, Leuko *et al.* (2017) reported the disappearance of the deinoxanthin signal in *D. radiodurans* after exposure to simulated Mars-like conditions in LEO for a prolonged period as part of the BIOMEX project. Our results suggested that melanins are promising biomarkers of microbial life being preserved under space and Mars-like exposure, as well as potentially on the Martian subsurface, due to their distinctive and stable fingerprint by Raman spectroscopy. Among spectroscopy techniques, FTIR is the most appropriate technique to analyze spectral composition assignments of functional groups by associating them to their respective absorption bands (Centeno and Shamir, 2008). The ESA ExoMars rover includes within its payload three IR spectrometers, namely ISEM (Infrared Spectrometer for ExoMars), MicrOmega, and Ma-

MISS (Mars Multispectral Imager for Subsurface Studies). It offers a collection of different methods for the mineralogical and organic characterization of the Martian soil at landing site. Near-IR spectroscopic observations of the Martian surface have not been performed from any surface platform to date. Therefore, the close-up near-IR capability of ISEM on the ExoMars rover offers a very high diagnostic potential (Vago *et al*., 2018). Here, IR spectra complemented the mineralogical information obtained by Raman analyses and showed the main molecular vibrations of some organic compounds (Fig. S4). The assignment of the main bands (assignment cm^{-1}, Fig. 5) to several vibrational functional groups of organics was at the 3401 [O-H stretch, with potential contribution of N-H stretch], 2960 [C-H asymmetric stretch (CH_3)], 1740 [C=O stretch stretching (Fabian *et al.,* 1995)], 1650 [amide I: C= O, C-N, N-H], 1540 [amide II: N-H, C-N], 1423 [C-H bending], 1315 [ester C-O], 1168 [C-OH asymmetric stretch], and 863 [possibly the aromatic C-H out of plane bend] regions. The presence of amide I and II was potentially due to peptides from proteins, while bands around 2800 cm^{-1} are due to the stretching vibrations of CH_2 and CH_3 of phospholipids in cell membranes. Bands around 2917, 2843, 1621, and 1024 cm^{-1} are indicative for melanin pigments. The organic functional groups that could be attributed to melanin, carboxylic acids and amides were hard to be unambiguously discerned, due to the strong and similar mineralogical absorptions. However, as for the Raman investigation, no significant differences were found among the treatments. The MOMA (Mars Organic Molecule Analyzer) instrument, onboard the ExoMars rover, will carry a GC-MS for the extraction and robotic characterization of organic molecules, including carboxylic acids and amino acids, and their degradation products (Vago *et al*., 2017). Our GC-MS data suggested the presence of carboxylic acids as well as the occurrence of appreciable degradative processes for the samples exposed on the ISS facility. Low molecular weight carboxylic acids, such as pyruvic acid and lactic acid, were most probably produced by radiolysis of glucose and fructose occurring in the growth medium, in accordance with the results previously reported for the formation of simple carboxylic acids during the oxidative transformation of monosaccharides (Novotný *et al*., 2008). In a similar way, glycerol and ethylene glycol may be derived from an extensive degradation of the

sugars present in the samples (Baraldi, 1973). Contrary, high molecular weight carboxylic acids, including azelaic, myristic, stearic and palmitic acids (Table 1) cannot be directly related to the radiolysis of monosaccharides; among them, the azelaic acid was clearly associated to the presence of *C. antarcticus* irrespective of the treatments. Azelaic acid is known to be an inhibitor of tyrosinase, one of the key enzymes for melanogenesis process, of mitochondrial enzymes of the respiratory chain, and of DNA synthesis (Nazzaro-Porro, 1987). It remains unclear if the other carboxylic acid derivatives can actually act as biomarkers, even if some of them appeared as possible degradation products of *C. antarcticus*. Carboxylic acids are key intermediates of numerous processes as the production of energy and the biosynthesis of primary and secondary metabolites; the long-chain carboxylic acids (C_9-C_{20}) are especially important because they are constituents of lipids. Indeed, fatty acids are ubiquitous and abundant constituents of bacterial and eukaryotic cellular membranes, bound in phospholipids and glycolipids (Vestal and White, 1989). The hydrocarbon-based acids and alcohols that contribute to the amphiphilic properties of membrane lipids in most bacteria (eubacteria) and eukaryotes have typical chain lengths between 14 and 18 carbons (Georgiou and Deamer, 2014); we found myristic acid (C_{14}), palmitic acid (C_{16}) and stearic acid (C_{18}) in our samples. Fatty acids derived from microbial cellular metabolic processes have an even-over-odd carbon chain length preference due to enzymatically formed acetyl (C_2) units derived from glucose (Volkman and Brown, 2006). However, the carbon chain length and carbon number preference are not always diagnostics of biotic versus abiotic genesis (Williams *et al.,* 2019). Short-chain carboxylic acids may be metabolic products not incorporated into membranes, and Fischer-Tropsch-type reactions can generate long-chain carboxylic acids. In addition, abiotic hydrocarbon derivatives were identified in the Murchison meteorite (Naraoka *et al*., 1999) and they can spontaneously self-assemble into membranous bilayer vesicles in aqueous phases (Deamer and Pashley, 1989). Therefore, we must consider that biotic and abiotic carboxylic acids produce distinctly different GC-MS patterns and these patterns can be used as biomarkers (Georgiou and Deamer, 2014). Nevertheless, the most important outcome of this approach is the identification of azelaic acid as a distinctive feature of the fungal presence, despite

the treatments and the substrata (Fig. S6); therefore, azelaic acid should be taken into account as a biomarker. Lastly, even if PCR-based instruments have not been planned for the future Mars missions, our purpose was to detect nucleic acids from Martian analogue samples using the PCR technique, to test its applicability to an *in-situ* DNA detection technique on Mars for future exploration campaigns. In fact, currently the detection of nucleic acids as biomarkers is one of the strategies under development for life-detection missions destined for Mars (Maggiori *et al*., 2020). PCR is a useful technique that allows amplifying fragments of a DNA molecule, making it possible to detect even minimal traces; therefore, recent efforts have focused on developing robotic instruments able to perform PCR or direct DNA sequencing on environmental samples with low DNA amount (Carr *et al*., 2013). Nucleic acids are excellent biological markers for several reasons including their presence in all forms of life and their specificity as a marker of terrestrial life, their endurance upon adsorption to rocks, the resistance of the information contained therein, and the formation of polymeric, double-stranded chain, improbable under abiotic conditions (Trevors, 2003). The results reported here revealed the extraordinary resistance of *C. antarcticus* DNA, being always detectable after 16 months of space exposure (Fig. 6). The presence of DNA-like molecules in Martian soils is plausible due to large meteoritic exchanges between Mars and Earth and there is an acceptable chance that potential past or eventually present life on Mars could be related to life on Earth (Thiel *et al*., 2011). These results also highlighted the risk of the "forward contamination" of spacecraft hardware, consisting of terrestrial microbes and/or their components (Rummel *et al*., 2014) that can generate false-positive results.

3.3.5 Implications for the search of Earth-like life on Mars

The outcomes of this research are very timely and relevant for space exploration considering that the imminent robotic exploration of Mars will carry Raman, FTIR, and GC-MS instruments. Raman and FTIR spectroscopies offer complementary elemental and mineralogical analysis techniques; they highlighted the presence in our samples of melanin pigments, carboxylic acids and amides. Even if

the detection of organic compounds by IR spectroscopy is challenging due the huge overlap between organic and mineralogical vibrations, it should be highlighted that aliphatic structures were observed, as indicated by C-H stretching vibrations in the region 2960-2850 cm^{-1}. Since C-H bonds exist in virtually all organic compounds, the C-H stretch vibration may be considered the most characteristic for recognizing organic compounds; in addition, this region is free of any mineralogical vibration and therefore of utmost importance for organic compounds detection. Nevertheless, it should be noted that even if IR spectroscopy showed the presence of carboxylic acids and amides, these molecules are not recorded in the Raman analysis. On the contrary, the Raman analyses are dominated mainly by the melanin spectrum; the presence of melanin can also be found by FTIR spectroscopy, but it is difficult to unequivocally assign the bands to the presence of melanin due to vibration overlapping with other organic compounds (as carboxylic acids) and minerals. The identification of carboxylic acids by FTIR spectroscopy was confirmed by the GC-MS analyses; they identified, for the first time, the azelaic acid as a potential biomarker. The detection of nucleic acids by amplification methods in all the samples, and the non-detection by the other used techniques, may suggest new designs for future payloads in the search for life in the solar system. Overall, our results underlined that each technique has its own constraints and limitations on the kind of given information. These results do not have to discourage, instead they highlight the importance to use a suite of complementary analytical techniques to support any identification of organic compounds in the future space robotic exploration. To conclude, we reported on the persistence of fungal biomolecules after 16 months of space and Mars-like conditions exposure outside the ISS, and we discussed their potential use for searching traces of extant or recently extinct Earth-like life on Mars. We have demonstrated i) the robustness of the fungal melanin detection by Raman spectroscopy, ii) the presence of carboxylic acids and amides functional groups by FTIR spectroscopy, iii) the detection of azelaic acid as a distinctive sign of fungal presence by GC-MS, and iv) the detection of nucleic acids by amplification methods. Our analytical techniques are also consistent, for some extent, with the ones proposed in the current and near-future exploration mission to Mars. Results from this study will contribute to the

development of a data library to support the interpretation of data generated by future missions to Mars. Besides, our results suggest that the used techniques should be added in the analysis of the Mars Samples Return (MSR), compared to the life-detection protocol reported in Kminek *et al*. (2014). These researches also have implications in the planetary protection issue, since a hypothetical contaminant could persist under the harsh conditions of an extraterrestrial celestial body. However, some Martian conditions may be deleterious to potential organisms or organic molecules, but could also offer protection, especially for extremophilic organisms or their remains, thanks to their extraordinary adaptation mechanisms (Hallsworth, 2021).

Acknowledgments

We thank the European Space Agency (ESA) for offering the flight opportunity on the ISS and the Russian cosmonauts who took care of the samples between launch and landing. The Italian National Program of Antarctic Researches (PNRA) and the Italian National Antarctic Museum "Felice Ippolito" (MNA) are also acknowledged for funding the collection of Antarctic samples and the CCFEE.

3.4 Spectroscopic investigations of fungal biomarkers after exposure to heavy ion irradiation

Abstract

The main objective of the ongoing and future space exploration missions is the search for traces of extant or extinct life (biomarkers) on Mars. One of the main limiting factors on the survival of Earth-like life is the presence of harmful space radiation, therefore understanding the effects of radiation on terrestrial biomolecules stability and detectability is of utmost importance. Which terrestrial molecules could be preserved in a Martian radiation scenario? Here, we investigated the potential endurance of fungal biomolecules, by exposing de-hydrated colonies of the Antarctic cryptoendolithic black fungus *Cryomyces antarcticus* mixed with Antarctic sandstone and with two Martian regolith analogues to increasing doses (0, 250 and 1000 Gy) of accelerated ions, namely iron (Fe), argon (Ar) and helium (He) ions. We analyzed the feasibility to detect fungal compounds with Raman and Infrared spectroscopies after exposure to these space-relevant radiations.

Keywords: Mars exploration, ionizing radiation, biomarkers stability, Raman and FTIR spectroscopies

Cassaro A., Pacelli C., Baqué M., Maturilli A., Bottger U., Fujimori A., Moeller R., de Vera J-P.P., Onofri S. Spectroscopic investigations of fungal biomarkers after exposure to heavy ion irradiation. Submitted on “Astrobiology”.

3.4.1 Introduction

The concept of habitability requires the presence of "an environment able to support the activity of at least one organism, where activity is considered as metabolic activity allowing for survival, maintenance, growth, or reproduction" (Cockell et al., 2016). This concept is strictly related to life detection on other planets. Nowadays, Mars is considered as one of the potential habitable planets in our Solar System, because it contains carbon, potential energy sources to support life, and water in different forms, such as polar ice cap, subsurface deposits, hydrated salts and water vapor (Malin and Edgett, 2000, 2003; Michalski et al., 2017; Rasmussen et al., 2009). However, one of the main factors limiting the habitability and the detection of life is its high radiation environment. In fact, the Martian surface is reached by different particles, which include Galactic Cosmic Rays (GCRs) and Solar Energetic Particles (SEP). GCRs occur afterwards cosmic events, such as supernova explosion (Chancellor et al., 2018), and are composed of energetic particles, which cover a wide spectrum of energy and mass values: light particles (85% of hydrogen-ions and 14% of helium ions) and the so-called High charged Z and Energy particles (HZE). These particles constitute about 1% of GCRs, and because of their high energy and penetration depth, they represent the main damaging component for organic matter (Ferrari and Szuszkiewicz, 2009; Horneck et al., 2010, 2016). Besides, SEP are characterized by non-ionizing UV radiation, X-rays and solar flares mostly composed of protons (Sliney, 2007).

The lacking of a global dipole magnetic field and a sufficient atmosphere (<1%) able to deflect charged particles on Mars, allows them to penetrate and react with Martian regolith, creating other particles leading to an oxidizing environment on the Martian surface. The radiation dose of GCRs reaching the Martian surface was estimated to be about 0.210 ± 0.040 mGy/day (Hassler et al., 2014), while the SEP dose was measured at 50 μGy/event (Hassler et al., 2014) by the Radiation Assessment Detector (RAD) onboard the Mars Science Laboratory (MSL) rover. This highly irradiated environment could cause the chemical alteration of regoliths, altering the hypothetical organic matter preserved therein, and making difficult the detection of traces of life.

Indeed, each particle induces a track of electrons and ionization of atoms inside molecules characterized by a well-defined diameter and energy deposition, which produce different areas and biological damages. When radiation interact with matter through an ionization process, it may induce direct effects on biomolecules (i.e. nucleic acids and proteins) by energy absorption and secondary effects with radiation-induced radicals (radiolysis) (Moeller et al., 2010).

The ionization of these particles in a medium is characterized by a physical parameter named Linear Energy Transfer (LET) defined as the average energy transferred by a single particle and deposited per unit length (expressed in keV/μm, which is referred to a particle's charge and velocity—energy per nucleon— and the elemental composition of the traversing medium) (Hamada et al., 2010) and used to quantify the effects of ionizing radiation on biological matter. Particles with increasing LET, such as iron ions are able to produce dense ionization (that produces clusters of lesions very close to each other) compared to sparse ionization (that produces lesions separated from each other) of low LET X-rays (Hagiwara et al., 2019). Despite the low abundance of iron ions (0.03% of HZE, Horneck et al., 2010) in the cosmic radiation spectrum, they are considered the particles with the highest lethal value in terms of released energy (Leuko and Rettberg, 2017; Moeller et al., 2017). However, the effects of accelerated heavy ions with atomic number Z >18 cannot be related exclusively to LET value, as has been found for lighter ions, but also depending on the spatial distribution of ionizing energy around the particle's trajectory. The energy depositing released by heavy ions can be subdivided into a densely ionizing core and a penumbra where energy transfer takes place by far reaching secondary electrons (Baltschukat et al., 1986), excluding only localized effects. The different organization in spatial distribution of ionization implies different types of biological damages: sparse ionizing radiation (low-LET) induce single strand breaks (SSBs) compared with clustered DNA damages, such as double strand breaks (DSBs) of dense ionizing radiation (high-LET). DSBs are the most damaging radiation effects since the majority of living organisms are not able to repair this kind of damages. For example, 10,000 Gy of irradiation (γ-rays) induced almost 100 DSBs per chromosome in *Deinococcus radiodurans*, (Daly and Minton, 1996). Nevertheless,

many organisms (mainly fungi) have demonstrated to survive after exposure to ionizing radiation, recovering from multiple damages (Zhdanova et al., 2000; Liu et al., 2003; Dadachova and Casadevall, 2008; Schultzhaus et al., 2019, 2021).

Considering the Martian radiative surface conditions, the most probable place to find life is in the subsurface of the planet. Indeed, it was demonstrated that the effects of GCRs diminished at 3 meters depth on the beneath of the Martian surface and model predictions showed that 1-meter depth should be enough to find resistant and hypothetical microbial life (Hassler et al., 2014).

In addition, minerals could provide support and preserve of organic molecules over geological scale as reported for well-preserved organic matter in 3 billion-year-old mudstones of Gale Crater (Eigenbrode et al., 2018).

In this scenario, what is the potential shielding ability of Martian regoliths against radiation? Are they able to protect hypothetical biomarkers in the subsurface?

To answer this question, in the frame of the STARLIFE 2018 irradiation campaign, various microorganisms and their associated molecules have been investigated for testing their resistance to different space-relevant ionizing radiation exposure. Among them, de-hydrated colonies of the Antarctic black fungus *Cryomyces antarcticus* were mixed with two Martian regolith analogues, Phyllosilicate Mars Regolith Simulant (P-MRS) and Sulfatic Mars Regolith Simulant (S-MRS) and exposed to different doses (250 and 1000 Gy) of ions of Fe (500MeV/n), Ar (500MeV/n) and He (150MeV/n). The extraordinary radio-resistance of the black fungus in terms of survivability and DNA resistance has already been widely investigated in ground-based experiments (Pacelli et al., 2017a, b; Cassaro et al., 2021) and space exposure outside the International Space Station (ISS) (Onofri et al., 2012, 2015, 2019; Pacelli et al., 2021). Recently, its resistance, in terms of survival and cellular damages, to exposure up to 1000 Gy of He ions when mixed with P-MRS analogue (Pacelli et al., 2020a) and to 1000 Gy of Fe ions (Aureli et al., 2020) has been reported. Here, we aim at investigating the protective role of Martian regolith analogues on the stability of fungal biomolecules by using Raman and Infrared spectroscopies after exposure to this ionizing radiation. This is notably

important also considering that, in samples containing a mixture of abiotic and biotic components, the unambiguous identification of biological molecule can be extremely difficult (Messmer et al., 2022). This work gives essential support in space exploration, contributing to a correct interpretation of data from missions, and helping to develop specific methods for the identification of signs of Earth-like life on planetary sub-surfaces through *in-situ* analysis with dedicated instrumentation.

3.4.2 Materials and Methods

3.4.2.1 Fungal colonies and mineral mixtures preparation

The investigated organism was the black fungus *C. antarcticus* MNA-CCFEE 515, isolated from sandstone rocks collected by L. Vishniac at Linnaeus Terrace (McMurdo Dry Valleys, Southern Victoria Land, Antarctica) during the expedition in 1980-1981. The fungus was supplied by the Italian National Antarctic Museum's Culture Collection of Fungi from Extreme Environment (MNA-CCFEE) of Mycological Section of the University of Tuscia (Viterbo, Italy). Colonies for irradiation were obtained spreading 2000 Colony-Forming Units (CFU) on MEA medium (malt extract, powdered 30 g/L; agar 15 g/L; Applichem, GmbH) on Petri dished. Fungal samples were incubated at 15 °C for 3 months. After growth, the colonies were de-hydrated under a laminar flow, at room temperature. Once de-hydrated, colonies were mixed in standard 200 µl volume PCR tubes with three distinct minerals mixture, previously dried-sterilized at 140 °C for 4 hours. Three sample's sets were thus investigated**: i)** colonies mixed with grinded Antarctic sandstone that is the Original Substratum (referred as "OS") where the fungus naturally occurs, **ii)** colonies mixed with Phyllosilicatic Mars Regolith Simulant (referred as **"**P-MRS"), simulating the early evolutionary stages of Mars and rich in montmorillonite, **iii)** colonies mixed with Sulfatic Mars Regolith Simulant (referred as "S-MRS"), simulating the late evolutionary stages of Mars and with abundant plagioclase and gypsum minerals (Böttger et al., 2012).

3.4.2.2 Radiation exposure

Triplicate samples of each set were individually exposed on PCR tubes to three different types of high-energy-charged ions: Fe, with energy of 500 MeV/nucleon (LET = 200 keV/μm), Ar, with energy of 500 MeV/nucleon (LET=95.6 keV/μm) and He, with energy of 150 MeV/nucleon (LET= 2.2 keV/μm) (Table 1). Irradiations were performed at the heavy ion medical accelerator (HIMAC) facility of the National Institute for Radiological Sciences (NIRS) in Chiba, Japan. The geometry of irradiation of the HIMAC and dose calculations have been described in Okayasu et al., (2006).

Table 1. Radiation values experienced during STARLIFE experiments

Ion	**Energy (MeV/n)**	**LET (keV(μm)**	**Intensity (in particles per second)**	**Dose rate (Gy/min)**
Iron	500	200	$2.5 \cdot 10^8$	12.1
Argon	500	95.6	$2.4 \cdot 10^8$	6.8
Helium	150	2.2	$2 \cdot 10^9$	4.2

3.4.2.3 Fourier transformed infrared resonance (FT-IR) spectroscopy analysis

FT-IR spectroscopy has been used for the investigation of microorganisms and microscopic biological structures (Schmitt and Flemming, 1998; Igisu et al., 2009; Preston et al., 2015). It allows the identification of vibrational modes of chemical bonds in an organic and inorganic substratum. The resulted spectra are obtained by passing radiation through a sample and determining what the fraction of radiation and which energy is absorbed. This energy, able to generate any absorption peak in a spectrum, corresponds to the frequency of the vibration of a functional group in a molecule, which may be diagnostic for different molecules.

In this work, samples were scanned with an IR Bruker Vertex80V FTIR Spectrometer, housed at the Planetary Spectroscopy Laboratory (PSL) of the German Aerospace Center (DLR) in Berlin.

Reflectance measurements, were performed over a spectral range of 600–4000 cm^{-1} at a resolution of 4-5 cm^{-1} and an average of 250 scanning; in total three spectra were acquired for each sample. Measurements were performed directly on samples without preparation, at room temperature, operating under evacuated conditions to remove atmospheric features from the spectra. Bands assignment were performed with a 3-hreshold value; 3% of maximum intensity and a noise factor of 2. All data analyzes were performed with the Spectragryph software version 1.2.14.

3.4.2.4 Data analysis

Heat Map (HM)

In this work, we used the HM to evaluate potential difference in band positions, as a direct consequence of the radiation exposure. HM is a graphical representation of a set of measurements that allows a direct comparison among data, through a color map (Monti et al., 2013). In this work, a heat map was generated using RStudio (RStudio Software 3.6.3), considering the wavelength values of organic and inorganic compounds bands, measured with FT-IR analysis for *C. antarcticus* colonies after exposure to different heavy ions (Fe, Ar and He), in all irradiation conditions (0, 250 and 1000 Gy).

3.4.2.5 Confocal Raman spectroscopy analysis

Confocal Raman analyses were performed to investigate the stability of protective pigments, mainly melanin, and the potential shielding of the mineral mixture. Raman spectroscopy analyses were performed at the German Aerospace Center in Berlin, using a 532 nm excitation laser, with a WITec alpha300 Confocal Raman microscope. The samples were analyzed without further preparation, by removing the colonies from each minerals mixture and depositing them on glass slides; at room temperature, under ambient atmospheric conditions. Acquisitions and data analyses were performed according to the optimized protocol from Pacelli et al. (2021).

3.4.3 Results

3.4.3.1 Fourier Transform Infrared Resonance Spectroscopy (FT-IR) detection

FTIR spectroscopy was used to identify functional groups, such as carboxyl, phosphate, and amine groups, through their characteristic absorption bands in defined regions of the spectrum (Orsini et al., 2000; Caccamo et al., 2020). This analysis was used to determine structural and biochemical changes occurring in irradiated samples in comparison with untreated samples. Numerous compounds (inorganics and organics) were identified in the Mid-infrared (MIR) spectra of *C. antarticus* and they are summarized in Table 2.

Table 2. Organic and mineralogical FTIR reflectance band frequencies from all tested samples, including assignments and potential origins

Wavenumber (cm^{-1})	Assignment	Potential origin
657	CH bend	alkyne
700	O–H out-of-plane deformation vibration or to the C–S stretching vibrations	phenols or thiols and thioethers
790	CH out-of-plane deformation	benzenes
815	C–H out-of-plane deformation vibrations	Aromatic compounds
880	stretching and bending ν_2 vibrational modes of C-O	carbonate
1000	ν_1 symmetric and ν_3 asymmetric stretching vibrational modes of SO_4 tetrahedra	Quartz
1020	carbon ring breathing vibrations	cyclic compounds (melanin pigments)
1080	CO_3^{-2} ion in-plane bend	Carbonates
1161-1100	C–O–C antisymmetric stretching or to the Si–O–Si and Si–O–C stretching vibrations	aliphatic ethers or silicon-oxy compounds
1250	C-O-C stretching	esters
1450	CH_2 bending (scissors) vibration	Aliphatic compounds
1620	vibration modes of aromatic ring C=C or C=N	melanin pigments
1750	C=C bond	lipids and fatty acids
1820	C=O bond	acid halides
1870	C=O bond	β-lactones
2000	C≡N stretching vibrations	nitriles and thiols
2037	C≡N stretching vibrations	nitriles and thiols
2135	C≡N stretching	nitriles and thiols
2230	C≡N stretching	nitriles and thiols
2510	C-N-H vibration	
2600	H-bonded NH vibration band	
2680-2630	stretching N-H (NH^{3+})	
2850	methyl C–H asymmetric/symmetric stretching	aliphatic compounds
2930	methyl C–H asymmetric/symmetric stretching	Aliphatic primary amine
3200	asymmetric and symmetric OH stretching	fully hydrogen bonded pure water molecules
3375	stretching O-H bands	alcohols and phenols
3550	OH stretching	
3640	ν_3 antisymmetric stretching	Water molecules
3700-3600	OH stretch of –OH	alcohols and phenols

3.4.3.2 Mineralogy

Bands at 1161, 1100 and 1000 cm^{-1} arise from the Si–O–Si and Si–O–C stretching vibrations in silicon-oxy compounds (Coates, 2006; Shurvell, 2006) and from the ν_1 symmetric and ν_3 asymmetric stretching vibrational modes of SO_4 tetrahedra (Preston et al., 2020), respectively have been detected in all set of samples (Figs 1, 1S and 2S). However, the first band appears sharper in OS samples due to the presence of quartz as main component of sandstone (Fig. 1A, 1SA, 2SA, Prinsloo et al., 2014), in comparison with P-MRS (Figs. 1B, 1SB and 2SB) and S-MRS samples (Figs. 1C, 1SC and 2SC). The band near 1080 cm^{-1}, assigned to carbonate ions (CO_3^{2-}) (Bourgier, 2007), appears in the MIR spectra of S-MRS (Figs. 1C, 1SC and 2SC). Some bands in MIR spectra of P-MRS samples are unaltered after irradiation, ~880, 700, and 610 cm^{-1} (Fig. 1, 1S and 2S): these bands could be attributed to the stretching and bending ν_2 vibrational modes of C-O of carbonates (Preston et al., 2020), and to SO_2 deformation in sulfonyl chlorides (Shurvell, 2006); respectively.

3.4.3.2 Organics

MIR spectra of samples exposed to Fe ions

Figure 1 shows the MIR spectra of samples irradiated with Fe ions (Fig. 1A, B, and C; respectively). Alcohols and phenols [3700-3600 cm^{-1} (Shurvell, 2006)] have been detected in all MIR spectra (Fig. 1B, C and D). These bands resulted less pronounced in the MIR spectra of S-MRS control (Fig. 1C, green line). The presence of aliphatic compounds (attributed to the methyl C–H asymmetric/symmetric stretching vibrations) are highlighted at 2930 and ~2850 cm^{-1} (Coates, 2006; Shurvell, 2006; Movasaghi et al., 2008; Sajjan et al., 2013). These bands are well preserved in the MIR spectra of colonies mixed with OS (Fig. 1B). These bands are not clearly visible in spectra with the Martian analogues regolith and disappear at the highest radiation dose (1000 Gy, Fig. 1B red line) and at the highest and intermediate irradiation doses of samples mixed with S-MRS analogue (Fig. 1C blue and red lines).

The bands observed near 2680, 2600 and 2510 cm^{-1} assigned to stretching N-H (NH_3^+) (Dovbeshko et al., 2000), H-bonded NH vibration band (Dovbeshko et al., 2000; Movasaghi et al., 2008), and C-N-H vibration (Rinaudo, 2006); respectively, have been detected only in OS, (where they remain unchanged, Fig. 1A) and in P-MRS spectra (flattened in control sample, Fig. 1B).

The presence of nitriles and thiols [2230 and 2135 cm^{-1} (Coates, 2006; Shurvell, 2006)], identified by C≡N stretching vibrations, have been reported in all experimental conditions; less pronounced in control samples of P-MRS spectra (Fig. 1B, green line) and absent in S-MRS control sample (Fig. 1C, green line).

The band near 1750 cm^{-1} attributed to C=C bond in lipids and fatty acids (Movasaghi et al., 2008), maintained its stability in all experimental conditions, excepting in S-MRS spectra of control sample (Fig. 1C, green line). The presence of melanin bands at 1621 and 1024 cm^{-1} [due to the bending vibration modes of aromatic ring C=C or C=N (Mbonyiryivuze et al., 2015) and to carbon ring breathing vibrations in cyclic compounds (Pal et al., 2014; Shurvell, 2006)] could be identified in all analyzed spectra.

The MIR spectra report the presence of amide I band near 1660–1628 cm^{-1} (Böcker et al., 2017) (Fig. 1A, B, and C). The band near 1250 cm^{-1} may be associated to C-O-C stretching in esters (Shurvell, 2006) or to polysaccharides (Schulz and Baranska, 2007; Forfang et al., 2017); it occurs in MIR spectra of P-MRS and S-MRS samples (Fig. 1B and C).

The MIR spectra of OS samples exposed to Fe ions show a similar shape. Particularly, no differences between irradiated and control samples have been reported (Fig. 1A).

On the contrary, MIR spectra of P-MRS samples (Fig. 1B) revealed a higher similarity between control and 250 Gy irradiated samples (green and blue lines) compared with 1000 Gy irradiated samples (red line), that showed more pronounced bands; and the MIR spectra of S-MRS (Fig. 1C), 250 and 1000 Gy irradiated samples (red and blue lines) show a higher similarity compared with the control sample (green line).

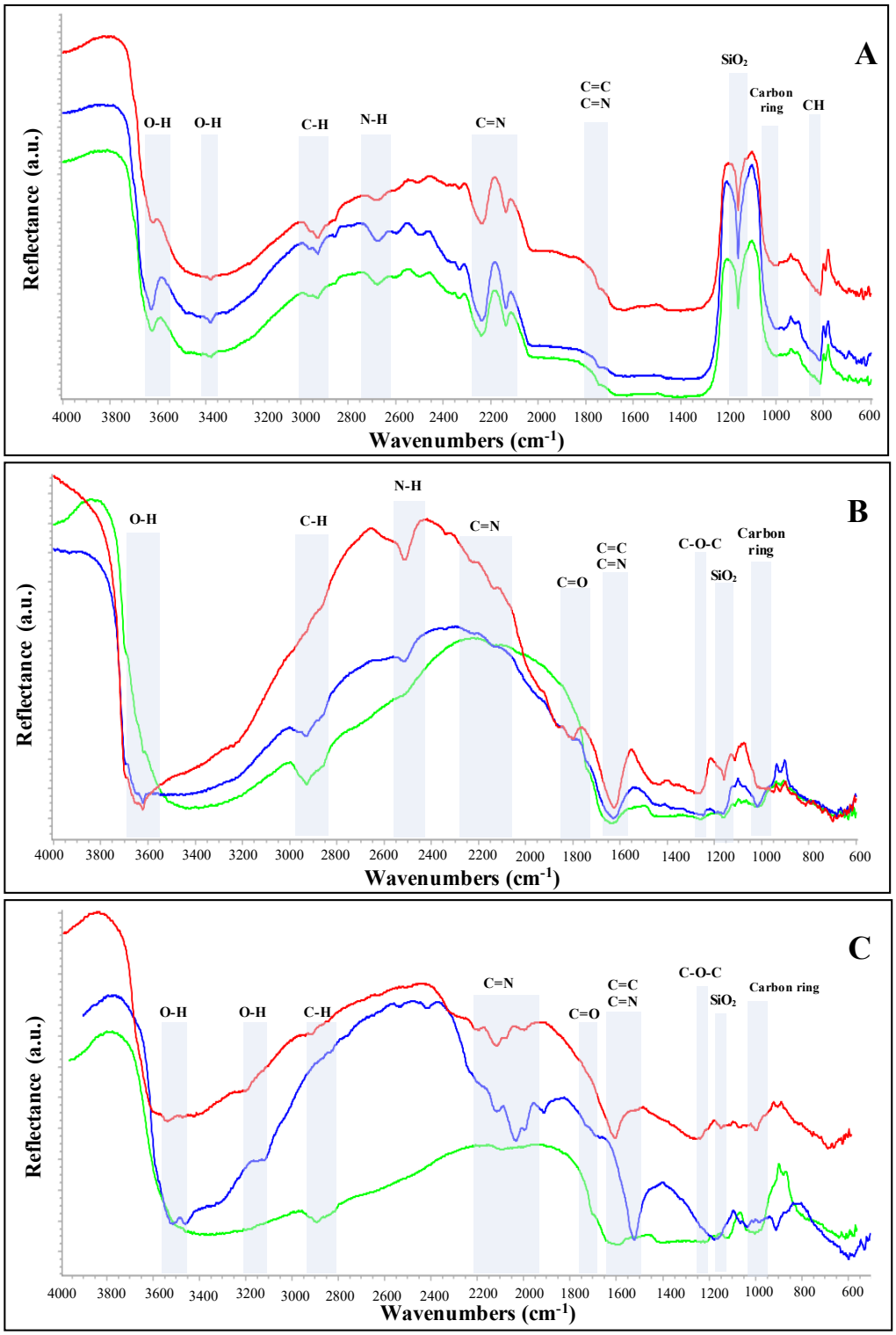

Figure 1. FT-IR reflectance spectra of *C. antarcticus* colonies mixed with A) OS substratum B) P-MRS and C) S-MRS analogues exposed to increasing doses of Fe ions (500MeV/n). Different spectra colors represent the different irradiation doses: control 0 Gy (not irradiated) = green line; irradiated with 250 Gy = blue line and irradiated with 1000 Gy = red line.

3.4.3.3 MIR spectra of samples exposed to Ar ions

Figure 1S shows the MIR spectra of samples irradiated with Ar ions (Fig. 1SA, B, and C; respectively). Bands assignment references are reported in the paragraph "MIR spectra of samples exposed to Fe ions". Alcohols and phenols [3700-3600 cm^{-1}] have been detected in all MIR spectra of samples mixed with the different minerals (Fig. 1SA, B and C); although, these bands appear evident in MIR spectra of OS samples (Fig. 1SA) but less pronounced in the MIR spectra of P-MRS and S-MRS control samples (Fig. 1SB and C, green lines). The presence of aliphatic compounds (attributed to the methyl C–H asymmetric/symmetric stretching vibrations) are highlighted at 2930 and ~2850 cm^{-1}. These bands are less pronounced in MIR spectra of P-MRS and S-MRS samples in 250 and 1000 Gy irradiated samples (Fig. 1SB and C, blue and red lines; respectively), in comparison to the control samples (Fig. 1SB and C, green lines).

The bands observed near 2680, 2600 and 2510 cm^{-1} assigned to stretching N-H (NH_3^+), H-bonded NH vibration band, and C-N-H vibration; respectively, have been detected only in OS and P-MRS samples (Fig. 1SA and B). In control samples of S-MRS spectra (Fig. 1SC, green line), the band is less pronounced. We report the presence of nitriles and thiols [2230 and 2135 cm^{-1}, identified by C≡N stretching vibrations, in all experimental conditions; with the exception of control sample of S-MRS spectra (Fig. 1SC, green line). The band at 1750 cm^{-1} (Fig. 2 A, B, C and D) may be correspond to C=C bond in lipids and fatty acids. The presence of melanin bands 1621 and 1024 cm^{-1} [due to the bending vibration modes of aromatic ring C=C or C=N and to carbon ring breathing vibrations in cyclic compounds were identified in all analyzed spectra, except in control samples of S-MRS spectra (Fig. 1SC, green line). The MIR spectra report the presence of amide I band near 1660–1628 cm^{-1} (Fig. 1SA, B and C). A weak band at ~1250 cm^{-1} may be related to C-O-C stretching in esters or polysaccharides, and occurs in the MIR spectra of P-MRS and S-MRS samples (Fig. 1SB and C).

Overall, the MIR spectra of samples exposed to Ar ions show a similar shape, regardless the irradiation dose (250 and 1000 Gy). Particularly, the results obtained in OS spectra show only minor

differences among control and irradiated samples (Fig. 1SA); while in P-MRS and S-MRS spectra more bands have been identified in irradiated samples than in the control sample (Fig. 1SB and C).

3.4.3.4 MIR spectra of samples exposed to He ions

Figure 2S shows the MIR spectra of samples irradiated with He ions (Fig. 2SA, B, and C; respectively). Bands assignment references are reported in the paragraph "MIR spectra of samples exposed to Fe ions". The spectra revealed the presence of several bands associated with different functional groups of organic molecules. The MIR spectra of OS, P-MRS and S-MRS samples (Fig. 2SA, B and C; respectively) show bands in the range of 3700-3600 cm^{-1} that are attributed to the OH stretch of –OH in alcohols and phenols in all experimental conditions. A further confirmation of the presence of the functional group related to alcohols and phenols is determined by a weak band at ~3375 cm^{-1}, which occurs only in the MIR spectra of OS samples (Fig. 2SA) and a band at 3200 cm^{-1} associated to asymmetric and symmetric OH stretching vibration of fully hydrogen bonded detected S-MRS samples (Fig. 2SC).

A band near 3640 cm^{-1} assigned to the ν_3 antisymmetric stretching vibrational modes of H_2O (Preston et al., 2020) occurs only in OS samples irradiated with He ions (Fig. 2SA).

The presence of aliphatic compounds (attributed to the methyl C–H asymmetric/symmetric stretching vibrations) are highlighted at 2930 and ~2850 cm^{-1} in OS samples for all the experimental conditions (Fig. 2SA, green, blue and red lines). The region near 2510 cm^{-1} associated to C-N-H vibration has been detected only in OS and P-MRS samples (Fig. 2SA and B) in all experimental conditions, with the exception of the control sample spectrum of P-MRS (Fig. 2SB, green line).

Several bands correspond to the C≡N stretching vibrations in nitriles and thiols, (2230 and 2135 cm^{-1}, which occur unaltered in the MIR spectra of OS samples (Fig. 2SA); while appear less pronounced in P-MRS and S-MRS control samples (Figures 2SB and C, green lines), and slightly accentuated in samples irradiated with 250 and 1000 Gy doses (Fig. 2SB and C, blue and red lines respectively). A bulge at 1750 cm^{-1} assigned to C=C bond in lipids and fatty acids occurs in all spectra for all

irradiation conditions (Fig. 2SA, B and C). The spectra report the presence of amide I band near 1660–1628 cm^{-1} (Fig. 2SA, B and C). The presence of melanin bands at 1621 and 1024 cm^{-1}, due to the bending vibration modes of aromatic ring C=C or C=N and to carbon ring breathing vibrations in cyclic compounds are confirmed.

The occurrence of bands at 1250, 1161 and 1100 cm^{-1} may be related to polysaccharides. Overall, the MIR spectra of samples exposed to He ions show a similar shape, regardless the irradiation dose (250 and 1000 Gy). On other hand, OS samples revealed no significant differences among control (green line) and irradiated samples (blue and red lines) (Fig. 2SA) in comparison with P-MRS and S-MRS samples (Figs. 2SB and C).

3.4.3.5 Heatmap (HM) analysis on the FT-IR spectra

The reflectance values of the detected FT-IR band positions were used to produce the HM with the aim to evaluate any differences among different sets of samples and treatments. By simultaneously capturing the characteristics and the relationships among groups of spectra and vibrational bands, HMs are helpful to extract all the accessible multivariate information coded in the FT-IR data set (Monti et al., 2013). In the HMs, different colors visually map the entire range of spectral reflectance of each wavenumbers value relative to its mean value across the spectra: lower values tend towards brighter red tones while higher values tend toward brighter green ones. Lower values (brighter red tones) and higher ones (brighter green tones) should coincide with flattened bands and with accentuated ones of IR spectra; respectively. Overall, HM representation (Figs. 3S, 4S and 5S) did not revealed significant differences among treatments reflecting the bands preservation of the respective IR spectra (Figs. 1, 1S and 2S).

Figures 3S and 4S reported the HM representation of sets of samples irradiated with Fe and Ar ions, showing the same differences profile. Differences among the samples have been detected in all OS samples, in comparison with P-MRS and S-MRS analogues in both irradiation type (Fe and Ar ions). OS samples shown a color difference between 1250 and 1000 cm^{-1}. In addition, a color change has

been identified between 2080-1750 cm^{-1} of OS samples in comparison with P-MRS and S-MRS samples (Figs. 1B and C).

Differences have been detected comparing HM results of OS samples with P-MRS and S-MRS samples irradiated with He ions (Fig. 5S). In particular, bands near 2100 and 1750 cm^{-1} show different colors code (from green to red) similarly, to bands between 1250 and 1000 cm^{-1}, as previously reported for samples irradiated with Fe and Ar ions. HM differences (near 3100-2800 cm^{-1}) in P-MRS and S-MRS samples have been found among controls and irradiated samples (Fig. 5S). A slight color change (~980-890 cm^{-1}) has been revealed between control and irradiated samples only for S-MRS samples (Fig. 5S).

3.4.3.6 Pigment detection by confocal Raman spectroscopy

The confocal Raman spectra of colonies of *C. antarcticus* mixed with either OS substratum, P-MRS and S-MRS analogues, after exposure to different doses of accelerated Fe, Ar and He ions are reported in Figures 2, 6S and 7S, respectively.

The Raman analyses identified a specific fingerprint of fungal colonies with two main peaks: an intense and broad peak at 1590-1605 cm^{-1} and a second peak at low wavelength near 1340 cm^{-1} (Figs. 2, 6S and 7S). These specific peaks are associated with the occurrence of fungal melanin pigments (Culka et al., 2017; Pacelli et al., 2021): they are associated to the aromatic C-N bonds (peak at at 1590-1605 cm^{-1}, Samokhvalov et al., 2004), and to the stretching of the C-C bonds within the rings of the aromatic melanin monomers (peak at 1340 cm^{-1}, Galván et al., 2013).

The Raman analyses identified an additional peak near 1425 cm^{-1}, that allows to i) discern melanin pigments from burnt organic matter and/or amorphous carbon (Böttger et al., 2012) and to confirm that the samples did not undergo thermal degradation and ii) further confirm the presence of *C. antarcticus* melanin pigments (Pacelli et al., 2021).

Similar peak positions (1602-1604 cm^{-1}) were observed in samples exposed to different doses of Fe, Ar and He accelerated ions, for all set of samples (Figs. 8SA, B and C respectively). Despite the

treatments, the collected spectra do not change significantly under all experimental conditions, maintaining the peak around 1425 cm^{-1} that is a distinctive trait of *C. antarcticus*'s melanin.

However, colonies mixed with P-MRS analogue have revealed the presence of amorphous carbon (Fig. 2B, black line), as a component of the regolith analogue (Pacelli et al., 2021). For this reason, colonies mixed with the P-MRS analogue were previously cleaned to remove the excess of the analogue before Raman measurements. No additional relevant spectrum was recorded in the samples, confirming that the only spectroscopic feature revealed by Raman analyses is the spectrum of melanin.

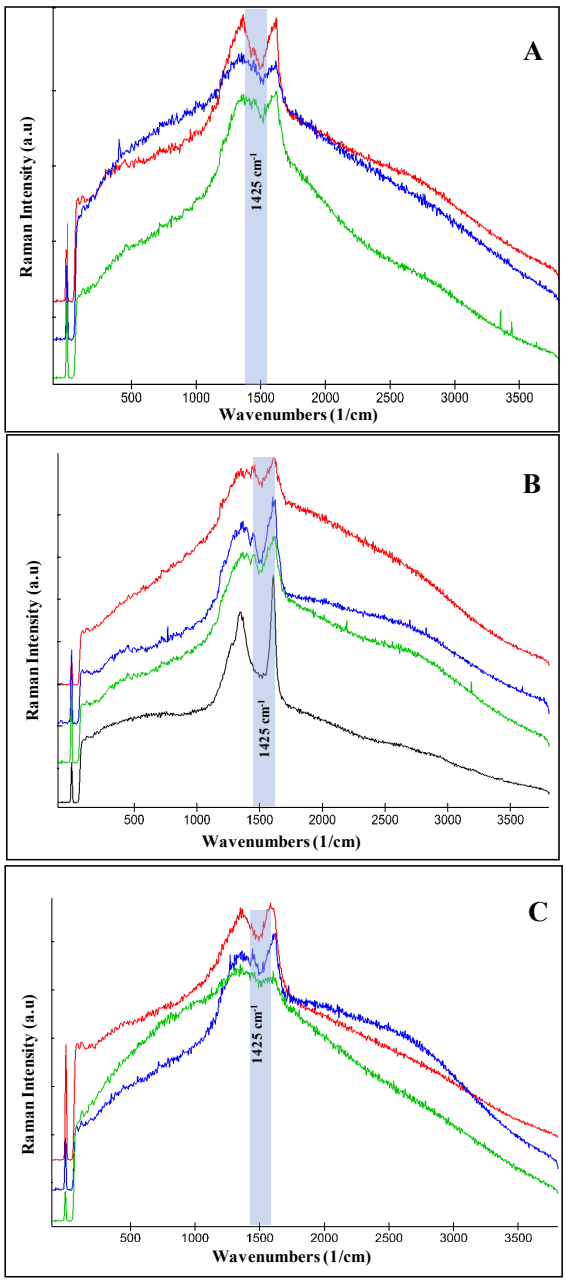

Figure 2. Raman spectra of melanin pigments of *C. antarcticus* colonies mixed with A) OS substratum, B) P-MRS analogue with amorphous carbon spectrum added and C) S-MRS analogue and exposed to increasing doses of Fe ions. Colors reference as reported in Fig. 1. Amorphous carbon spectrum = black curve.

3.4.4 Discussion

Each planetary body is dipped in a highly radiative environment composed of energetic particles from GCRs and SEP source. If a strong magnetic field exists around the planets, these particles are deflected before the interaction with the atmosphere's molecules and atoms and planetary surfaces. Differently from Earth, where the magnetosphere traps the majority of ionizing particles, Mars does not have a thick atmosphere nor a magnetic field, therefore the radiation environment on the surface is dangerous for any terrestrial biological system. This is especially true when considering the HZE component of the cosmic rays, because they can penetrate also in the shallow surface, damaging hypothetical biological systems and their associated molecules, with implication for life resistance and detection. In the context of space exploration missions, the damages of organic compounds induced by ionizing radiation represent one of the major challenges to search for extant or extinct life. Therefore, understanding the alteration of organics under similar Martian conditions (mainly the effects of GCRs irradiation) is essential to support the robotic *in situ* analyses. Which molecules of biological origin are better preserved and under which conditions?

Our study aimed at investigating the effects of accelerated heavy ions (Fe, Ar and He) on the biomolecules of the black fungus *C. antarcticus*, using Infrared and Raman spectrometers, as they are two of the devices onboard current and future rovers on Mars.

The absence of evidences of life on Martian surface suggests that hypothetical microorganisms or their remains may occupy a subsurface niche, where the conditions appear more favorable for life as we know it; for this reason, in our study, we mixed the fungal colonies with two Martian regolith analogues (P-MRS and S-MRS). These mixtures have been applied to evaluate their protective role. In fact the persistence of a biosignature may be enhanced by the matrix in which putative organisms

are embedded. With this in mind and looking to the robotic mission to Mars we used FTIR and Raman spectroscopies to evaluate the stability of fungal biomolecules.

The rover Rosalind Franklin is equipped with three infrared instruments that will provide the detection of organics within its mineral niches. To date, FTIR spectroscopy has been used on a number of space missions especially for remote detection of rocks and minerals (Anderson et al., 2005); however, given the rapidity and non-destructiveness, its use has been extended to drilled samples (Gordon and Septhon, 2016). The effects of the accelerated Fe, Ar and He ions on fungal biomolecules were investigated by using the FTIR technique, comparing irradiated with non-irradiated samples.

Overall, we observed no significant changes in the shape of all recorded spectra. The spectra of colonies mixed with the OS analogue highlighted no differences among irradiated and control samples (Figs. 1A, 1SA, 2SA). However, on the P-MRS and S-MRS samples the presence of additional bands was revealed in irradiated samples compared to the controls; in particular, the most evident difference occurs between bands at 2230 and 2135 cm^{-1}, which are attributed to nitriles and thiols, which appears very clear in S-MRS and P-MRS irradiated samples (250 and 1000 Gy; Figs. 1B and C; 1SB and C; 2SB and C), but are not present in the respective control samples. The appearance of nitrile compound bands may be considered as reaction products. As previously reported in Poch et al. (2014), adenine leads to the formation of many secondary products, such as nitriles, when exposed to UV radiation. Two experiments that have exposed the same nucleobase and a thin oxygen ice, deposited on the pre-irradiated adenine film at 5 keV electrons as a charged particle component of the GCRs, have revealed the production of nitriles. The nitriles are known to be stable over geological periods and they can be accumulated and preserved in regolith (Evans et al., 2011).

Our results highlight the needs for a better understanding of the production of nitrile compounds and a deeply investigation of nucleobases under accelerated heavy ions irradiation. The preliminary results obtained by the Sample Analysis at Mars (SAM) instrument aboard the Curiosity rover detected nitriles (Stern et al., 2015; Ming et al., 2014) on the Martian soil. Despite that, the origin of

Martian nitriles has not been confirmed, due to the fact that they could be derived from decomposition of organic reactants of terrestrial origin (i.e. the degradation of adenine) under Mars environmental conditions (Glavin et al., 2013).

The band at 1630 cm^{-1} was referred to the H_2O bending mode (McIntosh et al., 2017) and the 3500 cm^{-1} band is characteristic for bend H_2O and OH mode.

Other FT-IR bands (Figs. 1, 1S and 2S) observed in this study belong to several vibrational functional groups of organics, such as alcohols and phenols [3700-3600 cm^{-1}, OH stretch (Shurvell, 2006)], aliphatic compounds [2930 and ~2850 cm^{-1}, methyl C–H asymmetric/symmetric stretching vibrations (Coates, 2006; Shurvell, 2006; Movasaghi et al., 2008; Sajjan et al., 2013)], or lipids and fatty acids [1750 cm^{-1} assigned to C=C bond (Movasaghi et al., 2008)]. The presence of polysaccharides is evidenced by bands at 1250, 1161 and 1100 cm^{-1} and may be related to the fungal cell wall components such as chitin or glucuronans (Schulz and Baranska, 2007; Forfang et al., 2017). Chitin is an abundant macromolecule that usually occurs in complexes with other polysaccharides, pigments, and/or proteins. Chitin has been shown to possess a long-term stability in the fossil records (Briggs and Summons, 2014) as evidenced in 25-million-year-old fossils (Stankiewicz et al., 1997) and in an 810 to 715 million-year-old shale rocks (Bonneville et al., 2020). Chitin is also more resistant to decay when complexed with proteins (Flannery et al., 2001).

In addition, melanin pigments have been detected by the presence of bands at 1621 and 1024 cm^{-1} (Mbonyiryivuze et al., 2015) and to carbon ring vibrations in cyclic compounds (Pal et al., 2014).

We also performed a FT-IR characterization of the regolith without fungal colonies. Mineral bands have been assigned mainly to stretching vibrational modes of SO_4 tetrahedra (Preston et al., 2020), as component of quartz. In addition, the presence of carbonates has been largely reported [1080 cm^{-1}, vibrational modes of CO_3^{2-} (Bourgier, 2007); 880, 700, and 610 cm^{-1}; stretching and bending ν_2 vibrational modes of C-O (Preston et al., 2020)]. Carbonates are produced by the interaction between CO_2, water and rocks on Earth; while on Mars –where carbonates have been found on the surface and

in the dust (Bandfield et al., 2003)– it has been hypothesized that they were produced in a CO_2-rich atmosphere and wet climate conditions, probably during the Noachian epoch (~3.8-4 Gyr; Ramirez and Craddock, 2018). Carbonates are related to biological activity and could be considered as an astrobiological target compound, because of their presence on planetary surfaces (Barbieri and Cavalazzi, 2004). Some bacterial communities promote carbonates' precipitation that may be preserved in the fossil record (Bailey et al., 2009). Our results confirm the presence of carbonates, which could be helpful to protect biomolecules against part of GCR spectrum exposure.

The present and future space exploration missions to Mars are carrying Raman spectroscopes, whose role will be to analyze the chemical and structural composition of surface and subsurface materials on Mars.

Basing on previous studies (Pacelli et al., 2021), confocal Raman spectroscopy has been applied focusing on the detection of fungal melanin pigments, which constitute one of the components of the fungal cell-walls. The acquired Raman signals are characterized by two broad bands at 1590-1605 and 1340 cm^{-1} (Figs. 2, 6S and 7S), both used as indicator for any biomolecule's damages, considering the difference position with the amorphous carbon bands (Pacelli et al., 2021). An intermediate peak at 1425 cm^{-1}, a distinctive traits of *C. antarcticus* melanin pigment (Pacelli et al., 2021), is always maintained despite the radiation dose and ions exposure (Figs. 2, 6S and 7S). This peak allows to distinguish unequivocally melanin pigments from amorphous carbon (Pacelli et al., 2021). Previously work focusing on the detection of fungal melanin after simulated and real space exposure (Pacelli et al., 2021) reported a high stability of the fungal pigments, and already suggested to consider these pigments as biosignatures. Our results of melanin stability after exposure to increasing doses and different ions, being part of the GCRs spectrum, corroborate the necessity to confirm melanin as a good stabile biosignatures of Earth-like life. Indeed, melanin is a well-known protective factor against different extreme environmental stresses, including UV radiation (Jacobson, 2000). Melanin pigments helps many Antarctic black fungi to stand the radiation exposure (Dadachova and Casadevall, 2008; Singaravelan et al., 2008).

Recently, Shunk et al. (2020) reported the capability of 1.7 mm thick lawn of the melanized radiotrophic fungus *Cladosporium sphaerospermum* to attenuate also ionizing radiation. In our case, the extraordinary resistance given by melanic pigments against ionizing radiation is probably related to the peculiarity of the black fungus to exhibit two melanin types (produced via DHN and L-DOPA pathways, Pacelli et al., 2020b). Accordingly, *Aspergillus niger*, which has a high melanin content in the cell coat produced through DHN and DOPA pathways, showed a good viability after five months exposure aboard the International Space Station (ISS).

To conclude, our results showed the importance to use multiple and connected analytical techniques in astrobiological-related studies, since they provide complementary and important information for detecting and characterizing biosignatures. First of all, we confirmed the detectability of melanin pigments with two complementary devices, even in the presence of a multitude of biomolecules; this evidence corroborates the suggestion to use this biomolecule, diffused among all biological Kingdoms, as a biosignature in the search for Earth-like life elsewhere in our Solar System. Our analyses also highlighted two new molecules such as nitrile and chitin whose role as possible biosignatures will be further investigated.

Acknowledgments: We thank the PNRA (Italian National Program for Antarctic Research) for supporting sample collection in Antarctica, and the Italian National Antarctic Museum "Felice Ippolito", for funding MNA-CCFEE. We acknowledge the HIMAC team at the NIRS in Chiba, Japan for the irradiation.

3.5 The protective role of Antarctica sandstone: new results from Lichens and Fungi EXperiment

Abstract

Ongoing and near future space exploration missions (ESA-Roscomos ExoMars and NASA Mars 2020) aim to detect and identify chemical and biological indicators of life, or biomarkers, on Mars. Because of the highly radiative conditions on Mars surface, unfavorable for life as we know it, ESA Rosalind Franklin rover will drill the Martian subsurface (up to 2 meters depth) in order to find well preserved biomarkers. In the frame of Lichen and Fungi Experiment (LIFE), small fragments of Antarctic sandstone colonized by cryptoendolithic microbial communities were exposed to space and Mars-like conditions in Low Earth Orbit (LEO) for 16 months, aboard the EXPOSE-E payload. Here, we explore the protective role of mineral matrix in preserving organic compounds, through the combined use of Raman and Infrared spectroscopies. The results revealed that pigments, as melanin and carotenoids, lipids and polysaccharides are able to maintain their stability in space and Mars-like environment, when protected by minerals, and therefore can be proposed as biomarkers for search for life on Mars.

Keywords: microbial communities, mineral protection, spectroscopy, pigments, polysaccharides

Cassaro A., Pacelli C., Baqué M., Rabbow E., Maturilli A., de Vera J-P.P., Onofri S. The protective role of Antarctica sandstone: new results from Lichens and Fungi Experiment. (draft)

3.5.1 Introduction

Cryptoendolithic microbial communities, discovered in the extremely cold, hyper-arid McMurdo Dry Valleys of Antarctica (Friedmann, 1982), one of the closest terrestrial environments to the Martian surface (Wynn-Williams and Edwards 2000; Onofri et al., 2004), have been considered a candidate for supporting the search of life on Mars. In such harsh conditions, characterized by very low temperatures, ranging from -20 to -50 °C in winter, with annual average temperature below 0 °C, wide thermal fluctuations, frequent freeze/thaw cycles, dryness, high salt concentrations, low nutrient availability and high radiation including UV (Onofri et al., 2007), the endolithic growth represent the last chance for survival before extinction (Selbmann et al., 2016).

In these regions, microorganisms find refuge dwelling among the airspace of the rocks, forming well-stratified communities. These communities are highly adapted to withstand to extreme low temperature, radiation, and desiccation also by producing protective pigments and compatible solutes, assuring their survival (Selbmann et al., 2005).

In the frame of the Lichen and Fungi experiment (LIFE), small sandstones fragments colonized by cryptoendolithic microbial communities were exposed for 16 months to real space environment and to Mars-like conditions in Low Earth Orbit (LEO, Onofri et al., 2012, 2015). Aboard the EXPOSE-E payload attached to the exterior of the ISS, samples have experienced to space stressors, such as vacuum (10^{-7} to 10^{-4} Pa) (Horneck et al., 2010), galactic cosmic radiation (≤190mGy) (Berger et al., 2012), the full spectrum of solar extraterrestrial electromagnetic radiation and to Mars-like conditions. For a set of samples, the spectral range of solar UV radiation was attenuated with an optical filter, allowing only a small UV radiation dose to penetrate. Once back on Earth, samples were subjected to molecular and culture-dependent analyses in order to investigate the viability of microoganisms (Onofri et al., 2012). A few cryptoendolithic organisms, as the lichenized fungus *Acarospora,* were able to recover and grow after exposure to space dark; and only one green alga belonging to the genus *Stichococcus* were recovered in samples exposed to attenuated Mars-like conditions (Scalzi et al., 2012). These results increased our knowledge about the resistance of

cryptoendolithic microorganisms under space and Mars-like stressors and confirmed that microorganisms extracted from Antarctic microbial communities are a perfect test organism to investigate the resistance of life to space environments and to support the future exploration missions. Indeed, one of the most important challenges of our time is the *in situ* exploration of Mars to detect traces of extant or recently extinct life. The strong radiation environment on the Martian surface is considered enough to destroy any potential sign of life (Pavlov et al., 2013), such as cells or cellular elements, which could hypothetically be present within the top few meters of the Martian regolith (ten Kate et al., 2005; Schuerger et al., 2006). To achieve space mission's primary objective, it is important to understand the role played by mineralogy in preserving organics (Preston at al., 2019; Carrizo et al., 2020). In this context, the development of new spectroscopic techniques (Storrie-Lombardi et al., 2009, Eshelman et al., 2017; Uckert et al., 2018) connected with the possibility for the Rosalind Franklin rover to drill the Martian subsurface at two meters depth (Vago et al., 2017; Debus et al., 2018), could increase the possibility to detect and identify molecules potentially associated with the presence of life. Indeed, the ongoing ExoMars mission will drive Mars exploration with a rover equipped with several instruments on Pasteur payload: the samples preparation and distribution system will be able to crush drilled samples to deliver to the infrared (IR) micro-imaging spectrometer (MicrOmega), to IR spectrometer (ISEM) (Vaitua et al., 2017) and to Raman Laser Spectrometer (RLS) (Lopez-Reyes et al., 2013).

Raman spectroscopy has been considered an excellent tool for the detection of inorganic and organic components. For example, microbial pigments have a very distinct Raman signals, allowing a direct detection in their natural environment (Jehlicˇka et al., 2014). One of the key features of Raman spectroscopy is the ability to acquire experimental data without chemical or mechanical pre-treatment of the samples (Edwards et al., 2012) and its potential to detect compounds from extant or extinct microbes in rock samples has been widely proved (Edward et al., 2010; 2014). Moreover, Fourier transform infrared (FT-IR) spectroscopy has been already used successfully for the microorganisms and microscopic biological structures identification (Naumann et al., 1991; Schmitt and Flemming,

1998; Igisu et al., 2009, Preston et al., 2015) and it may provide information about mineralogical composition, allowing to detect the presence of different target molecules in the same spectra. Both techniques were also adopted for their non-destructive properties, making the samples available for further analyses with other instruments.

Here, we investigate the persistence of organic compounds of biological origin, in Antarctic sandstones fragments exposed to space and Mars-like conditions, through Raman and FT-IR spectroscopies. Due to high meteoritic exchange and assuming that hypothetical life on Mars would likely be based on life as we known on Earth, our focus was on microbial macromolecules, such as lipids, amino-acids, polysaccharides and pigments. The aim of this work was to i) compare the information of complementary techniques and to evaluate the role of mineral matrix in protection the detection of microbial biomarkers, in order to guide and support the ongoing and future life detection missions beyond Earth.

3.5.2 Materials and Methods

3.5.2.1 Colonized Sandstone

Battleship Promontory (Fig. 1B) (76°54'37.6" S, 160°55'27.5" E) is a sandstone promontory in Southern Victoria Land, Antarctica (Fig 1A, up-right); for its environmental conditions (Selbmann et al., 2015; 2018) it can be considered analogues to Mars environment.

In the frame of LIFE (Lichens and Fungi Experiment) project, fragments of sandstones colonized by a stratified cryptoendolithic community (Fig. 1B), collected by L. Zucconi in January 2004, were selected to be exposed to space environment in LEO. Excised fragments were dehydrated at room temperature and glued, using Wacker silicone glue RTV-S 69, on sterile Teflon disks (12 mm diameter). These fragments were then accommodated in different trays of the EXPOSE-E payload (Rabbow et al., 2012).

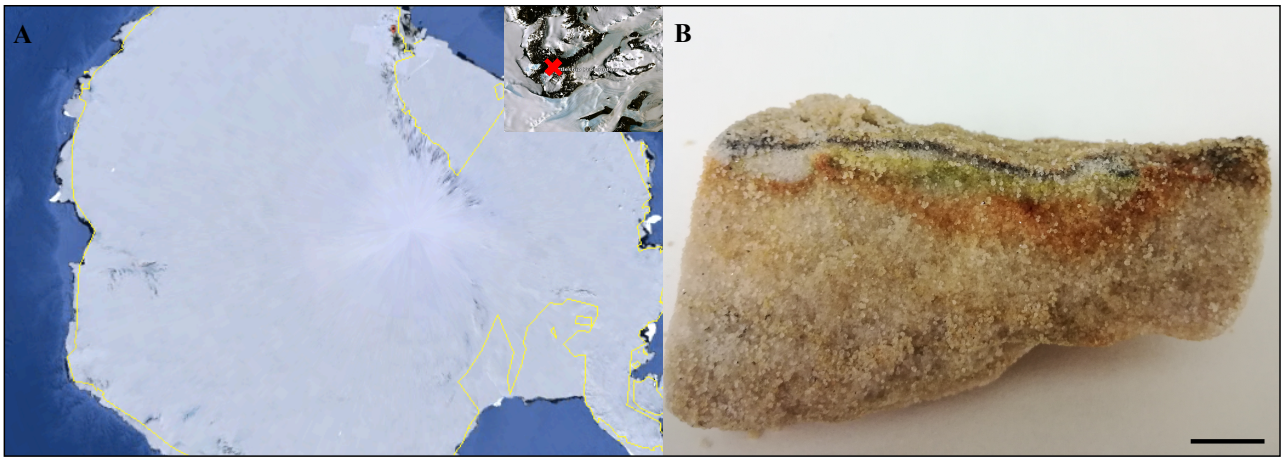

Figure 1. A) Overview (up right) and detailed map of the location of sampling location (Batteship Promontory, Southern Victoria Land; CREDIT: Google Earth); **B)** Section of a dried sandstone fragment, colonized by a stratified cryptoendolithic microbial community. Scale bar= 1cm.

3.5.2.2 Hardware and exposure conditions

In February 2008, the samples of LIFE experiment were loaded in a small chamber (1.4 cm in diameter) on the EXPOSE-E facility, a part of the European Technology Exposure Facility (EuTEF), developed to expose different type of samples in space environment. Colonized samples were launched on board the Space Shuttle STS-122 and, on 15 February 2008, the facility was installed outside the Columbus module by an extravehicular activity. The infrastructure EXPOSE-E was bringing back to Earth on 12 September 2009 with STS-128. During the exposure period, the rock samples were loaded on two different trays (Fig. 2A and B) and exposed on EXPOSE-E payload as follow:

- Tray 1: samples (referred as "space 100% UV") were exposed to space vacuum (10^{-7} to 10^{-4} Pa) (Horneck et al., 2010), two intensities of solar extraterrestrial electromagnetic radiation of $\lambda > 110$ nm, cosmic ionizing radiation (≤190 mGy) (Berger et al., 2012), and temperature fluctuation.
- Tray 2: samples (referred as "Mars 100% UV") were exposed to simulated Martian conditions with an atmosphere composed of 1.6% argon, 0.15% oxygen, and 2.7% nitrogen, and

*370ppm H_2O in CO_2 at a starting pressure of 10^3 Pa. The radiation parameters involved two intensities of solar extraterrestrial electromagnetic radiation of λ> 200 nm, which simulated the UV radiation on Mars, including cosmic ionizing radiation and temperature fluctuation.

In each tray, temperature fluctuation has covered a range between −21.7 and +42.9 °C (Rabbow et al., 2012; Onofri et al., 2012). Both compartments were covered by an 8 mm thick optical window to allow access of selected spectral ranges of solar electromagnetic radiation (Top samples): MgF_2 window (MaTeck GmbH, Germany) for tray 1 and quartz (MaTeck GmbH, Germany) for tray 2, the latter complemented by a long-pass cutoff filter of approximately 50% transmission at 216 nm (Wisag AG, Switzerland). For this set of samples, the UV (200-400 nm) fluences, calculated in according to the orientation of the ISS to the sun, reached 6.34×108 Jm^{-2} (space 100% UV and Mars 100% UV samples). In addition, a set of samples for each tray were covered with neutral-density filters (ND) made of MgF_2 (MaTeck GmbH, Germany; Moltech GmbH, Germany, coatings from Thin Film Physics AG, Switzerland) for tray 1 or of quartz (Moltech GmbH, Germany, coatings from Thin Film Physics AG, Switzerland) for tray 2, allowing only to 0.1% of radiation to penetrate (referred as "space 0.1% UV" and "Mars 0.1% UV" samples; respectively). The UV fluences for this set of samples reached 9.19×105 Jm^{-2}. Below the irradiated samples, an identical set of samples (referred as "space dark" and "Mars dark" samples) was kept in the dark and experienced all simulation parameters except UV radiation exposure. All tested conditions are reported in Table 1.

Although the samples were exposed 10 years before the analyses, they were stored in the dark under sterile conditions so any effects from external microbes, oxidation or humidity can be discarded. The only effect that we may expect during this period is a minimal increase of organic matter degradation.

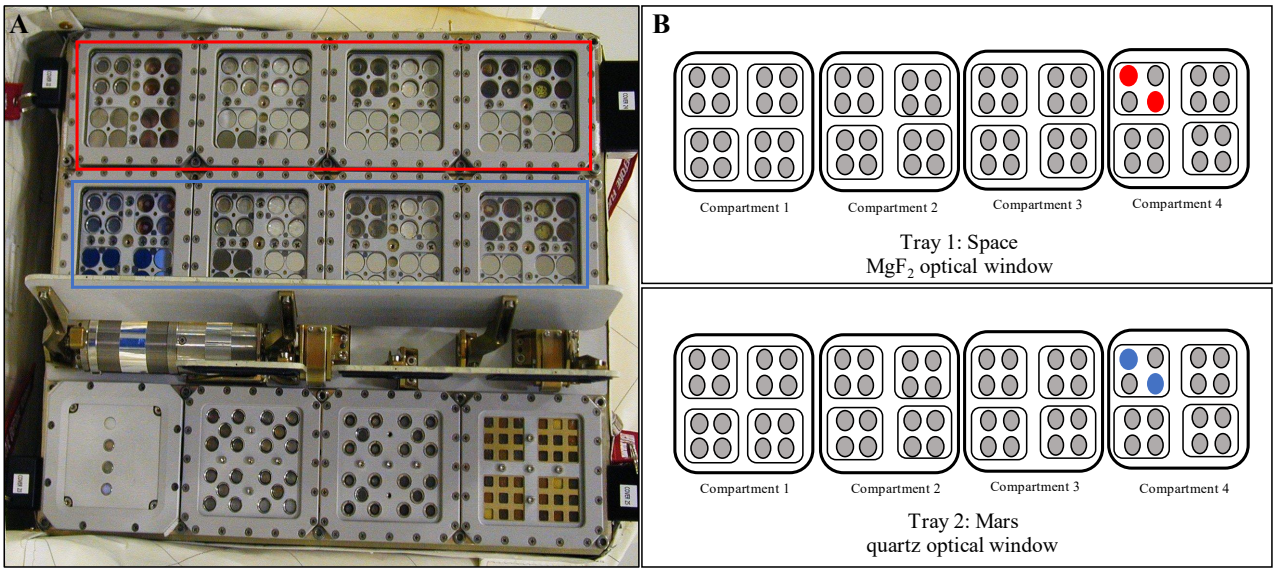

Figure 2. A) EXPOSE-E flight hardware, red and blue squares highlight Tray 1 and Tray 2, respectively. **B)** detail of dried sandstone fragment samples accomodation in the two trays.

Table 1. Real space and Mars-like exposure conditions experienced during 16 months outside the ISS (from Berger et al., 2012 and Rabbow et al., 2012)

Samples	Atmosphere	Solar UV radiation 200-400 nm (MJ/m^2)*	Cosmic radiation (mGy)**	Temperature (°C)
Space 0.1 % UV (Space 0.1 % solar UV radiation)	Space vacuum (10^{-7} to 10^{-4} Pa)	0.92	238	-21.7 to +42.9
Space 100 % UV (Space 100 % solar UV radiation)	Space vacuum (10^{-7} to 10^{-4} Pa)	634	238	-21.7 to +42.9
Space dark	Space vacuum (10^{-7} to 10^{-4} Pa)	0	220	-21.7 to +42.9
Mars 0.1 % UV (Simulated Mars 0.1% solar UV radiation)	95% CO_2 atmosphere 1000 Pa	0.63	238	-21.7 to +42.9
Mars 100 % UV (Simulated Mars 100% solar UV radiation)	95% CO_2 atmosphere 1000 Pa	475	238	-21.7 to +42.9
Simulated Mars dark	95% CO_2 atmosphere 1000 Pa	0	220	-21.7 to +42.9
Control (Ground control)	Dark, room temperature, 1 atm	0	0	+25 °C

*Solar spectral UV and visible irradiances were calculated from the RedShift-Modeled Data and the Composite Solar Irradiance Reference Spectrum for the Wavelength Range of 200-400 nm

** Dosimetry of the ionizing radiation was calculated with R3DE and DOSIS/DOBIES experiments, determining d daily dose rates of the three essential components of the radiation field encountered at the orbit of the ISS and the total mission dose, respectively.

3.5.2.3 Confocal Raman spectroscopy analysis

Raman analysis of exposed samples were performed at the German Aerospace Center (DLR, Berlin) with a confocal Raman microscope (WITec alpha300 Raman system) under ambient atmospheric conditions. The Raman laser excitation wavelength was set at 532 nm and the spectral resolution of the spectrometer 4-5 cm^{-1}. The spectrometer was calibrated with a pure silicon and paracetamol test samples. A 10X Nikon objective, with a 0.25 numerical aperture, was used to focus the laser on a 1.5-μm spot. Raman spectroscopic analyses were performed directly on the sandstone fragments and zones of colonization have been studied preferentially after an *image scan* of the area. *Line scans* were obtained with 1s integration with 1 accumulation to avoid signal saturation from fluorescing pigments and minerals, with-up to 50 image points. All data analyzes were performed with the WITec Project FIVE software.

3.5.2.4 Fourier transformed infrared resonance (FT-IR) spectroscopy analysis

FT-IR analysis was performed at the Planetary Spectroscopy Laboratory (PSL) of German Aerospace Center (DLR) in Berlin at room temperature, operating under evacuated conditions to remove atmospheric features from the spectra. Infrared spectra were recorded using a FT-IT Bruker Vertex80V, in the wavenumber region from visible, to UV and to Middle Infrared (MIR), by using reflectance. The infrared spectra were obtained between 4000 and 400 cm^{-1}, using 4 cm^{-1} resolution and an average of 250 scannings; in total three spectra were acquired for each sample. With the purpose to remove as much noise as possible from spectra, without degrading signals, a 15 points Savitzky-Golay smoothing was applied in all samples and in the same range, with a polynomial value

of 3. Peaks assignment were performed with a threshold value of 3; 3% of maximum intensity and a noise factor of 2. All data analyzes were performed with the ACD/Spectrus Lab 2019 software.

3.5.3 Results

3.5.3.1 Detection of pigments by Confocal Raman spectroscopy

Raman spectroscopy is widely proven to be an efficient way to characterize microbiological pigments (Jehlička et al., 2014). This technique is able to identify pigments, such as melanin and carotenoids (de Oliveira et al., 2010; Jehlička et al., 2013) in a mineral substrate, as from endolithic microbial communities inside rocks (Storme et al., 2015).

Raman spectra of samples in all exposure conditions, revealed the presence of organic pigments. First, it has been detected a strong signal of melanin pigment (Fig. 3A and B), due to the two typically bands, respectively at 1340 and 1600-1604 cm^{-1}(Culka et al., 2017). According to literature, the first band is probably associated to the aromatic C-N bonds (Samokhvalov et al., 2004), and the second one to the stretching of the C-C bonds within the rings of the aromatic melanin monomers (Galvan et al., 2013). Probably, the key features of melanin are composed of overlapping bands, due to the many vibrations of the monomer's constituent. An additional band is showed in the range of 1425 cm^{-1}, as previously reported by Pacelli et al. (2021). This band allow to discern unequivocally the presence of fungal melanin pigments (Pacelli et al., 2021).

The Raman analyses revealed also the presence of carotenoid pigments (Fig. 4). The spectra showed a specific fingerprint consisting by two bands located at 1515 cm^{-1} and 1155 cm^{-1}, attributed to the in-phase C=C (ν_1) and C-C stretching (ν_2) vibrations of the polyene chain in carotenoids, respectively; and a third peak at lower intensity (near 1008 cm^{-1}), associated to the in-plane rocking modes of CH_3 groups linked to the polyene chain coupled with C-C bonds (Marshall et al., 2007).

While the carotenoid signal was detected with a high intensity in all the samples, a lower band located in the range of 400-500 cm^{-1}, was found only in carotenoid spectra of dark samples exposed to real

space conditions and in Mars dark and Mars 0.1% UV samples exposed Mars-like conditions in space (Fig. 4A and B). No change in melanin and carotenoid spectra has been reported in all experimental conditions.

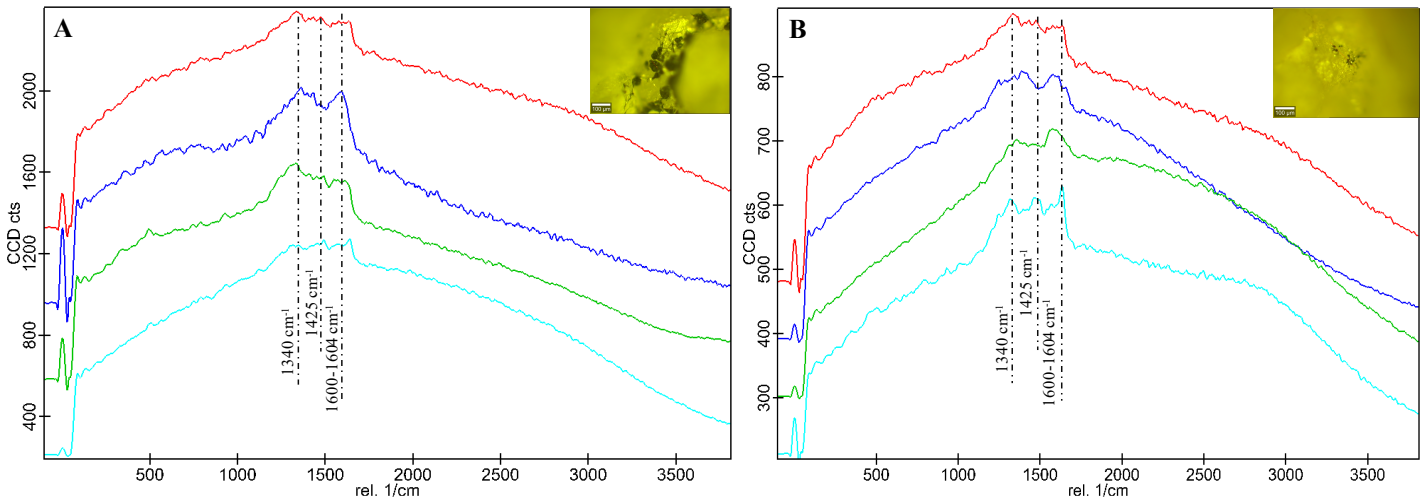

Figure 3. Melanin Raman spectra of samples exposed to A) real space and B) Mars-like conditions in space. Control: red, dark: blue, UV 0.1%: green, UV 100%: pale blue.

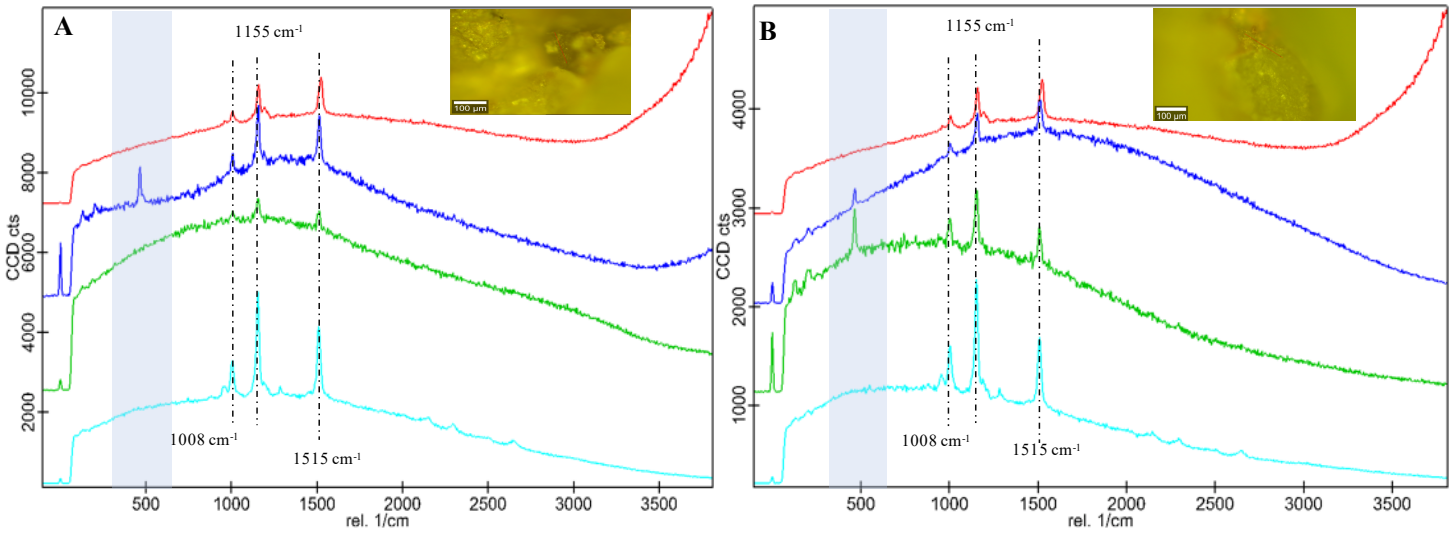

Figure 4. Carotenoids Raman spectra of samples exposed to A) real space and B) Mars-like conditions in space. Control: red, dark: blue, UV 0.1%: green, UV 100%: pale blue.

3.5.3.2 Infrared spectroscopy analysis: organic and inorganic detection

During the upcoming ExoMars mission the visual/infrared micro-imaging spectrometer and the ISEM will assist the RSL instruments to investigate mineralogical and molecular composition of Martian samples (rocks, outcrops, and regolith). The absorbance values of each samples were calculated as the height of the peak with respect to a base line. Overall, FT-IR bands in the MIR region, may be distinguished by four main regions: i) the fingerprint region (500-1500 cm^{-1}) that usually contains a very complicated absorption bands; due to all manner of bending vibrations within the molecules (Mathias, 2018), ii) the double bounds region (1500-2000 cm^{-1}), iii) the triple bounds region (2000-2500 cm^{-1}) and iv) the single bounds region (2500-4000 cm^{-1}). The MID region is very informative because it includes the major classes of biomarkers, as pigments and lipids, and the mineral bands. Figure 5A and B show infrared spectra comparison among samples exposed to space and Mars-like conditions in LEO.

The characteristic absorption band of the quartz, mainly found in sandstone and correspond to the main peaks in the MIR, occur at 786, 864, 1122, 1194 and 3248 cm^{-1}. In samples exposed to real space conditions (Fig. 5A) was shown an additional band at 1101 cm^{-1}, referred to asymmetric stretching vibrational modes of SO_4 tetrahedra (Preston et al., 2020). The infrared spectra highlighted

the presence of many functional groups that can be assigned to the presence of organic molecules. The melanin pigments may be associated to a broad absorption band at 3371-3020 cm^{-1} in samples exposed to real space conditions (Fig. 5A) and at 3369-3020 cm^{-1} in samples exposed to Mars-like conditions in space (Fig. 5B), indicative of stretching vibration of OH groups and NH stretch, respectively (Pal et al., 2013; Pacelli et al., 2020). The band at 1026 cm^{-1} was detected for all the samples in all the experimental conditions (Fig. 5A and B), and it was attributed to aromatic ring CH stretching (Pal et al., 2013; Pacelli et al., 2021). The representative band at 1452 cm^{-1} in space exposed samples (Fig. 5A) and at 1448 cm^{-1} in Mars-like conditions exposed samples (Fig. 5B), appears due to the bending vibration of methylene $–CH_2$ (scissoring) and may be assigned to carotenoid pigments (Kushwaha et al., 2014). Controversially, this band of CH_2 bending signal could be also associated with CH_2 bending of proteins or chitin, a major component in the fungal cells wall (Ivshin et al., 2007; Bowman and Free, 2006), or to in plane-scissoring of CH_2 in lipid chain (Shulz and Baranska, 2007). The band at 1526 cm^{-1} and 1524 cm^{-1} (Fig. 5A and B) may be clearly assigned to ν(C=C) of β-carotene. The lipid content may be identified in all analyzed samples by bands at 1664, 2889 and 3020 cm^{-1}, due to ν(C=C) cis, $\nu_s(CH_3)$ and ν_{as}(=C–H), respectively (Schulz and Baranska, 2007). In addition, the band at 1664 cm^{-1}, associated to ν(C=C) cis, could be assigned as a part of chlorophyll (Kushwaha et al., 2014). The bands at 1553 and 1572 cm^{-1}, may be associated to the presence of the chlorophyll a and chlorophyll b, respectively (Schulz et al., 2007). Similar bands (1549 and 1570 cm^{-1}) were reported in samples exposed to Mars-like conditions in space. The presence of chlorophyll may be further confirmed by the presence of the band at 1718 cm^{-1}, due to ν(C=O) obtained from the aliphatic macromolecule algenan, isolated from microalgae. The band at 1501 cm^{-1} (1502 cm^{-1} for samples exposed to Mars-like conditions) may be associated to an N-H bending vibration coupled to C-N stretching in amide II (Fabian et al., 1995). The absorbance bands at 3057 cm^{-1} and 3061 cm^{-1}, may be associated with amide B, due to N-H stretching. The band at 1410 cm^{-1} (Fig. 5A) and 1402 cm^{-1} (Fig. 5B) can be related to ν(C–N), ν(N–H) of amide III (Marshall, 2006). As reported in Shetty et al. (2006), the bands at 970 (976 cm^{-1} in Mars-like conditions samples) and 1335 cm^{-1}, probably

due to OCH_3, could be determined to polysaccharides or pectin. The spectrum part assigned to the single bonds to H (2500-4000 cm^{-1}), was characterized by the bands at 2633, 2731-2735, 2826 cm^{-1} attributable to the stretching NH_3; 3169 cm^{-1}, owed to N-H stretching and at 2995-2997 cm^{-1}, due to C-H ring (Dovbeshko et al., 1997). In addition, the band at 3508-3512 cm^{-1} is related to O-H stretching (Smith and Rehman, 1994).

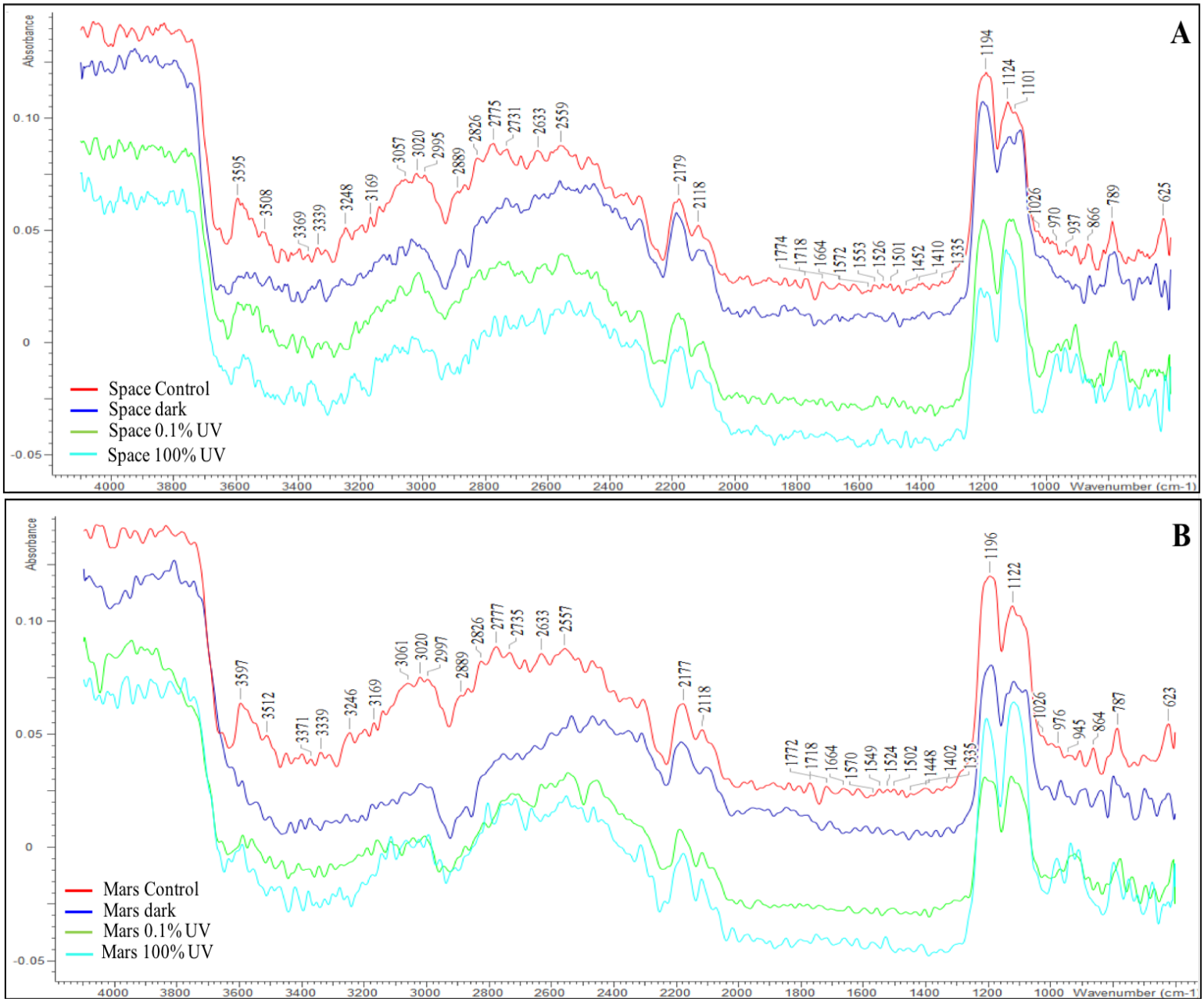

Figure 5. Mid Infrared comparison spectra with the main identified peaks of samples exposed to **A)** real space and **B)** Mars-like conditions in space.

3.5.4 Discussions

3.5.4.1 The preservation of molecular biomarkers in quartz minerals

To discern if Mars was habitable and if host or hosted life-like forms in the subsurface, life-detection missions are necessary. Considering the highly oxidative and radiative environment on Martian surface, the near future ExoMars mission will search for sign of extant or extinct on the subsurface, up to 2 meters depth (Vago et al., 2017). In this context, to understand the protection potential of mineral matrix in relation with organic components, is of outmost importance. Minerals could play a dual role in protection organic matter: they could act as protector or affect the reactivity of hypothetical molecules or their remains (Fornaro et al., 2018).

The previous aims of LIFE experiment were to assess the survivability of microbial communities after exposure to space and Mars-like conditions in LEO. During this period, dried sandstone fragments were exposed within the EXPOSE-E payload (Fig. 2A) and accommodated in two trays (Fig. 2B); vented with access to space vacuum in tray 1 and sealed and filled with a simulated Mars gas mixture in tray 2. Based on previously results reported by Scalzi et al. (2012), only few cryptoendolithic microorganisms were able to survive after 16 months of exposure.

In this context, we have deepened our knowledge about the resistance of microbial communities, investigating the stability of organic biomarkers inside mineral grains of sandstone, 10 years after the exposure.

This work aimed ii) to determine the detectability of different classes of biomolecules through a multidisciplinary approach, verifying the possibility that these molecules will be a useful biomarker to detect life in the ongoing space exploration missions and ii) to deepen the interaction between minerals and organic compounds. The detectability of biomolecules after the exposure to real space and Mars-like conditions in space, was investigated by Raman and Infrared spectroscopies, two non-destructive devices that will be onboard the Rosalind Franklin and Perseverance rovers. The potential of these instruments is the sensibility to detect the presence of organic compounds, even in small quantities, within mineral matrix (Freissinet et al, 2015). The use of Raman spectrometer with an

excitation wavelength of 532 nm in our analyses is for its abilities to detect biomarkers from samples collected in extreme environments and in fossilized microorganisms in rock samples (Edwards et al., 2005, 2014; Jorge Villar et al., 2006; Vítek et al., 2010; Winters et al., 2013) and for the similarity with the wavelength of the instrument that will be employed by Rosalind Franklin rover.

Our results detected melanin and carotenoids in the exposed sandstones. The spectra in Fig. 3a and B clearly revealed the presence of fungal melanin. It is characterized by distinguished two broad bands: a main band located in the region 1590-1605 cm^{-1} and a second band around 1350 cm^{-1} (Culka et al., 2017). The third band near 1425 cm^{-1} was unequivocally associated to lipids, polysaccharides or proteins of the fungal cell wall (Culka et al., 2017), allowing to assign the obtained spectra to melanin pigments (according to Pacelli et al., 2021). Besides, Raman signatures of carotenoids were characterized by two bands, respectively at 1515 cm^{-1} and 1155 cm^{-1}, attributed to in-phase ν_1(C=C) and ν_2(C-C) stretching vibrations of the polyene chain and a third band at near 1008 cm^{-1}, due to in-plane rocking modes of CH_3 groups attached to the polyene chain coupled with C-C bonds (Fig. 4A and B) (Gill et al., 1970; Vítek et al., 2009). Raman analyses highlighted also the presence of mineral components, such as quartz near 400 cm^{-1} (Bottger et al., 2012), identified only in dark sample exposed to real space conditions (Fig. 4A) and in Mars dark and Mars 0.1% UV samples exposed Mars-like conditions in space (Fig. 4B). The non detection of quartz, the main constituent of sandstones, is probably due to the high fluorescence of mineral grains during the measurements: the fluorescence background of the minerals may interfere with the ability to detect organic matter and should be therefore considered for the robotic exploration. Our results, highlighted no change or alteration in Raman spectra of melanin and carotenoids, in all tested conditions. In this context, we may consider these pigments as biomarkers of life, owing to its high stability when detected in sandstone samples after the exposure to real space and Mars-like conditions in space. These pigments may be used by extremophiles as strategy to withstand the harmful conditions of the environment. The role of these pigments as UV-protectors is largely reported (Edwards et al., 2005a, b, c; Villar and Edwards, 2006). Indeed, melanin pigments play a crucial role against environmental pressures

including ultraviolet (UV) light, oxidizing agents and ionizing radiation (Eisenman and Casadevall, 2012). On other hand, carotenoids are used as accessory pigments in the light-harvesting complexes of photosynthetic organisms (Tian and Hua, 2010) or scavenge reactive oxygen species like singlet oxygen and peroxyl radicals in non-phototrophic (Armstrong, 1997; Stahl and Sies, 2003; Slade and Radman, 2011). Also, carotenoids protect DNA from oxidative damage (Shahmohammadi et al., 1998), proteins from carbonylation (Tian et al., 2009) and membranes from lipid peroxidation (Sy et al., 2015). β-Carotene is an important antioxidant pigment found in the various extremophilic organisms, and therefore its presence is evidence of biologic processes in extreme habitats. Previously results showed the detectability and stability of melanin pigments after the exposure to simulated and real space exposure in combination with Martian regolith analogues or alone (Pacelli et al., 2021a, b; Cassaro et al., 2021). On the contrary, Raman β-carotene signal was dropped after the exposure to 570 MJ/m^2 of polychromatic UV irradiation, when mixed with Martian regolith analogues (Baqué et al., 2016). On the contrary, its signal is still detectable after the exposure to 113 kGy of gamma rays, even if reduced in intensity (Baqué et al., 2020). Other studies suggested a good preservation of β-carotene signal after an intense exposure to UV-C radiation, when protected by halite (Jehlicˇka et al., 2014; Perl and Baxter, 2020; Perl et al., 2020).

To complement and enhance the capabilities to detect functional groups of biomolecules within sandstone, an infrared spectrometer was used to distinguish mineral and organic components. Similarly, the ISEM instrument onboard the Rosalind Franklin rover, will capable of recognizing organics and minerals, which are indicative of the presence of water as well as organic indicators (Korablev et al., 2017). In this context, FT-IR analyses were performed in the MID infrared region (4000-600 cm^{-1}), focusing on lipids, pigments, polysaccharides.

The lipids content was identified by bands at 1664, 2889 and 3020 cm^{-1} (Fig. 5A and B) and associated to ν(C=C) cis, $\nu_s(CH_3)$ and ν_{as}(=C–H), respectively (Schulz and Baranska, 2007). Lipids, the building blocks of life, are considered one of the high-priority organic compounds in the search for life on Mars (Aerts et a., 2014), thanks to their great chemical stability and potential for persisting

for billions of years in the geological record (Aubrey et al., 2006; Kminek and Bada, 2006) (e.g. in the 2.7 billion-year-old shales from the Pilbara Craton, Australia; Brocks et al., 1999). The finding of lipid functional groups within sandstone, may be helpful to support life-detection missions. As reported in Peters et al. (2005), the majority of molecular fossils in geological samples derives from lipids or cellular membranes components. In particular, the recalcitrant hydrocarbon backbone, acts to promote the high preservation potential of lipid-derived molecular fossils. Moreover, previously studies show that lipid composition may reflect biological and environmental features of possible ecosystems (Eingenbrode, 2008); and know the exact molecular composition of lipids or the entire molecules, could be helpful in life-search space missions. De Leeuw and Largeau (1993) suggested that some classes of lipids, in particular glycolipids and lipopolysaccharides, are one of the most resistant to degradation in depositional environments.

The infrared spectra further confirm the presence of melanin pigments, with a broad absorption bands at 3371-3020 cm^{-1} in samples exposed to real space conditions (Fig. 5A); and at 3369-3020 cm^{-1} in samples exposed to Mars-like conditions in space (Fig. 5B), both due to the stretching vibration of OH groups and NH stretch (Pal et al., 2013; Pacelli et al., 2020, 2021). The band observed at 1026 cm^{-1} and detected in all tested samples (Fig. 5A and B), may be attributed to aromatic ring CH stretching (Pal et al., 2013; Pacelli et al., 2020, 2021). The presence of carotenoid pigments was not entirely unambiguous: the band at 1452 cm^{-1} in space exposed samples and at 1448 cm^{-1} in Mars-like conditions exposed samples appears due to the bending vibration of methylene $–CH_2$ (scissoring) and could be assigned to carotenoid pigments (Kushwaha et al., 2014). Similarly, this band may be occurring in CH_2 bending of proteins or chitin, the main components of the fungal cells wall (Ivshin et al., 2007; Bowman and Free, 2006) or to in plane-scissoring of CH_2 in lipid chain (Shulz and Baranska, 2007). On other hand, the band at 1526 cm^{-1} and 1524 cm^{-1} (Fig. 5A and B), can be clearly assigned to ν(C=C) of β-carotene.

Overall, infrared spectroscopy confirmed the results obtained with Raman analyses: the presence of melanin and carotenoids pigments occur in all tested samples without any alteration. Similar results

have been obtained for melanin pigments of fungal colonies exposed for 16 months to space and Mars-like conditions outside the ISS, aboard EXPOSE-R2 payload (Pacelli et al., 2021).

The band at 1664 cm^{-1}, associated to $\nu(C=C)_{cis}$, previously reported as a lipid absorption, could be identify also as a band of chlorophyll (Kushwaha et al., 2014). The presence of chlorophyll a and chlorophyll b, was revealed both in samples exposed to real space conditions either in samples exposed to Mars-like conditions, with the bands at 1553 and 1572 cm^{-1} and at 1549 and 1570 cm^{-1}, respectively (Schulz et al., 2007).

The presence of chlorophyll may be further confirmed by the presence of the band at 1718 cm^{-1}, due to $\nu(C=O)$ obtained from the aliphatic biomacromolecule algenan, a non-hydrolyzable, insoluble biopolymer (Tegelaar et al., 1989) isolated from a variety of unicellular algae and involved as the source of a sizable proportion of the aliphatic refractory organic matter in sedimentary rocks (Kodner et al., 2009). Its role as a protective compound, reinforcing cell walls (Blokker et al., 1999; Graham and Wilcox, 2000; Versteegh and Blokker, 2004) and conferring resistance to environmental stress (Allard and Templier, 2000; Versteegh and Blokker, 2004) is still debated. In contrast to other compounds, such as DNA and proteins, which are highly susceptible to hydrolysis and oxidation (Lindahl, 1993) and able to persist as traces in fossils more than about 100000 years old (Bada et al., 1999; Collins et al., 1999), algaenan is more decay-resistant, showing a higher preservation potential. Moreover, the discovery of an algaenan-like signature in kerogens (Derenne et al., 1994; 1992; Goth et al., 1988), confirm the hypothesis of the high preservation potential of this compound, leading us to understand that biopolymers plays a principal role in kerogen formation (Derenne et al., 1991; Gelin et al., 1996; Tegelaar et al., 1989) and this could be useful in the search of recently extinct life on Mars. Even if, this molecule can be analyzed with the traditional methods, infrared spectroscopy is unable to provide the exact molecular composition. In this context, pyrolysis-gas chromatography-mass spectrometry (py-GC-MS) has been widely used to evaluate the molecular entities comprising algaenan (Kodner et al., 2009) and this is relevant information to take into account in the near space exploration missions.

Researches highlighted that amide functional groups, occur at 1501 cm^{-1} in samples exposed to space conditions and at 1502 cm^{-1} for samples exposed to Mars-like conditions and could be assigned to an N-H bending vibration coupled to C-N stretching in amide II (Fabian et al., 1995; Preston et al., 2014). The absorbance at 3057 cm^{-1} and 3061 cm^{-1}, can be associated with amide B, due to N-H stretching. Finally, the band at 1410 cm^{-1} (Fig. 5A) and 1402 cm^{-1} (Fig. 5B) can be related to ν(C–N), ν(N–H) of amide III (Marshall, 2006). The presence of amide II and III bands could represent components of proteins, lipids, and polysaccharides within the samples. If we assume that the found vibrational mode are correlate with a proteins backbone vibrations, they could reveal the presence of the protein secondary structure (Preston et al., 2011). The detection of α-helical and β-structures may suggest that hydrolysis has not occurred and that intact proteins have been preserved in the mineral matrix (Gleeson et al., 2012). The finding of amides band constitutes an additional evidence that organics are preserved within samples exposed to space and Mars-like conditions.

The bands at 970 (976 cm^{-1} in Mars-like conditions samples) and 1335 cm^{-1}, probably due to OCH_3, could highlight the presence of polysaccharides or pectin. The region from 2500 to 4000 cm^{-1}, was characterized by the bands at 2633, 2731-2735, 2826 cm^{-1} attributable to the stretching NH_3; 2995-2997 cm^{-1}, due to C-H ring and at 3169 cm^{-1} for presence of N-H stretching (Dovbeshko et al., 1997). Then, the band at 3508-3512 cm^{-1} is created by the presence of O-H stretching (free) (Smith and Rehman, 1994). In contrast to Raman spectroscopy, with infrared detection it is always possible to identify inorganic materials, as minerals. With a main focus on the fingerprint region, the quartz presence was correlated to the absorption bands at 786, 864, 1122, 1194 and 3248 cm^{-1}, found in samples exposed to real space and Mars-like conditions. Only the samples exposed to real space conditions (Fig. 5A) were characterized to an additional band at 1101 cm^{-1}, referred to asymmetric stretching vibrational modes of SO_4 tetrahedra (Preston et al., 2020). As reported in Preston et al. (2020) for sulfate analogues, the difficulty to distinguish organics within a silica mineral grains, has profound implications for the search for life on Mars. Indeed, many bands associated with organic matter could be correlated also to the presence of mineral elements and this could be considered in

the frame of *in situ* explorations. These results demonstrated that the combined use of two spectroscopies, is useful to confirm the presence of organic compounds within a sample. The synergic work of these spectroscopies is highly requested: the RLS instrument can be used after identification of potential targets using the MicrOmega visible/near-IR microscope, which has a wider footprint on the sample. The MicrOmega device can performed the analyses in a point identified in the initial analysis with the RSL (Stevens et al., 2019). Deepen the detectability about organic molecules inside sandstone after exposure to space and Mars-like conditions allowed to highlight that minerals acting as an effective protection for organic matter. Indeed, cryptoendolithic microbial communities, if appropriately protected by minerals matrix, can be detected via spectroscopy-based techniques, even after 16 months of exposure and also 10 years after the exposure.

Acknowledgments

This work was supported by the Italian Space Agency (BioSigN MicroFossils – ASI N. 2018-6- U.0). The Italian National Program of Antarctic Researches (PNRA) and the Italian National Antarctic Museum “Felice Ippolito” (MNA) are also acknowledged for funding the collection of Antarctic samples CCFEE.

4. General discussion

The main scientific drivers of Solar System exploration are the habitability potential and the search for past or present signs of life (biomarkers), near the surface or in the subsurface of planetary bodies. Nowadays, Mars is considered one of the main targets to the search for life, because it contains most of the fundamental ingredients for life: carbon, potential energy sources to support life, and water under different forms (Malin and Edgett, 2000, 2003; Michalski et al., 2017; Rasmussen et al., 2009). However, its surface is characterized by a high radiative environment, consisted of UV and ionizing radiation, the Galactic Cosmic Rays (GCRs) and Solar Energetic Particles (SEP). If UV radiation is no longer a problem at depth greater than 1 mm in the subsurface, due to the limited penetration capability, ionizing radiation constitutes a problem for life in the first 1.5 meters of subsurface.

This highly irradiated environment could i) affect the survivability of hypothetical life forms and limiting the habitability and ii) cause chemical alteration of regoliths, damaging the hypothetical organic matter preserved therein, and making difficult the detection of putative traces of life.

In this context, this thesis aimed to deepen these two fundamental topics of astrobiological researches by i) investigating the responses of the Antarctic cryptoendolithic black fungus *C. antarcticus* after the exposure to different stressors (radiation, vacuum, perchlorates, etc) to investigate the limits of terrestrial life and to expand the concept of habitability; and ii) studying the behavior of fungal biomolecules after the exposure to the above-mentioned stressors, in order to identify a group of molecules to be accounted as biomarkers of life. These researches have been performed in the frame of different astrobiological projects (see paragraph #1.8 “Astrobiology projects”, Chapter 1), using the astrobiological well-established eukaryotic test organism, the black fungus *C. antarcticus*. This organism showed an extraordinary resistance in terms of survivability and DNA damages in ground-based experiments (Pacelli et al., 2017a, b, 2018) and under space exposure conducted outside the International Space Station (Onofri et al., 2012, 2015, 2019). Moreover, it withstands an exposure up to 1000 Gy of He ions when mixed with P-MRS analogue (Pacelli et al., 2020) and to 1000 Gy of Fe

ions (Aureli et al., 2020). The use of a terrestrial organism in support of life detection is based on the idea that terrestrial life is the only example of life we have so far and that extraterrestrial life, if exists, may share chemical characteristics of life on Earth.

One the fundamental requisite that may define a planetary surface habitable is the availability of liquid water. Contrary to what was assumed in the past, its presence is widely reported outside the Earth as well. For example, it was demonstrated that water may persist on Martian surface, even if only in certain circumstances and for a short period of time because of the surface conditions (e.g., low temperature and atmospheric pressure) (Orosei et al., 2020). Also Martian subsurface hosts numerous aquifer reservoirs, such as a stable water body, located 1.5 km beneath the South polar ice cap, discovered by NASA in 2016 (Orosei et al., 2018). The discovery of transient liquid water on the surface of the planet, has important implications for the habitability concept, enhancing the focus on this planet for the search for life. On the one hand liquid water could favor the proliferation of hypothetical life forms. But the high radiative environment of the Martian surface, should be considered. The exposure of metabolically active life forms to ionizing radiation could cause a direct ionization of DNA or the ionization of water causing OH•, H• and aqueous electrons (e-aq) formation (Becker and Sevilla, 1993; von Sonntag, 2006). These reactive species may be dangerous for biological molecules, such as DNA, enzymes, and lipid membranes (Adam et al., 2003; Krieger, 2004). In this context and in the frame of "Starlife" irradiation campaign and "Life in space" ASI project, the responses of metabolically active cells of the fungus *C. antarcticus,* after the exposure to increasing doses of **i)** heavy ions (iron ions, Fe^{26+}) and **ii)** γ-rays, have been tested. The results showed a strong fungal survivability after the exposure to iron ions, even at the higher doses (1000 and 2000 Gy; Pacelli et al., 2021a). On the contrary, no microbial growth was detected for samples exposed to γ-rays (see paragraphs #2.1 and 2.2; Cassaro et al., in prep.). Although the effects of densely (heavy ions) radiation may be considered more dangerous than sparsely (γ-rays) radiation because of the different linear energy transfer (LET, amount of energy transferred to a material when traveling a given distance through it), the value of the tested doses should be taken into account (the minimum

of the applied heavy ions doses was 0.1 kGy, while γ-rays doses was 27 kGy). Differences in microorganism's tolerance to sparse and dense radiation, were also reported for the cyanobacterium *Chroococcidiopsis* spp. Indeed, the exposure to light and heavy ions (He and Fe ions) and to X- and γ-rays, resulted in different survival values (up to 1 kGy of He-ions, 2 kGy of Fe-ions, 5 kGy of X-rays and 12 kGy of γ-rays, Verseux et al., 2017). In different halophilic archaea (*Halobacterium salinarum NRC-1, Halococcus hamelinensis, Halococcus morrhuae*) exposed to Fe-ions, γ- and X-rays in metabolic active conditions, the recorded survival was up to 2 kGy for Fe-ions and X-rays and up to 6 kGy of γ-rays, indicating the radiation with high-LET values as the limit for the survival of organisms in space (Leuko and Rettberg, 2017). While, the whole-genome oligonucleotide microarray analysis of the α-proteobacterium *Rhodospirillum rubrum* S1H exposed to a combination of single beams of low-LET γ-rays and high-LET neutron rays, revealed significant changes at the transcriptomic level but only a few considerable variations in the expression of proteins, and no alteration in cell viability (Mastroleo et al., 2009). Transcriptomic responses of *Saccharomyces cerevisiae* after the exposure to X- and γ-rays, revealed that the up-regulated genes were mainly involved in cell cycle and DNA processing, cell rescue defence and virulence, protein and cell fate and metabolism (Kimura et al., 2006). Further -omics analysis on *C. antarcticus* will be performed to investigate the molecular effects of high- and low-LET radiation exposure.

On the contrary, similar results, among the two experimental sets, were obtained in evaluating the metabolic activity recovery (MTT assay), cellular membrane damages (PMA assay) and the nucleic acids damages (qPCR). In overall, an increase in metabolic activity was recorded for both irradiated set of samples (Pacelli et al., 2021a). On the contrary, a reduction in the amplified copy numbers, as the radiation dose increase, was obtained both for PMA assay and qPCR technique. Lastly, nucleic acid damages were evaluated also through a single gene PCR amplification. The samples irradiated with iron ions showed a good amplification even at the highest doses longest gene sequences tested (ITS5-LR5 and ITS5-LR7) (Pacelli et al., 2021a), while samples exposed to γ-rays showed a

gradually reduced ITS amplification up to 56 kGy and the loss of amplification for the longest tested sequences, comparing to control samples (see paragraphs #2.1 and 2.2).

One of the factors that could contribute to the occurrence of liquid water on Mars is the widespread presence of perchlorates on the surface. In 2008, the Phoenix's Wet Chemistry Laboratory analysis, detected a mixture of $Ca(ClO_4)_2$ and $Mg(ClO_4)_2$ with a concentration of 0.4-0.6 wt% and a small amount of Na^+ and K^+ (Hecht et al., 2009) in Martian regolith. Perchlorates are highly hygroscopic compounds, that may act by lowering the freezing temperature of water (Möhlmann and Thomsen, 2011) and in appropriate range of temperature they form aqueous solution (brines), which remain stable at room temperature (Martin-Torres et al., 2015). The aqueous solutions may favor the presence of liquid water for hypothetical life forms, but perchlorates could act as a toxic and oxidant species for microorganisms (Soudi et al., 2017). For these reasons, investigating the microbial tolerance in presence of perchlorates is of utmost importance to support life-detection missions, since they could interfere with the detection of hypothetical life-forms or organic compounds on the planet (Quinn et al., 2013; Wadsworth and Cockell, 2017). In the context of "Life in space" project, the perchlorates tolerance of the black fungus *C. antarticus* has been tested. In particular, fungal colonies were grown on i) increasing concentrations of four perchlorate salts (Na-, K-, Mg- and Ca-perchlorates) and ii) Mars relevant perchlorate salts (0.4-0.6 wt%) cultivation media. Results showed a good growth rate at lower concentrations with a decrease as the concentration increases (see paragraph #2.3). The fungus was able to grow up to 220 mM of Na-perchlorate, while a concentration of 100 mM of Mg-perchlorate drastically reduced the growth, until the complete loss of vitality at 150 mM. A similar trend was observed for colonies grown on Ca-perchlorate, in which a concentration of 100 mM reduced the survivability and a concentration of 220 mM completely inhibited the growth. The solubility of K-perchlorate limited the survivability at 90 mM (see paragraph #2.3).

Since 2.4 mM perchlorate ions were reported to occur on Mars as a 60 and 40% mixture of Mg- and Ca-perchlorate, respectively (Hassler et al., 2014), the survivability of the fungus was tested in 2.4 mM culture media. 80% of survivors was detected in comparison to control samples (see paragraph

#2.3). *C. antarcticus* demonstrated a high survivability in presence of different perchlorate species and concentrations, compared to prokaryotic tolerance. A concentration of 100 mM of Mg- and Ca-perchlorates completely inhibit the growth of the cyanobacterium *Chroococcidiopsis* CCMEE 029 (Billi et al., 2021). This study reported, for the first time, the survivability of a non-halophilic microorganism, confirming its role as a test organism in the search for life outside Earth. Also, expand the knowledge about the limits of life and Martian habitability. Even if future experiments through the use of the modern -omic techniques will be necessary to highlights the mechanisms at the basis of fungal perchlorates tolerance and metabolism, the resistance of this fungal specie to salt species might be exploited in In Situ Resources Utilization (ISRU) to removing perchlorate in Martian soil.

The second topic of this thesis was developed through the investigation of the stability of fungal biomarkers after the exposure of *C. antarcticus* colonies to different stressors. To achieve this goal, similar techniques to those will be utilized by Perseverance and Rosalind Franklin rovers (Raman and FT-IR spectroscopies and Gas Chromatography-Mass Spectrometry), have been used. In addition, new life-detection instruments (PCR and qPCR) might be suggested for future missions.

In the frame of BIOMEX project, de-hydrated fungal samples were exposed to i) simulated space and Martian conditions (EVTs and SVT ground-based experiments) in preparation for the space exposure and ii) real space exposure and simulated Martian conditions in LEO (de Vera et al., 2012, 2019). Before the exposure, fungal samples were grown on two Martian regolith analogues (P-MRS and S-MRS) and on Antarctic sandstone (OS), in which the fungus naturally occurs.

During the EVTs tests, *C. antarcticus* colonies were exposed to increasing doses of UV irradiation simulating the whole Solar UV spectrum expected in LEO for the mission duration (up to 16 months). Here, samples were analyzed through qPCR, spectroscopic techniques (Raman and Infrared techniques) and spectrophotometric assay. As reported in Pacelli et al. (2021b), nucleic acids may be considered as a potential biomarker of life, despite their high sensitivity to degradation, since a good amplification was recorded even at the high dose of 5.5×10^5 kJ/m^2.

Among other biomarkers, this work focused on melanin pigments. The spectrophotometric detection reported the typical spectral profile of fungal melanins with a maximum absorbance peak at around 230 nm (Pacelli et al., 2021b; Pal et al., 2013; Suryanarayanan et al., 2004; Yuan et al., 2007). Similarly, Raman spectra recorded two main peaks at 1340 and 1590-1604 cm^{-1} and an additional peak at 1425 cm^{-1}, characteristic of the fungal melanin pigments. Since no changes were detected in both techniques, melanin pigments may be considered as a highly resistant compounds, suggesting their use as biomarker of life. The results of FT-IR analyses, confirmed the presence and the preservation of melanin pigments.

Melanins are secondary compounds chemically synthesized from phenolic compounds and indolic rings (Nguyen et al., 2013) with remarkable structural diversity (Chang et al., 2020) that are widespread in animals, plants, and microorganisms (Riley, 1997; Plonka and Grabacka, 2006).

Melanins are among the most important molecules related to stress tolerance; the peculiar characteristic is the high protection they offer against ultraviolet (UV) and ionizing radiation, solar radiation, desiccation (Henson et al., 1999), enzymatic lysis (Jacobson, 2000; Rosas and Casadevall, 2001), extreme environmental conditions (Nosanchuk et al., 1999), metals, salinity (Gunde-Cimerman et al., 2000), and oxidants (Wang and Casadevall, 1994). Previous studies showed that the melanization enhances the resistance of *C. antarcticus* to acute and chronic ionizing radiation, compared to the non-melanized counterparts (Pacelli et al., 2017 a, b, 2018).

Besides, other molecules belonging to the groups of fatty acids, proteins and carbohydrates have been detected, among which, chitin is the most interesting (Pacelli et al., 2021b). This compound is known as one of the specific biosignature for fungi, and it has been demonstrated its high stability in fossil records (Ivarsson et al., 2011) and up to 5.5×10^5 kJ/m^2 of UV radiation (Pacelli et al., 2021b). These results corroborating the use of chitin as a suitable biomarker for the search for life.

In the second set of ground-based tests (SVT), fungal colonies were grown on i) OS and exposed to vacuum (10^{-5} Pa) and cycling temperatures between -25 °C (16 h in the dark) and +10 °C (8 h during irradiation) and polychromatic UV radiation (200-400 nm) and on ii) P-MRS and S-MRS and exposed

to Mars-like atmosphere (95.55% CO_2, 2.70% N_2, 1.60% Ar, 0.15% O_2, *370 ppm H_2O), Mars-like pressure of 10^3 Pa and polychromatic UV radiation (200-400 nm). After the exposure, samples were analyzed with the same techniques reported for EVT samples (Pacelli et al., 2021b) and with the innovative GC-MS analysis. As reported for EVT treatments, UV-Vis and Raman analyses confirmed the stability of fungal melanin (Chapter 3, Cassaro et al., 2021). No noticeable damages were reported for nucleic acids, even if a decrease in copy numbers amplification have been detected in comparison to EVT treatments (Pacelli et al., 2021b). The innovative GC-MS approach, was used to test any possible thermal destruction and transformation of organic matter induced by pyrolysis. The results highlighted the presence of unaltered low molecular weight carboxylic acids, such as pyruvic and myristic acids (Cassaro et al., 2021). The most interesting detected compound is the azelaic acid, which was detected in all tested samples and never in samples without fungal colonies. Further studies finalized to the evaluation of azelaic acids as a suitable biomarker of life will be performed.

The last step of BIOMEX project was the launch of selected samples in LEO on the International Space Station. After the success of the ground-based tests, the fungus *C. antarcticus* was included among different organisms in the space experiment. Fungal samples prepared with the same procedure of EVTs and SVT treatments, were exposed for 16 months aboard the ISS within the EXPOSE-R2 payload (de Vera et al., 2012, 2019). To provide new insights about pigment stability after the real space exposure, Raman analyses were developed. Similar results to EVT and SVT treatments were obtained. Here, we optimized the detection of melanin pigments in order to discern these compounds from amorphous carbon, which represents one of the most important challenges in the search for traces of life of unambiguous biological origin. As reported in Pacelli et al. (2021c), the melanin and amorphous carbon Raman spectra appear different: i) the positions of the bands of amorphous carbon differ from the recorded melanin spectra with a higher shift for each feature and ii) an additional band around 1457 cm^{-1} was found only in spectra acquired from fungal colony, therefore is the proof of molecules derived from biotic process. These results confirmed the stability and the easy detection of melanin pigments, as to be considered as a promising biomarker to search

beyond Earth. The limits of the instrument in detecting melanin pigments should be considered. According to Lopez-Reyes et al. (2013), a prototype of the Raman instrument was built to test the scientific capabilities of the Rosalind Franklin rover instrument, demonstrating that the instrument is able to detect most of the mineral phases present on the sample, with a detection threshold down to 1 % with 30 random point acquisitions. Further investigations on melanic pigment mixed with Martian regolith analogues in varying quantities will be performed to determine the melanin detection threshold with a comparable Exomars equipment.

Similar results of EVT analyses were obtained through FT-IR technique: functional groups of proteins, lipids, carboxylic acids and pigments have been detected (Pacelli et al., 2021b). qPCR technique has proven as a useful technique once again to detect nucleic acids, even with a minimal amount of sample, highlighting the necessity to develop miniaturized PCR devices onboard the future rover instrumentation.

In the above-mentioned works, the presence of Martian regolith analogues did not interfere with the biomolecule's extraction and detection. The preservation of biomolecules might be enhanced by the presence of a protection, such as a mineral matrix (Preston at al., 2019). The mineral matrix (e.g. regolith of Martian surface) could play a dual role in protection organic matter: on the one hand the active minerals could affect the reactivity of hypothetical molecules, on the other hand they could act as protector (Fornaro et al., 2018). For these reasons, the upcoming ExoMars 2022 mission will search for sign of life up to 2 meters depth in the subsurface, in order to provide the best chance yet to gain access to biomarkers (Vago et al., 2017). Thus, the study of the mineral matrix role is of utmost importance. In this context, part of this thesis focused on the detection of i) fungal biomarkers after the exposure of *C. antarcticus* colonies mixed with two Martian regolith analogues to heavy ions (Fe, Ar and He ions) and ii) cryptoendolithic communities' biomarkers within sandstone fragments, after the exposure to space and Mars-like conditions in space.

The first study aimed at investigating the effects of accelerated heavy ions (Fe, Ar and He) on the biomolecules of the black fungus *C. antarcticus*, using Raman and Infrared spectroscopies (see

paragraph #3.4). The results of Raman spectroscopy, revealed unaltered melanin pigments bands (Pacelli et al., 2021b, c), even at the higher dose (1000 Gy of heavy ions). This study confirms the stability of melanin pigments after the exposure to increasing doses and different heavy ions, corroborating the necessity to confirm melanin as a good stabile biosignatures of Earth-like life.

FT-IR bands detected in this study belong to several vibrational functional groups of organics, such as alcohols and phenols (Shurvell, 2006), aliphatic compounds (Coates, 2006; Shurvell, 2006; Movasaghi et al., 2008; Sajjan et al., 2013), or lipids and fatty acids (Movasaghi et al., 2008) and melanin pigments (Mbonyiryivuze et al., 2015). The presence of polysaccharides is highlighted by bands at 1250, 1161 and 1100 cm^{-1} and may be related to the fungal cell wall components such as chitin or glucuronans (Schulz and Baranska, 2007; Forfang et al., 2017). As reported in Pacelli et al. (2021b), chitin confirmed a good detection potential, even after heavy ions irradiation. Furthermore, nitrile compounds have been identified. These compounds could be derived by adenine secondary products, that may be formed after irradiation (Poch et al., 2014), but are known to be stable over geological periods and they can be accumulated and preserved in regolith (Evans et al., 2011). The results of this work highlight a good preservation of different classes of fungal biomolecules, when mixed with two Martian regolith analogues. Also, we confirmed the detectability of melanin pigments with two complementary devices. Further analyses to account chitin and nitriles as a suitable biomarker should be performed. In the second study, dried sandstone fragments, colonized by cryptoendolithic microbial communities were exposed to space and Mars-like conditions in space within the EXPOSE-E payload (Onofri et al., 2012; Rabbow et al., 2015), in the frame of LIFE project. After 10 years from the exposure, the detectability of microbial communities' biomarkers and the protective role of mineral matrix were investigated through Raman and Infrared analytical devices (see paragraph #3.5). Although it is reasonable to hypothesize that minerals may affect the biomarker's detectability, here we assert that sandstone (mainly composed to quartz grains) acts as protection against prohibitive conditions of the space environment, maintain unaltered microbial

biomarkers (mainly melanin and carotenoids pigments; see paragraph #3.5). This work could be considered as a starting point and driving work to detect signs of extinct life on Mars.

Assuming that environmental conditions on the planet were favorable in the past (Benner et al., 2020), the proliferation of life might have been supported (Cockell, 2014; Westall et al., 2015). The drastic environmental changes on the Martian surface could have led to the extinction of these hypothetical life-forms (Schwartz and Mancinelli, 1989), that have once evolved on the surface or subsurface. These life-forms may have left behind fossilized traces in minerals, rocks, and in surrounding areas where its metabolism has finished (Schwartz and Mancinelli, 1989). However, these signs could be affected or degraded by the harsh environmental Martian conditions (e.g. radiation, regolith, oxidant species). Indeed, the cumulative effects of radiation could have destroyed all traces on and beneath the surface, or modified organics (Dartnell, 2011; Hassler et al., 2014), such as not to be detected by standard spectroscopy techniques. Thus, these preliminary studies finalized to test the application of spectroscopic techniques on terrestrial samples and the interference of mineral matrix on the detection of signs of life, are very useful for interpreting data obtained from the ongoing and future life-detection missions and for the next Mars Samples Return Missions (MSR).

5. Conclusion

This thesis has been focused on the survival of the black fungus *C. antarcticus* and on fungal biomarkers detection, after the exposure to different stressors. This research is relevant and has deep implications to support the ongoing and near future life-detection missions beyond Earth. One of the main challenges in the search for life outside Earth, is the habitability of a target planet. Indeed, many factors (radiation, availability of water, oxidant species, temperatures, etc), could limiting the proliferation of life forms. In this context, we tested the responses of the black fungus after the exposure to i) heavy ions, ii) γ-rays and iii) different perchlorates concentrations. Here, we reported a good survivability up to 1000 Gy of heavy ions, while no growth was detected after γ-rays exposure

in metabolically active conditions. The fungus demonstrated to withstand up to 220 mM of Na-, 200 mM of Ca-, 145 mM of Mg- and 90 mM of K-perchlorates and at 0.4-0.6 wt% of $Mg(ClO_4)_2$ and $Ca(ClO_4)_2$, concentrations similar to those found on Mars by the Phoenix lander. These results confirmed the stunning ability of *C. antarcticus* to survive under stressors normally neglected by or precluded to the majority of terrestrial life-forms. Besides, this work expands our knowledge of the boundaries of terrestrial life as well as of the potential for habitability of other worlds in our Solar System by improving our ability to identify environments that could support life. Further studies about the mechanisms at the basis of the fungal tolerance will be performed, trying to identify the genes involved in the resistance. This finding could be exploited through synthetic biology to create resistant strains to be used as component of the Bioregenerative Life Support Systems (BLSS).

The fungal biomarkers detection was performed after the exposure of *C. antarcticus* grown on two Martian regolith analogues, to ground-based tests (EVT and SVT treatments) and to real space exposure in Low Earth Orbit. Our results showed the importance to use multiple and connected analytical techniques (such as Raman and FT-IR spectroscopies) in astrobiology-related studies, since they provide complementary and important information for detecting and characterizing biomarkers. We confirmed the detectability of melanin pigments, even in the presence of a multitude of biomolecules and its discernibility from amorphous carbon spectra. In this context, we corroborated to use melanin pigments, diffused among all biological Kingdoms, as biomarkers in the search for Earth-like life in our Solar System. Surprisingly, we identified azelaic acid, a carboxylic acid strictly related to the fungus, as a potential biomarker. Our investigations also encourage to consider nucleic acids as biomarker, despite their high susceptibility to degradation over time scales, because we demonstrated its detectability upon radiation exposure with amplification methods, and to develop miniaturized devices to design new life-detection rovers. Lastly, experiments on fungal colonies embedded in two Martian regolith analogues and on sandstone fragments colonized by cryptoendolithic microbial communities, were performed in order to investigate the role of minerals in protecting microbial biomolecules and to test the potential of spectroscopic devices to detect

biomarkers entombed in minerals. Our results confirmed the use of melanin and carotenoid pigments as suitable biomarkers and the protective role of minerals that could act as radiation shielding material. In order to quantify the threshold of the instrument for the melanin detection, further analysis on quantity-controlled samples will be performed.

Two new molecules such as nitrile and chitin will be further investigated as possible biosignatures. Further investigations of these molecules will allow to integrate the current biomarkers database and to identify novel extreme biomolecules to be exploited in biotechnological applications. This study represents a starting point to investigate and detect signs of extinct life on Mars.

References

Acuna, M. H., Connerney, J. E. P., Ness, Lin, R. P., Mitchell, D., Carlson, C. W., ... & Cloutier, P. (1999). Global distribution of crustal magnetization discovered by the Mars Global Surveyor MAG/ER experiment. *science*, *284*(5415), 790-793.

Adam, G., Lauger, P., and Stark, G. (2003) Physikalische Chemie und Biophysik, Springer-Verlag, Berlin, Chapter 11.

Aerts, J. W., Riedo, A., Melton, D. J., Martini, S., Flahaut, J., Meierhenrich, U. J., ... & Ehrenfreund, P. (2020). Biosignature analysis of Mars soil analogs from the Atacama Desert: challenges and implications for future missions to Mars. *Astrobiology*, *20*(6), 766-784.

Aerts, J.W.; Röling, W.F.; Elsaesser, A.; Ehrenfreund, P. Biota and biomolecules in extreme environments on Earth: implications for life detection on Mars. *Life* 2014, 4(4), 535-565.

Al Soudi, A. F., Farhat, O., Chen, F., Clark, B. C., & Schneegurt, M. A. (2017). Bacterial growth tolerance to concentrations of chlorate and perchlorate salts relevant to Mars. International Journal of Astrobiology, 16(3), 229-235.

Alvarez, M.; Zeelen, J.P.; Mainfroid, V.; Rentier-Delrue, F.; Martial, J.A.; Wyns, L.; Maes, D. Triose-phosphate Isomerase (TIM) of the Psychrophilic Bacterium Vibrio marinus Kinetic And Structural Properties. *J. Biol. Chem.* 1998, 273(4), 2199-2206.

Amaral Zettler, L. A., Gómez, F., Zettler, E., Keenan, B. G., Amils, R., & Sogin, M. L. (2002). Eukaryotic diversity in Spain's River of Fire. Nature, 417(6885), 137-137.

Amarelle, V., Carrasco, V., & Fabiano, E. (2019). The hidden life of Antarctic rocks. In *The Ecological Role of Micro-organisms in the Antarctic Environment* (pp. 221-237). Springer, Cham.

Anchordoguy, T. J., Carpenter, J. F., Cecchini, C. A., Crowe, J. H., & Crowe, L. M. (1990). Effects of protein perturbants on phospholipid bilayers. Archives of biochemistry and biophysics, 283(2), 356-361.

Anderson, M. S., Andringa, J. M., Carlson, R. W., Conrad, P., Hartford, W., Shafer, M., ... & Hand, K. (2005). Fourier transform infrared spectroscopy for Mars science. *Review of Scientific Instruments*, *76*(3), 034101.

Arevalo, R., Brinckerhoff, W., van Amerom, F., Danell, R., Pinnick, V., Li, X., ... & Steininger, H. (2015, March). Design and demonstration of the Mars Organic Molecule Analyzer (MOMA) on the ExoMars 2018 rover. In *2015 IEEE Aerospace Conference* (pp. 1-11). IEEE.

Aubrey, A., Cleaves, H. J., Chalmers, J. H., Skelley, A. M., Mathies, R. A., Grunthaner, F. J., ... & Bada, J. L. (2006). Sulfate minerals and organic compounds on Mars. *Geology*, *34*(5), 357-360.

Aureli, L., Pacelli, C., Cassaro, A., Fujimori, A., Moeller, R., & Onofri, S. (2020). Iron ion particle radiation resistance of dried colonies of *Cryomyces antarcticus* embedded in Martian regolith analogues. *Life*, *10*(12), 306.

Baccaro, S., Cemmi, A., & Di Sarcina, I. (2019). Calliope ^{60}Co gamma irradiation facility for space qualification at ENEA-casaccia research centre (Rome). *Phys Astron Int J*, *3*(2), 94-100.

Bada, J. L. (2013). New insights into prebiotic chemistry from Stanley Miller's spark discharge experiments. *Chemical Society Reviews*, *42*(5), 2186-2196.

Bailey, J. V., Orphan, V. J., Joye, S. B., & Corsetti, F. A. (2009). Chemotrophic microbial mats and their potential for preservation in the rock record. Astrobiology, 9(9), 843-859.

Baltschukat, K., Horneck, G., Bücker, H., Facius, R., & Schäfer, M. (1986). Mutation induction in spores of *Bacillus subtilis* by accelerated very heavy ions. *Radiation and environmental biophysics*, *25*(3), 183-187.

Bandfield, J. L., Glotch, T. D., & Christensen, P. R. (2003). Spectroscopic identification of carbonate minerals in the Martian dust. *Science*, *301*(5636), 1084-1087.

Baqué, M., Scalzi, G., Rabbow, E., Rettberg, P., & Billi, D. (2013). Biofilm and planktonic lifestyles differently support the resistance of the desert cyanobacterium *Chroococcidiopsis* under space and Martian simulations. Origins of Life and Evolution of Biospheres, 43(4), 377-389.

Baqué, M., Hanke, F., Böttger, U., Leya, T., Moeller, R., & de Vera, J.-P. (2018). Protection of cyanobacterial carotenoids' Raman signatures by Martian mineral analogues after high-dose gamma irradiation. *Journal of Raman Spectroscopy*, *49*(10), 1617-1627.

Baraldi, D. Effect of Gamma Radiation on D-Glucose Present in Apple Juice. 1973, *J. Food Sci.*, 38, 108–111.

Barbieri, R., & Cavalazzi, B. (2004). Astrobiological implications of microbial morphologies in cold fluid-generated carbonates. *Advances in Space Research*, *33*(8), 1262-1267.

Bargagli, R. (2005). *Antarctic ecosystems: environmental contamination, climate change, and human impact* (Vol. 175). Springer Science & Business Media.

Bauermeister, A., Rettberg, P., & Flemming, H. C. (2014). Growth of the acidophilic iron–sulfur bacterium *Acidithiobacillus ferrooxidans* under Mars-like geochemical conditions. Planetary and Space Science, 98, 205-215.

Baumstark-Khan, C., & Horneck, G. (Eds.). (2002). *Astrobiology: the Quest for the Conditions of Life*. Berlin: Springer-Verlag.

Beblo-Vranesevic, K., Huber, H., & Rettberg, P. (2017). High tolerance of *Hydrogenothermus marinus* to sodium perchlorate. Frontiers in Microbiology, 8, 1369.

Beblo-Vranesevic, K., Bohmeier, M., Schleumer, S., Rabbow, E., Perras, A. K., Moissl-Eichinger, C., ... & Rettberg, P. (2020). Impact of simulated martian conditions on (facultatively) anaerobic bacterial strains from different Mars analogue sites. Current Issues in Molecular Biology, 38(1), 103-122.

Becker, D., & Sevilla, M. D. (1993). The chemical consequences of radiation damage to DNA. In Advances in radiation biology (Vol. 17, pp. 121-180). Elsevier.

Bell, A. A., & Wheeler, M. H. (1986). Biosynthesis and functions of fungal melanins. *Annual review of phytopathology*, *24*(1), 411-451.

Benner, S. A., Ricardo, A., & Carrigan, M. A. (2004). Is there a common chemical model for life in the universe?. *Current opinion in chemical biology*, *8*(6), 672-689.

Berelson, W. M., Corsetti, F. A., Pepe-Ranney, C., Hammond, D. E., Beaumont, W., & Spear, J. R. (2011). Hot spring siliceous stromatolites from Yellowstone National Park: assessing growth rate and laminae formation. *Geobiology*, *9*(5), 411-424.

Berger, T., Bilski, P., Hajek, M., Puchalska, M., Reitz, G. 2013, The MATROSHKA Experiment: Results and Comparison from Extravehicular Activity (MTR-1) and Intravehicular Activity (MTR-2A/2B) Exposure. *Radiat. Res.*, 180, 622–637.

Bernard, S., & Papineau, D. (2014). Graphitic carbons and biosignatures. *Elements*, *10*(6), 435-440.

Bhartia, R.; Hug, W.F.; Salas, E.C.; Reid, R.D.; Sijapati, K.K.; Tsapin, A.; Conrad, P.G. Classification of organic and biological materials with deep ultraviolet excitation. *Appl. Spectrosc.* 2008, 62(10), 1070-1077.

Bibring, J. P., Hamm, V., Pilorget, C., & Vago, J. L. (2017). The micrOmega investigation onboard ExoMars. *Astrobiology*, *17*(6-7), 621-626.

Bibring, J.P., Langevin, Y., Mustard, J.F., Poulet, F., Arvidson, R., Gendrin, A., Berthe, M. 2006, Global mineralogical and aqueous Mars history derived from OMEGA/Mars express data. *Science,* 312, 400–404.

Biemann, K. 2007, On the ability of the Viking gas chromatograph-mass spectrometer to detect organic matter. *Proceed. Nat. Acad. Sci. U.S.A,* 104, 10310–10313.

Billi, D., Verseux, C., Fagliarone, C., Napoli, A., Baqué, M., & de Vera, J. P. (2019). A desert cyanobacterium under simulated Mars-like conditions in low Earth orbit: implications for the habitability of Mars. Astrobiology, 19(2), 158-169.

Billi, D., Fernandez, B. G., Fagliarone, C., Chiavarini, S., & Rothschild, L. J. (2021). Exploiting a perchlorate-tolerant desert cyanobacterium to support bacterial growth for in situ resource utilization on Mars. International Journal of Astrobiology, 20(1), 29-35.

Bishop, J. L., Englert, P. A., Patel, S., Tirsch, D., Roy, A. J., Koeberl, C., ... & Jaumann, R. (2014). Mineralogical analyses of surface sediments in the Antarctic Dry Valleys: coordinated analyses of Raman spectra, reflectance spectra and elemental abundances. Philosophical Transactions of the Royal Society A: Mathematical, Physical and Engineering Sciences, 372(2030), 20140198.

Blois, M.S. 1965, Random polymers as a matrix for chemical evolution. In Fox S.W. (Ed.), The origins of pre-biological systems and of their molecular matrices, *Proceedings of a Conference, Wakulla Springs, Florida, 27–30 October 1963***,** pp.19-38 pp.

Blomberg, A., & Adler, L. (1992). Physiology of osmotolerance in fungi. *Advances in microbial physiology*, *33*, 145-212.

Böcker, U., Wubshet, S. G., Lindberg, D., & Afseth, N. K. (2017). Fourier-transform infrared spectroscopy for characterization of protein chain reductions in enzymatic reactions. *Analyst*, *142*(15), 2812-2818.

Bockheim, J. G. (Ed.). (2015). *The soils of Antarctica*. Springer.

Bonner, T. G., & Duncan, A. (1962). Infra-red spectra of some melanins. *Nature*, *194*(4833), 1078-1079.

Bonneville, S., Delpomdor, F., Préat, A., Chevalier, C., Araki, T., Kazemian, M., ... & Benning, L. G. (2020). Molecular identification of fungi microfossils in a Neoproterozoic shale rock. *Science advances*, *6*(4), eaax7599.

Borucki, W. J., Agol, E., Fressin, F., Kaltenegger, L., Rowe, J., Isaacson, H., ... & Winn, J. N. (2013). Kepler-62: a five-planet system with planets of 1.4 and 1.6 Earth radii in the habitable zone. *Science*, *340*(6132), 587-590.

Böttger, U., de Vera, J. P., Fritz, J., Weber, I., Hübers, H. W., & Schulze-Makuch, D. (2012). Optimizing the detection of carotene in cyanobacteria in a martian regolith analogue with a Raman spectrometer for the ExoMars mission. *Planetary and Space Science*, *60*(1), 356-362.

Böttger, U., Meeßen, J., Martínez-Frías, J., Hübers, H. W., Rull, F., Sánchez, F. J., de la Torre, R., & de Vera, J. P. (2014). Raman spectroscopic analysis of the calcium oxalate producing extremotolerant lichen Circinaria gyrosa. *International Journal of Astrobiology*, *13*(1), 19-27.

Bounichou, M. (2010). *LA METHODE DIAMS: Desorption/Ionization on self-Assembled Monolayer Surface Une nouvelle technique de désorption ionisation laser sans matrice pour la Spectrométrie de Masse* (Doctoral dissertation, Université d'Angers).

Bourgier, V. (2007). *Influence des ions monohydrogénophosphates et fluorophosphates sur les propriétés des phosphogypses et la réactivité des phosphoplâtres* (Doctoral dissertation, Ecole Nationale Supérieure des Mines de Saint-Etienne).

Brandes, J. A., Devol, A. H., Yoshinari, T., Jayakumar, D. A., & Naqvi, S. W. A. (1998). Isotopic composition of nitrate in the central Arabian Sea and eastern tropical North Pacific: A tracer for mixing and nitrogen cycles. *Limnology and Oceanography*, *43*(7), 1680-1689.

Brandt, A., Meeßen, J., Jänicke, R. U., Raguse, M., & Ott, S. (2017). Simulated space radiation: impact of four different types of high-dose ionizing radiation on the lichen Xanthoria elegans. *Astrobiology*, *17*(2), 136-144.

Briggs, D. E., & Summons, R. E. (2014). Ancient biomolecules: their origins, fossilization, and role in revealing the history of life. *BioEssays*, *36*(5), 482-490.

Broady, P. A. (1996). Diversity, distribution and dispersal of Antarctic terrestrial algae. *Biodiversity & Conservation*, *5*(11), 1307-1335.

Brocks, J. J., Buick, R., Summons, R. E., & Logan, G. A. (2003). A reconstruction of Archean biological diversity based on molecular fossils from the 2.78 to 2.45 billion-year-old Mount Bruce Supergroup, Hamersley Basin, Western Australia. *Geochimica et Cosmochimica Acta*, *67*(22), 4321-4335.

Busch, K. L. (1995). Special feature: Tutorial. Desorption ionization mass spectrometry. *Journal of mass spectrometry*, *30*(2), 233-240.

Butler, M. J., & Day, A. W. (1998). Destruction of fungal melanins by ligninases of Phanerochaete chrysosporium and other white rot fungi. *International journal of plant sciences*, *159*(6), 989-995.

Caccamo, M. T., Mavilia, G., Mavilia, L., Lombardo, D., & Magazù, S. (2020). Self-assembly processes in hydrated montmorillonite by FTIR investigations. *Materials*, *13*(5), 1100.

Cady, S. L., Farmer, J. D., Grotzinger, J. P., Schopf, J. W., & Steele, A. (2003). Morphological biosignatures and the search for life on Mars. *Astrobiology*, *3*(2), 351-368.

Campbell, N.A., Reece, J.B., and Markl, J. (2003) Biologie. Spektrum Akademischer Verlag, 533–639.

Campbell, I. B., & Claridge, G. G. (2009). Antarctic permafrost soils. In *Permafrost soils* (pp. 17-31). Springer, Berlin, Heidelberg.

Capozzi, V., Perna, G., Gallone, A., Biagi, P. F., Carmone, P., Fratello, A., Cicero, R. 2005, Raman and optical spectroscopy of eumelanin films. *J. Mol. Struct*., 744, 717-721.

Carbone, I. and Kohn, L.M. 1999, A method for designing primer sets for speciation studies in filamentous ascomycetes. *Mycologia*, 91, 553–556.

Carr, M. H. (1996). Channels and valleys on Mars: Cold climate features formed as a result of a thickening cryosphere. Planetary and Space Science, 44(11), 1411-1423.

Carr, C.E., Rowedder, H., Vafadari, C., Lui, C.S., Cascio, E., Zuber, M.T., Ruvkun, G. 2013, Radiation resistance of biological reagents for in situ life detection. *Astrobiology*, 13, 68–78.

Carrier, B. L., & Kounaves, S. P. (2015). The origins of perchlorate in the Martian soil. *Geophysical Research Letters*, *42*(10), 3739-3745.

Cassaro, A., Pacelli, C., Aureli, L., Catanzaro, I., Leo, P., & Onofri, S. (2021). Antarctica as a reservoir of planetary analogue environments. *Extremophiles*, *25*(5), 437-458.

Cassaro, A., Pacelli, C., Baqué, M., de Vera, J. P. P., Böttger, U., Botta, L., ... & Onofri, S. (2021). Fungal Biomarkers Stability in Mars Regolith Analogues after Simulated Space and Mars-like Conditions. *Journal of Fungi*, *7*(10), 859.

Castro-Wallace, S.L.; Chiu, C.Y.; John, K.K.; Stahl, S.E.; Rubins, K.H.; McIntyre, A.B.; Stephenson, T.A. Nanopore DNA sequencing and genome assembly on the International Space Station. *Sci. Rep.* 2017, 7(1), 1-12.

Catling, D. C., Claire, M. W., Zahnle, K. J., Quinn, R. C., Clark, B. C., Hecht, M. H., & Kounaves, S. (2010). Atmospheric origins of perchlorate on Mars and in the Atacama. Journal of Geophysical Research: Planets, 115(E1).

Catling, D. C. (2013). *Astrobiology: a very short introduction* (Vol. 370). Oxford University Press.

Centeno, S. A., & Shamir, J. (2008). Surface enhanced Raman scattering (SERS) and FTIR characterization of the sepia melanin pigment used in works of art. *Journal of Molecular Structure*, *873*(1-3), 149-159.

Chancellor, J. C., Blue, R. S., Cengel, K. A., Auñón-Chancellor, S. M., Rubins, K. H., Katzgraber, H. G., & Kennedy, A. R. (2018). Limitations in predicting the space radiation health risk for exploration astronauts. *npj Microgravity*, *4*(1), 1-11.

Checinska Sielaff, A., & Smith, S. A. (2019). Habitability of Mars: How Welcoming Are the Surface and Subsurface to Life on the Red Planet?. *Geosciences*, *9*(9), 361.

Chevrier, V. and Mathé, P.E. 2007, Mineralogy and evolution of the surface of Mars: A review. *Planet. Space Sci.* 55, 289–314.

Chevrier, V. F., Hanley, J., & Altheide, T. S. (2009). Stability of perchlorate hydrates and their liquid solutions at the Phoenix landing site, Mars. *Geophysical Research Letters*, *36*(10).

Chyba, C. F., & Hand, K. P. (2005). Astrobiology: the study of the living universe. *Annu. Rev. Astron. Astrophys.*, *43*, 31-74.

Chung, Y. S., J. Kim, D. Han, K. Chae, and K. Jahng. 2003. Ultrastructure of the cell wall of a null pigmentation mutant, npgA1, in Aspergillus nidulans. J. Microbiol. 41:224–231.

Ciaravella, A., Scappini, F., Franchi, M., Cecchi-Pestellini, C., Barbera, M., Candia, R., ... & Micela, G. (2004). Role of clays in protecting adsorbed DNA against X-ray radiation. *International Journal of Astrobiology*, *3*(1), 31-35.

Clifford, S.M.; Lasue, J.; Heggy, E.; Boisson, J.; McGovern, P.; Max, M.D. Depth of the Martian cryosphere: Revised estimates and implications for the existence and detection of subpermafrost groundwater. *J. Geophys. Res. Planets* 2010, 115(E7).

Coates, J. (2000). Interpretation of infrared spectra, a practical approach. *Encyclopedia of analytical chemistry: applications, theory and instrumentation* (pp. 1-24). John Wiley & Sons

Coates, J. D., & Achenbach, L. A. (2004). Microbial perchlorate reduction: rocket-fuelled metabolism. *Nature Reviews Microbiology*, *2*(7), 569-580.

Coates, J. P., & Shelley, P. H. (2006). Infrared spectroscopy in process analysis. *Encyclopedia of Analytical Chemistry: Applications, Theory and Instrumentation*.

Cockell, C. S. (2014). 11 The subsurface habitability of terrestrial rocky planets: Mars. *Microbial life of the deep biosphere*, 225-260.

Cockell, C. S., & Knowland, J. (1999). Ultraviolet radiation screening compounds. *Biological Reviews*, *74*(3), 311-345.

Cockell, C. S., & Raven, J. A. (2004). Zones of photosynthetic potential on Mars and the early Earth. *Icarus*, *169*(2), 300-310.

Cockell, C. S., Schuerger, A. C., Billi, D., Friedmann, E. I., & Panitz, C. (2005). Effects of a simulated martian UV flux on the cyanobacterium, *Chroococcidiopsis* sp. 029. *Astrobiology*, *5*(2), 127-140.

Cockell, C. S., Balme, M., Bridges, J. C., Davila, A., & Schwenzer, S. P. (2012). Uninhabited habitats on Mars. *Icarus*, *217*(1), 184-193.

Cockell, C. S., Bush, T., Bryce, C., Direito, S., Fox-Powell, M., Harrison, J. P., ... & Zorzano, M. P. (2016). Habitability: a review. *Astrobiology*, *16*(1), 89-117.

Cockell, C. S., Stevens, A. H., & Prescott, R. (2019). Habitability is a binary property. *Nature Astronomy*, *3*(11), 956-957.

Coleine, C.; Masonjones, S.; Sterflinger, K.; Onofri, S.; Selbmann, L.; Stajich, J.E. Peculiar genomic traits in the stress-adapted cryptoendolithic Antarctic fungus *Friedmanniomyces endolithicus*. *Fungal Biol.* 2020.

Cooper, G.; Reed, C.; Nguyen, D.; Carter, M.; Wang, Y. Detection and formation scenario of citric acid, pyruvic acid, and other possible metabolism precursors in carbonaceous meteorites. *PNAS* 2011, 108(34), 14015-14020.

Cowan, D. A., & Tow, L. A. (2004). Endangered antarctic environments. *Annu. Rev. Microbiol.*, *58*, 649-690.

Crawford, I. A., Fagents, S. A., Joy, K. H., & Rumpf, M. E. (2010). Lunar palaeoregolith deposits as recorders of the galactic environment of the Solar System and implications for astrobiology. *Earth, Moon, and Planets*, *107*(1), 75-85.

Cubeta, M. A., Echandi, E., Abernethy, T., & Vilgalys, R. (1991). Characterization of anastomosis groups of binucleate Rhizoctonia species using restriction analysis of an amplified ribosomal RNA gene. *Phytopathology*, 81(11), 1395-1400.

Culka, A., Jehlička, J., Ascaso, C., Artieda, O., Casero, C. M., & Wierzchos, J. (2017). Raman microspectrometric study of pigments in melanized fungi from the hyperarid Atacama desert gypsum crust. *Journal of Raman Spectroscopy*, *48*(11), 1487-1493.

Da Pieve, F., Botek, E., Pierrard, V., & Vandaele, A. C. (2019, January). Radiation environment and Habitability on Mars at Oxia Planum and Mawrth Vallis: influence of mineralogy, atmospheric depth and Solar activity. In *Geophysical Research Abstracts* (Vol. 21).

Dabney, J.; Meyer, M.; Pääbo, S. Ancient DNA damage. *Csh. Perspect. Biol.* 2013, 5(7), a012567.

Dadachova, E., & Casadevall, A. (2008). Ionizing radiation: how fungi cope, adapt, and exploit with the help of melanin. *Current opinion in microbiology*, *11*(6), 525-531.

Daly, M. J., & Minton, K. W. (1996). An alternative pathway of recombination of chromosomal fragments precedes recA-dependent recombination in the radioresistant bacterium *Deinococcus radiodurans*. *Journal of Bacteriology*, *178*(15), 4461-4471.

Dartnell, L.R.; Desorgher, L.; Ward, J.M.; Coates, A.J. Modelling the surface and subsurface martian radiation environment: implications for astrobiology. *Geophys. Res.* 2007, 34(2).

Dartnell, L. R., Storrie-Lombardi, M. C., Mullineaux, C. W., Ruban, A. V., Wright, G., Griffiths, A. D., Muller, J. P., & Ward, J. M. (2011). Degradation of cyanobacterial biosignatures by ionizing radiation. *Astrobiology*, *11*(10), 997-1016.

Dartnell, L. R., Patel, M. R., Storrie-Lombardi, M. C., Ward, J. M., & Muller, J. P. (2012). Experimental determination of photostability and fluorescence-based detection of PAHs on the Martian surface. *Meteoritics & Planetary Science*, *47*(5), 806-819.

Dartnell, L. R., & Patel, M. R. (2014). Degradation of microbial fluorescence biosignatures by solar ultraviolet radiation on Mars. *International Journal of Astrobiology*, *13*(2), 112-123.

Davila, A.F.; Duport, L.G.; Melchiorri, R.; Jaenchen, J.; Valea, S.; de Los Rios, A.; Wierzchos, J. Hygroscopic salts and the potential for life on Mars. *Astrobiology* 2010, 10(6), 617-628.

De Angelis, S., De Sanctis, M. C., Ammannito, E., Di Iorio, T., Carli, C. R. I. S. T. I. A. N., Frigeri, A. L. E. S. S. A. N. D. R. O., ... & Piccioni, G. I. U. S. E. P. P. E. (2013). VNIR spectroscopy of Mars analogues with the ExoMars-Ma_Miss instrument. *Memorie della Societa Astronomica Italiana Supplement*, *26*, 121-127.

De Gussem, K., Vandenabeele, P., Verbeken, A., & Moens, L. (2005). Raman spectroscopic study of Lactarius spores (Russulales, Fungi). *Spectrochimica Acta Part A: Molecular and Biomolecular Spectroscopy*, *61*(13-14), 2896-2908.

De Hoog, G. S., & Hermanides-Nijhof, E. J. (1977). Survey of the black yeasts and allied fungi. *Stud Mycol*, *15*, 178-223.

De Sanctis, M. C., Altieri, F., Ammannito, E., Biondi, D., De Angelis, S., Meini, M., ... & Vago, J. L. (2017). Ma_MISS on ExoMars: mineralogical characterization of the martian subsurface. *Astrobiology*, *17*(6-7), 612-620.

de Vera, J. P., Boettger, U., de la Torre Noetzel, R., Sánchez, F. J., Grunow, D., Schmitz, N., ... & Spohn, T. (2012). Supporting Mars exploration: BIOMEX in Low Earth Orbit and further astrobiological studies on the Moon using Raman and PanCam technology. *Planetary and Space Science*, *74*(1), 103-110.

de Vera, J. P., Dulai, S., Kereszturi, A., Koncz, L., Lorek, A., Mohlmann, D., ... & Pocs, T. (2014). Results on the survival of cryptobiotic cyanobacteria samples after exposure to Mars-like environmental conditions. *International Journal of Astrobiology*, *13*(1), 35-44.

de Vera, J. P., Alawi, M., Backhaus, T., Baqué, M., Billi, D., Böttger, U., ... & Zucconi, L. (2019). Limits of life and the habitability of Mars: the ESA space experiment BIOMEX on the ISS. *Astrobiology*, *19*(2), 145-157.

Deamer, D.W. and Pashley, R.M. 1989, Amphiphilic components of the murchison carbonaceous chondrite: Surface properties and membrane formation. *Orig. Life Evol. Biosph.,* 19, 21–38.

Des Marais, D. J., & Jahnke, L. L. (2019). Biosignatures of cellular components and metabolic activity. In *Biosignatures for Astrobiology* (pp. 51-85). Springer, Cham.

Des Marais, D. J., Nuth III, J. A., Allamandola, L. J., Boss, A. P., Farmer, J. D., Hoehler, T. M., ... & Spormann, A. M. (2008). The NASA astrobiology roadmap. *Astrobiology*, *8*(4), 715-730.

Dhole, P.D., Khollam, Y.B., Gunjal, S.D., Shelke, P.N., Jadkar, S.R. 2016, Melanin Thin Films Prepared by Electrochemical Deposition Method and Their Characterizations. *Int. J. Chem. Phys. Sci.* 5, 1–10.

Dick, S. J. (2007). From exobiology to astrobiology. *Planets and Life: The Emerging Science of Astrobiology, edited by WT Sullivan III and JA Baross, Cambridge University Press, Cambridge, UK*, 46-65.

Dick, S. J., & Strick, J. E. (2005). The living universe: NASA and the development of astrobiology. *Journal of the History of Biology*, *38*(2).

DiGregorio, B. E., Levin, G. V., & Straat, P. A. (1997). Mars: the living planet. *Mars: the living planet/Barry E. DiGregorio with Gilbert V. Levin and Patricia Ann Straat. Berkeley*.

Dohm, J. M., Baker, V. R., Boynton, W. V., Fairén, A. G., Ferris, J. C., Finch, M., ... & Wheelock, S. J. (2009). GRS evidence and the possibility of paleooceans on Mars. Planetary and Space Science, 57(5-6), 664-684.

Domagal-Goldman, S. D., Wright, K. E., Adamala, K., De La Rubia, L. A., Bond, J., Dartnell, L. R., ... & Wong, T. (2016). The astrobiology primer v2. 0. *Astrobiology*, *16*(8), 561.

Doran, P. T., McKay, C. P., Clow, G. D., Dana, G. L., Fountain, A. G., Nylen, T., & Lyons, W. B. (2002). Valley floor climate observations from the McMurdo Dry Valleys, Antarctica, 1986–2000. *Journal of Geophysical Research: Atmospheres*, *107*(D24), ACL-13.

Dorn, E.D.; Nealson, K.H.; Adami, C. Monomer abundance distribution patterns as a universal biosignature: examples from terrestrial and digital life. *J. Mol. Evol.* 2011, 72(3), 283-295.

Dovbeshko, G. I., Gridina, N. Y., Kruglova, E. B., & Pashchuk, O. P. (2000). FTIR spectroscopy studies of nucleic acid damage. Talanta, 53(1), 233-246.

Durante, M., & Cucinotta, F. A. (2011). Physical basis of radiation protection in space travel. Reviews of modern physics, 83(4), 1245.

Edwards, A. A. (2001). RBE of radiations in space and the implications for space travel. Physica Medica: PM: an International Journal Devoted to the Applications of Physics to Medicine and Biology: Official Journal of the Italian Association of Biomedical Physics (AIFB), 17, 147-152.

Edwards, H. G., Hutchinson, I. B., Ingley, R., Parnell, J., Vítek, P., & Jehlička, J. (2013). Raman spectroscopic analysis of geological and biogeological specimens of relevance to the ExoMars mission. *Astrobiology*, *13*(6), 543-549.

Edwards, H.G.M., Jehlička, J., Culka, A. 2021, Portable Raman Spectroscopy in Field Geology and Astrobiology Applications. *Portable Spectroscopy and Spectrometry 1: Applications*, **2**, 377-400.

Eglinton, T.I.; Damsté, J.S.S.; Pool, W.; de Leeuw, J.W.; Eijk, G.; Boon, J.J. Organic sulphur in macromolecular sedimentary organic matter. II. Analysis of distributions of sulphur-containing pyrolysis products using multivariate techniques. *Geochimic. Cosmochim. Acta* 1992, 56(4), 1545-1560.

Ehlmann, B. L., Mustard, J. F., Fassett, C. I., Schon, S. C., Head III, J. W., Des Marais, D. J., ... & Murchie, S. L. (2008). Clay minerals in delta deposits and organic preservation potential on Mars. *Nature Geoscience*, *1*(6), 355-358.

Ehlmann, B.L.; Mustard, J.F.; Murchie, S.L.; Bibring, J.P.; Meunier, A.; Fraeman, A.A.; Langevin, Y. Subsurface water and clay mineral formation during the early history of Mars. *Nature* 2011, *479*(7371), 53-60.

Ehlmann, B. L., & Buz, J. (2015). Mineralogy and fluvial history of the watersheds of Gale, Knobel, and Sharp craters: A regional context for the Mars Science Laboratory Curiosity's exploration. *Geophysical Research Letters*, *42*(2), 264-273.

Eigenbrode, J. L., Summons, R. E., Steele, A., Freissinet, C., Millan, M., Navarro-González, R., ... & Coll, P. (2018). Organic matter preserved in 3-billion-year-old mudstones at Gale crater, Mars. *Science*, *360*(6393), 1096-1101.

Eisenman, H.C.; Casadevall, A. Synthesis and assembly of fungal melanin. *Appl. Microbiol Biotechnol* 2012, 93(3), 931-940.

El Maarry, M. R., Kodikara, J., Wijessoriya, S., Markiewicz, W. J., & Thomas, N. (2012). Desiccation mechanism for formation of giant polygons on Earth and intermediate-sized polygons on Mars: Results from a pre-fracture model. Earth and Planetary Science Letters, 323, 19-26.

Ellery, A.; Wynn-Williams, D. Why Raman spectroscopy on Mars?-a case of the right tool for the right job. *Astrobiology* 2003, 3(3), 565-579.

Encrenaz, T., Greathouse, T. K., Lefèvre, F., & Atreya, S. K. (2012). Hydrogen peroxide on Mars: observations, interpretation and future plans. *Planetary and Space Science*, *68*(1), 3-17.

Evans, N. L., Bennett, C. J., Ullrich, S., & Kaiser, R. I. (2011). On the interaction of adenine with ionizing radiation: Mechanistical studies and astrobiological implications. *The Astrophysical Journal*, *730*(2), 69.

Fabian, H., Jackson, M., Murphy, L., Watson, P.H., Fichtner, I., and Mantsch, H.H.A. 1995, Comparative Infrared Spectroscopic Study of Human Breast Tumors and Breast Tumor Cell Xenografts. *Biospectroscopy*, 1, 37–45.

Fairén, A. G., Davila, A. F., Lim, D., Bramall, N., Bonaccorsi, R., Zavaleta, J., ... & McKay, C. P. (2010). Astrobiology through the ages of Mars: the study of terrestrial analogues to understand the habitability of Mars. Astrobiology, 10(8), 821-843.

Fajardo-Cavazos, P.; Schuerger, A.C.; Nicholson, W.L. Exposure of DNA and Bacillus subtilis spores to simulated Martian environments: use of quantitative PCR (qPCR) to measure inactivation rates of DNA to function as a template molecule. *Astrobiology* 2010, 10(4), 403-411.

Fassett, C. I., & Head III, J. W. (2008). Valley network-fed, open-basin lakes on Mars: Distribution and implications for Noachian surface and subsurface hydrology. Icarus, 198(1), 37-56.

Faure, P.; Jeanneau, L.; Lannuzel, F. Analysis of organic matter by flash pyrolysis-gas chromatography–mass spectrometry in the presence of Na-smectite: When clay minerals lead to identical molecular signature. *Org. Geochem.* 2006, 37(12), 1900-1912.

Ferrari, A. C., Rodil, S. E., & Robertson, J. 2003, Interpretation of infrared and Raman spectra of amorphous carbon nitrides. *Phys. Rev. B.*, 67, 155306.

Ferrari, F., & Szuszkiewicz, E. (2009). Cosmic rays: a review for astrobiologists. *Astrobiology*, *9*(4), 413-436.

Fisk, M. R., & Giovannoni, S. J. (1999). Sources of nutrients and energy for a deep biosphere on Mars. *Journal of Geophysical Research: Planets*, *104*(E5), 11805-11815.
Flannery, M. B., Stott, A. W., Briggs, D. E., & Evershed, R. P. (2001). Chitin in the fossil record: identification and quantification of D-glucosamine. *Organic Geochemistry*, *32*(5), 745-754.

Forfang, K., Zimmermann, B., Kosa, G., Kohler, A., & Shapaval, V. (2017). FTIR spectroscopy for evaluation and monitoring of lipid extraction efficiency for oleaginous fungi. *PloS one*, *12*(1), e0170611.

Formisano, V., Grassi, D., Orfei, R., Biondi, D., Mencarelli, E., Mattana, A., ... & Gobbi, P. (2004, August). Pfs: the planetary fourier spectrometer for mars express. In *Mars Express: The Scientific Payload* (Vol. 1240, pp. 71-94).

Foucher, F., Lopez-Reyes, G., Bost, N., Rull-Perez, F., Rüßmann, P., & Westall, F. (2013, September). Effects of powdering rock and mineral samples on optical observations and Raman analyses: consequences for ExoMars measurements. In *European Planetary Science Congress* (pp. EPSC2013-200).

Foucher, F., Hickman-Lewis, K., Hutzler, A., Joy, K. H., Folco, L., Bridges, J. C., ... & Westall, F. (2021). Definition and use of functional analogues in planetary exploration. *Planetary and Space Science*, *197*, 105162.

Freissinet, C., Glavin, D. P., Mahaffy, P. R., Miller, K. E., Eigenbrode, J. L., Summons, R. E., ... & MSL Science Team. (2015). Organic molecules in the sheepbed mudstone, gale crater, mars. *Journal of Geophysical Research: Planets*, *120*(3), 495-514.

Friedmann, E. I. (1982). Endolithic microorganisms in the Antarctic cold desert. *Science*, *215*(4536), 1045-1053.

Friedmann, E. I., & Ocampo-Friedmann, R. (1984). The Antarctic cryptoendolithic ecosystem: relevance to exobiology. *Origins of life*, *14*(1), 771-776.

Friedmann, E.I. 1986, The antarctic cold desert and the search for traces of life on Mars. *Adv. Sp. Res,* 6, 265–268.

Friedmann, E. I., McKay, C. P., & Nienow, J. A. (1987). The cryptoendolithic microbial environment in the Ross Desert of Antarctica: satellite-transmitted continuous nanoclimate data, 1984 to 1986. *Polar Biology*, *7*(5), 273-287.

Friedmann, E. I., Hua, M., & Ocampo-Friedmann, R. (1988). 3.6 Cryptoendolithic lichen and cyanobacterial communities of the Ross Desert, Antarctica. *Polarforschung*, *58*(2/3), 251-259.

Friedmann, E. I., & Koriem, A. M. (1989). Life on Mars: how it disappeared (if it was ever there). *Advances in Space Research*, *9*(6), 167-172.

Friedmann, E. I., Kappen, L., Meyer, M. A., & Nienow, J. A. (1993). Long-term productivity in the cryptoendolithic microbial community of the Ross Desert, Antarctica. *Microbial Ecology*, *25*(1), 51-69.

Galván, I.; Jorge, A.; Ito, K.; Tabuchi, K.; Solano, F.; Wakamatsu, K. Raman spectroscopy as a non-invasive technique for the quantification of melanins in feathers and hairs. *Pigment Cell Melanoma Res.* 2003, 26(6), 917-923.

Galván, I., Jorge, A., Ito, K., Tabuchi, K., Solano, F., & Wakamatsu, K. (2013). Raman spectroscopy as a non-invasive technique for the quantification of melanins in feathers and hairs. *Pigment Cell & Melanoma Research*, *26*(6), 917-923.

Gellert, R., Rieder, R., Anderson, R. C., Bruckner, J., Clark, B. C., Dreibus, G., ... & Zipfel, J. (2004). Chemistry of rocks and soils in Gusev Crater from the Alpha Particle X-ray Spectrometer. *Science*, *305*(5685), 829-832.

Georgiou, C. D., & Deamer, D. W. (2014). Lipids as universal biomarkers of extraterrestrial life. *Astrobiology*, *14*(6), 541-549.

Ghosal, D., Omelchenko, M. V., Gaidamakova, E. K., Matrosova, V. Y., Vasilenko, A., Venkateswaran, A., ... & Daly, M. J. (2005). How radiation kills cells: survival of Deinococcus radiodurans and Shewanella oneidensis under oxidative stress. *FEMS microbiology reviews*, *29*(2), 361-375.

Gibson, E. K., Wentworth, S. J., & McKay, D. S. (1983). Chemical weathering and diagenesis of a cold desert soil from Wright Valley, Antarctica: An analog of Martian weathering processes. *Journal of Geophysical Research: Solid Earth*, *88*(S02), A912-A928.

Glass, K., Ito, S., Wilby, P.R., Sota, T., Nakamura, A., Bowers, C.R., Wakamatsu, K. 2012, Direct chemical evidence for eumelanin pigment from the Jurassic period. *Proc. Natl. Acad. Sci. U.S.A.*, 109, 10218–10223.

Glavin, D. P., Freissinet, C., Miller, K. E., Eigenbrode, J. L., Brunner, A. E., Buch, A., Mahaffy, P. R. (2013). Evidence for perchlorates and the origin of chlorinated hydrocarbons detected by SAM at the Rocknest aeolian deposit in Gale Crater. *Journal of Geophysical Research: Planets*, *118*(10), 1955-1973.

Goesmann, F., Brinckerhoff, W. B., Raulin, F., Goetz, W., Danell, R. M., Getty, S. A., ... & van Amerom, F. H. (2017). The Mars Organic Molecule Analyzer (MOMA) instrument: characterization of organic material in martian sediments. *Astrobiology*, *17*(6-7), 655-685.

Goetz, W., Brinckerhoff, W. B., Arevalo, R., Freissinet, C., Getty, S., Glavin, D. P., ... & Brucato, J. R. (2016). MOMA: the challenge to search for organics and biosignatures on Mars. *International Journal of Astrobiology*, *15*(3), 239-250.

Golubic, S., Friedmann, I., & Schneider, J. (1981). The lithobiontic ecological niche, with special reference to microorganisms. *Journal of Sedimentary Research*, *51*(2).

Gómez-Elvira, J., Armiens, C., Carrasco, I., Genzer, M., Gómez, F., Haberle, R., Hamilton, V. E., Harri, A.-M., Kahanpää, H., Kemppinen, O., Lepinette, A., Martín Soler, J., Martín-Torres, J., Martínez-Frías, J., Mischna, M., Mora, L., Navarro, S., Newman, C., De Pablo, M. A., Peinado, V., Polkko, J., Rafkin, S. C. R., Ramos, M., Rennõ, N. O., Richardson, M., Rodríguez-Manfredi, J. A., Romeral Planellõ, J. J., Sebastián, E., De La Torre Juárez, M., Torres, J., Urquí, R., Vasavada, A. R., Verdasca, J., & Zorzano, M. P. (2014). Curiosity's rover environmental monitoring station: Overview of the first 100 sols. *Journal of Geophysical Research: Planets*, *119*(7), 1680-1688.

Gorbushina, A. (2003). Microcolonial fungi: survival potential of terrestrial vegetative structures. *Astrobiology*, *3*(3), 543-554.

Gorbushina, A. A., Andreas, B. E. C. K., & Schulte, A. (2005). Microcolonial rock inhabiting fungi and lichen photobionts: evidence for mutualistic interactions. *Mycological Research*, *109*(11), 1288-1296.

Gordon, P. R., & Sephton, M. A. (2016). Organic matter detection on Mars by pyrolysis-FTIR: an analysis of sensitivity and mineral matrix effects. *Astrobiology*, *16*(11), 831-845.

Gostinčar, C., Muggia, L., & Grube, M. (2012). Polyextremotolerant black fungi: oligotrophism, adaptive potential, and a link to lichen symbioses. *Frontiers in Microbiology*, *3*, 390.

Gronstal, A., Cockell, C. S., Perino, M. A., Bittner, T., Clacey, E., Clark, O., ... & Wathiong, S. (2007). Lunar astrobiology: a review and suggested laboratory equipment. *Astrobiology*, *7*(5), 767-782.

Grotzinger, J. P., & Knoll, A. H. (1999). Stromatolites in Precambrian carbonates: evolutionary mileposts or environmental dipsticks?. *Annual review of earth and planetary sciences*, *27*(1), 313-358.

Grotzinger, J.P.; Sumner, D.Y.; Kah, L.C.; Stack, K.; Gupta, S.; Edgar, L.; Milliken, R.A habitable fluvio-lacustrine environment at Yellowknife Bay, Gale Crater, Mars. *Sci* 2014, 343(6169), 1242777.

Grotzinger, J. P., Crisp, J. A., Vasavada, A. R., & MSL Science Team. (2015). Curiosity's mission of exploration at Gale Crater, Mars. *Elements*, *11*(1), 19-26.

Guillén, M. D., & Cabo, N. (1999). Usefulness of the frequency data of the Fourier transform infrared spectra to evaluate the degree of oxidation of edible oils. *Journal of agricultural and food chemistry*, *47*(2), 709-719.

Haberle, R.M.; de la Torre Juárez, M.; Kahre, M.A.; Kass, D.M.; Barnes, J.R.; Hollingsworth, J. L.; Kahanpää, H. Detection of northern hemisphere transient eddies at Gale crater Mars. *Icarus* 2018, 307, 150-160.

Hagiwara, Y., Oike, T., Niimi, A., Yamauchi, M., Sato, H., Limsirichaikul, S., Shibata, A. (2019). Clustered DNA double-strand break formation and the repair pathway following heavy-ion irradiation. *Journal of radiation research*, *60*(1), 69-79.

Halliwell, B., & Gutteridge, J. M. (2015). Free radicals in biology and medicine. Oxford university press, USA.

Hallsworth, J.E. (2021), Mars' surface is not universally biocidal. *Environ Microbiol*.

Hansen, A. J., Mitchell, D. L., Wiuf, C., Paniker, L., Brand, T. B., Binladen, J., ... & Willerslev, E. (2006). Crosslinks rather than strand breaks determine access to ancient DNA sequences from frozen sediments. Genetics, 173(2), 1175-1179.

Hamada, N., Imaoka, T., Masunaga, S. I., Ogata, T., Okayasu, R., Takahashi, A., ... & Teshima, T. (2010). Recent advances in the biology of heavy-ion cancer therapy. *Journal of radiation research*, *51*(4), 365-383.

Harel, Y., Ohad, I., & Kaplan, A. (2004). Activation of photosynthesis and resistance to photoinhibition in cyanobacteria within biological desert crust. Plant Physiology, 136(2), 3070-3079.

Hart, M. H. (1979). Habitable zones about main sequence stars. *Icarus*, *37*(1), 351-357.

Harutyunyan, S., Muggia, L., & Grube, M. (2008). Black fungi in lichens from seasonally arid habitats. *Studies in Mycology*, *61*(1), 83-90.

Hassler, D. M., Zeitlin, C., Wimmer-Schweingruber, R. F., Ehresmann, B., Rafkin, S., Eigenbrode, J. L., Berger, G. (2014). Mars' surface radiation environment measured with the Mars Science Laboratory's Curiosity rover. *science*, *343*(6169), 1244797.

Hecht, M. H., Kounaves, S. P., Quinn, R. C., West, S. J., Young, S. M., Ming, D. W., ... & Smith, P. H. (2009). Detection of perchlorate and the soluble chemistry of martian soil at the Phoenix lander site. *Science*, *325*(5936), 64-67.

Heinz, J., Waajen, A. C., Airo, A., Alibrandi, A., Schirmack, J., & Schulze-Makuch, D. (2019). Bacterial growth in chloride and perchlorate brines: halotolerances and salt stress responses of *Planococcus halocryophilus*. Astrobiology, 19(11), 1377-1387.

Heinz, J., Krahn, T., & Schulze-Makuch, D. (2020). A new record for microbial perchlorate tolerance: fungal growth in $NaClO_4$ brines and its implications for putative life on Mars. Life, 10(5), 53.

Heinz, J., Rambags, V., & Schulze-Makuch, D. (2021). Physicochemical Parameters Limiting Growth of *Debaryomyces hansenii* in Solutions of Hygroscopic Compounds and Their Effects on the Habitability of Martian Brines. Life, 11(11), 1194.

Heldmann, J. L., Pollard, W., McKay, C. P., Marinova, M. M., Davila, A., Williams, K. E., ... & Andersen, D. T. (2013). The high elevation Dry Valleys in Antarctica as analog sites for subsurface ice on Mars. *Planetary and Space Science*, *85*, 53-58.

Hennings, E., Heinz, J., Schmidt, H., & Voigt, W. (2013). Freezing and hydrate formation in aqueous sodium perchlorate solutions. Zeitschrift für anorganische und allgemeine Chemie, 639(6), 922-927.

Henson, J.M.; Butler, M.J.; Day, A.W. The dark side of the mycelium: melanins of phytopathogenic fungi. *Annu. Rev. Phytopathol* 1999, 37(1), 447-471.

Hölker, U., Bend, J., Pracht, R., Tetsch, L., Müller, T., Höfer, M., & Hoog, G. S. (2004). Hortaea acidophila, a new acid-tolerant black yeast from lignite. *Antonie van Leeuwenhoek*, *86*(4), 287-294.

Holland, P.M.; Chutjian, A.; Darrach, M.R.; Orient, O.J. Miniaturized GC/MS instrumentation for in situ measurements: micro gas chromatography coupled with miniature quadrupole array and Paul ion trap mass spectrometers. In *First Jet Propulsion Laboratory in Situ Instruments Workshop*. *International Society for Optics and Photonics* 2003. 4878, 1-7.

Hopple Jr, J. S., & Vilgalys, R. (1999). Phylogenetic relationships in the mushroom genus Coprinus and dark-spored allies based on sequence data from the nuclear gene coding for the large ribosomal subunit RNA: divergent domains, outgroups, and monophyly. *Molecular phylogenetics and evolution*, *13*(1), 1-19.

Horneck, G. (1981). Survival of microorganisms in space: a review. Advances in Space Research, 1(14), 39-48.

Horneck, G., Stöffler, D., Ott, S., Hornemann, U., Cockell, C. S., Moeller, R., ... & Artemieva, N. A. (2008). Microbial rock inhabitants survive hypervelocity impacts on Mars-like host planets: first phase of lithopanspermia experimentally tested. *Astrobiology*, *8*(1), 17-44.

Horneck, G., Klaus, D. M., & Mancinelli, R. L. (2010). Space microbiology. *Microbiology and Molecular Biology Reviews*, *74*(1), 121-156.

Horneck, G., Walter, N., Westall, F., Grenfell, J. L., Martin, W. F., Gomez, F., ... & Capria, M. T. (2016). AstRoMap European astrobiology roadmap. *Astrobiology*, *16*(3), 201-243.

Horsfield, B. Practical criteria for classifying kerogens: some observations from pyrolysis-gas chromatography. *Geochimic. Cosmochim. Acta* 1989, 53(4), 891-901.

Hou, R., Liu, X., Xiang, K., Chen, L., Wu, X., Lin, W., Zheng, M., & Fu, J. (2019). Characterization of the physicochemical properties and extraction optimization of natural melanin from *Inonotus hispidus* mushroom. *Food chemistry*, *277*, 533-542.

Huang, S. S. (1960). Life outside the solar system. *Scientific American*, *202*(4), 55-63.

Huang, Z., Lui, H., Chen, M. X., Alajlan, A., McLean, D. I., & Zeng, H. (2004). Raman spectroscopy of in vivo cutaneous melanin. *Journal of biomedical optics*, *9*(6), 1198-1206.

Hunter, S. E., Jung, D., Di Giulio, R. T., & Meyer, J. N. (2010). The QPCR assay for analysis of mitochondrial DNA damage, repair, and relative copy number. Methods, 51(4), 444-451.

Hynek, B. M., Beach, M., & Hoke, M. R. (2010). Updated global map of Martian valley networks and implications for climate and hydrologic processes. Journal of Geophysical Research: Planets, 115(E9).

Igisu, M., Ueno, Y., Shimojima, M., Nakashima, S., Awramik, S. M., Ohta, H., & Maruyama, S. (2009). Micro-FTIR spectroscopic signatures of bacterial lipids in Proterozoic microfossils. *Precambrian Research*, *173*(1-4), 19-26.

Irudayaraj, J., Sivakesava, S., Kamath, S., & Yang, H. (2001). Monitoring chemical changes in some foods using Fourier transform photoacoustic spectroscopy. *Journal of food science*, *66*(9), 1416-1421.

Isenbarger, T.A.; Carr, C.E.; Johnson, S.S.; Finney, M.; Church, G.M.; Gilbert, W.; Ruvkun, G. The most conserved genome segments for life detection on Earth and other planets. *Origins Life Evol. B.* 2008, 38(6), 517-533.

Isola, D., Selbmann, L., de Hoog, G. S., Fenice, M., Onofri, S., Prenafeta-Boldú, F. X., & Zucconi, L. (2013). Isolation and screening of black fungi as degraders of volatile aromatic hydrocarbons. *Mycopathologia*, *175*(5), 369-379.

Ivarsson, M., Broman, C., Holmström, S. J., Ahlbom, M., Lindblom, S., & Holm, N. G. (2011). Putative fossilized fungi from the lithified volcaniclastic apron of Gran Canaria, Spain. *Astrobiology*, *11*(7), 633-650.

Ivshin, V. P., Artamonova, S. D., Ivshina, T. N., & Sharnina, F. F. (2007). Methods for isolation of chitin-glucan complexes from higher fungi native biomass. *Polymer Science Series B*, *49*(11), 305-310.

Jacobson, E. S. (2000). Pathogenic roles for fungal melanins. *Clinical microbiology reviews*, *13*(4), 708-717.

Jacobson, E. S., & Ikeda, R. (2005). Effect of melanization upon porosity of the cryptococcal cell wall. Medical Mycology, 43(4), 327-333.

Jackson, W. A., Böhlke, J. K., Andraski, B. J., Fahlquist, L., Bexfield, L., Eckardt, F. D., ... & Harvey, G. J. (2015). Global patterns and environmental controls of perchlorate and nitrate co-occurrence in arid and semi-arid environments. Geochimica et Cosmochimica Acta, 164, 502-522.

Jackson, A., Davila, A. F., Böhlke, J. K., Sturchio, N. C., Sevanthi, R., Estrada, N., ... & Zacny, K. (2016). Deposition, accumulation, and alteration of Cl^-, NO_3^-, ClO_4^- and ClO_3^- salts in a hyper-arid polar environment: Mass balance and isotopic constraints. Geochimica et Cosmochimica Acta, 182, 197-215.

Jakosky, B. M., & Phillips, R. J. (2001). Mars' volatile and climate history. *nature*, *412*(6843), 237-244.

Jaramillo, E. A., Royle, S. H., Claire, M. W., Kounaves, S. P., & Sephton, M. A. (2019). Indigenous organic-oxidized fluid interactions in the Tissint Mars meteorite. Geophysical Research Letters, 46(6), 3090-3098.

Jaumann, R., Hiesinger, H., Anand, M., Crawford, I. A., Wagner, R., Sohl, F., ... & Oberst, J. (2012). Geology, geochemistry, and geophysics of the Moon: Status of current understanding. *Planetary and Space Science*, *74*(1), 15-41.

Javaux, E.J. Extreme life on Earth—past, present and possibly beyond. *Res. Microbiol.* 2006, 157(1), 37-48.

John, K.K.; Botkin, D.S.; Burton, A.S.; Castro-Wallace, S.L.; Chaput, J.D.; Dworkin, J.P.; Stahl, S. The Biomolecule Sequencer Project: Nanopore sequencing as a dual-use tool for crew health and astrobiology investigations 2016.

Johnson, S. S., Anslyn, E. V., Graham, H. V., Mahaffy, P. R., & Ellington, A. D. (2018). Fingerprinting non-terran biosignatures. *Astrobiology*, *18*(7), 915-922.

Joiner, M. C., & Marples, B. (1993). The response of chinese hamster V79 cells to low radiation doses: evidence of enhanced of the whole cell population sensitivity. *Radiat. Res.*, *133*, 41-51.

Jones, R. A. (1970). Physicochemical Properties of Pyrroles. *Advances in Heterocyclic Chemistry*, 383–472.

Jones, L., Hoban, P., & Metcalfe, P. (2001). The use of the linear quadratic model in radiotherapy: a review. *Australasian Physics & Engineering Sciences in Medicine*, *24*(3), 132-146.

Jones, B. W. (2004). The Nature of Exoplanetary Systems. *An Introduction to Astrobiology*, 233.

Jones, E. G., Lineweaver, C. H., & Clarke, J. D. (2011). An extensive phase space for the potential martian biosphere. Astrobiology, 11(10), 1017-1033.

Josset, J.-L., Westall, F., Hofmann, B.A., Spray, J., Cockell, C., Kempe, S., Griffiths, A.D., De Sanctis, M.C., Colangeli, L., Koschny, D., Fo¨llmi, K., Verrecchia, E., Diamond, L., Josset, M., Javaux, E.J., Esposito, F., Gunn, M., Souchon-Leitner, A.L., Bontognali, T.R.R., Korablev, O., Erkman, S., Paar, G., Ulamec, S., Foucher, F., Martin, P., Verhaeghe, A., Tanevski, M., and Vago, J.L. (2017) The Close-Up Imager onboard the ESA ExoMars Rover: objectives, description, operations, and science validation activities. Astrobiology 17:595–611.

K. SACHS, P. HAHNFELD and DJ BRENNER, R. (1997). Review the link between low-LET dose-response relations and the underlying kinetics of damage production/repair/misrepair. *International journal of radiation biology*, *72*(4), 351-374.

Kannan, P., & Ganjewala, D. (2009). Preliminary characterization of melanin isolated from fruits and seeds of *Nyctanthes arbortristis*. *Journal of Scientific Research*, *1*(3), 655-661.

Kargel, J. S. (2004). Proof for water, hints of life?. *Science*, *306*(5702), 1689-1691.

Kashefi, K., and Lovley, D.R. (2003) Extending the upper temperature limit for life. Science 301: 934.

Kasting, J. F. (1988). Runaway and moist greenhouse atmospheres and the evolution of Earth and Venus. *Icarus*, *74*(3), 472-494.

Kasting, J. F., Whitmire, D. P., & Reynolds, R. T. (1993). Habitable zones around main sequence stars. *Icarus*, *101*(1), 108-128.

Kasting, J. F., & Catling, D. (2003). Evolution of a habitable planet. *Annual Review of Astronomy and Astrophysics*, *41*(1), 429-463.

Keller, J. M., Eckert, C. M., & Clarkson, P. J. (17). others, 2006. Equatorial and midlatitude distribution of chlorine measured by Mars Odyssey GRS: Journal of Geophysical Research, 111, E03S08.

Kendall, C., Isabelle, M., Bazant-Hegemark, F., Hutchings, J., Orr, L., Babrah, J., Baker, R., Stone, N. (2009). Vibrational spectroscopy: A clinical tool for cancer diagnostics. *Analyst*, *134*(6), 1029–1045.

Kenig, F., Chou, L., McKay, C. P., Jackson, W. A., Doran, P. T., Murray, A. E., & Fritsen, C. H. (2016). Perchlorate and volatiles of the brine of Lake Vida (Antarctica): Implication for the in situ analysis of Mars sediments. *Journal of Geophysical Research: Planets*, 121(7), 1190-1203.

Kieffer, H. H., Chase Jr, S. C., Miner, E. D., Palluconi, F. D., Münch, G., Neugebauer, G., & Martin, T. Z. (1976). Infrared thermal mapping of the Martian surface and atmosphere: First results. *Science*, *193*(4255), 780-786.

Klein, H. P. (1978). The Viking biological experiments on Mars. *Icarus*, *34*(3), 666-674.

Kminek, G., & Bada, J. L. (2006). The effect of ionizing radiation on the preservation of amino acids on Mars. *Earth and Planetary Science Letters*, *245*(1-2), 1-5.

Kogej, T., Gorbushina, A. A., & Gunde-Cimerman, N. (2006). Hypersaline conditions induce changes in cell-wall melanization and colony structure in a halophilic and a xerophilic black yeast species of the genus Trimmatostroma. *Mycological research*, *110*(6), 713-724.

Kogej, T., Stein, M., Volkmann, M., Gorbushina, A. A., Galinski, E. A., & Gunde-Cimerman, N. (2007). Osmotic adaptation of the halophilic fungus *Hortaea werneckii*: role of osmolytes and melanization. Microbiology, 153(12), 4261-4273.

Kolb, V. M. (Ed.). (2018). *Handbook of Astrobiology*. CRC Press.

Korablev, O., Ivanov, A., Fedorova, A., Kalinnikov, Y. K., Shapkin, A., Mantsevich, S., ... & Kiselev, A. V. (2015, September). Development of a mast or robotic arm-mounted infrared AOTF

spectrometer for surface Moon and Mars probes. In *Infrared Remote Sensing and Instrumentation XXIII* (Vol. 9608, pp. 45-54). SPIE.

Korablev, O. I., Dobrolensky, Y., Evdokimova, N., Fedorova, A. A., Kuzmin, R. O., Mantsevich, S. N., ... & Ivanov, A. Y. (2017). Infrared spectrometer for ExoMars: a mast-mounted instrument for the rover. *Astrobiology*, *17*(6-7), 542-564.

Kosa, G., Kohler, A., Tafintseva, V., Zimmermann, B., Forfang, K., Afseth, N. K., Tzimorotas, D., Vuoristo, K. S., Horn, S. J., Mounier, J., & Shapaval, V. (2017). Microtiter plate cultivation of oleaginous fungi and monitoring of lipogenesis by high-throughput FTIR spectroscopy. *Microbial cell factories*, *16*(1), 1-12.

Kounaves, S. P., Hecht, M. H., Kapit, J., Gospodinova, K., DeFlores, L., Quinn, R. C., ... & Young, S. M. M. (2010). Wet Chemistry experiments on the 2007 Phoenix Mars Scout Lander mission: Data analysis and results. Journal of Geophysical Research: Planets, 115(E1).

Kounaves, S. P., Chaniotakis, N. A., Chevrier, V. F., Carrier, B. L., Folds, K. E., Hansen, V. M., ... & Weber, A. W. (2014). Identification of the perchlorate parent salts at the Phoenix Mars landing site and possible implications. Icarus, 232, 226-231.

Krasnopolsky, V. A., Maillard, J. P., & Owen, T. C. (2004). Detection of methane in the martian atmosphere: evidence for life?. Icarus, 172(2), 537-547.

Krieger, H. (2004) Grundlagen der Strahlenphysik und des Strahlenschutzes. Vieweg+Teubner Verlag, Germany.

Kuhn, W. R., & Atreya, S. K. (1979). Solar radiation incident on the Martian surface. *Journal of Molecular Evolution*, *14*(1-3), 57-64.

Kulikov, Y. N., Lammer, H., Lichtenegger, H. I., Penz, T., Breuer, D., Spohn, T., ... & Biernat, H. K. (2007). A comparative study of the influence of the active young Sun on the early atmospheres of Earth, Venus, and Mars. *Space Science Reviews*, *129*(1), 207-243.

Langseth, M. G., Clark, S. P., Chute, J. L., Keihm, S. J., & Wechsler, A. E. (1972). The Apollo 15 lunar heat-flow measurement. *The Moon*, *4*(3), 390-410.

Lasne, J., Noblet, A., Szopa, C., Navarro-González, R., Cabane, M., Poch, O., ... & Coll, P. (2016). Oxidants at the surface of Mars: a review in light of recent exploration results. *Astrobiology*, *16*(12), 977-996.

Laurent, B., Cousins, C. R., Pereira, M. F. C., & Martins, Z. (2019). Effects of UV-organic interaction and Martian conditions on the survivability of organics. *Icarus*, *323*, 33-39.

Laye, V. J., & DasSarma, S. (2018). An Antarctic extreme halophile and its polyextremophilic enzyme: effects of perchlorate salts. Astrobiology, 18(4), 412-418.

Lesage, G., & Bussey, H. (2006). Cell wall assembly in *Saccharomyces cerevisiae*. Microbiology and molecular biology reviews, 70(2), 317-343.

Leuko, S., & Rettberg, P. (2017). The effects of HZE particles, γ and X-ray radiation on the survival and genetic integrity of *Halobacterium salinarum* NRC-1, *Halococcus hamelinensis*, and *Halococcus morrhuae*. *Astrobiology*, *17*(2), 110-117.

Léveillé, R. (2009). Validation of astrobiology technologies and instrument operations in terrestrial analogue environments. *Comptes Rendus Palevol*, *8*(7), 637-648.

Levy, J. (2013). How big are the McMurdo Dry Valleys? Estimating ice-free area using Landsat image data. *Antarctic Science*, *25*(1), 119-120.

Li, X., Danell, R. M., Brinckerhoff, W. B., Pinnick, V. T., van Amerom, F., Arevalo Jr, R. D., ... & Goesmann, F. (2015). Detection of trace organics in Mars analog samples containing perchlorate by laser desorption/ionization mass spectrometry. *Astrobiology*, *15*(2), 104-110.

Liu, Y., Zhou, J., Omelchenko, M. V., Beliaev, A. S., Venkateswaran, A., Stair, J., ... & Daly, M. J. (2003). Transcriptome dynamics of *Deinococcus radiodurans* recovering from ionizing radiation. *Proceedings of the National Academy of Sciences*, *100*(7), 4191-4196.

López Reyes, G. (2015). Development of algorithms and methodological analyses for the definition of the operation mode of the Raman Laser Spectrometer instrument.

Mach, H., Volkin, D. B., Burke, C. J., & Middaugh, C. R. (1995). Ultraviolet absorption spectroscopy. *Protein stability and folding*, 91-114.

Macko, S. A., Engel, M. H., & Parker, P. L. (1993). Early diagenesis of organic matter in sediments. In *Organic geochemistry* (pp. 211-224). Springer, Boston, MA.

Magarelli, M., Passamonti, P., & Renieri, C. (2010). Purification, characterization and analysis of sepia melanin from commercial sepia ink (*Sepia Officinalis*). *Revista CES Medicina Veterinaria y Zootecnia*, *5*(2), 18-28.

Maggiori, C., Stromberg, J., Blanco, Y., Goordial, J., Cloutis, E., García-Villadangos, M., Parro, V., & Whyte, L. (2020). The Limits, Capabilities, and Potential for Life Detection with MinION Sequencing in a Paleochannel Mars Analog. *Astrobiology*, *20*(3), 375-393.

Mahaffy, P. 2008, Exploration of the habitability of mars: Development of analytical protocols for

measurement of organic carbon on the 2009 mars science laboratory. *Space Sci. Rev.*, **135**, 255–268.

Mahaffy, P.R.; Webster, C.R.; Cabane, M.; Conrad, P.G.; Coll, P.; Atreya, S.K.; Brinckerhoff, W.B. The sample analysis at Mars investigation and instrument suite. *Space Sci. Rev.* 2012, 170(1-4), 401-478.

Mahaffy, P. R., Webster, C. R., Atreya, S. K., Franz, H., Wong, M., Conrad, P. G., ... & Gasnault, O. (2013). Abundance and isotopic composition of gases in the Martian atmosphere from the Curiosity rover. *Science*, *341*(6143), 263-266.

Malin, M. C., & Edgett, K. S. (2000). Evidence for recent groundwater seepage and surface runoff on Mars. *Science*, *288*(5475), 2330-2335.

Malin, M. C., & Edgett, K. S. (2003). Evidence for persistent flow and aqueous sedimentation on early Mars. *Science*, *302*(5652), 1931-1934.

Mancinelli, R. L., & Banin, A. (2003). Where is the nitrogen on Mars?. *International Journal of Astrobiology*, *2*(3), 217-225.

Mandal, P., Roy, T. S., Das, T. K., Banerjee, U., Xess, I., & Nosanchuk, J. D. (2007). Differences in the cell wall architecture of melanin lacking and melanin producing *Cryptococcus neoformans* clinical isolates from India: an electron microscopic study. Brazilian Journal of Microbiology, 38, 662-666.

Maquelin, K., Choo-Smith, L. P., Kirschner, C., Ngo-Thi, N. A., Naumann, D., & Puppels, G. J. (2006). Vibrational spectroscopic studies of microorganisms. *Handbook of Vibrational Spectroscopy*.

Marlow, J. (2016). *Physical, metabolic, and energetic investigations of methane-metabolizing microbial communities*. California Institute of Technology.

Marschall, M., Dulai, S., & Kereszturi, A. (2012). Migrating and UV screening subsurface zone on Mars as target for the analysis of photosynthetic life and astrobiology. *Planetary and Space Science*, *72*(1), 146-153.

Martin, P. E., Farley, K. A., Baker, M. B., Malespin, C. A., Schwenzer, S. P., Cohen, B. A., ... & Navarro-González, R. (2017). A two-step K-Ar experiment on Mars: Dating the diagenetic formation of jarosite from Amazonian groundwaters. Journal of Geophysical Research: Planets, 122(12), 2803-2818.

Martins, Z., Alexander, C. O. D., Orzechowska, G. E., Fogel, M. L., & Ehrenfreund, P. (2007). Indigenous amino acids in primitive CR meteorites. *Meteoritics & Planetary Science*, *42*(12), 2125-2136.

Martins, Z. (2011). In situ biomarkers and the Life Marker Chip. *Astronomy & Geophysics*, *52*(1), 1-34.

Martín-Torres, F. J., Zorzano, M. P., Valentín-Serrano, P., Harri, A. M., Genzer, M., Kemppinen, O., ... & Vaniman, D. (2015). Transient liquid water and water activity at Gale crater on Mars. Nature Geoscience, 8(5), 357-361.

Mbonyiryivuze, A., Mwakikunga, B. W., Dhlamini, S. M., & Maaza, M. (2015). Fourier transform infrared spectroscopy for sepia melanin.

McCauley, J. F., Carr, M. H., Cutts, J. A., Hartmann, W. K., Masursky, H., Milton, D. J., ... & Wilhelms, D. E. (1972). Preliminary Mariner 9 report on the geology of Mars. *Icarus*, *17*(2), 289-327.

McCollom, T.M. and Hynek, B.M. 2005, A volcanic environment for bedrock diagenesis at Meridiani Planum on Mars. *Nature*, 438, 1129–1131.

McCollom, T. M. (2006). The habitability of Mars: past and present. In *Solar System Update* (pp. 159-175). Springer, Berlin, Heidelberg.

McCreery, R. L. (2005). *Raman spectroscopy for chemical analysis* (Vol. 225). John Wiley & Sons.

McIntosh, I. M., Nichols, A. R., Tani, K., & Llewellin, E. W. (2017). Accounting for the species-dependence of the 3500 cm^{-1} H_2O infrared molar absorptivity coefficient: Implications for hydrated volcanic glasses. *American Mineralogist: Journal of Earth and Planetary Materials*, *102*(8), 1677-1689.

McKay, C. P., Friedman, E. I., Wharton, R. A., & Davies, W. L. (1992). History of water on Mars: a biological perspective. *Advances in Space Research*, *12*(4), 231-238.

McKay, C.P. What is life—and how do we search for it in other worlds? *PLoS biol.* 2004, 2(9).

Mckay, C. P., Trigo–rodrÝguez, J. M., Ehrenfreund, P., Martin, E. L., Lammer, H., Penz, T., ... & Teodorani, M. (2006). The Distribution of Life in the Universe. In Life as We Know It (pp. 373-503). Springer, Dordrecht.

McMahon, S. 2021, Astrobiology (Overview). In Oxford Research Encyclopedia of Planetary Science.

McMahon, S., O'Malley-James, J., & Parnell, J. (2013). Circumstellar habitable zones for deep terrestrial biospheres. *Planetary and space science*, *85*, 312-318.

McMahon, S., Parnell, J., & Reekie, P. B. R. (2020). Mars-analog calcium sulfate veins record evidence of ancient subsurface life. Astrobiology, 20(10), 1212-1223.

Meeßen, J., Sánchez, F. J., Sadowsky, A., de la Torre, R., Ott, S., & de Vera, J. P. (2013). Extremotolerance and resistance of lichens: comparative studies on five species used in astrobiological research II. Secondary lichen compounds. *Origins of Life and Evolution of Biospheres*, *43*(6), 501-526.

Meeßen, J., Backhaus, T., Brandt, A., Raguse, M., Böttger, U., de Vera, J. P., & de la Torre, R. (2017). The effect of high-dose ionizing radiation on the isolated photobiont of the astrobiological model lichen *Circinaria gyrosa*. *Astrobiology*, *17*(2), 154-162.

Meierhenrich, U. (2008). Minority Report: Life's Chiral Molecules of Opposite Handedness. In *Amino Acids and the Asymmetry of Life* (pp. 47-59). Springer, Berlin, Heidelberg.

Melosh, H. J. (2003). Exchange of meteorites (and life?) between stellar systems. Astrobiology, 3(1), 207-215.

Menges, F. (2019). *Spectragryph - optical spectroscopy software* (version 1.2.14) [Computer software]. Retrieved from http://www.effemm2.de/spectragryph/ (7th February 2020).

Merk, R., & Prialnik, D. (2006). Combined modeling of thermal evolution and accretion of trans-neptunian objects—Occurrence of high temperatures and liquid water. Icarus, 183(2), 283-295.

Messmer, M. W., Dieser, M., Smith, H. J., Parker, A. E., & Foreman, C. M. (2021). Investigation of Raman spectroscopic signatures with multivariate statistics: an approach for cataloguing microbial biosignatures. *Astrobiology*, 22(1), 1-11.

Mewaldt, R. A. (1994). Galactic cosmic ray composition and energy spectra. Advances in Space Research, 14(10), 737-747.

Michalski, J. R., Cuadros, J., Niles, P. B., Parnell, J., Deanne Rogers, A., & Wright, S. P. (2013). Groundwater activity on Mars and implications for a deep biosphere. *Nature Geoscience*, *6*(2), 133-138.

Michalski, J. R., Dobrea, E. Z. N., Niles, P. B., & Cuadros, J. (2017). Ancient hydrothermal seafloor deposits in Eridania basin on Mars. *Nature communications*, *8*(1), 1-10.

Michalski, J. R., Onstott, T. C., Mojzsis, S. J., Mustard, J., Chan, Q. H., Niles, P. B., & Johnson, S. S. (2018). The Martian subsurface as a potential window into the origin of life. *Nature Geoscience*, *11*(1), 21-26.

Millar, C. D., & Lambert, D. M. (2013). Ancient DNA: towards a million-year-old genome. *Nature*, *499*(7456), 34-35.

Ming, D. W., Archer, P. D., Glavin, D. P., Eigenbrode, J. L., Franz, H. B., Sutter, B., ... & Yingst, R. A. (2014). Volatile and organic compositions of sedimentary rocks in Yellowknife Bay, Gale Crater, Mars. *Science*, *343*(6169).

Moeller, R., Reitz, G., Berger, T., Okayasu, R., Nicholson, W. L., & Horneck, G. (2010). Astrobiological aspects of the mutagenesis of cosmic radiation on bacterial spores. *Astrobiology*, *10*(5), 509-521.

Moeller, R., Raguse, M., Leuko, S., Berger, T., Hellweg, C. E., Fujimori, A., ... & STARLIFE Research Group. (2017). STARLIFE—An international campaign to study the role of galactic cosmic radiation in astrobiological model systems. *Astrobiology*, *17*(2), 101-109.

Möhlmann, D., & Thomsen, K. (2011). Properties of cryobrines on Mars. *Icarus*, *212*(1), 123-130.

Mojarro, A., Ruvkun, G., Zuber, M. T., & Carr, C. E. (2017). Nucleic acid extraction from synthetic Mars analog soils for in situ life detection. *Astrobiology*, *17*(8), 747-760.

Moldoveanu, S.C. Pyrolysis of carboxylic acids. *Tech. Instrum. Anal. Chem.* 2010, 28, 471-526.

Monti, F., Dell'Anna, R., Sanson, A., Fasoli, M., Pezzotti, M., & Zenoni, S. (2013). A multivariate statistical analysis approach to highlight molecular processes in plant cell walls through ATR FT-IR microspectroscopy: The role of the α-expansin PhEXPA1 in *Petunia hybrida*. *Vibrational Spectroscopy*, *65*, 36-43.

Morris, R. V., Klingelhoefer, G., Schröder, C., Rodionov, D. S., Yen, A., Ming, D. W., ... & Arvidson, R. E. (2006). Mössbauer mineralogy of rock, soil, and dust at Meridiani Planum, Mars: Opportunity's journey across sulfate-rich outcrop, basaltic sand and dust, and hematite lag deposits. *Journal of Geophysical Research: Planets*, *111*(E12).

Morris, R.V., Ruff, S.W., Gellert, R., Ming, D.W., Arvidson, R.E, Clark, B.C., Fleischer, I. 2010, Identification of carbonate-rich outcrops on Mars by the spirit rover. *Science,* 329, 421–424.

Movasaghi, Z., Rehman, S., & Rehman, I. U. (2007). Raman spectroscopy of biological tissues. *Applied Spectroscopy Reviews*, *42*(5), 493-541.

Movasaghi, Z., Rehman, S., & Rehman, D. I. (2008). Fourier transform infrared (FTIR) spectroscopy of biological tissues. *Applied Spectroscopy Reviews*, *43*(2), 134-179.

Muirhead, B. K., Nicholas, A. K., Umland, J., Sutherland, O., & Vijendran, S. (2020). Mars sample return campaign concept status. *Acta Astronautica*, *176*, 131-138.

Mumma, M. J., DiSanti, M. A., Russo, N. D., Magee-Sauer, K., Gibb, E., & Novak, R. (2003). Remote infrared observations of parent volatiles in comets: A window on the early solar system. *Advances in Space Research*, *31*(12), 2563-2575.

Musilova, M., Wright, G., Ward, J. M., & Dartnell, L. R. (2015). Isolation of radiation-resistant bacteria from Mars analog Antarctic Dry Valleys by preselection, and the correlation between radiation and desiccation resistance. *Astrobiology*, *15*(12), 1076-1090.

Mustard, J.F.; Ehlmann, B.L.; Murchie, S.L.; Poulet, F.; Mangold, N.; Head, J.W.; Roach, L.H. Composition, morphology, and stratigraphy of Noachian crust around the Isidis basin. *J. Geophys. Res. Planets* 2009, 114(E2).

Mustard, J.F.; Adler, M.; Allwood, A.; Bass, D.S.; Beaty, D.W.; Bell, J.F.; Edgett, K.S. Report of the Mars 2020 science definition team. *Mars Explor. Progr. Anal. Gr*. 2013, 150, 155-205.

Nagler, K., & Moeller, R. (2015). Systematic investigation of germination responses of Bacillus subtilis spores in different high-salinity environments. FEMS Microbiology Ecology, 91(5), fiv023.

Nakajima, S., Hayashi, Y. Y., & Abe, Y. (1992). A study on the "runaway greenhouse effect" with a one-dimensional radiative–convective equilibrium model. *Journal of Atmospheric Sciences*, *49*(23), 2256-2266.

Nakamura, T., Takagi, H., & Shima, J. (2009). Effects of ice-seeding temperature and intracellular trehalose contents on survival of frozen Saccharomyces cerevisiae cells. *Cryobiology*, *58*(2), 170-174.

Naraoka, H., Shimoyama, A. and Harada, K. 1999, Molecular distribution of monocarboxylic acids in Asuka carbonaceous chondrites from Antarctica. *Orig. Life Evol. Biosph.*, **29**, 187–201.

Nazari-Sharabian, M., Aghababaei, M., Karakouzian, M., & Karami, M. (2020). Water on Mars—a literature review. Galaxies, 8(2), 40.

Nerenberg, R. (2013). Breathing perchlorate. science, 340(6128), 38-39.

Neveu, M.; Hays, L.E.; Voytek, M.A.; New, M.H.; Schulte, M.D. The ladder of life detection. *Astrobiology* 2018, 18(11), 1375-1402.

Nienow, J. A., McKay, C. P., & Friedmann, E. I. (1988). The cryptoendolithic microbial environment in the Ross Desert of Antarctica: light in the photosynthetically active region. *Microbial ecology*, *16*(3), 271-289.

Noack, L., Höning, D., Lammer, H., & Bredehöft, J. H. (2014, April). Exotic water worlds: how life-friendly is a deep ocean?. In *European Planetary Science Congress* (Vol. 9, pp. EPSC2014-514).

Novotný, O., Cejpek, K. and Velíšek, J. 2008, Formation of Carboxylic Acids during Degradation of Monosaccharides. *Czech J. Food Sci.*, 26, 117–131.

Nuding, D. L., Rivera-Valentin, E. G., Davis, R. D., Gough, R. V., Chevrier, V. F., & Tolbert, M. A. (2014). Deliquescence and efflorescence of calcium perchlorate: An investigation of stable aqueous solutions relevant to Mars. *Icarus*, *243*, 420-428.

Nylen, T. H., Fountain, A. G., & Doran, P. T. (2004). Climatology of katabatic winds in the McMurdo dry valleys, southern Victoria Land, Antarctica. *Journal of Geophysical Research: Atmospheres*, *109*(D3).

OCAMPO-FRIEDMANN, R. O. S. E. L. I., & FRIEDMANN, E. I. (1993). Biologically active substances produced by antarctic cryptoendolithic fungi. *Group*, *459*(F9), A801147.

Okayasu, R., Okada, M., Okabe, A., Noguchi, M., Takakura, K., & Takahashi, S. (2006). Repair of DNA damage induced by accelerated heavy ions in mammalian cells proficient and deficient in the non-homologous end-joining pathway. *Radiation research*, *165*(1), 59-67.

Okland, I., Huang, S., Dahle, H., Thorseth, I. H., & Pedersen, R. B. (2012). Low temperature alteration of serpentinized ultramafic rock and implications for microbial life. *Chemical Geology*, *318*, 75-87.

Onofri, S. (1999). Antarctic microfungi. In *Enigmatic microorganisms and life in extreme environments* (pp. 323-336). Springer, Dordrecht.

Onofri, S.; Selbmann, L.; Zucconi, L.; Pagano, S. Antarctic microfungi as models for exobiology. *Planet. Space Sci. 2004*, 52(1-3), 229-237.

Onofri, S., Selbmann, L., De Hoog, G. S., Grube, M., Barreca, D., Ruisi, S., & Zucconi, L. (2007). Evolution and adaptation of fungi at boundaries of life. *Advances in Space Research*, *40*(11), 1657-1664.

Onofri, S., de la Torre, R., de Vera, J. P., Ott, S., Zucconi, L., Selbmann, L., ... & Horneck, G. (2012). Survival of rock-colonizing organisms after 1.5 years in outer space. *Astrobiology*, *12*(5), 508-516.

Onofri, S., de Vera, J. P., Zucconi, L., Selbmann, L., Scalzi, G., Venkateswaran, K. J., ... & Horneck, G. (2015). Survival of Antarctic cryptoendolithic fungi in simulated Martian conditions on board the International Space Station. *Astrobiology*, *15*(12), 1052-1059.

Onofri, S., Selbmann, L., Pacelli, C., Zucconi, L., Rabbow, E., & de Vera, J. P. (2019). Survival, DNA, and ultrastructural integrity of a cryptoendolithic Antarctic fungus in Mars and Lunar rock analogs exposed outside the International Space Station. *Astrobiology*, *19*(2), 170-182.

Onofri, S., Balucani, N., Barone, V., Benedetti, P., Billi, D., Balbi, A., ... & OPPS Project Team. (2020). The Italian National Project of Astrobiology—Life in Space—Origin, Presence, Persistence of Life in Space, from Molecules to Extremophiles.

Osinski, G. R., Tornabene, L. L., Banerjee, N. R., Cockell, C. S., Flemming, R., Izawa, M. R., ... & Southam, G. (2013). Impact-generated hydrothermal systems on Earth and Mars. Icarus, 224(2), 347-363.

Orosei, R., Ding, C., Fa, W., Giannopoulos, A., Hérique, A., Kofman, W., ... & Xu, Y. (2020). The global search for liquid water on Mars from orbit: Current and future perspectives. *Life*, *10*(8), 120.

Orosei, R., Lauro, S. E., Pettinelli, E., Cicchetti, A. N. D. R. E. A., Coradini, M., Cosciotti, B., ... & Seu, R. (2018). Radar evidence of subglacial liquid water on Mars. *Science*, *361*(6401), 490-493.

Orsini, F., Ami, D., Villa, A. M., Sala, G., Bellotti, M. G., & Doglia, S. M. (2000). FT-IR microspectroscopy for microbiological studies. *Journal of microbiological methods*, *42*(1), 17-27.

Øvstedal, D. O., & Smith, R. L. (2001). *Lichens of Antarctica and South Georgia: a guide to their identification and ecology*. Cambridge University Press.

Owen, T., Biemann, K., Rushneck, D. R., Biller, J. E., Howarth, D. W., & Lafleur, A. L. (1977). The composition of the atmosphere at the surface of Mars. *Journal of Geophysical research*, *82*(28), 4635-4639.

Pacelli, C., Selbmann, L., Zucconi, L., Raguse, M., Moeller, R., Shuryak, I., & Onofri, S. (2017a). Survival, DNA integrity, and ultrastructural damage in Antarctic cryptoendolithic eukaryotic microorganisms exposed to ionizing radiation. *Astrobiology*, *17*(2), 126-135.

Pacelli, C., Selbmann, L., Moeller, R., Zucconi, L., Fujimori, A., & Onofri, S. (2017b). Cryptoendolithic Antarctic black fungus *Cryomyces antarcticus* irradiated with accelerated helium ions: survival and metabolic activity, DNA and ultrastructural damage. *Frontiers in Microbiology*, *8*, 2002.

Pacelli, C., Bryan, R. A., Onofri, S., Selbmann, L., Zucconi, L., Shuryak, I., & Dadachova, E. (2018). The effect of protracted X-ray exposure on cell survival and metabolic activity of fast and slow growing fungi capable of melanogenesis. *Environmental microbiology reports*, *10*(3), 255-263.

Pacelli, C., Selbmann, L., Zucconi, L., Coleine, C., de Vera, J. P., Rabbow, E., ... & Onofri, S. (2019). Responses of the Black Fungus *Cryomyces antarcticus* to simulated mars and space conditions on rock analogs. *Astrobiology*, *19*(2), 209-220.

Pacelli, C., Cassaro, A., Aureli, L., Moeller, R., Fujimori, A., & Onofri, S. (2020a). The responses of the black fungus *Cryomyces antarcticus* to high doses of accelerated helium ions radiation within martian regolith simulants and their relevance for Mars. *Life*, *10*(8), 130.

Pacelli, C., Cassaro, A., Maturilli, A., Timperio, A. M., Gevi, F., Cavalazzi, B., Stefan, M., Ghica, D., & Onofri, S. (2020b). Multidisciplinary characterization of melanin pigments from the black fungus *Cryomyces antarcticus*. *Applied Microbiology and Biotechnology*, *104*, 6385–6395.

Pacelli, C., Alessia, C., Siong, L. M., Lorenzo, A., Moeller, R., Fujimori, A., ... & Silvano, O. (2021a). Insights into the Survival Capabilities of *Cryomyces antarcticus* Hydrated Colonies after Exposure to Fe Particle Radiation. *Journal of Fungi*, *7*(7), 495.

Pacelli, C., Cassaro, A., Catanzaro, I., Baqué, M., Maturilli, A., Böttger, U., ... & Onofri, S. (2021b). The Ground-Based BIOMEX Experiment Verification Tests for Life Detection on Mars. *Life*, *11*(11), 1212.

Pacelli, C., Cassaro, A., Baqué, M., Selbmann, L., Zucconi, L., Maturilli, A., ... & Onofri, S. (2021c). Fungal biomarkers are detectable in Martian rock-analogues after space exposure: Implications for the search of life on Mars. *International Journal of Astrobiology*, *20*(5), 345-358.

Paim, S., Linhares, L. F., Mangrich, A. S., & Martin, J. P. (1990). Characterization of fungal melanins and soil humic acids by chemical analysis and infrared spectroscopy. *Biology and Fertility of Soils*, *10*(1), 72-76.

Pal, A. K., Gajjar, D. U., & Vasavada, A. R. (2013). DOPA and DHN pathway orchestrate melanin synthesis in Aspergillus species. *Medical mycology*, *52*(1), 10-18.

Pál, B., Kereszturi, Á., Forget, F., & Smith, M. D. (2019). Global seasonal variations of the near-surface relative humidity levels on present-day Mars. *Icarus*, *333*, 481-495.

Palerme, C., Kay, J. E., Genthon, C., L'Ecuyer, T., Wood, N. B., & Claud, C. (2014). How much snow falls on the Antarctic ice sheet?. *The Cryosphere*, *8*(4), 1577-1587.

Panieri, G., Lugli, S., Manzi, V., Roveri, M., Schreiber, B. C., & Palinska, K. A. (2010). Ribosomal RNA gene fragments from fossilized cyanobacteria identified in primary gypsum from the late Miocene, Italy. *Geobiology*, *8*(2), 101-111.

Parnell, J., Cullen, D., Sims, M. R., Bowden, S., Cockell, C. S., Court, R., ... & Vago, J. (2007). Searching for life on Mars: selection of molecular targets for ESA's Aurora ExoMars mission. *Astrobiology*, *7*(4), 578-604.

Pasek, M. A., Dworkin, J. P., & Lauretta, D. S. (2007). A radical pathway for organic phosphorylation during schreibersite corrosion with implications for the origin of life. *Geochimica et Cosmochimica Acta*, *71*(7), 1721-1736.

Patel, M. R., Zarnecki, J. C., & Catling, D. C. (2002). Ultraviolet radiation on the surface of Mars and the Beagle 2 UV sensor. Planetary and Space Science, 50(9), 915-927.

Pavlov, A. K., Shelegedin, V. N., Vdovina, M. A., & Pavlov, A. A. (2010). Growth of microorganisms in martian-like shallow subsurface conditions: laboratory modelling. *International Journal of Astrobiology*, *9*(1), 51-58.

Pavlov, A. A., Vasilyev, G., Ostryakov, V. M., Pavlov, A. K., & Mahaffy, P. (2012). Degradation of the organic molecules in the shallow subsurface of Mars due to irradiation by cosmic rays. *Geophysical research letters*, *39*(13).

Pepe-Ranney, C., Berelson, W. M., Corsetti, F. A., Treants, M., & Spear, J. R. (2012). Cyanobacterial construction of hot spring siliceous stromatolites in Yellowstone National Park. *Environmental Microbiology*, *14*(5), 1182-1197.

Pessoni, R. A., Freshour, G., Figueiredo-Ribeiro, R. D. C. L., Hahn, M. G., & Braga, M. R. (2005). Cell-wall structure and composition of Penicillium janczewskii as affected by inulin. Mycologia, 97(2), 304-311.

Peters, K. E., Walters, C. C., & Moldowan, J. M. (2004). The biomarker guide: II. Biomarkers and isotopes in petroleum systems and earth history. Cambridge University Press.

Pilorget, C., & Bibring, J. P. (2013). NIR reflectance hyperspectral microscopy for planetary science: Application to the MicrOmega instrument. *Planetary and Space Science*, *76*, 42-52.

Pimblott, S. M., & LaVerne, J. A. (1994). Diffusion-kinetic theories for LET effects on the radiolysis of water. *The Journal of Physical Chemistry*, *98*(24), 6136-6143.

Pinkert, S. and Zeuss, D. 2018, Thermal Biology: Melanin-Based Energy Harvesting across the Tree of Life. *Curr. Biol.,* **28**, R887–R889.

Plaut, J. J., Picardi, G., Safaeinili, A., Ivanov, A. B., Milkovich, S. M., Cicchetti, A., ... & Edenhofer, P. (2007). Subsurface radar sounding of the south polar layered deposits of Mars. *science*, *316*(5821), 92-95.

Poch, O., Noblet, A., Stalport, F., Correia, J. J., Grand, N., Szopa, C., & Coll, P. (2013). Chemical evolution of organic molecules under Mars-like UV radiation conditions simulated in the laboratory with the "Mars organic molecule irradiation and evolution" (MOMIE) setup. *Planetary and Space Science*, *85*, 188-197.

Poch, O., Kaci, S., Stalport, F., Szopa, C., & Coll, P. (2014). Laboratory insights into the chemical and kinetic evolution of several organic molecules under simulated Mars surface UV radiation conditions. *Icarus*, *242*, 50-63.

Pointing, S. B., & Belnap, J. (2012). Microbial colonization and controls in dryland systems. *Nature Reviews Microbiology*, *10*(8), 551-562.

Pollack, J. B., Colburn, D. S., Flasar, F. M., Kahn, R., Carlston, C. E., & Pidek, D. (1979). Properties and effects of dust particles suspended in the Martian atmosphere. Journal of Geophysical Research: Solid Earth, 84(B6), 2929-2945.

Pontefract, A., Hachey, J., Zuber, M. T., Ruvkun, G., & Carr, C. E. (2018). Sequencing nothing: exploring failure modes of nanopore sensing and implications for life detection. *Life sciences in space research*, *18*, 80-86.

Ponti, M., Souhami, R. L., Fox, B. W., & Hartley, J. A. (1991). DNA interstrand crosslinking and sequence selectivity of dimethanesulphonates. *British journal of cancer*, *63*(5), 743-747.

Potts, M. (1994). Desiccation tolerance of prokaryotes. Microbiological reviews, 58(4), 755-805.

Pouget, J. P., & Mather, S. J. (2001). General aspects of the cellular response to low-and high-LET radiation. European journal of nuclear medicine, 28(4), 541-561.

Poulet, F., Bibring, J. P., Mustard, J. F., Gendrin, A., Mangold, N., Langevin, Y., ... & Gomez, C. (2005). Phyllosilicates on Mars and implications for early Martian climate. *Nature*, *438*(7068), 623-627.

Preston, L. J., & Dartnell, L. R. (2014). Planetary habitability: lessons learned from terrestrial analogues. *International Journal of Astrobiology*, *13*(1), 81-98.

Preston, L. J., Johnson, D., Cockell, C. S., & Grady, M. M. (2015). Fourier transform infrared spectral detection of life in polar subsurface environments and its application to Mars exploration. *Applied spectroscopy*, *69*(9), 1059-1065.

Preston, L. J., Barcenilla, R., Dartnell, L. R., Kucukkilic-Stephens, E., & Olsson-Francis, K. (2020). Infrared spectroscopic detection of biosignatures at Lake Tírez, Spain: implications for Mars. *Astrobiology*, *20*(1), 15-25.

Price, J. R., Velbel, M. A., & Patino, L. C. (2005). Rates and time scales of clay-mineral formation by weathering in saprolitic regoliths of the southern Appalachians from geochemical mass balance. GSA Bulletin, 117(5-6), 783-794.

Primm, K. M., Gough, R. V., Wong, J., Rivera-Valentin, E. G., Martinez, G. M., Hogancamp, J. V., ... & Tolbert, M. A. (2018). The effect of Mars-relevant soil analogs on the water uptake of magnesium perchlorate and implications for the near-surface of Mars. Journal of Geophysical Research: Planets, 123(8), 2076-2088.

Quinn, R. C., Martucci, H. F., Miller, S. R., Bryson, C. E., Grunthaner, F. J., & Grunthaner, P. J. (2013). Perchlorate radiolysis on Mars and the origin of martian soil reactivity. *Astrobiology*, *13*(6), 515-520.

R Core Team. (2018). *R: a language and environment for statistical computing* (version 3.5.2) [Computer software]. Retrieved from http://www.R-project.org/ (8th August 2019).

Rabbow, E.; Rettberg, P.; Barczyk, S.; Bohmeier, M.; Parpart, A.; Panitz, C.; Baglioni, P. EXPOSE-E: an ESA astrobiology mission 1.5 years in space. *Astrobiology* 2012, 12(5), 374-386.

Rabbow, E.; Rettberg, P.; Barczyk, S.; Bohmeier, M.; Parpart, A.; Panitz, C.; Pereira, C. The astrobiological mission EXPOSE-R on board of the International Space Station. *Int. J. Astrobiology* 2015, 14(1), 3-16.

Rabbow, E., Rettberg, P., Parpart, A., Panitz, C., Schulte, W., Molter, F., ... & Willnecker, R. (2017). EXPOSE-R2: the astrobiological ESA mission on board of the International Space Station. *Frontiers in Microbiology*, *8*, 1533.

Rai, Y., Pathak, R., Kumari, N., Sah, D. K., Pandey, S., Kalra, N., ... & Bhatt, A. N. (2018). Mitochondrial biogenesis and metabolic hyperactivation limits the application of MTT assay in the estimation of radiation induced growth inhibition. Scientific reports, 8(1), 1-15.

Raman, N. M., & Ramasamy, S. (2017). Genetic validation and spectroscopic detailing of DHN-melanin extracted from an environmental fungus. *Biochemistry and biophysics reports*, *12*, 98-107.

Ramirez, R. M., & Craddock, R. A. (2018). The geological and climatological case for a warmer and wetter early Mars. *Nature Geoscience*, *11*(4), 230-237.

Rasmussen, B., Blake, T. S., Fletcher, I. R., & Kilburn, M. R. (2009). Evidence for microbial life in synsedimentary cavities from 2.75 Ga terrestrial environments. *Geology*, *37*(5), 423-426.

Reinhardt, M.; Goetz, W.; Thiel, V. Testing Flight-Like Pyrolysis Gas Chromatography–Mass Spectrometry as Performed by the Mars Organic Molecule Analyzer Onboard the ExoMars 2020 Rover on Oxia Planum Analog Samples. *Astrobiology* 2020.

Rieder, R., Gellert, R., Anderson, R. C., Bruckner, J., Clark, B. C., Dreibus, G., ... & Zipfel, J. (2004). Chemistry of rocks and soils at Meridiani Planum from the Alpha Particle X-ray Spectrometer. *Science*, *306*(5702), 1746-1749.

Rinaudo, C., Cairo, S., Gastaldi, D., Gianfagna, A., Tagliani, S. M., Tosi, G., & Conti, C. (2006). Characterization of fluoro-edenite by μ-Raman and μ-FTIR spectroscopy. *Mineralogical Magazine*, *70*(3), 291-298.

Rinaudo, M. (2006). Chitin and chitosan: Properties and applications. *Progress in polymer science*, *31*(7), 603-632.

Robinson, S. A., Wasley, J., & Tobin, A. K. (2003). Living on the edge–plants and global change in continental and maritime Antarctica. *Global Change Biology*, *9*(12), 1681-1717.

Rontó, G., Bérces, A., Lammer, H., Cockell, C. S., Molina-Cuberos, G. J., Patel, M. R., & Selsis, F. (2003). Solar UV Irradiation Conditions on the Surface of Mars¶. Photochemistry and photobiology, 77(1), 34-40.

Rosas, Á.L., Nosanchuk, J.D., Gómez, B.L., Edens, W.A., Henson, J.M., Casadevall, A. (2000), Isolation and serological analyses of fungal melanins. *J. Immunol. Methods*, **244**, 69–80.

Rösch, P., Harz, M., Peschke, K. D., Ronneberger, O., Burkhardt, H., & Popp, J. (2006). Identification of single eukaryotic cells with micro-Raman spectroscopy. *Biopolymers: Original Research on Biomolecules*, *82*(4), 312-316.

Rothschild, L. J., & Cockell, C. S. (1999). Radiation: microbial evolution, ecology, and relevance to Mars missions. Mutation Research/Fundamental and Molecular Mechanisms of Mutagenesis, 430(2), 281-291.

RStudio Team. (2016). *RStudio: Integrated Development for R* (version 1.1.423) [Computer software]. Retrieved from http://www.rstudio.org/ (8th August 2019).

Ruibal, C., Gueidan, C., Selbmann, L., Gorbushina, A. A., Crous, P. W., Groenewald, J. Z., ... & De Hoog, G. S. (2008). Phylogeny of rock-inhabiting fungi related to Dothideomycetes. *Studies in Mycology*, *61*(1), 131-136.

Ruibal, C., Platas, G., & Bills, G. F. (2005). Isolation and characterization of melanized fungi from limestone formations in Mallorca. *Mycological Progress*, *4*(1), 23-38.

Ruisi, S., Barreca, D., Selbmann, L., Zucconi, L., & Onofri, S. (2007). fungi in Antarctica. *Reviews in Environmental Science and Bio/Technology*, *6*(1), 127-141.

Rull, F., Maurice, S., Hutchinson, I., Moral, A., Perez, C., Diaz, C., ... & Vago, J. L. (2017). The Raman laser spectrometer for the ExoMars rover mission to Mars. *Astrobiology*, *17*(6-7), 627-654.

Rummel, J. D., Beaty, D. W., Jones, M. A., Bakermans, C., Barlow, N. G., Boston, P. J., ... & Wray, J. J. (2014). A new analysis of Mars "special regions": findings of the second MEPAG Special Regions Science Analysis Group (SR-SAG2).

Safar, M., Bertrand, D., Robert, P., Devaux, M. F., & Genot, C. (1994). Characterization of edible oils, butters and margarines by Fourier transform infrared spectroscopy with attenuated total reflectance. *J Am Oil Chem Soc*, *71*(4), 371-377.

Saif, F. A., Yaseen, S. A., Alameen, A. S., Mane, S. B., & Undre, P. B. (2020). Identification and characterization of Aspergillus species of fruit rot fungi using microscopy, FT-IR, Raman and UV–Vis spectroscopy. *Spectrochimica Acta Part A: Molecular and Biomolecular Spectroscopy*, *246*, 119010.

Sajjan, S.S., Anjaneya, O., Guruprasad, B.K., Anand, S.N., Suresh, B.M., & Karegoudar, T.B. (2013). Properties and functions of melanin pigment from Klebsiella sp. GSK. Journal of Microbiology and Biotechnology, 41(1), 60-69.

Salman, A., Shufan, E., Tsror, L., Moreh, R., Mordechai, S., & Huleihel, M. (2014). Classification of *Colletotrichum coccodes* isolates into vegetative compatibility groups using infrared attenuated total reflectance spectroscopy and multivariate analysis. *Methods*, *68*(2), 325-330.

Samokhvalov, A., Liu, Y., & Simon, J. D. (2004). Characterization of the Fe (III)-binding Site in Sepia Eumelanin by Resonance Raman Confocal Microspectroscopy. *Photochemistry and photobiology*, *80*(1), 84-88.

Scalzi, G., Selbmann, L., Zucconi, L., Rabbow, E., Horneck, G., Albertano, P., & Onofri, S. (2012). LIFE experiment: isolation of cryptoendolithic organisms from Antarctic colonized sandstone exposed to space and simulated Mars conditions on the International Space Station. *Origins of Life and Evolution of Biospheres*, *42*(2), 253-262.

Scappini, F., Casadei, F., Zamboni, R., Franchi, M., Gallori, E., & Monti, S. (2004). Protective effect of clay minerals on adsorbed nucleic acid against UV radiation: possible role in the origin of life. *International Journal of Astrobiology*, *3*(1), 17-19.

Schmitt, J., & Flemming, H. C. (1998). FTIR-spectroscopy in microbial and material analysis. *International Biodeterioration & Biodegradation*, *41*(1), 1-11.

Schopf, J. W., Farmer, J. D., Foster, I. S., Kudryavtsev, A. B., Gallardo, V. A., & Espinoza, C. (2012). Gypsum-permineralized microfossils and their relevance to the search for life on Mars. *Astrobiology*, *12*(7), 619-633.

Schuerger, A. C., Mancinelli, R. L., Kern, R. G., Rothschild, L. J., & McKay, C. P. (2003). Survival of endospores of Bacillus subtilis on spacecraft surfaces under simulated martian environments: implications for the forward contamination of Mars. *Icarus*, *165*(2), 253-276.

Schuerger, A. C. (2004). Microbial ecology of the surface exploration of Mars with human-operated vehicles (AAS 03-322). *Martian Expedition Planning*, *107*, 363.

Schuerger, A. C., Moores, J. E., Smith, D. J., & Reitz, G. (2019). A lunar microbial survival model for predicting the forward contamination of the Moon. *Astrobiology*.

Schultzhaus, Z., Chen, A., Kim, S., Shuryak, I., Chang, M., & Wang, Z. (2019). Transcriptomic analysis reveals the relationship of melanization to growth and resistance to gamma radiation in *Cryptococcus neoformans*. *Environmental microbiology*, *21*(8), 2613-2628.

Schultzhaus, Z., Chen, A., Shuryak, I., & Wang, Z. (2021). The transcriptomic and phenotypic response of the melanized yeast Exophiala dermatitidis to ionizing particle exposure. Frontiers in microbiology, 3442.

Schulz, H., & Baranska, M. (2007). Identification and quantification of valuable plant substances by IR and Raman spectroscopy. *Vibrational Spectroscopy*, *43*(1), 13-25.

Schulze-Makuch, D., & Irwin, L. N. (2006). The prospect of alien life in exotic forms on other worlds. *Naturwissenschaften*, *93*(4), 155-172.

Schwieterman, E. W., Cockell, C. S., & Meadows, V. S. (2015). Nonphotosynthetic pigments as potential biosignatures. *Astrobiology*, *15*(5), 341-361.

Segura, A., & Navarro-González, R. (2005). Nitrogen fixation on early Mars by volcanic lightning and other sources. *Geophysical research letters*, *32*(5).

Selbmann, L., De Hoog, G. S., Mazzaglia, A., Friedmann, E. I., & Onofri, S. (2005). Fungi at the edge of life: cryptoendolithic black fungi from Antarctic desert. *Stud Mycol*, *51*(1), 1-32.

Selbmann, L., Isola, D., Zucconi, L., & Onofri, S. (2011). Resistance to UV-B induced DNA damage in extreme-tolerant cryptoendolithic Antarctic fungi: detection by PCR assays. *Fungal Biology*, *115*(10), 937-944.

Selbmann, L., Zucconi, L., Isola, D., & Onofri, S. (2015). Rock black fungi: excellence in the extremes, from the Antarctic to space. *Current Genetics*, *61*(3), 335-345.

Selbmann, L., Onofri, S., Coleine, C., Buzzini, P., Canini, F., & Zucconi, L. (2017). Effect of environmental parameters on biodiversity of the fungal component in lithic Antarctic communities. *Extremophiles*, *21*(6), 1069-1080.

Sephton, M. A. (2002). Organic compounds in carbonaceous meteorites. *Natural product reports*, *19*(3), 292-311.

Sert, H. B., Sümbül, H., & Sterflinger, K. (2007). Microcolonial fungi from antique marbles in Perge/side/Termessos (Antalya/Turkey). *Antonie Van Leeuwenhoek*, *91*(3), 217-227.

Sephton, M. A. (2010). Organic geochemistry and the exploration of Mars. Journal of Cosmology, 5, 1141-1149.

Shunk, G. K., Gomez, X. R., & Averesch, N. J. (2020). A Self-Replicating Radiation-Shield for Human Deep-Space Exploration: Radiotrophic Fungi can Attenuate Ionizing Radiation aboard the International Space Station. *BioRxiv*.

Shurvell, H.F. (2006). Spectra–structure correlations in the mid-and far-infrared. *Handbook of vibrational spectroscopy* (pp. 1-34). John Wiley & Sons.

Sibirny, A. A. (Ed.). (2017). *Biotechnology of yeasts and filamentous fungi*. Springer.

Simoneit, B. R., Summons, R. E., & Jahnke, L. L. (1998). Biomarkers as tracers for life on early Earth and Mars. *Origins of Life and Evolution of the Biosphere*, *28*(4), 475-483.

Singh, H., Anurag, K., & Apte, S. K. (2013). High radiation and desiccation tolerance of nitrogen-fixing cultures of the cyanobacterium Anabaena sp. strain PCC 7120 emanates from genome/proteome repair capabilities. Photosynthesis research, 118(1), 71-81.

Singaravelan, N., Grishkan, I., Beharav, A., Wakamatsu, K., Ito, S., & Nevo, E. (2008). Adaptive melanin response of the soil fungus *Aspergillus niger* to UV radiation stress at "Evolution Canyon", Mount Carmel, Israel. *PloS one*, *3*(8), e2993.

Sliney, D. H. (2007). Radiometric quantities and units used in photobiology and photochemistry: recommendations of the Commission Internationale de l'Eclairage (International Commission on Illumination). *Photochemistry and photobiology*, *83*(2), 425-432.

Smith, H.G. (1992). Distribution and ecology of the testate rhizopod fauna of the continental Antarctic zone. *Polar Biology*, *12*(6-7), 629-634.

Smith, H.G. (1996). Diversity of Antarctic terrestrial protozoa. *Biodiversity & Conservation*, *5*(11), 1379-1394.

Smits, G. J., van den Ende, H., & Klis, F. M. (2001). Differential regulation of cell wall biogenesis during growth and development in yeast. Microbiology, 147(4), 781-794.

Soppa, J. (2013). Evolutionary advantages of polyploidy in halophilic archaea.

Squyres, S. W., Arvidson, R. E., Bell Iii, J. F., Bruckner, J., Cabrol, N. A., Calvin, W., ... & Yen, A. (2004). The opportunity rover's athena science investigation at meridiani planum, mars. *science*, *306*(5702), 1698-1703.

Stalport, F., Coll, P., Szopa, C., Cottin, H., & Raulin, F. (2009). Investigating the photostability of carboxylic acids exposed to Mars surface ultraviolet radiation conditions. *Astrobiology*, *9*(6), 543-549.

Stamenković, V., Ward, L.M., Mischna, M. and Fischer, W.W. 2018, O_2 solubility in martian near-surface environments and implications for aerobic life. *Nat. Geosci.*, **11**, 905–909.

Stan-Lotter, H., & Fendrihan, S. (2015). Halophilic archaea: life with desiccation, radiation and oligotrophy over geological times. *Life*, *5*(3), 1487-1496.

Stankiewicz, B. A., Briggs, D. E., Evershed, R. P., Flannery, M. B., & Wuttke, M. (1997). Preservation of chitin in 25-million-year-old fossils. *Science*, *276*(5318), 1541-1543.

Steininger, H., Goesmann, F., & Goetz, W. (2012). Influence of magnesium perchlorate on the pyrolysis of organic compounds in Mars analogue soils. *Planetary and Space Science*, *71*(1), 9-17.

Sterflinger, K. (2006). Black yeasts and meristematic fungi: ecology, diversity and identification. In *Biodiversity and ecophysiology of yeasts* (pp. 501-514). Springer, Berlin, Heidelberg.

Sterflinger, K., & Krumbein, W. E. (1995). Multiple stress factors affecting growth of rock-inhabiting black fungi. *Botanica Acta*, *108*(6), 490-496.

Sterflinger, K., De Hoog, G. S., & Haase, G. (1999). Phylogeny and ecology of meristematic ascomycetes. *Studies in mycology*, 5-22.

Stern, J. C., Sutter, B., Freissinet, C., Navarro-González, R., McKay, C. P., Archer, P. D., ... & Mahaffy, P. R. (2015). Evidence for indigenous nitrogen in sedimentary and aeolian deposits from the Curiosity rover investigations at Gale crater, Mars. *Proceedings of the National Academy of Sciences*, *112*(14), 4245-4250.

Stevenson, A., Cray, J. A., Williams, J. P., Santos, R., Sahay, R., Neuenkirchen, N., ... & Hallsworth, J. E. (2015). Is there a common water-activity limit for the three domains of life?. The ISME journal, 9(6), 1333-1351.

Stuart, B. H. (2004). Organic molecules. *Infrared Spectroscopy: Fundamentals and Applications* (pp. 71-93). John Wiley & Sons.

Summers, D. P., & Khare, B. (2007). Nitrogen fixation on early Mars and other terrestrial planets: experimental demonstration of abiotic fixation reactions to nitrite and nitrate. *Astrobiology*, *7*(2), 333-341.

Summons, R. E. (1993). Biogeochemical cycles. In Organic geochemistry (pp. 3-21). Springer, Boston, MA.

Summons, R. E., Albrecht, P., McDonald, G., & Moldowan, J. M. (2008). Molecular biosignatures. In *Strategies of Life Detection* (pp. 133-159). Springer, Boston, MA.

Summons, R. E., Amend, J. P., Bish, D., Buick, R., Cody, G. D., Des Marais, D. J., ... & Sumner, D. Y. (2011). Preservation of martian organic and environmental records: final report of the Mars Biosignature Working Group. *Astrobiology*, *11*(2), 157-181.

Sun, S., Zhang, X., Sun, S., Zhang, L., Shan, S., & Zhu, H. (2016). Production of natural melanin by Auricularia auricula and study on its molecular structure. *Food Chemistry*, *190*, 801-807.

Suryanarayanan, T. S., Ravishankar, J. P., Venkatesan, G., & Murali, T. S. (2004). Characterization of the melanin pigment of a cosmopolitan fungal endophyte. *Mycological research*, *108*(8), 974-978.

Takai, K., Nakamura, K., Toki, T., Tsunogai, U., Miyazaki, M., Miyazaki, J., ... & Horikoshi, K. (2008). Cell proliferation at 122 C and isotopically heavy CH4 production by a hyperthermophilic methanogen under high-pressure cultivation. *Proceedings of the National Academy of Sciences*, *105*(31), 10949-10954.

Terato, H., & Ide, H. (2004). Clustered DNA damage induced by heavy ion particles. *Biological Sciences in Space*, *18*(4), 206-215.

Thiel, C.S., Pletser, V. and Foing, B. 2011, Human crew-related aspects for astrobiology research. *Int. J. Astrobiol.*, **10**, 255–267.

Thomas, R.J.; Hynek, B.M.; Osterloo, M.M.; Kierein-Young, K.S. Widespread exposure of Noachian phyllosilicates in the Margaritifer region of Mars: Implications for paleohydrology and astrobiological detection. *J. Geophys. Res. Planets* 2017, 122(3), 483-500.

Tian, F. (2009). Thermal escape from super Earth atmospheres in the habitable zones of M stars. *The Astrophysical Journal*, *703*(1), 905.

Toner, J. D., & Catling, D. C. (2016). Water activities of NaClO4, Ca (ClO4) 2, and Mg (ClO4) 2 brines from experimental heat capacities: water activity> 0.6 below 200 K. Geochimica et Cosmochimica Acta, 181, 164-174.

Travis, B.J.; Rosenberg, N.D.; Cuzzi, J.N. On the role of widespread subsurface convection in bringing liquid water close to Mars' surface. *J. Geophys. Res. Planets* 2003, 108(E4).

Trevors, J.T. 2003, Possible origin of a membrane in the subsurface of the Earth. *Cell Biol. Int.,* 27, 451–457.

Trumpolt, C. W., Crain, M., Cullison, G. D., Flanagan, S. J., Siegel, L., & Lathrop, S. (2005). Perchlorate: sources, uses, and occurrences in the environment. Remediation Journal: The Journal of Environmental Cleanup Costs, Technologies & Techniques, 16(1), 65-89.

Turk, M., Mejanelle, L., Šentjurc, M., Grimalt, J. O., Gunde-Cimerman, N., & Plemenitaš, A. (2004). Salt-induced changes in lipid composition and membrane fluidity of halophilic yeast-like melanized fungi. Extremophiles, 8(1), 53-61.

Turner, J., Bindschadler, R., Convey, P., Di Prisco, G., Fahrbach, E., Gutt, J., ... & Summerhayes, C. (2009). *Antarctic climate change and the environment*.

Urbanski, S. P., Stickel, R. E., & Wine, P. H. (1998). Mechanistic and kinetic study of the gas-phase reaction of hydroxyl radical with dimethyl sulfoxide. The Journal of Physical Chemistry A, 102(51), 10522-10529.

Usui, T., McSween Jr, H. Y., & Clark III, B. C. (2008). Petrogenesis of high-phosphorous Wishstone Class rocks in Gusev Crater, Mars. *Journal of Geophysical Research: Planets*, *113*(E12).

Vago, J. L., Westall, F., Coates, A. J., Jaumann, R., Korablev, O., Ciarletti, V., ... & Carreau, C. (2017). Habitability on early Mars and the search for biosignatures with the ExoMars Rover. *Astrobiology*, *17*(6-7), 471-510.

Vago, J., Witasse, O., Svedhem, H., Baglioni, P., Haldemann, A., Gianfiglio, G., de Groot, R. 2015, ESA ExoMars program: The next step in exploring Mars. *Sol. Syst. Res.,* **49**, 518–528.

Vago, J.L., Coates, A.J., Jaumann, R., Korablev, O., Ciarletti, V., Mitrofanov, I., Rull, F. 2018, Searching for Traces of Life With the ExoMars Rover. in *From Habitability to Life on Mars* 309–347.

van de Meent, D.; Brown, S.C.; Philp, R.P.; Simoneit, B.R. Pyrolysis-high resolution gas chromatography and pyrolysis gas chromatography-mass spectrometry of kerogens and kerogen precursors. *Geochimic. Cosmochim. Acta* 1980, 44(7), 999-1013.

Varnali, T., Edwards, H. G., & Hargreaves, M. D. (2009). Scytonemin: molecular structural studies of a key extremophilic biomarker for astrobiology. *International Journal of Astrobiology*, *8*(2), 133-140.

Vera, J. P. D., Möhlmann, D., Butina, F., Lorek, A., Wernecke, R., & Ott, S. (2010). Survival potential and photosynthetic activity of lichens under Mars-like conditions: a laboratory study. *Astrobiology*, *10*(2), 215-227.

Verseux, C., Baqué, M., Cifariello, R., Fagliarone, C., Raguse, M., Moeller, R., & Billi, D. (2017). Evaluation of the resistance of Chroococcidiopsis spp. to sparsely and densely ionizing irradiation. *Astrobiology*, *17*(2), 118-125.

Vestal, J.R. and White, D.C. 1989, Lipid Analysis in Microbial Ecology. *Bioscience*, **39**, 535–541.

Vilgalys, R., & Hester, M. (1990). Rapid genetic identification and mapping of enzymatically amplified ribosomal DNA from several Cryptococcus species. *Journal of bacteriology*, *172*(8), 4238-4246.

Vítek, P., Jehlička, J., Edwards, H. G., & Osterrothová, K. (2009). Identification of β-carotene in an evaporitic matrix—evaluation of Raman spectroscopic analysis for astrobiological research on Mars. *Analytical and bioanalytical chemistry*, *393*(8), 1967-1975.

Volkman, J.K. and Brown, M.R. 2006, Nutritional value of microalgae and applications. *Algal Cult. Analog. Bloom. Appl. Sci. Publ. Inc New Hampsh.*, 407–457.

von Sonntag, C. (2006). Free-radical-induced DNA damage and its repair (pp. 282-284). Berlin: Springer.

Vreeland, R. H., Rosenzweig, W. D., & Powers, D. W. (2000). Isolation of a 250 million-year-old halotolerant bacterium from a primary salt crystal. *Nature*, *407*(6806), 897-900.

Wackett, L.P., Dodge, A.G., and Ellis, L.B.M. (2004) Microbial genomics and the Periodic Table. Appl Environ Microbiol 70:647–655.

Wadsworth, J., & Cockell, C. S. (2017). Perchlorates on Mars enhance the bacteriocidal effects of UV light. Scientific reports, 7(1), 1-8.

Walker, J. J., & Pace, N. R. (2007). Phylogenetic composition of Rocky Mountain endolithic microbial ecosystems. *Applied and environmental microbiology*, *73*(11), 3497-3504.

Weiss, B. P., Yung, Y. L., & Nealson, K. H. (2000). Atmospheric energy for subsurface life on Mars?. *Proceedings of the National Academy of Sciences*, *97*(4), 1395-1399.

Wentworth, S. J., Gibson, E. K., Velbel, M. A., & McKay, D. S. (2005). Antarctic Dry Valleys and indigenous weathering in Mars meteorites: Implications for water and life on Mars. *Icarus*, *174*(2), 383-395.

Westall, F., Brack, A., Hofmann, B., Horneck, G., Kurat, G., Maxwell, J., ... & Vassaux, D. (2000). An ESA study for the search for life on Mars. *Planetary and Space Science*, *48*(2-3), 181-202.

Westall, F., & Cavalazzi, B. (2011). Biosignatures in rocks. In *Encyclopedia of geobiology*.

Westall, F., Loizeau, D., Foucher, F., Bost, N., Betrand, M., Vago, J., & Kminek, G. (2013). Habitability on Mars from a microbial point of view. *Astrobiology*, *13*(9), 887-897.
Westall, F.; Foucher, F.; Bost, N.; Bertrand, M.; Loizeau, D.; Vago, J.L.; Gautret, P. Biosignatures on Mars: what, where, and how? Implications for the search for martian life. *Astrobiology* 2015, 15(11), 998-1029.

White, T. J., Bruns, T., Lee, S. J. W. T., & Taylor, J. (1990). Amplification and direct sequencing of fungal ribosomal RNA genes for phylogenetics. PCR protocols: a guide to methods and applications, 18(1), 315-322.

Wierzchos, J., Ríos, A. D. L., & Ascaso, C. (2012). Microorganisms in desert rocks: the edge of life on Earth.

Williams A.J., Eigenbrode, J. Floyd, M. Wilhelm M.B., O'Reilly S., Johnson S.S., Craft K.L., Knudson, C.A. Andrejkovičová S., Lewis J.M.T., Buch A., Glavin D.P., Freissinet C., Williams R.H., Szopa C., Millan M., Summons R.E., McAdam A., Benison K., Navarro-González R., Malespin C., and Mahaffy P.R. 2019, Recovery of fatty acids from mineralogic Mars analogs by TMAH thermochemolysis for the sample analysis at mars wet chemistry experiment on the Curiosity Rover. *Astrobiology* 522-546.

Wollenzien, U., De Hoog, G. S., Krumbein, W. E., & Urzi, C. (1995). On the isolation of microcolonial fungi occurring on and in marble and other calcareous rocks. *Science of the total Environment*, *167*(1-3), 287-294.

Wright, D. J., Wittenmyer, R. A., Tinney, C. G., Bentley, J. S., & Zhao, J. (2016). Three planets orbiting Wolf 1061. The Astrophysical Journal Letters, 817(2), L20.

Wynn-Williams, D. D. (1990). Ecological aspects of Antarctic microbiology. In *Advances in microbial ecology* (pp. 71-146). Springer, Boston, MA.

Wynn-Williams, D. D. (1996). Antarctic microbial diversity: the basis of polar ecosystem processes. *Biodiversity & Conservation*, *5*(11), 1271-1293.

Wynn-Williams, D.D.; Edwards, H.G.M. Antarctic ecosystems as models for extraterrestrial surface habitats. *Planet. Space Sci.* 2000, 48(11), 1065-1075.

Yoshimura, Y. (2019). The Search for Life on Mars. In *Astrobiology* (pp. 367-381). Springer, Singapore.

Yuan, X., Xiao, S., and Taylor, T.N. (2005) Lichen like symbiosis 600 million years ago. Science 308:1017–1020.

Yuan, W., Burleigh, S. H., & Dawson, J. O. (2007). Melanin biosynthesis by Frankia strain CeI5. *Physiologia plantarum*, *131*(2), 180-190.

Zhdanova, N. N., Zakharchenko, V. A., Vember, V. V., & Nakonechnaya, L. T. (2000). Fungi from Chernobyl: mycobiota of the inner regions of the containment structures of the damaged nuclear reactor. *Mycological Research*, *104*(12), 1421-1426.

Zhdanova, N. N., Tugay, T., Dighton, J., Zheltonozhsky, V., & Mcdermott, P. (2004). Ionizing radiation attracts soil fungi. *Mycological research*, *108*(9), 1089-1096.

Zorzano, M. P., Mateo-Martí, E., Prieto-Ballesteros, O., Osuna, S., & Renno, N. (2009). Stability of liquid saline water on present day Mars. *Geophysical Research Letters*, *36*(20).